Waste Package Materials Performance Peer Review

A Compilation of Special Topic Reports

Compiled and Edited by
Frank M.G. Wong and Joe H. Payer

May 31, 2002

THIS PAGE INTENTIONALLY LEFT BLANK

Table of Contents

Introduction

At the request of the U.S. Department of Energy, Bechtel SAIC Company, LLC, formed the Waste Package Materials Performance Peer Review Panel (the Panel) in February, 2001. The Panel's charge was to conduct a consensus peer review of the current technical basis and the planned experimental and modeling program for the prediction of the long-term performance of waste package materials being considered for use in a proposed repository at Yucca Mountain, Nevada. The Panel has issued two reports: an Interim Report, dated September 4, 2001 and a Final Report, of February 28, 2002.

During its review, the Panel called on the expertise of a group of Subject Matter Experts, engaged to provide technical advice to Panel members in areas such as corrosion, materials science, and geochemistry. These experts were given a general description of the proposed repository; for the most part, however, they were not asked to consider the specific conditions and operating procedures expected at the proposed repository or to base their reports extensively on information and research results from the Yucca Mountain Project. Rather they were to draw on their own expertise and understanding of the current state of knowledge within their topic areas.

The Subject Matter Experts provided advice to Panel members by participating in meetings, responding to questions, and preparing papers, called Special Topic Reports. The purpose of each Special Topic Report was to assist the Panel's review by presenting information about a factor relevant to the evaluation of the long-term performance of waste packages. Several members of the Panel also prepared Special Topic Reports.

This volume, "A Compilation of Special Topic Reports", contains these reports. Summaries drawn from the reports are also presented in Section 11 of the Panel's Final Report. The Panel used the reports as background and input for its review. Any views and comments expressed in the summaries and the full reports do not necessarily reflect the opinion and findings of the Panel. Further, opinions expressed in the reports are not necessarily those of the Panel or reflected in the Panel's reports and recommendations.

Special Topic Report Authors

The following authors provided advice and information and prepared helpful background reports to assist the Panel in its deliberations.

Name	Location	Technical Area
United States		
John A. Beavers	CC Technologies, Dublin, Ohio	Corrosion, stress corrosion cracking
Craig M. Bethke	University of Illinois, Champaign, Illinois	Hydrogeology
Clyde L. Briant	Brown University, Providence, Rhode Island	Metallurgy
Thomas M. Devine, Jr.	University of California at Berkeley, Berkeley, California	Corrosion-passivity
Stephen C. Dexter	University of Delaware, Newark, Delaware	Corrosion-MIC
Stephen Floreen	Schenectady, New York	Metallurgy
Gerald S. Frankel	Ohio State University, Columbus, Ohio	Corrosion-passivity
Robert P. Frankenthal	Basking Ridge, New Jersey	Corrosion-passivity
Carl E. Jaske	CC Technologies, Dublin, Ohio	Fracture mechanics-life prediction
Russell H. Jones	Battelle Northwest Laboratories, Richland, Washington	Metallurgy, environmental interactions
John C. Lippold	Ohio State University, Columbus, Ohio	Welding
Kathryn L. Nagy	University of Colorado, Boulder, Colorado	Geochemistry
Robert A. Rapp	Ohio State University, Columbus, Ohio	Oxidation
Frank M.G. Wong	Stone & Webster Inc., Las Vegas, Nevada	Metallurgy, fabrication processes
International		
Masatsune Akashi	Ishikawajima-Harima Heavy Industries Co., (IHI), Tokyo, Japan	Life prediction-corrosion
Hannu Hanninen	Helsinki University of Technology, Helsinki, Finland	Metallurgy-Corrosion
Roger C. Newman	UMIST, Manchester, UK	Corrosion-passivity
Bo Rosborg	Rosborg Consulting, Nyköping, Sweden	Corrosion-SCC
Toshio Shibata	Fukui University of Technology, Fukui, Japan	Corrosion-passivity
Alan Turnbull	National Physics Laboratory, Teddington, UK	Corrosion

1. Fabrication Processes and Metallurgy: Peer Review Sub-Panel Meeting with International Materials Experts

Frank M.G. Wong
Stone & Webster, Inc.
Las Vegas, Nevada, USA

EDITORIAL NOTE

This volume, "A Compilation of Special Topic Reports," contains a series of reports that were prepared for the Waste Package Materials Performance Peer Review Panel to use as background and input to the peer review. Summaries drawn from the reports were also presented in Section 11 of the Panel's Final Report. The Panel used the reports as background and input for its review. Any views and comments expressed in the summaries and the full reports do not necessarily reflect the opinion and findings of the Panel. Further, opinions expressed in the reports are not necessarily those of the Panel or reflected in the Panel's reports and recommendations.

CONTENTS

Special Topic Report prepared for the Waste Package Materials Performance Peer Review. The Final Report of the Peer Review was submitted to U.S. Department of Energy and Bechtel SAIC Company, LLC on February 28, 2002.

INTRODUCTION

This paper summarizes the discussion and feedback from the Waste Package Performance Peer Review Sub-Panel Meeting on *Fabrication Processes and Metallurgy and Industrial Experience with Long-Term Corrosion Degradation* that was held on August 10, 2001 at the Lawrence Livermore National Laboratory (LLNL). The objective of the meeting was to obtain technical input on fabrication metallurgical issues of the waste package fabrication process from a group of international materials and corrosion experts, who had been attending the International Environmental Degradation Conference at Lake Tahoe earlier in the week. Several of the international experts are Subject Matter Experts (SMEs) for the YMP International Waste Package Materials Performance Peer Review (M. Akashi, H. Hänninen, B. Rosborg, and T. Shibata). Two Panel members also attended this meeting, J. Payer and R. Jones. A list of the meeting participants is included as an Appendix. A list of the international experts and their affiliations is shown in Table 1. Several of the international experts had also toured the facilities at Yucca Mountain during the previous week (B. Aghili, J. Daret, H. Hänninen, and B. Rosborg).

TABLE 1
International Materials Experts

Aghili, Behnaz	Swedish Nuclear Power Inspectorate (SKI), Sweden
Akashi, Masatsune	Ishikawajima-Harima Heavy Industries Co. Ltd. (IHI), Japan
Daret, Jacques	CEA/LETC, France
Hänninen, Hannu	Helsinki University of Technology/VTT, Finland
Haruna, Takumi	Osaka University, Japan
Hwang, Il Soon	Seoul National University, South Korea
Kubo, Tatsuya	Toshiba Corporation, Japan
Rosborg, Bo	Rosborg Consulting, Sweden
Shibata, Toshio	Fukui University of Technology, Japan

The three Discussion Topics for the meeting were included with the meeting agenda (see Appendices 1 and 2). The YMP documents, FY00 Waste Package Fabrication and Closure Weld Reports, were also distributed as background material. Two Project overview presentations were made at the beginning of the meeting: 1) Overview of the Waste Package Fabrication Sequence and 2) Overview of the Waste Package Materials Testing Program. The remainder of the meeting focused on informal discussions of the three Discussion Topics. The international experts were asked to reply to the three Discussion Topics based on their industrial experience and the SMEs (and the other experts on a volunteer basis) were also requested to forward a brief write-up of this Discussion Topics after the meeting (those received to date are included in the Appendices).

This meeting summary highlights the key points raised by the experts during the discussions of these three Discussion Topics.

DISCUSSION OF WASTE PACKAGE FABRICATION METHODS

It was noted that fabrication of the waste package is similar to that of suction rolls, which are used in paper mills. The suction roll is a large cylindrical metal shell having very high tolerance requirements. The length of the suction roll is approximately the width of the paper machine (up to 10 m). The wall thickness of the roll can be about 50 to 100 mm, and the outer diameter varies between 800 to 1800 mm. The materials processing and the metallurgical considerations used in the fabrication of suction rolls were deemed to be similar to those of the waste package.

The experts agreed that the fabrication processes proposed for the waste package are mostly routine methods that are widely used in many industries. However, the tolerances required of the waste package were viewed as a critical aspect in the manufacturing process. There was much discussion on the effects of mis-alignments between the inner and outer shells of the waste package, as these could lead to significant bending moments in the circumferential welds of the waste package. The bending moments would arise from random contact between the shells. Of all of the manufacturing steps described, the tolerances were viewed as the most difficult requirement. The Project noted that machining tolerances were also deemed the "rate-determining" step in the waste package fabrication sequence by fabricators at the 2000 Waste Package Fabrication Workshop sponsored by the Nickel Development Institute. It was also discussed that the proposed waste container (carbon steel with a titanium overpack) for the Japanese program uses a larger gap than that shown for the YMP waste packages.

There was also some discussion on the timetable required for the manufacturing issues and schemes of the YMP waste package to be resolved and finalized. It was noted that in the Finnish program it is planned that 1) the welding and manufacturing issues must be resolved by the end of 2007, and 2) the construction licensing process of the facility is expected to start in 2010.

DISCUSSION OF WASTE PACKAGE WELDING

There was a significant amount of discussion on waste package welding and its effects on material performance. Many experts noted that from a metallurgical perspective, the welds are the areas of the waste package that would most affect long-term performance. Of all the fabrication processes described, it was viewed that welding would have the largest impact on the metallurgical condition of the waste package.

A summary of the key issues discussed about waste package welding:

- What is the industrial experience base for TIG welding of Alloy 22? The experts were not aware of wide experience in industry.

- The closure weld metallurgy requires particular attention, especially the heat-affected zone and affected microstructure. Electrochemical coupling from precipitates may be possible.

- Boron has a large impact on liquation cracking susceptibility in welding of nickel-base alloys, which is related to boron segregation to grain boundaries. It was noted that boron should not be alloyed to the filler materials, and perhaps it should be controlled in the base material (there may be a number of other elements needing control in addition to B, such as S, P, Si, Nb, C, Fe etc.), in order to avoid liquation cracking and other forms of high temperature cracking at the weld zone, such as solidification cracking and ductility dip cracking.

- Lack of fusion type defects are related to the alloying elements enhancing/decreasing weld penetration and wettability as well as to the welding method itself. With nickel-base alloys lack of fusion is the major problem in welding, and this issue needs attention.

- Different types of oxide films form during manufacturing and they need to be analyzed in detail. The metal matrix composition and microstructure under these oxide films, as well as air-formed oxide film, need to be determined. Weld segregation issues need also to be considered.

- During the discussion of weld repair, it was noted that the weld repair process used should not cause increased susceptibility to stress corrosion cracking (SCC).

- During the discussion of microbiologically-induced corrosion (MIC), it was noted that biofilm growth and MIC mostly affect the corrosion performance of welds. A paper was cited that observed and studied MIC on Alloy 625 welds (Ref. Le Guyader et al., "Crevice Corrosion of Ni Base Alloys and Highly Alloyed Stainless Steels in Sea Water," Solution of Corrosion Problems in Advanced Technologies, Proceedings of Eurocorr '99, European Corrosion Congress, September 1999).

- It was also noted that the surface condition of waste package after welding and annealing is very important to long-term corrosion performance.

DISCUSSION OF LASER PEENING

Of the two stress mitigation techniques applied to the closure weld in the reference waste package design, there was a fair amount of discussion on laser peening (local induction annealing was mentioned, but the experts focused the discussion on laser peening). T. Kubo of Toshiba gave a presentation that described industrial applications of laser peening (developed by Toshiba). The presentation concentrated on Toshiba's methods for laser peening BWR core shroud welds in-situ in the pressure vessel of a nuclear power station. Toshiba developed a laser peening system that uses a fiber optic delivery system (about a 40 meter run) to laser peen welds near the bottom of the BWR core shroud. These welds are under water, and the amount of space

near these welds is very limited (about 10 cm), which necessitated the need for a remote laser peening system. As a result of laser peening, residual surface compressive stresses, approximately 2 to 3 mm in depth, are produced in the shroud welds. The Toshiba system employed a feedback-controlled beam tracking system. Using this system, the laser spot placement is ∂ 1 mm at the end of a 40-meter fiber optic run. This laser peening system by Toshiba has been in production since 1999 and has been used in two nuclear power stations in Japan. The system is scheduled to be used in other nuclear power plants during scheduled maintenance shutdowns.

The discussion on laser peening concentrated on its effects on the metallurgical condition of the weld, and how this would affect corrosion performance:

- It was noted that the transition region between the peened and non-peened regions at the surface of the welds needs to be carefully studied. Examples were cited from the French experience with laser peening processes in steam generator tubing, where there were numerous failures at these transition regions. The effects of residual and applied stresses on the transition regions between peened and non-peened also need to be evaluated.

- The material characteristics and stress profiles after laser peening need to be studied as they may change over time under repository conditions.

- The effect of dislocations and dislocation densities on corrosion performance should be investigated (any peening process affects dislocations near the surface).

- It was noted that the issues raised in the discussions on laser peening and stress mitigation techniques today are similar to (or the same as) those raised and addressed in Toshiba's programs over the last 10 to 20 years.

DISCUSSION OF OTHER WASTE PACKAGE ISSUES THAT WOULD AFFECT CORROSION PERFORMANCE

During the course of the discussions, several other issues were noted and are summarized in this section. These issues were deemed to be significant because they could impact the corrosion performance of the waste package.

Localized Corrosion

The waste package design contains features that may cause some areas of the container to be susceptible to localized corrosion. In evaluating and modeling an alloy's susceptibility to localized corrosion, it is necessary to sufficiently determine the critical potential. The experts from Japan described a new measurement technique, known as the step-down potential method or $E_{R\text{-}CREV}$ technique, for determining the critical potential. M. Akashi gave a presentation on the $E_{R\text{-}CREV}$ technique (see Appendix 6). It was also discussed that to adequately address the susceptibility of localized or crevice corrosion, a map of susceptibility should be constructed to

determine conditions where localized corrosion is either "go" or "no go." Using such a map would allow scenarios to be determined that would avoid crevice corrosion.

It was also suggested that based on the waste package design presented, waste package positioning strategies should be exercised to help avoid crevice corrosion conditions. For example, it was noted that waste package should be placed on the emplacement pallet in such a manner that avoids having any weld regions in contact with the pallet.

The passive behavior of Alloy 22 was viewed to be stable against localized breakdown. Experts were confident that there were no known mechanisms in such an oxidizing environment that would lead to localized breakdown (as the surface of the alloy would be quite homogeneous in the base metal). It was noted that there are quite large variations in chemical composition locally in the weld metal, but it may not be critical for passive breakdown in the anticipated conditions.

Effects of Radiation

Related to the discussion of passive breakdown, it was noted that the NiO film is a p-type semiconductor that contains a low electron density. The effects of gamma radiation from the waste form on the behavior and stability of this NiO film needs to be evaluated, because gamma ray interactions will increase electron densities.

The experts noted that the effects of radiation on the alloy microstructure after laser peening should be studied. It was not obvious what microstructural characteristics may be altered.

The experts also inquired about what are the expected radiation fluence levels. It was noted that the expected fluence is approximately 1.5×10^{16} n/cm^2 in 10,000 years.

Need for Mock-ups/Prototypes

Several experts strongly recommended that several full-scale mock-ups and prototypes should be fabricated and metallurgically examined and tested. These mock-ups/prototypes should also be produced from different fabricators to be able to determine what are the variances in the processes used by different fabricators.

Accelerated Testing

Due to the long timeframe in materials performance required for the waste package, it was also suggested that especially for SCC tests, accelerated tests and measurement techniques would be very useful. Accelerated testing would allow data to be obtained quickly. In addition, it would allow certain test parameters to be perturbed and the effects sampled to assess the susceptibility of the alloys to SCC mechanisms.

Lessons from Experience

- Hydrogen cracking for titanium components is a very significant issue. Predicting hydrogen cracking through 1) hydrogen uptake and diffusion, 2) hydride formation, and 3) repeated crack extension and hydride formation is not easy. Due to such difficulties, the Finnish program decided more than 10 years ago not to use titanium in their waste package.

- Based on uncertainties in predicting and testing, anticipated heat fluxes have always been difficult to quantify. Heat flux uncertainties used in laboratory tests always underestimate what is observed in the field. Nuclear power components were cited as examples.

- Probability analyses are very important in predicting performance over very long time periods.

- Fabrication does have a significant effect on corrosion performance.

Appendix 1

Agenda for

Waste Package Performance Peer Review Sub-Panel Meeting on

Fabrication Processes and Metallurgy and Industrial Experience with Long-Term Corrosion Degradation.

August 10, 2001

Lawrence Livermore National Laboratory

7:30 am	For international visitors staying at the Hampton Inn Livermore: Meet F. Wong in Lobby, and we will go over to the LLNL Badge Office	
8:00 am	International visitors sign-in at LLNL Westgate Badge Office (Also any US visitors requiring a LLNL Visitor Badge)	
8:30 am	Welcoming Remarks/Meeting Outline	T. Summers/J. Payer/ F. Wong
8:45 am	Overview of Waste Package Fabrication Sequence	J. Cogar
9:15 am	Overview of Waste Package Materials Testing Program	T. Summers
9:45 am	**Discussion Topic 1**: Waste Package Fabrication Strategy Assessment (See below for details): Participants are asked to comment on the WP fabrication process based on their industrial experiences: - Forming - Welding - Stress Mitigation Techniques: Laser Peening & Local Induction Annealing of the Closure Weld - NDE methods - Process Metallurgy	
10:30 am	*Break*	
10:45 am	Continue Discussion Topic 1	
11:15 am	**Discussion Topic 2**: Locations and Geometries on the Waste Package that would be more susceptible to corrosion degradation based on industrial experience	
12:15 – 1:30 pm	*Lunch*	

1:00 – 1:30 pm	WP Peer Review Subject Matter Experts (SMEs): Hänninen, Rosborg, Akashi, and Shibata meet with J. Payer	J. Payer / F. Wong
1:30 – 2:30 pm	**Discussion Topic 3**: Procedures and Methods Used in Long-term Corrosion Applications in Industry: - Examples of Long-term Corrosion Applications - Industrial approaches and methods used to resolve such corrosion problems - Model predictions: Did models adequately predict phenomena observed in the field? - How to increase confidence in model predictions	
2:30 – 2:45 pm	*Break*	
2:45 – 4:15 pm	**Tour of LLNL Corrosion Facilities**	D. McCright
4:15 – 5:00 pm	Wrap-up Discussions	
5:00 pm	Adjourn	

Appendix 2

Detailed Questions and Information for Discussion Topics

Each corrosion engineering or materials expert participating in this meeting is kindly requested to prepare a brief 1-2 page write-up on the following discussion topics and email them to F. Wong by August 20, 2001.

Discussion Topic 1: Waste Package Fabrication Strategy Assessment

Based on the information you have received about the waste package fabrication methods and strategy (from the background information in this email and presentations by Yucca Mountain personnel) and your industrial experience, please comment on:

A. Waste Package Fabrication processes, methods, techniques that are widely used in industry that are reliable and have a wide experience base.

B. Waste Package Fabrication processes, method, and techniques that in your judgment are novel or custom tailored for this application.

C. Waste Package Forming Methods: Please let us know in your judgment how this task compares to other industrial projects that involve forming (e.g. easy, standard practice, difficult?).

D. Waste Package Welding and Stress Mitigation Methods: Please let us know in your judgment how this task compares to other industrial project that involve similar types of welding and stress mitigation methods (e.g. easy, standard practice, difficult?).

E. Waste Package NDE Methods: Please let us know in your judgment how this task compares to NDE methods used in other industrial applications (e.g. easy, standard practice, difficult?).

F. Waste Package Process Metallurgy: Please let us know in your judgment whether any of the waste package fabrication methods will be beneficial or detrimental to the Alloy 22 metallurgy that would affect long-term performance of the alloy.

Discussion Topic 2: Locations and Geometries on the Waste Package that would be more susceptible to corrosion degradation based on industrial experience

Based on your industrial experience, please comment on any locations or geometries that are a result of the waste package fabrication process that would promote corrosion degradation processes over long time periods.

Discussion Topic 3: Procedures and Methods Used in Long-term Corrosion Applications in Industry:

Based on your industrial experience, please comment on:

A. Examples of applications that addresses long-term corrosion issues.

B. Industrial approaches and methods used to resolve such corrosion problems

C. Corrosion model predictions: Did models adequately predict corrosion phenomena and performance observed in the field?

D. From the information you have received about the Waste Package Materials Testing and Modeling Programs, is there anything additional that you feel should be included or added to improve confidence in model predictions over long-time periods?

Appendix 3

BACKGROUND INFORMATION ON ALLOY 22 AND WASTE PACKAGE FABRICATION ACTIVITIES

For Waste Package Performance Peer Review Sub-Panel Meeting
August 10, 2001
Lawrence Livermore National Laboratory

This information package summarizes the waste package fabrication sequence with particular emphasis on the Alloy 22 outer barrier/shell of the waste package. This also includes some background information on Alloy 22.

ALLOY 22 BACKGROUND INFORMATION

Alloy 22 (also known as Hastelloy C-22 or equivalent) is a nickel-chromium-molybdenum-tungsten alloy, and its nominal chemical composition is shown in the table below (Alloys C-276 and C-4 are included for comparative purposes). Alloy 22 is an austenitic alloy that is solid-solution strengthened.

Nominal Chemical Compositions (wt %) of some Ni-Cr-Mo Alloys

	Ni	Co	Cr	Mo	W	Fe	Si	Mn	C	V	Others (max)
C-22	**56**	**2.5 max**	**22**	**13**	**3**	**3**	**0.08 max**	**0.50 max**	**0.010 max**	**0.35 max**	
C-22 Filler (GTAW)	**Bal**	**2.5 max**	**20.0 - 22.5**	**12.5 - 14.5**	**2.5 - 3.5**	**2.0 – 6.0**	**0.08 max**	**0.50 max**	**0.015 max**	**0.35 max**	**P: 0.02 S: 0.010 Cu: 0.50**
C-276	57	2.5 max	14.5 – 16.5	15.0 – 17.0	3.0 – 4.5	4.0 – 7.0	0.08 max	1.0 max	0.01 max	0.35 max	P: 0.025 S: 0.010
C-4	65	2.0 max	14.0-18.0	14.0-17.0	-	3.0 max	0.08 max	1.0 max	0.01 max	-	Ti: 0.70 P: 0.025 S: 0.010

The following information about Alloy 22 is excerpted from the Hastelloy C-22 Alloy brochure from Haynes International (Ref: Haynes International, "Hastelloy C-22 Alloy," Brochure No. H-2019E, 1997):

- Specifications: C-22 alloy is covered by ASME Section VIII, Division I. Plate, sheet, strip, bar, tubing, and pipe are covered by ASME specifications SB-574, SB-575, SB-619, SB-622, and SB-626 and by ASTM specifications B-574, B-575, B-619, B-622, and B-626. DIN specification is 17744 No. 2.4602 (all forms), TUV Werkstoffblatt 479 (all forms). NACE

specification is MR-01-75. C-22 alloy falls within the range of UNS number N06022 but has a more restricted composition for improved performance.

- C-22 alloy is a Ni-Cr-Mo-W alloy with better overall corrosion resistance than other Ni-Cr-Mo alloys available today, including C-276, C-4, and 625 alloys.

- C-22 alloy has outstanding resistance to pitting, crevice corrosion, and stress corrosion cracking. It has excellent resistance to oxidizing aqueous media including wet chlorine and mixtures containing nitric acid or oxidizing acids with chloride ions.

- C-22 alloy offers optimum resistance where reducing and oxidizing conditions are encountered in process streams.

- C-22 alloy has exceptional resistance to a wide variety of chemical process environments, including strong oxidizers such as ferric and cupric chlorides, chlorine, hot contaminated solutions (organic and inorganic), formic and acetic acids, acetic anhydride, and seawater and brine solutions.

- C-22 alloy resists the formation of grain-boundary precipitates in the weld heat-affected zone, thus making it suitable for most chemical process applications in the as-welded condition.

- C-22 alloy is readily welded by gas tungsten arc (GTAW), gas metal arc (GMAW), and shielded metal arc (SMAW) welding techniques. Its welding characteristics are similar to C-276 and C-4 alloys. Submerged arc welding is not recommended as this process is characterized by high heat input to the base metal and slow cooling of the weld.

- C-22 alloy has excellent forming characteristics. Cold forming is the preferred method of forming. Because of its good ductility, it can be easily cold-worked. The alloy is generally stronger than the austenitic stainless steels. Therefore, more energy is required during cold forming.

- Examples of typical industrial applications of C-22 alloy can be found in the reference above for Haynes International.

SUMMARY OF WASTE PACKAGE FABRICATION SEQUENCE

The "Waste Package Operations Fabrication Process Report" (September 2000) and "Waste Package FY-00 Closure Methods Report" (September 2000) describe the details of the waste package fabrication logic and sequence. A brief outline of the fabrication sequence is included here. An exploded-view illustration of a typical waste package is included at the end of this information memo.

The waste package fabrication sequence is for the Alloy 22 outer barrier/shell comprised of the following basic steps (Steps 1-6 are performed at the vendors' factories):

1. Fabrication begins with a hot-rolled plate, 25 mm thick.
2. Plate is roll-formed into a cylinder and a longitudinal seam is welded and inspected.
3. A second roll-formed cylinder is circumferentially butt welded to the first cylinder to achieve the desired cylinder length, and the weld is inspected.
4. The bottom lid is circumferentially welded to close the lower end of the cylinder, and the weld is inspected.
5. The Alloy 22 cylinder with the bottom lid is solution annealed.
6. The 316NG stainless steel inner shell with its bottom lid (included for structural purposes) is inserted into the Alloy 22 cylinder.
7. The "open" cylinders (no top lids attached) are delivered to the surface facilities of the repository.
8. The fuel assemblies are inserted into the open 316NG/Alloy 22 cylinder assemblies.
9. The 316NG closure weld is performed.
10. The Alloy 22 closure welds are performed.
11. Stress mitigation techniques are performed on the Alloy 22 closure welds after welding.

Please see the attached fabrication and closure methods reports provide for an in-depth description of the waste package fabrication sequence outlined above.

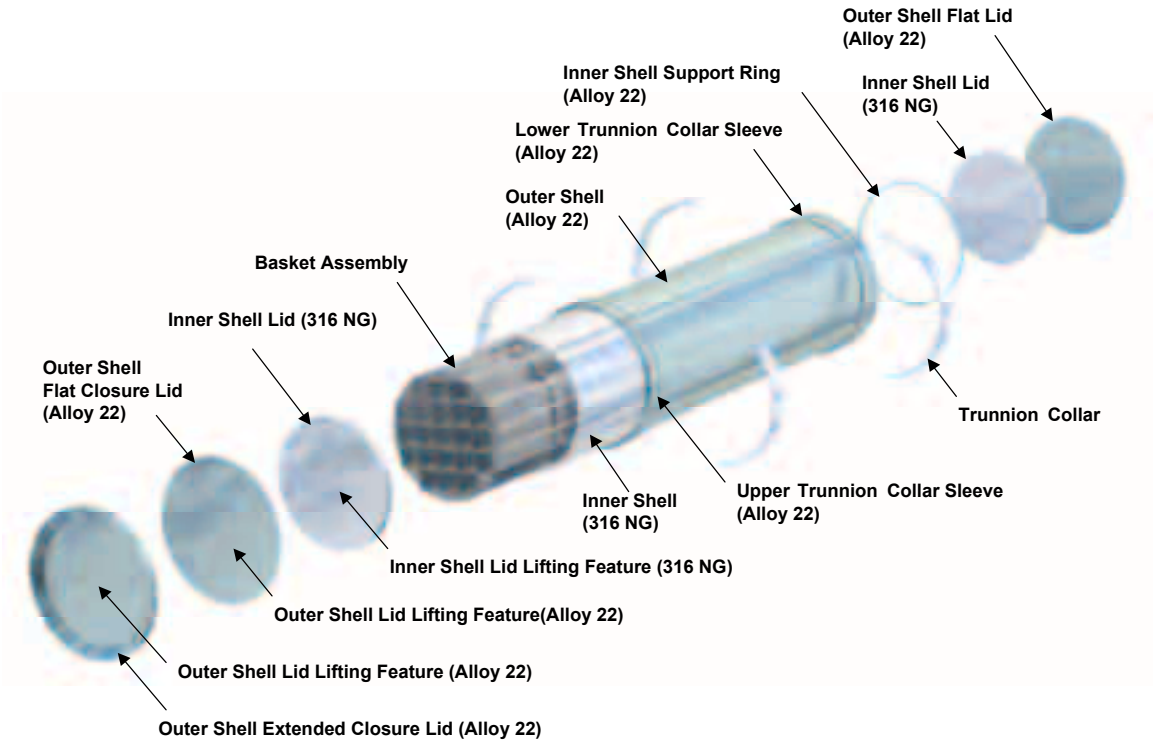

Example 21-PWR Waste Package Assembly Configuration

(Ref: U.S. Dept of Energy, CRWMS, Yucca Mountain Science and Engineering Report, DOE/RW-0539, May 2001).

Appendix 4

List of Meeting Participants

Name: Last	Name: First	Affiliation
Aghili	Behnaz	SKI
Akashi	Masatsune	IHI
Cogar	Jerry	BSC
Cowan	Robert	LLNL
Daret	Jacques	CEA
Di Bella	Carl	US NWTRB
Farmer	Joe	LLNL
Gdowski	Greg	LLNL
Gordon	Gerry	BSC (Framatome)
Hänninen	Hannu	HUT (Helsinki Univ. Tech.)
Haruna	Takumi	Osaka University
Hwang	Il Soon	Seoul National Univ.
Ilevbare	Gabriel	LLNL
Jones	Russ	Battelle (PNNL)
Jones	Denny	LLNL/UNR
Joon	Lee	SNL
Kubo	Tatsuya	Toshiba
Lingenfelter	Al	LLNL
McCright	Daniel	LLNL
Pasupathi	V. (Pasu)	BSC (DOE)
Payer	Joe	CWRU
Rebak	Raul	LLNL
Rosborg	Bo	Rosborg Consulting
Shibata	Toshio	Fukui Univ. Tech.
Summers	Tammy	LLNL
Wong	Frank	Stone & Webster/YMSCO

Appendix 5

Comments on Discussion Topics

Bo Rosborg
Rosborg Consulting, SWEDEN

Please find below my comments on the given discussion topics (the latter in italics). The comments on waste package fabrication are based upon telephone conversations with several persons in Sweden with experience of fabrication of large components in stainless alloys.

Discussion Topic 1: Waste Package Fabrication Strategy Assessment

Based on the information you have received about the waste package fabrication methods and strategy (from the background information in this email and presentations by Yucca Mountain personnel) and your industrial experience, please comment on:

A. *Waste Package Fabrication processes, methods, techniques that are widely used in industry that are reliable and have a wide experience base.*

B. *Waste Package Fabrication processes, method, and techniques that in your judgment are novel or custom tailored for this application.*

C. *Waste Package Forming Methods: Please let us know in your judgment how this task compares to other industrial projects that involve forming (e.g. easy, standard practice, difficult?).*

D. *Waste Package Welding and Stress Mitigation Methods: Please let us know in your judgment how this task compares to other industrial project that involve similar types of welding and stress mitigation methods (e.g. easy, standard practice, difficult?).*

E. *Waste Package NDE Methods: Please let us know in your judgment how this task compares to NDE methods used in other industrial applications (e.g. easy, standard practice, difficult?).*

F. *Waste Package Process Metallurgy: Please let us know in your judgment whether any of the waste package fabrication methods will be beneficial or detrimental to the Alloy 22 metallurgy that would affect long-term performance of the alloy.*

Comments Topic 1:

A similar case (considering fabrication of either the outer or the inner shell) is fabrication of suction rolls for the pulp and paper industry. Large suction rolls are either made by

centrifugal casting or by roll-forming of rolled plates and welding. The latter method is practiced in Sweden and suction rolls as long as 10 m are produced. The requirements on tolerances and life performance are high. My comments below originate from a comparison of the fabrication strategy for the waste package with the proven technology of producing suction rolls.

1A – Considering one container at a time no problems are foreseen for the fabrication of either the inner or outer container. Proven technology will be used. It is a matter of required tolerances, workmanship and cost.

1B – The challenge is "the sizeable container within another sizeable container" design with preference for a quite small gap, or even a close fit, and machining before annealing. (I have understood that the tolerances are not finally settled. From the Las Vegas meeting on August 3rd, I also have a note saying that "the present plans call for machining after annealing".) This may be new and will definitely call for very strict requirements on dimensional control. Early verification by means of full-scale mock-ups is recommended.

1C – No problems foreseen. The machining of the outer shell has to be performed with adequate support for dimensional control. However, machining of large "flexible" components to required tolerances is proven technology. Possible ovalness from the rolling operation and mis-alignments from the welding operation give requirements on machining allowance. Dimensional changes during heat treatment have to be mastered, if machining will be performed before annealing. There is a trade-off as to the degree of compressive stresses on the outer surface and dimensional control for machining before or after annealing and quenching. For dimensional control it is preferable that machining is performed after annealing.

1D – No problems foreseen. Proven methods will be used.

1E – No problems foreseen.

1F – The quenching after annealing may be critical.

General Comments – Fabrication of a number of mock-ups in order to obtain convincing evidence and verification of practically achievable tolerance levels is advisable. It could also be advisable to order several mock-ups from one or two suppliers rather than only a single from several suppliers.

Discussion Topic 2: Locations and Geometries on the Waste Package that would be more susceptible to corrosion degradation based on industrial experience

Based on your industrial experience, please comment on any locations or geometries that are a result of the waste package fabrication process that would promote corrosion degradation processes over long time periods.

Comments Topic 2:

- Welds and in particular machined welds, since turning or grinding may open weld defects that can facilitate initiation of corrosion attack.
- Weld repairs (performed during fabrication). Extensive weld repairing should be avoided.
- Other defects in the plate material that have passed NDT.

The following items are not "a result of the waste package fabrication process" but are nevertheless mentioned:

- crevices between waste package and emplacement pallet
- cold-worked areas (from manufacturing, transportation, and handling)
- deposits formed by dripping and evaporation

Discussion Topic 3: Procedures and Methods Used in Long-term Corrosion Applications in Industry:

Based on your industrial experience, please comment on:

A. *Examples of applications that addresses long-term corrosion issues.*

B. *Industrial approaches and methods used to resolve such corrosion problems*

C. *Corrosion model predictions: Did models adequately predict corrosion phenomena and performance observed in the field?*

D. *From the information you have received about the Waste Package Materials Testing and Modeling Programs, is there anything additional that you feel should be included or added to improve confidence in model predictions over long-time periods?*

Comments Topic 3:

General – The life requirement for the waste package is of course unique. Adequate industrial performance is most often of the order 10-50 years. A lesson learned worth considering from industrial performance of components as regards environmentally assisted cracking (which probably also applies to other forms of localized corrosion): The difference between success and trouble can be fairly small.

3A – (i) the copper canister in a final repository for spent nuclear fuel (the approach adopted in Canada, Finland and Sweden); (ii) pressure vessels in nuclear power plants and environmentally assisted cracking; (iii) PWR steam generator tubing; (iv) polymer piping for district heat systems and environmentally assisted cracking.

3B – (i) natural analogs/archaeological findings; model predictions; verification tests; (ii) extensive NDT programs, international co-operation to achieve a database on environmentally

assisted cracking (time-consuming and expensive testing); (iii) stainless steels not chosen because of the well-known risk for environmentally assisted cracking in chloride containing solutions, and Alloy 800 (Siemens-KWU) and Alloy 600 (Westinghouse, Combustion Engineering and B&W) considered far better alternatives; (iv) laboratory testing of actual piping in water at different temperatures higher than for field applications; extrapolations to lower temperatures to establish the highest allowable temperature to give an anticipated life of 50 years.

3C – (i) verification tests in progress; yes, obtained results for exposure during oxic conditions agree with model predictions; (ii) no, performance observed in plants is better than the bulk of laboratory data predicts; some data predicts immediate repair, while hardly any cracking at all has been observed (only a few isolated cases); one reason for the discrepancy could be laboratory testing in off-normal chemistries, in retrospect too conservative testing; (iii) no, performance observed in plants for Alloy 600 inferior to early predictions based on laboratory data; a large heat-to-heat variability may be one of the reasons, another an underestimated susceptibility to cold-work; (iv) yes, the model predictions have worked quite well.

3D – Possible additions to (or modifications of) the materials testing program "to improve confidence in model predictions over long-time periods":

- Corrosion testing of actual plate and weld material from mock-ups.

- It is recommended to also include less corrosion resistant stainless steels and alloys in the test program for comparison purposes and to obtain information about and verify the aggressiveness of the test environments. Even if Alloy 22 does not show any obvious corrosion attack in a certain environment within the possible time frame for testing, it may be possible to make extrapolations to predict its behavior over longer times by using the results from the less corrosion resistant alloys tested in the very same environment.

- Part of the slow strain rate testing should be performed at lower nominal strain rates. (Pre-loading of the specimens could be used to limit test duration.)

Appendix 6

Comments on Discussion Topics

Hannu Hänninen
Helsinki University of Technology, FINLAND

Discussion Topic 1: Waste Package Fabrication Strategy Assessment:

Based on the information you have received about the waste package fabrication methods and strategy (from the background information in this email and presentations by Yucca Mountain personnel) and your industrial experience, please comment on:

A. Waste Package Fabrication processes, methods, techniques that are widely used in industry that are reliable and have a wide experience base.

In general, the large-scale industrial components such as the present waste packages with similar tolerance range requirements are not common in the industrial manufacturing. A comparable widely used product is the suction roll shell of the paper machine. The suction roll is a large cylindrical metal shell having very high tolerance requirements. The length of the suction roll is approximately the width of the paper machine, i.e., up to 10 m. The wall thickness of the roll can be 50 to 100 mm and the outer diameter varies between 800 to 1800 mm. The materials processing and the metallurgical considerations used in the fabrication of suction rolls are quite similar to those of the waste package. In suction roll shell manufacturing, a new advanced P/M HIP method has been recently adopted in addition to forming and casting.

B. Waste Package Fabrication processes, method, and techniques that in your judgement are novel or custom tailored for this application.

The narrow gap (NG) GTAW welding proposed for longitudinal (probably also circumferential) welding of the cylinder segment and closure welding of the inner lid (AISI 316 nuclear grade) and the outer barrier closure lid (Alloy 22) are not widely used in the industry. Stainless steel welding is better known from experience in the nuclear power plant applications as well as more recently in paper machine applications in welding the suction roll shells. The experience with nickel-base alloys is much more limited. In NG-GTAW, the repair welding experience especially is limited, and also the real time weld monitoring/inspection method needs to be developed. The other technique needing custom tailoring for this application is the final residual stress mitigation: laser peening and local induction annealing of the closure weld. Verification of these methods needs extensive full-scale mock-up manufacturing and demonstration as well as development of the reliable residual stress measurement methods for in-depth analysis. If the

flaw detection requirements are very tight, then the NDT inspection methods have to be developed further for weld inspection.

C. *Waste Package Forming Methods: Please let us know in your judgement how this task compares to other industrial projects that involve forming (e.g. easy, standard practice, difficult?).*

The outer and inner cylinders are planned to be made by roll forming to make first two half-cylinders which are welded longitudinally and circumferentially and then machined for size and tolerance range required. Here marked weld shrinkage can be expected based on the experience on welding of large-thickness stainless steel components, which may require extensive machining. The cylinders are then solution annealed at high annealing temperatures, up to 1150°C (3.5 h). At such a high temperature, creep may take place under the own weight of the cylinders, and therefore, a new machining phase is required, which forms a cold worked layer to the surfaces of the cylinders, but takes away the high-temperature oxide film from the surface. This task will be difficult in the beginning, but after a number of mock-up manufacturing exercises it may become a standard practice.

D. *Waste Package Welding and Stress Mitigation Methods: Please let us know in your judgement how this task compares to other industrial project that involve similar types of welding and stress mitigation methods (e.g. easy, standard practice, difficult?).*

This task will be the most difficult of all, since novel NG-GTAW welding techniques are used and especially the nickel-base alloy is difficult to weld. A large number of trials and mock-ups are needed for careful characterisation of the possible weld defects and their detection by various NDT methods. Residual stress mitigation after final closure lid welding by local induction annealing (1000 to 1100°C/30 s and cooling down to 600°C in less than 10 min) or by local laser peening needs also careful demonstration. It may only move the residual stresses to a new location in the base metal. Induction annealing will produce a high-temperature surface oxide film different from the other surface including alloy depletion under the oxide film in the metal side. Laser peening produces additional cold work to the surface layer in the area of the weld metal and HAZ where recrystallisation has also occurred during welding. Thus, a very complicated final condition is obtained consisting of the closure weld metal with segregations and phase transformations, HAZ with recrystallised microstructure possibly with some precipitates, unknown (at present) residual stress distribution and local high temperature oxide film (induction annealing) or unspecified cold work layer (laser peening).

E. *Waste Package NDE Methods: Please let us know in your judgement how this task compares to NDE methods used in other industrial applications (e.g. easy, standard practice, difficult?).*

The intention is to use NDT methods in accordance with the existing ASME Code. Therefore this task should be a standard practice well known from the power plant inspections. Difficulties may arise from special requirements related to NG-GTAW welds of the nickel-base alloy (specific type of defects and their difficult sizing). In order to improve the reliability of inspection, the complete inspection system (equipment, personnel, procedure) has to be qualified, which is an additional task itself.

F. *Waste Package Process Metallurgy: Please let us know in your judgement whether any of the waste package fabrication methods will be beneficial or detrimental to the Alloy 22 metallurgy that would affect long-term performance of the alloy.*

Alloy 22 is a complicated alloy where a number of phase transformations and ordering phenomena are possible. Most of these are under careful study at present. However, more attention should be paid to these phenomena in the weld metals where major segregation takes place during the solidification and a number of phases can be expected to be present already after welding. Welding will be markedly affected by the heat-to-heat variations both in the base metal and the filler material. These variations can be seen as differences in weld penetration and as susceptibility to various forms of high temperature cracking in welds as well as other weld defects. The long-term behaviour of the weld metals should be also studied carefully. In final closure lid welding and during possible subsequent local induction annealing a high temperature oxide film is formed. This film may be thick and highly enriched in the alloying elements as well as have under it a depleted layer in the metal side. The depleted layer (also the segregated zones in the weld metal) may be more susceptible to various forms of localised corrosion than the base metal. Initiation of corrosion attack should also be considered from this point of view, which is so well known in the case of heat-tinted stainless steels.

Discussion Topic 2: Locations and Geometries on the Waste Package that would be more susceptible to corrosion degradation based on industrial experience:

Based on your industrial experience, please comment on any locations or geometries that are a result of the waste package fabrication process that would promote corrosion degradation processes over long time periods.

As a summary of the previous comments, it is obvious that the most susceptible locations for corrosion are the welds of the waste package, and especially the final lid closure weld. This weld will not be solution annealed as the other welds and therefore it contains all the segregations formed during solidification and the precipitated phases formed during slow

cooling. These may have an effect on all forms of localised corrosion. Also in this region the high-temperature oxide film from local induction annealing is present, which may decrease the localised corrosion resistance due to depleted layer under the oxide film. If localised corrosion is able to initiate there, it may create autocatalytically concentrated local environments inside the pits or crevices (occluded cell formation), even though the bulk environmental conditions were mild. In this region also the tensile residual stresses and weld defects may be present and make the structure susceptible to environment-assisted cracking (EAC), stress corrosion cracking or hydrogen embrittlement.

Discussion Topic 3: Procedures and Methods Used in Long-term Corrosion Applications in Industry:

Based on your industrial experience, please comment on:

A. Examples of applications that addresses long-term corrosion issues.

In order to satisfy the corrosion resistance of the waste package (the most important barrier) for at least 10,000 years, it is evident that the basic knowledge on corrosion properties and mechanisms of Alloy 22 is very important. For such an extremely long-time extrapolation of corrosion behaviour natural analogues are often been used, but there may be no suitable case available. This means that the long-time corrosion behaviour extrapolations must be based on theories and assumptions, which have to be carefully verified with long-term experiments.

B. Industrial approaches and methods used to resolve such corrosion problems.

An extensive corrosion study program is being carried out to understand the mechanisms of various forms of corrosion in Alloy 22. All the necessary methods seem to be in use. More attention should only be paid to the inhomogeneous weld metals with a number of precipitated phases and the high-temperature oxide films with depleted zones as well as to the cold work effects due to surface machining and possible laser peening.

C. Corrosion model predictions: Did models adequately predict corrosion phenomena and performance observed in the field?

Because of the limited experience with Alloy 22, this question is difficult to answer. In general, alternative corrosion models should also be considered in the evaluations (e.g., slip dissolution/film rupture model for stress corrosion cracking may not be sufficient to describe the SCC susceptibility). In addition to corrosion, also the hydrogen embrittlement mechanisms should be considered and the hydrogen uptake should be modelled.

D. From the information you have received about the Waste Package Materials Testing and Modeling Programs, is there anything additional that you feel should be included or added to improve confidence in model predictions over long-time periods?

In corrosion behaviour modelling, the fundamental knowledge is based on the corrosion potential information. Therefore, in the first place there should be a clear understanding and scenario of the expected corrosion potential changes during the long-term storage. In addition, the expected pH-values in different conditions should be known based on the long-term mock-up experiments. This allows the possibility by the determined potential-pH diagrams to estimate the most critical phases for corrosion. These are expected to be the conditions where major structural and compositional changes will occur in the passive oxide films. More information of these things could perhaps be then obtained with very slow electrochemical polarisation measurements simulating the expected electrochemical potential changes during the long-term storage. Additionally, reliable data has to be available of critical potentials for localised corrosion (pitting, crevice and EAC) initiation and repassivation as well as on critical temperatures for occurrence of these phenomena.

Excessive mechanical loads may be possible during long-term storage from earthquakes and falling rocks, which may cause collapse of the tunnel on the waste packages. These extreme situations should also be examined.

Appendix 7

Comments on Discussion Topics

Masatsune Akashi
Ishikawajima-Harima Heavy Industries Co. Ltd. (IHI), JAPAN

Discussion Topic 1: Waste Package Fabrication Strategy Assessment

Stress Mitigation by Means of Laser Peening:

There exists a critical depth for the stress-corrosion crack to start steady propagation [1]. Therefore, the problems to be solved are:

(1) How the Laser-Peening effect extends beyond the critical depth, and
(2) How the post-fabrication NDE evaluates it

Discussion Topic 2: Locations and Geometries on the Waste Package that would be more susceptible to corrosion degradation based on industrial experience

Most of corrosion failures have generally been found near the weldment (weld metal plus weld heat-affected zone). You have to therefore evaluate the effects of heat/strain cycling during welding and microstructural changes on the corrosion degradation response.

Discussion Topic 3: Procedures and Methods Used in Long-Term Corrosion Applications in Industry

Generally for the localized corrosion in industrial plant materials, they do not apply the life estimated based on a life-prediction model, but apply the critical potential for initiation. For the crevice corrosion as the most important localized corrosion, the corrosion-crevice repassivation potential ($E_{R,CREV}$) concept [2] should be applied.

References

1. Masatsune Akashi, Guen Nakayama: "Effects of Acceleration Factors on the Probability Distribution of Stress-Corrosion Crack Initiation Life for Alloys 600, 182, and 82 in High-Temperature and High-Purity Water Environments," Proc. 9th International Conference on Environmental Degradation of Materials in Nuclear Power Systems –Water Reactors, F.P. Ford, S.M. Breummer, G.S. Was, Eds., TMS, pp. 389-397 (1999).

2. Masatsune Akashi, Guen Nakayama, Takanori Fukuda: "Initiation Criteria for Crevice Corrosion of Titanium Alloys Used for HLW Disposal Overpack," CORROSION/98, NACE International, Paper No. 158 (1998).

Appendix 8

Comments on Discussion Topics

Behnaz Aghili
Swedish Nuclear Power Inspectorate (SKI), SWEDEN

I have been reading the reports you have sent us, and even though I am not a member of the peer review group, I have provided some comments on these reports:

- Requirements and acceptance criteria for welding, repairs, production, etc., according to ASME are a good way to start. However, it must be pointed out that these requirements may change as the knowledge about the required performance of the waste package increases and evolves.

- Acceptance criteria should be related to the consequences of fractured canisters. Safety analyses are required.

- Production of the whole system seems to be valid and consistent to current industrial routines and practices.

- In my opinion, the concept for waste package production consists of many welding processes. Any metallurgical engineer knows that welding means introducing defects to the material. These defects may be small cracks and then they are not too difficult to detect. The difficult ones are inhomogeneities, different microstructure and residual stresses. I would suggest that the development program for production of waste package makes special attempts to reduce welding both in number and in total length.

- Even though the specimens used may fulfill all requirements, measurements in the actual waste package would give much more confidence. I would like to recommend that residual stress measurements be made on a mock-up or, even better, on a full-size canister made of actual materials.

- There is of course a worry about crevice corrosion with pedestal (palette) under the waste package, but we discussed this during the meeting.

Appendix 9

Comments on Discussion Topics

Jacques Daret
CEA/LETC, FRANCE

Two comments on laser peening:

- In the absence of any external applied load, a metal subjected to partial peening, if not deformed by the peening operation, will not only exhibit residual compressive stress in its peened area, but also to a residual tensile stress in its non-peened area (in absence of deformation, there must be a new stress equilibrium). So, at the distinct transition of the peened and non-peened areas, the non-peened areas exhibits tensile residual stresses, and this area can therefore be prone to SCC problems. This explains why laser peening was not applied to PWR steam generator tubes in France, since we proved that this transition region was very susceptible.

- Now, if an external load is applied to the peened region with residual compressive stresses, such as by the fall of a big rock in the YM repository, and if this load produces deformations (1 or 2% strain are sufficient), then huge tensile stresses (more than 1000 MPa) can be induced in the previously compressed area, while the bulk material exhibits stresses that are only slightly higher than the yield strength. This problem has been thoroughly investigated in France, especially for PWR wrought components, and is now systematically included in SCC prediction and modeling.

2. Welding Issues Associated with the Waste Packages

John C. Lippold
The Ohio State University
Columbus, Ohio, USA

EDITORIAL NOTE

This volume, "A Compilation of Special Topic Reports," contains a series of reports that were prepared for the Waste Package Materials Performance Peer Review Panel to use as background and input to the peer review. Summaries drawn from the reports were also presented in Section 11 of the Panel's Final Report. The Panel used the reports as background and input for its review. Any views and comments expressed in the summaries and the full reports do not necessarily reflect the opinion and findings of the Panel. Further, opinions expressed in the reports are not necessarily those of the Panel or reflected in the Panel's reports and recommendations.

Summary and Recommendations

The closure weld and its postweld processing are critical to the Yucca Mountain Project (YMP) goal to insure that nuclear waste storage canisters will survive their design lifetime in the emplacement environment. The current closure weld approach employs "off-the-shelf" technology to complete the weld by using the multipass, gas-tungsten arc welding (GTAW) process. The process is reliable and well proven, but completion of the closure weld will require multiple weld passes and hours of welding time to complete. This will increase the potential for weld defects such as lack-of-fusion, weld misalignment, shielding gas interruptions, etc. To account for this, a robust weld monitoring system must be in place and a repair welding procedure must be developed.

Following completion of the closure welds, they will be subjected to laser peening and local induction stress relieving to eliminate tensile residual stresses. Both these techniques have been demonstrated to be effective in the nuclear industries in France and Japan, but they are certain to be an "engineering challenge" in the hot cell environment of the YMP. It will be difficult to determine the efficacy of these techniques once they have been performed. Further investigation on the application and implementation of these techniques is required.

To date there has been little work to evaluate filler metal composition as it affects both weldability and long term metallurgical stability. The weld metal microstructure of C-22 and the matching ERNiCrMo-10 filler metal varies significantly from that of the base metal due to solidification and segregation effects. For example, there is considerable segregation of Mo to interdendritic regions (up to 18 wt%) in the microstructure, and both ω and P phases are present

Special Topic Report prepared for the Waste Package Materials Performance Peer Review. The Final Report of the Peer Review was submitted to U.S. Department of Energy and Bechtel SAIC Company, LLC on February 28, 2002.

in the as-welded condition. The effect of postweld annealing on the weld microstructure is not clear, nor is the long-term stability of the weld metal relative to long range ordering. Considerable work is needed to better characterize and quantify the microstructure and its stability. The ERNiCrMo-10 filler metal has been used in the early development studies because it is the matching composition to the C-22 base metal. It is possible that better long-term performance can be achieved by the use of an alternate filler metal.

A filler metal qualification program should also be put in place in order to better quantify the behavior of the filler metal with respect to its weldability. In highly restrained joints, nickel-base filler metals are known to be susceptible to a number of cracking phenomena including solidification cracking, weld metal liquation cracking, and solid-state "ductility-dip" cracking. Little or no weldability test data exists for ERNiCrMo-10 or comparable filler metals. Weldability test techniques now exist that can be used to develop a database that will allow the weldability of the filler metals to be quantified. This will ultimately allow selection or designation of filler metal compositions that optimize weldability. Any filler metal development program designed to improve another property, such as corrosion or long term stability, should be coupled with weldability testing to insure that an improvement in one property does not create a deficiency in another.

The YMP team should continue to evaluate alternate welding processes for the closure weld. While the GTAW process is reliable and dependable, it is very slow and results in high levels of residual stress that must subsequently be relieved by peening or induction heating. Electron beam welding is attractive because it eliminates the need for a weld joint and can be conducted in a single pass, thus reducing the weld time significantly. It also has inherent disadvantages, including high equipment cost and maintenance requirements, and how to deal with weld defects that may occur. A "single shot" process such as friction welding is also very attractive from both a metallurgical, residual stress, and productivity standpoint. Because friction welding is a solid-state process, many of the concerns regarding long term metallurgical stability resulting from segregation during weld solidification are minimized. However, because of the size of the canisters, the friction welding equipment would far exceed the capabilities of what is currently commercially available. There may also be other "hybrid" processes that are applicable. For example, coupling GTAW with laser welding has been shown to greatly improve penetration and productivity. These alternatives would require considerable development, but all would significantly improve productivity and would have a benefit with respect to reduction of residual stresses and improved metallurgical stability,

In closing, weld development activities and metallurgical studies involving C-22 and the ERNiCrMo-10 filler metal have been limited, but no "show-stopping" issues have been identified. The GTAW process and procedure selected is adequate for the initial development and prototype stage, but it has inherently low productivity and requires the use of complicated postweld processing to reduce residual stresses. Further optimization of this process is required for YMP applications and consideration of other processes is encouraged. The most significant metallurgical issue associated with welding involves the long-term stability of the weld metal and the potential negative effects with respect to corrosion resistance. A secondary issue is the

weldability of the filler metal and its resistance to cracking during fabrication. Both of these issues need to be evaluated in more detail.

3. Composition Effects within the Chemical Specification for Alloy 22

Stephen Floreen
Schenectady, New York, USA

EDITORIAL NOTE

This volume, "A Compilation of Special Topic Reports," contains a series of reports that were prepared for the Waste Package Materials Performance Peer Review Panel to use as background and input to the peer review. Summaries drawn from the reports were also presented in Section 11 of the Panel's Final Report. The Panel used the reports as background and input for its review. Any views and comments expressed in the summaries and the full reports do not necessarily reflect the opinion and findings of the Panel. Further, opinions expressed in the reports are not necessarily those of the Panel or reflected in the Panel's reports and recommendations.

Introduction

Composition specifications for Alloy 22 are relatively broad, and the microstructure and properties of Alloy 22 are likely to be sensitive to chemistry and processing history within the specified composition. Consequently, some heats may behave better or poorer than others. By determination of this behavior and optimizing these variables, it may be possible to achieve better behavior with this alloy. The author bases much of the following discussion on his experience with Alloy 625 while working at KAPL. An experimental program to investigate the effects of composition on Alloy 22 is recommended.

Alloys such as Alloy 22 were not designed for prolonged service at intermediate temperatures. Consequently, little thought was given to controlling the composition so as to prevent the precipitation of undesirable phases. Often, the composition specifications are left fairly broad to make melting and alloy production easier, and to prevent competitors from making another alloy too close to the one being considered. The result is that heats of the same alloy can have widely different properties, even though the compositions fall within the specifications for the alloy. This variability due to compositional factors was recognized when Alloy 625 was being examined for various applications. When the magnitude of the variability became evident an experimental program was undertaken to determine how to tighten the composition limits. Alloy 22 is not identical to Alloy 625, but is similar enough so that the Alloy 625 results can provide examples of the changes that can happen with changes in composition.

Special Topic Report prepared for the Waste Package Materials Performance Peer Review. The Final Report of the Peer Review was submitted to U.S. Department of Energy and Bechtel SAIC Company, LLC on February 28, 2002.

Alloy 625 Experience: Compositional Variability for Time- Temperature- Transformation (TTT) Diagrams

The attached Figures 96 and 8 show TTT diagrams for Alloy 22 and Alloy 625, respectively. For Alloy 22, the Project concludes that the carbides and the intermetallic compounds obey the same kinetics and precipitate at the same time. This is counter to the experience with Alloy 625. Carbides generally precipitate much sooner in nickel base alloys; because the kinetics are controlled by carbon diffusion while the intermetallics require substitutional element diffusion. In Alloy 625, the carbides came out over an order of magnitude sooner than the other phases. Several different carbides were precipitated, which is common.

The Project staff working with Alloy 22 apparently found another TTT diagram in the literature that looked similar to theirs, and they appear to have concluded that the TTT diagram was independent of chemistry variations. This is too optimistic. In Alloy 625, the diagram can be shifted significantly by changes in Nb content in particular. Experience with Alloy 718 TTT diagrams also showed wide variation in reported TTT curves. Examination of seven TTT curves from the literature showed that several resembled each other, but others were far different. There are probably several reasons for these differences, but a primary reason was likely to be the differences in alloy chemistry between the test materials.

Several practical consequences follow from the above discussion. If it takes about an hour to start forming intermetallics in Alloy 22 at high temperatures, then these phases should not be present in properly processed heats. Thus, these detrimental phases should not appear until late in the game. Carbides, however, may be present to start with and will come out sooner during service life.

Alloy 625 Experience: Effects on Mechanical Properties

Changes in chemistry had significant effects on the mechanical properties of Alloy 625. The enclosed Figure 12 shows the effects of thermal exposures on the impact properties of a normal heat and a heat with reduced Nb and C contents. Precipitation was significantly delayed in the low (Nb+C) heat, thus delaying the drop in impact strength.

One other chemistry variable that deserves mention is the level of tramp elements (e.g. S, P, O etc.). At elevated temperatures, these odd-sized elements fit within the lattice fairly well, and do not segregate too severely to the grain boundaries. At 300 C however, these elements want to segregate to the boundaries very badly. It may take them a long time to get there, but when they do they could cause serious problems (e.g. embrittlement). It should be noted that prolonged high temperature exposures to bring out secondary phase particles will not move these elements to the grain boundaries. There does not appear to be any practical method to test the effects these elements may eventually have at 300 C. Should these elements be problematic, the best approach would be to minimize their amounts. That is, use good melt practice (e.g. VIM – VAR) with selected melt stock. The performance benefit should be well defined, because this will increase the cost.

Alloy 625 Experience with Weld Metal

Weld metal is likely to be more sensitive to compositional variations than base material. For example, as shown in Figure 14, the TTT curves for Delta phase in Alloy 625 base material and in gas tungsten arc weld metal made the standard Alloy 625 filler metal differed greatly. The TTT curve for the weld metal was shifted to the right by more than an order of magnitude in time. This resulted directly from the segregation of the alloying elements in the cast structure of the weld. Carbides and\or intermetallic phases can be formed during solidification of the weld metal. Typically these will form in interdendritic regions where the final stages of solidification occur. The impact strength of GTA weldments was dramatically improved by switching from conventional Alloy 625 filler to a low (Si+Fe) wire. The improvement again resulted from a reduction in secondary phase particles. This improved wire chemistry was developed by Huntington Alloys and caught on with many people concerned about mechanical properties.

An Approach to Determine Composition Effects

The goal is to narrow the chemistry ranges so that detrimental phases are kept to a minimum while maintaining satisfactory mechanical properties and corrosion resistance. Based on the authors experience reducing the Mo, W, Fe,and C levels would be a fruitful approach, but other elements may also be important.

An approach to examining the effects of composition is an experimental program using small heats with systematic changes in chemistry. A set of vacuum melted ingots, weighing on the order, of 50 pounds could be hot rolled to plate stock, and this would provide a substantial supply of test material. The effects of thermal exposures could then be determined, along with spot checks of the mechanical properties and corrosion behavior. In addition, autogenous GTA weld beads could be made on test coupons and examined before and after thermal exposures to provide information on how to optimize the filler metal chemistry. It would also useful to make several heats of weld wire with modified compositions to check the weldability. This type of chemistry adjustment is common practice in industry, where experience shows that altering the composition of an alloy can significantly improve its performance in certain applications.

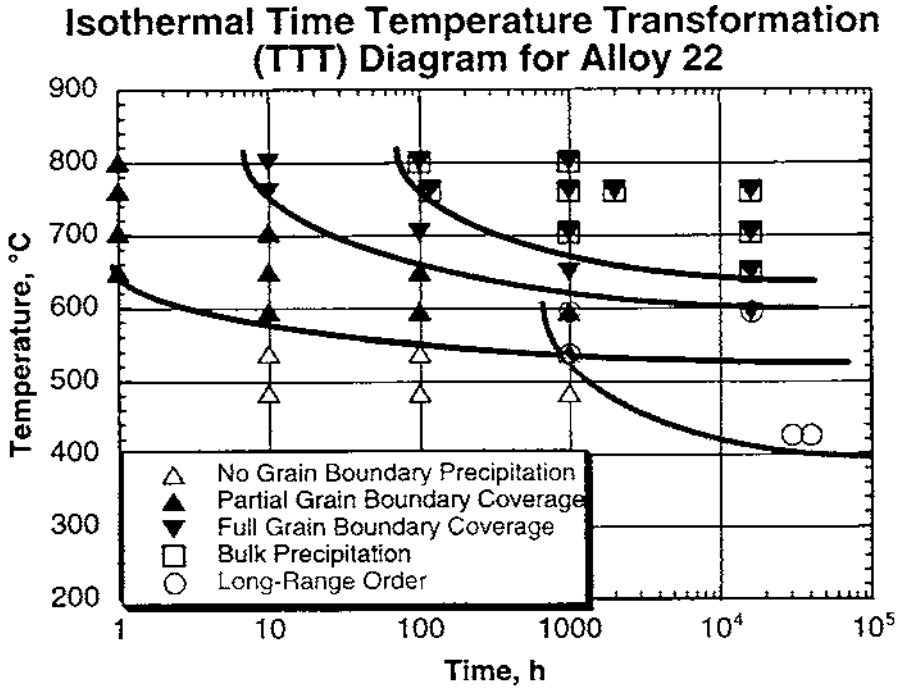

Figure 96. Isothermal TTT Diagram for Alloy 22 Base Metal [DTN # LL000116005924.114]

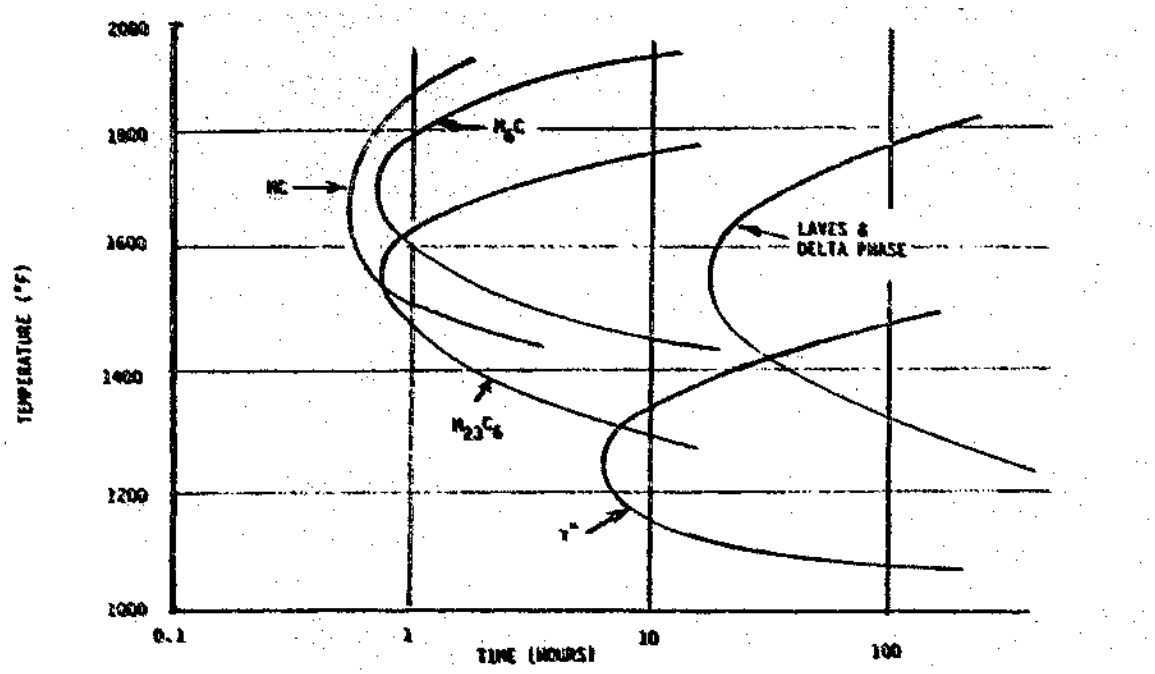

Figure 8. Approximate Time-Temperature-Transformation Diagram for Phases Forming at High Temperatures in A625

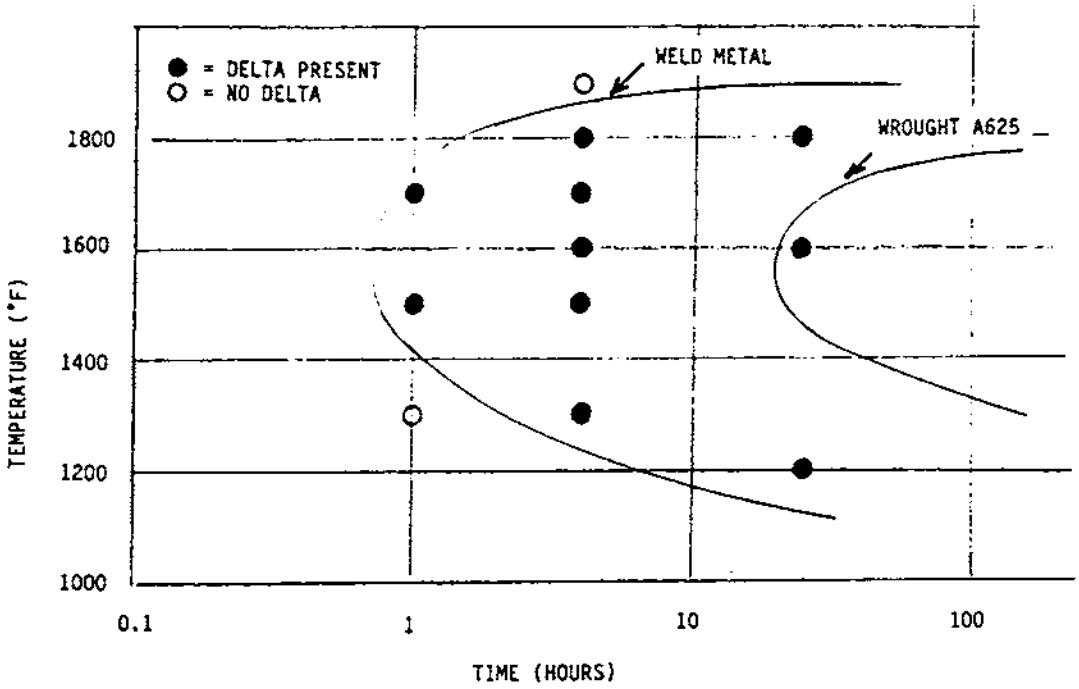

Figure 14. Thermal Exposure Conditions to Form Delta in Weld Metal Compared to Wrought A625

4. Residual Stress in Stainless Steel Cylinders from Quenching

Carl Jaske
CC Technologies Laboratories, Inc
Dublin, Ohio, USA

EDITORIAL NOTE

This volume, "A Compilation of Special Topic Reports," contains a series of reports that were prepared for the Waste Package Materials Performance Peer Review Panel to use as background and input to the peer review. Summaries drawn from the reports were also presented in Section 11 of the Panel's Final Report. The Panel used the reports as background and input for its review. Any views and comments expressed in the summaries and the full reports do not necessarily reflect the opinion and findings of the Panel. Further, opinions expressed in the reports are not necessarily those of the Panel or reflected in the Panel's reports and recommendations.

Large stainless steel cylinders are to be used for storage of nuclear waste at the Yucca Mountain facility.[1] The fabrication of such containers can produce significant residual stresses during metal forming and welding operations. Because high tensile residual stresses increase the susceptibility of stainless steel to stress corrosion cracking, it is important to minimize them. Residual stresses are typically relieved by heat treatment after fabrication. When stainless steel is solution annealed after fabrication, it provides the added benefit of removing sensitization in the heat-affected zones of welded joints. However, cooling after solution annealing can also produce significant tensile residual stresses in large stainless steel components.

Experience with the fabrication of suction roll shells in the pulp and paper industry provides insight into the importance of minimizing residual stresses in large stainless steel cylinders. A suction roll shell is a large stainless steel cylinder with a diameter up to about 1.5 m (1.6), a wall thickness up to about 75 mm (90), and length up to about 10 (10.2) m. They are made either by centrifugal casting or by rolling and welding plate. Either process may produce significant residual stresses. High tensile residual stresses coupled with operating stresses (and low resistance to corrosion-assisted cracking) have led to premature corrosion fatigue and stress corrosion cracking failures of suction rolls.

Early stainless steel suction rolls were made from Type 316 or CF-8M (the cast equivalent) materials (or early austenitic stainless steels with significant amounts of ferrite ie Alloy 63). As part of the manufacturing process, they were solution annealed and water quenched to remove sensitization and sigma phase. Premature failure problems were found with some of these rolls. Research studies revealed that these failures were caused by high tensile residual stresses

Special Topic Report prepared for the Waste Package Materials Performance Peer Review. The Final Report of the Peer Review was submitted to U.S. Department of Energy and Bechtel SAIC Company, LLC on February 28, 2002.

induced during the quenching process. It was found that slow air or furnace cooling after annealing was required to minimize tensile residual stresses in the large diameter, heavy section rolls. Slow cooling, however, sensitized Type 316 or CF-8M materials. For this reason, stainless steel alloys were developed that could be slow cooled without being sensitized. Today, typical suction rolls are made of proprietary grades of duplex stainless steels that are not sensitized by slow cooling after solution annealing.

In the fabrication of waste packages, the quenching process after solution annealing could produce unacceptably high tensile residual stresses. Two approaches can be employed to minimize tensile residual stresses induced by cooling after solution annealing. The first is to slowly cool the fabricated containers as is done for suction rolls. This approach would require the use of a corrosion resistant alloy that is not susceptible to sensitization or other detrimental metallurgical processes during the slow cooling process. The second is to carefully design and control the quenching process so that minimal levels of tensile residual stress are produced at or near free surfaces during the quenching operation. The selected approach should be verified by finite-element thermal and stress analysis and by experimental measurements on prototype containers.

REFERENCE

1. M. V. Veazey, "Nuclear Waste Storage Plan Under Review," Materials Performance**, Vol. 40**, No. 11, 2001, pp. 14-16.

5. Corrosion Product Passive Films: Effect of Surface Condition

Robert A. Rapp
The Ohio State University
Columbus, Ohio, USA

EDITORIAL NOTE

This volume, "A Compilation of Special Topic Reports," contains a series of reports that were prepared for the Waste Package Materials Performance Peer Review Panel to use as background and input to the peer review. Summaries drawn from the reports were also presented in Section 11 of the Panel's Final Report. The Panel used the reports as background and input for its review. Any views and comments expressed in the summaries and the full reports do not necessarily reflect the opinion and findings of the Panel. Further, opinions expressed in the reports are not necessarily those of the Panel or reflected in the Panel's reports and recommendations.

Preface

This memo describes the results of recent Ph.D. thesis by Florence Carrette entitled "Release (Dissolution) of Corrosion Products of Alloy 690 Steam Generator Tubes for the Primary Circuit of Pressurized Water Reactors."[1] While the environment studied (pressurized water at 325C at 155 atm pressure with pH = 7.2, containing additions of LiOH and H_3BO_3) is not directly relevant to the Yucca Mountain Project, the alloy composition and the nature and growth mechanism and kinetics of the passive film may be relevant. These careful and extensive thesis studies will be summarized for those concerned with the YMP, and some relevant interpretations will be offered.

Experimentation

Although the title of the thesis only refers to "Release (Dissolution)" of the corrosion products (in recirculating loops and a static autoclave), in fact the emphasis of the thesis was the experimental characterization of the corrosion product passive films by SEM, TEM, metallographic and surface roughness observations, X-ray diffraction, EDS, ESCA, marker observations, and precise gravimetric measurements. Although some studies also included the Alloy 800 (33Ni, 21Cr, 44 Fe...) and Alloy 600 (75Ni, 15Cr, 8.5Fe…), the emphasis was placed on Alloy 690 (60Ni, 29Cr, 9 Fe…). From a corrosion standpoint, the composition of Alloy 690, except for the absence of the refractory additions W and Mo and a lower Fe content, represents a Cr-rich Ni-base alloy similar to Alloy 22 intended for the YMP service. Indeed, these stated differences in their composition means that Alloy 22 would only be (much) more corrosion resistant than alloy 690. In the thesis, the experimental times extended to 2160 hours (45 days)

Special Topic Report prepared for the Waste Package Materials Performance Peer Review. The Final Report of the Peer Review was submitted to U.S. Department of Energy and Bechtel SAIC Company, LLC on February 28, 2002.

at a temperature of 325C, so that representative steady-state chromium-rich (spinel) passive films were formed. In fact, through careful weight measurements involving dissolution of the passive film following testing, the film growth kinetics could be separated from the film dissolution kinetics, although of course some considerable uncertainty arose from the slight weights of the passive films.

The mechanism for the growth of the passive films was identified principally by the use of implanted Xe (inert) markers, and by the use of a sequential double oxidation, involving corrosion for 144 hours in H_2O followed by 2016 hours in D_2O. The resulting concentration profiles were established by the use of SIMS. Three different surface preparations were compared: as-received, micro-ball-peened (deformed), and electropolished. The kinetics measurements were interpreted to separate the rate of scale growth from the rate of scale dissolution.

Results and Interpretations

Admittedly, the composition for the passive film formed in flowing pressurized water at 325C should not necessarily mimic that for thin-film atmospheric corrosion by an aerated aqueous film at much lower temperature. The former passive film might exhibit a higher dissolved proton content (OH^- ions), thereby supporting the inward growth of the chromium-rich corrosion product by anion diffusion. In fact, both the Xe marker motion (stayed close to the external surface) and the dual-stage corrosion involving deuterated water (deuterium enriched at the base of the passive film) supported this conclusion. Because of the simultaneous dissolution of the corrosion product, the passive films reached constant (limiting) thicknesses, on the order of 70-100 nm, and constant compositions (enriched in Cr, but with significant Ni and Fe), after about 144 hours. Significantly, the electropolished surface provided a tightly adherent, fine-grained product film with an important reduction in the growth rate of the passive film, while the peened (deformed) surface exhibited faster growth kinetics and a thicker corrosion product. Upon fitting the observed film growth kinetics to a power-law expression, $X = a\,t^n$, the exponent n for the electropolished surface equaled 0.39, i.e. “slower” than parabolic growth (n = 0.5). The time dependence would be affected by the evolving corrosion product composition resulting from the simultaneous dissolution process which favored the extraction of Fe.

In attempting the draw inferences from this study that are useful to the YMP, the importance of the electropolished surface preparation stands out. This advantage (compared to a deformed surface) should be realized whether the corrosion product film grows dominantly by outward cation grain-boundary diffusion over cation vacancies, or else by inward anion grain-boundary diffusion over anion vacancies. As shown in a study of the high-temperature gaseous sulfidation of Mo, any corrosion product grown by anion diffusion must form initially a fine-grained, tightly adherent product with a columnar morphology.[2] The fine scale grains result naturally because a given metal grain at the metal-scale interface offers multiple and redundant possible epitaxial orientations for the nucleation of a new product grain. However, the differing orientations for these scale grains cannot support grain intergrowth, i.e. their impingement stifles grain growth. Therefore, the repeated nucleation of new grains, all being epitaxial, but with differing orientations, continues the reaction, but leads to the formation of a columnar

morphology. The excellent adherence results from the continued epitaxial contact at the metal-scale interface. In contrast, for scales grown by cation diffusion with vacancy annihilation at the metal-scale interface, an eventual malfunction (tangling) of the interface dislocations whose climb normally results in vacancy annihilation can lead to void formation, poor adherence, and impurity segregation at the metal-scale interface. Thus, the thin protective anion-diffusing oxide films on W, Nb, Ta, Mo, and sometimes Cr are tightly adherent and slow growing. The oxidation problems for these reactive metals at really high temperatures (scale cracking, large volume increase upon reaction, oxygen dissolution, etc.) do not apply for the thin films.

Another interesting study is on the importance of hydrogen in the protection afforded by a chromia scale in high-temperature oxidation at 900C in pure oxygen.[3] The oxidation kinetics of pure Cr coupons containing some initial dissolved hydrogen (7 and 40 wt ppm) were compared to those for a vacuum-annealed (H-free) Cr coupon, using a two-step O^{16}/O^{18} ratio method. The presence of dissolved hydrogen led to faster scale growth and poor scale adherence compared to the hydrogen-free coupons. The authors interpreted these observations in terms of a point defect model whereby hydrogen (protons) dissolved in the scale increased the concentration of cation vacancies and thereby favored faster outward Cr diffusion and a badly adherent chromia scale. The thin inward grown chromia scale, resulting from inward anion diffusion for the hydrogen-free coupon, exhibited excellent adherence and very slow growth. As mentioned in a separate report[4], these advantageous changes can also be realized by the adsorption of yttrium or cerium ions at the Cr/Cr_2O_3 interface, the so-called Reactive Element Effect.[5] The point here is to emphasize the importance of a knowledge about the specific mode for film growth under the YMP conditions. The hydrogen dissolution in chromia at 900C is certainly not relevant to YMP, although dissolved hydrogen in the as-received Alloy 22 would not be advantageous. Hydrogen entry would not occur upon any (eventual) electropolishing of the Alloy 22 because of the high oxidation potential inherent to electropolishing.

References

1. F. Carrette, "Relachement des Produits de Corrosion des Tubes en Alliage 690 du Generateur de Vapeur du Circuit Primaire des Reacteurs a Eau Pressurisee", These of L'Institut National Polytechnique de Toulouse, Feb. 2002.

2. B. S. Lee and R. A. Rapp, "Gaseous Sulfidation of Pure Molybdenum at 700-950C, J. Electrochem. Soc. **131**, (1984) 2998.

3. B. Tveten, G. Hultquist and T. Norby, "Hydrogen in Chromium: Influence of the High-Temperature Oxidation Kinetics in O_2, Oxide Growth Mechanisms, and Scale Adherence", Oxidation of Metals, **52**, #3/4, (1999) 235.

4. R. A. Rapp, "Aspects of Waste Canister Corrosion Related to Oxidation and Scale Formation", Report to YMP Corrosion Team, Nov., 2001.

5. B. Pieraggi and R. A. Rapp, "Chromia Scale Growth in Alloy Oxidation and the Reactive Element Effect (REE)", J. Electrochem. Soc**.,** **140**, (1993) 2844.

6. Localized Corrosion Phenomenology and Controlling Parameters

Gerald S. Frankel
The Ohio State University
Columbus, Ohio, USA

EDITORIAL NOTE

This volume, "A Compilation of Special Topic Reports," contains a series of reports that were prepared for the Waste Package Materials Performance Peer Review Panel to use as background and input to the peer review. Summaries drawn from the reports were also presented in Section 11 of the Panel's Final Report. The Panel used the reports as background and input for its review. Any views and comments expressed in the summaries and the full reports do not necessarily reflect the opinion and findings of the Panel. Further, opinions expressed in the reports are not necessarily those of the Panel or reflected in the Panel's reports and recommendations.

Pitting and crevice corrosion are terms that describe a set of complex processes that are influenced by many different parameters, including the environment, metal composition, potential, temperature, and surface condition. Important environmental parameters include aggressive ion concentration, pH, and inhibitor concentration. Other phenomenological aspects of localized corrosion include the stochastic nature of the processes and the stages of localized attack, including passive film breakdown, metastable attack, stable growth, and stifling. This section will discuss the phenomenology and controlling parameters in localized corrosion in general. It will be divided into discussions on pitting and crevice corrosion. Much of the phenomenology will be described in relation to pitting because the understanding usually was developed vis-à-vis pitting. However, the phenomenology is largely applicable to crevice corrosion as well; the term "crevice corrosion" can simply be substituted for "pitting" in much of the following discussion. This is important since crevice corrosion will likely be more of a concern than pitting corrosion for the WP. The crevice corrosion section will discuss aspects unique to that phenomenon. Much of this section is taken from recent review articles (1,2).

1.1 Pitting Corrosion

1.1.1 Environment/Development of Local Environment

Classical pitting corrosion (caused by passive film breakdown) will only occur in the presence of aggressive anionic species, and chloride ions are usually, although not always, the cause. The severity of pitting tends to vary with the logarithm of the bulk chloride concentration (3). The reason for the aggressiveness of chloride has been pondered for some time and a

number of notions have been put forth. Chloride is an anion of a strong acid, and many metal cations exhibit considerable solubility in chloride solutions (4). Chloride is a relatively small anion with a high diffusivity, it interferes with passivation, and it is ubiquitous as a contaminant.

The presence of oxidizing agents in a chloride-containing environment is extremely detrimental, and will further enhance localized corrosion. Oxidizing agents enhance the likelihood of pitting corrosion by increasing the local potential. The influence of potential will be described below.

Pitting is considered to be autocatalytic in nature; once a pit starts to grow, the local conditions are altered such that further pit growth is promoted. The anodic and cathodic electrochemical reactions that comprise corrosion separate spatially during pitting. The local pit environment becomes depleted in cathodic reactant (e.g. oxygen), which shifts most of the cathodic reaction to the boldly-exposed surface where this reactant is more plentiful. The pit environment becomes enriched in metal cations and an anionic species such as chloride, which electromigrates into the pit to maintain charge neutrality by balancing the charge associated with the cation concentration. The pH in the pit is lower owing to cation hydrolysis:

$$Me^{2+} + 2H_2O \Downarrow Me(OH)^{+} + H^{+} + H_2O \Downarrow Me(OH)_2 + 2H^{+} \qquad (1)$$

and the absence of a local cathodic reaction. The acidic chloride environment thus generated in pits is aggressive to most metals and tends to propagate the pit growth.

A detailed analysis of the influence of pit chemistry changes on pit growth and stability was provided by Galvele (4,5). The concentration of various ionic species at the bottom of a model 1-dimensional pit geometry was determined as a function of current density based on a material balance that considered generation of cations by dissolution, outward diffusion, and thermodynamic equilibrium of various reactions such as cation hydrolysis, Eqn. 1. Galvele found that a critical value of the factor x≠i, where x is pit depth and i is current density, corresponded to a critical pit acidification for sustained pit growth. This value can be used to determine the current density required to initiate or sustain pitting at a defect of a given size. The model of pit chemistry based on reaction, hydrolysis, diffusion, and migration is a proper approach to the problem. The focus of Galvele's work on pit acidification, however, may not be totally appropriate since, at least for stainless steel and other corrosion resistant alloys such as alloy 22, the local chloride concentration is probably more important than local pH in terms of stabilizing pit growth and preventing repassivation. On the other hand, other factors describing the severity of the local environment, such as chloride concentration, will roughly scale with acidity, so a critical value of x≠i may in fact accurately predict pit stability.

As the pit current density increases, the ionic concentration in the pit solution increases, often reaching supersaturation conditions. A solid salt film may form on the pit surface, at which point the ionic concentration would drop to the saturation value, which is the value in equilibrium with the salt layer. Under these conditions, the pit growth rate is limited by mass transport out of the pit. Salt films are not required for pit stability (though some have suggested that they are (6-11)), but they enhance stability by providing a buffer of ionic species that can

dissolve into the pit to reconcentrate the environment in the event of a catastrophic event, such as the sudden loss of a protective pit cover. Under mass-transport-limited growth, pits will be hemispherical with polished surfaces. In the absence of a salt film (at lower potentials), pits may be crystallographically etched, or irregularly shaped in some other fashion.

1.1.2 Potential

Electrochemical studies of pitting corrosion have found that characteristic potentials exist. Stable pits form at potentials noble to the pitting potential, E_P, and will grow at potentials noble to the repassivation potential, E_R, which is lower than E_P. During upward scanning in a cyclic polarization experiment such as is shown schematically in Figure 1, a stable pit starts growing at E_P where the current increases sharply from the passive current level and, upon reversal of the scan direction, repassivates at E_R where the current drops back. It is generally considered that materials exhibiting higher values of E_P and E_R are more resistant to pitting corrosion, and cyclic polarization experiments are commonly used for this purpose. A correlation has been found such that metals with low experimentally-determined pitting potentials have a higher tendency to form pits naturally at open circuit (3).

It should be noted that several other names and subscripts have been used to describe these characteristic potentials. For instance, it is common to use the term breakdown potential (E_b) because one is not always sure if the form of localized attack is pitting, crevice corrosion, intergranular corrosion, or transpassive dissolution. The pitting potential is sometimes referred to as the pit nucleation potential, E_{np}, and the repassivation potential is sometimes called the protection potential, E_{prot}. If creviced samples are used, the potentials might be referred to as crevice potential, E_{crev}, and crevice repassivation potential, $E_{r,crev}$.

Other values that have been considered to be a measure of the susceptibility to localized corrosion include the difference between E_P and E_R, which is related to the extent of hysteresis in a cyclic potentiodynamic polarization curve, and the difference between the corrosion potential and E_P or E_R, which is an indication of the margin of safety between open circuit conditions and breakdown (12-14). However, there is abundant experimental evidence suggesting that consideration of these simplistic interpretations of the characteristic potentials alone is insufficient for the development of a fundamental understanding of the mechanism of pitting corrosion. For instance, the potentiodynamically-determined pitting potential of most materials exhibits a wide experimental scatter, of the order of hundreds of mV. Furthermore, E_P is in many cases a function of experimental parameters such as potential scan rate. As will be described below, so-called metastable pits initiate and grow for a period at potentials well below the pitting potential (15), which provides evidence in contradiction to the definition of the pitting potential as being the potential above which pits initiate. The meaning of the repassivation potential has also been called into question. Wilde showed that E_R of ferritic stainless steel decreased (i.e. moved in the active direction) with increasing values of the current density at which the potential scan direction was reversed (13,16). So deeper pits apparently repassivated at lower potentials. In contrast, the repassivation potential for pits in Al seemed to be relatively independent of the extent of prior pit growth for a limited number of experiments (17). Researchers at Southwest Research Institute have found a similar lack of dependence of E_R on

prior growth for pits in stainless steel and other corrosion resistant alloys, but only after the passage of large charge densities (18).

Thompson and Syrett have suggested that the highest-observed repassivation potential is the critical potential in pitting (19). They indicated that this value is associated with repassivation of very small pits, and is close to the lowest-observed value of pitting potential. No means was suggested, however, for accurate and reproducible determination of this critical potential.

The difference between the corrosion potential and some critical potential is being used as a design criterion for the YMP waste package. This is discussed in more detail in the body of this report.

1.1.3 Alloy Composition

The alloy composition and microstructure can have strong effects on the tendency for an alloy to pit (20). Cr concentration plays the dominant role in conferring passivity to ferrous alloys. The pitting potential was correspondingly found to increase dramatically as the Cr content increased above the critical 13% value needed to create stainless steel (21). Increasing concentration of Ni, which stabilizes the austenitic phase, moderately improves the pitting resistance of Fe-Cr (21). Small increases in certain minor alloying elements, such as Mo and N in stainless steels, can greatly reduce pitting susceptibility (20). Mo is particularly effective, but only in the presence of Cr. Various explanations have been given for the large influence of Mo on stainless steel corrosion (22-27). The majority of researchers seem to favor the notion that Mo influences localized corrosion via some kind of dissolution and pit growth consideration. Small amounts of other elements, such as N and W, also have a strong influence on the pitting resistance of stainless steels (28-30).

Various measures have been developed to describe the beneficial effects of alloy composition on resistance to localized corrosion. The pitting resistance equivalent number (PRE) was originally developed as a pitting index for stainless steels (29):

$$\text{PRE} = \text{wt.\% Cr} + 3.3\ \text{wt.\% Mo} + 16\ \text{wt.\% N} \qquad (2)$$

The multiplier value for N could be as high as 30. PRE has been correlated to various other measures of corrosion resistance for stainless steels, such as the critical pitting temperature, which will be described in the next section.

The Cr-containing nickel-based alloys, including Alloy 22, are extremely resistant to corrosion, and have found wide use in the chemical process industry, among others, for handling corrosive environments that are too severe for more common alloys, such as stainless steels (31,32). Except for Fe, the alloying elements in Alloy 22 (21.5% Cr, 13.5% Mo, 3% W, 3% Fe) provide enhanced passivity and localized corrosion resistance. The relationship between PRE as described in equation 2 and the critical pitting or crevice temperature is not linear for highly corrosion resistant Ni-based alloys in different aggressive solutions, such as the ASTM G-48

solution (6% $FeCl_3$) (33). This might be expected since the PRE does not account for the beneficial effects of W. A modified version of PRE has been offered to take the W concentration into account (34):

$$PRE' = wt.\%\ Cr + 3.3\ wt.\%\ (Mo + W) + 30\ wt.\%\ N \qquad (3)$$

It has been argued that it is better to use atomic % for Mo and W in this expression owing to the high atomic weight of W (33), but even this measure does not perfectly correlate with the critical pitting or crevice temperature for Ni-based alloys.

Pits almost always initiate at some chemical or physical heterogeneity at the surface, such as inclusions, second phase particles, solute-segregated grain boundaries, flaws, mechanical damage, or dislocations (20). Most engineering alloys have many or all of such defects, and pits will tend to form at the most-susceptible sites first. Pits in stainless steels are often associated with MnS inclusions, which are found in most commercial steels. Alloy 22 is largely devoid of MnS inclusions.

1.1.4 Temperature

Temperature is also a critical factor in pitting corrosion since many materials will not pit at a temperature below a certain value, which may be extremely sharp and reproducible (35-41). This effect can be seen either by varying the temperature at a range of fixed applied potentials, or varying the potential for a range of constant temperature experiments. At low temperatures, extremely high breakdown potentials are observed, corresponding to transpassive dissolution, not localized corrosion. Just above the critical pitting temperature (CPT), pitting corrosion occurs at a potential that is far below the transpassive breakdown potential. This value of CPT is independent of environmental parameters and applied potential over a wide range, and is a measure of the resistance to stable pit propagation (35). At higher temperatures, the pitting potential decreases with increasing temperature and chloride concentration. Pit initiation considerations play a role in this region (35). The CPT can be used, like pitting potential, as a means for ranking susceptibility to pitting corrosion; the higher the CPT, the more resistant the alloy to pitting (35). If crevice corrosion is the primary concern, as is the case for the WP, creviced samples can be used to determine a critical crevice temperature (CCT), which is typically lower than the corresponding CPT.

Temperature will play a critical role in the behavior of the WP since the repository will likely be hot for many years and then slowly cool.

1.1.5 Surface Condition

The exact condition of a surface can have a large influence on the pitting behavior of a material. In general, samples prepared with a rough surface finish are more susceptible to pitting and exhibit a lower pitting potential. For example, the pitting potential of 302 SS with a 120 grit finish was shown to be about 150 mV lower than that for the same material with a 1200 grit finish over a range of chloride concentrations (42). The effect of surface roughness on pitting is

related to the stabilization criteria described below. Rougher surfaces have more-occluded sites, which can sustain the conditions required for active dissolution at lower current densities and thus lower potentials because of the longer diffusion path length and slower rate of diffusion.

For stainless steels, heat treatment, grinding and abrasive blasting have been reported to be detrimental to pitting resistance, whereas pickling in HNO_3 + HF scales or passivation in HNO_3 is beneficial (29). Heat treatments in air generate a chromium oxide scale and a Cr depleted region under the scale. The scale is typically removed mechanically, and the Cr depleted region by pickling (29). Other common surface defects include heat tint from welding, embedded Fe particles from machining, and MnS inclusions. The detrimental effects of these defects are minimized and the overall surface condition improved by passivation in nitric acid, which increases the Cr content of the surface oxide film.

The effects of surface condition on localized corrosion are significant enough that care must be taken to not apply experimental data collected on samples with special preparation to a real application without taking the surface condition into account. This will play a role in the behavior of waste package canisters since there is no plan to provide special surface finishes or treatments. The surface condition will be a consequence of all of the prior processing and handling, as well as a possible extended exposure to high temperature air when the drift is closed.

1.1.6 Inhibitors/Inhibition Potential

Pitting can be inhibited by the same approaches that are commonly used to reduce corrosion in general. All of the factors described above can be used to mitigate pitting corrosion: environment, alloy composition and structure, potential, and temperature. Various chemicals, when added to corrosive solutions, will inhibit pitting (20). Common inorganic inhibitors include sulfates, nitrates, chromates and molybdates. Some, such as sulfate, may act simply by providing supporting electrolyte that reduces the migration of Cl^- into the pit. It was suggested that nitrate may reduce inside pits in Al, consuming protons and thereby reducing pH (43). Others may adsorb at active sites, or reduce pit growth kinetics.

The effect of these oxyanions on pitting is of particular importance to the behavior of waste packages in a Yucca Mountain repository since the environment is predicted to be rich in such anions. The behavior of stainless steel, Fe and Ni in mixtures of chloride and other anions, such as NO_3^-, SO_4^{2-}, ClO_4^-, and OH^- has been studied (3,44-47). These materials exhibit what is known as an inhibition potential, E_I, if the ratio of chloride to inhibitor ion is in the right range. In such an environment, the material might be spontaneously passive or exhibit an active/passive transition as the potential is increased in a potentiodynamic or stepped potential experiment. At the pitting potential, pitting corrosion is initiated on the passive surface and the measured current increases. In a pure chloride solution, the current increases monotonically with increasing potential, perhaps reaching a limiting value from mass transport effects. In solutions containing sufficient inhibitor and at a sufficiently high potential (E_I), however, the high current associated with pitting rapidly decreases back to a low passive current, in a fashion similar to that seen for active/passive transitions. The difference is that the high currents emanate from pits localized on

the surface rather than from the entire actively dissolving surface. Once the pits repassivate, the surface remains passive with increasing potential until the transpassive region is reached, Figure 2 (3).

The pitting potential decreases with increasing chloride concentration according to:

$$E_P = a_1 - b_1 \log [Cl^-] \quad (4)$$

A similar equation holds for solutions containing both chloride and an oxyanion inhibitor, I:

$$E_P = a_2 - b_2 \log ([Cl^-]/[I]) \quad (5)$$

The inhibition potential increases according to:

$$E_I = a_3 + b_3 \log ([Cl^-]/[I]) \quad (6)$$

These relationships are shown in Figure 3 for Ni in solutions containing Cl^- and NO_3^- (45). The lines representing the last two equations cross at low values of $[Cl^-]/[NO_3^-]$. When the [Cl-]/[I] ratio is extremely low, E_I is lower than E_P and pitting is not observed. This might explain the behavior of Alloy 22 in the concentrated solutions thought to represent the repository environment relative to the behavior in concentrated pure chloride solutions.

1.17 Stochastics

Since pitting events are relatively rare and unpredictable, pit initiation may be considered to be random in nature. Stochastic approaches have been developed to handle this randomness and the large scatter typically observed in measurements of pitting potential and induction time (which is the time for a stable pit to form following a sudden increase in potential into the pitting range, or following the injection of chloride into a nonaggressive solution). Stochastic approaches used to address metastable pits will be discussed later in this paper. Shibata showed that a large ensemble of pitting potential values follows a normal distribution, suggesting random variation, (48). The probability for pitting was determined by:

$$P(E) = n/(1+N) \quad (7)$$

where N is the total number of samples studied, and n is the number of samples that had pitted at a potential of E or lower. The potential at P = 0.5 is a representative value for a given material and surface preparation. Induction times at a given potential were also measured, and the survival probability, P(t), was determined using Eqn. 7, except that n was the number of samples that had pitted by time t after application of the potential. The pit generation rate, ς, was shown to be given by:

$$\varsigma(t) = -d\{\ln P(t)\}/dt \quad (8)$$

Three pit generation rates were found at successive time periods, with the second period exhibiting the highest rate (48).

1.1.8 Stages of Pitting

Pitting can be considered to consist of various stages: passive film breakdown, metastable pitting, pit growth, and pit stifling or death. Any of these stages may be considered to be the most critical. For instance, once the passive film breaks down and a pit initiates, there is a possibility that a stable pit will grow. The full range of available spectroscopic and analytical techniques has been applied to the study of the structure and composition of passive films in a hope to predict and understand pit initiation. To those who prefer the surface science approach, for example, it is often assumed that alloying affects localized corrosion via changes in the composition and structure of the passive film. According to this view, pit growth is considered to be well understood and to offer little in the way of fundamental understanding of the phenomenon of pitting. On the other hand, others feel that pit growth is pivotal and often controls the pitting process, since pits will not initiate if they cannot grow at least for a short while. It is considered that the passive state is required for pitting to occur, but details of the passive film composition and structure play a minor role in the pitting process. This view is supported by the fact that many observations of pitting tendency can be fully accounted for by growth considerations. Furthermore, pit growth is critical in practical applications of failure prediction. Finally, the metastable pitting stage may be thought to be the most important since only pits that survive this stage become stable growing pits. Metastable pits exist on the edge of stability. Studies of metastable pits can therefore provide insight into fundamental aspects of pitting since both initiation and stability are key factors in metastable pitting.

1.1.8.1 Initiation/Passive Film Breakdown

The breakdown of the passive film and very initiation of the pitting process is probably the least-understood aspect of the pitting phenomenon. Breakdown is a rare occurrence that happens extremely rapidly on a very small scale, making direct observation extraordinarily difficult. The passive film is often drawn schematically as a simple inert layer covering the underlying metal and blocking access of the environment to the metal. The reality is of course much more complicated. Depending on alloy composition, environment, potential, and exposure history, this film can have a range of thickness, structure, composition, and protectiveness. Typical passive films are quite thin, and support an extremely high electric field (on the order of 10^6-10^7 V/cm). The passage of a finite passive current density is evidence of continual reaction of the metal to result in film thickening, dissolution into the environment, or some combination of the two. The view of the passive film as being a dynamic structure, rather than static, is critical to the proposed mechanisms of passive film breakdown and pit initiation.

Theories for passive film breakdown and pit initiation have been categorized into three main mechanisms that focus on passive film penetration, film breaking, or adsorption, (49,50). As with most such situations, different mechanisms or combinations of these mechanisms may be valid for different metal/environment systems. These mechanisms are described below in

terms of pure metal systems. However, pits in real alloys are most often associated with inclusions or second phase particles, and these factors must be taken into consideration.

Penetration mechanisms for pit initiation involve the transport of the aggressive anions through the passive film to the metal/oxide interface where accelerated dissolution is promoted (51). Anion migration would be assisted by the high electric field in the film.

A related model for passive film breakdown is an outgrowth of the point-defect model developed by Macdonald and coworkers to describe passive film growth by the movement of point defects under the influence of an electrostatic field (52). The point defect model has been used to explain pit initiation by assuming that aggressive ion (chloride) adsorption and incorporation at the outer surface of the barrier oxide layer results in the formation of cationic vacancies (53). These vacancies diffuse to the metal/oxide surface where they are annihilated by the oxidative injection of cations from the metal. However, if the flux of vacancies is larger than can be accommodated by oxidation, the vacancies will condense at the metal/film interface to form a void that is presumed to be the first step in the pitting process according to this model. This model is therefore a "vacancy penetration" rather than a "chloride penetration" model.

Adsorption theories of initiation were first based on the notion of competitive adsorption of chloride ions and oxygen (54). It is now known that the passive film is at least several monolayers thick rather than just an adsorbed oxygen layer. However, aspects of the adsorption model are still relevant. For instance, exposure of Fe to chloride and other halides caused thinning of the passive film based on XPS measurements, even under conditions where a pit had not formed (50). When thinning occurs locally because of some local adsorbed species, the local electric field strength will increase, which may eventually lead to complete breakdown and the formation of a pit (51).

Pit initiation by a film-breaking mechanism considers that the thin passive film is in a continual state of breakdown and repair (55,56). Mechanical stresses at weak sites or flaws resulting from electrostriction and surface tension effects may cause the local breakdown events, which rapidly heal in non-aggressive environments. In fact, the background passive current density may be derived from a summation of many such breakdown and repair events. In chloride-containing solutions, however, there would be a lower likelihood for such a breakdown to heal because of the inhibition of repassivation by chloride. The film-breaking model really involves initiation based on pit growth stability. It assumes that breakdown will always occur, albeit at a rate that depends on many factors related to the passive film properties. According to this model, common and frequent breakdown will only lead to pitting under conditions where pit growth is possible.

If, as stated by the film-breaking theory, passive film breakdown is frequent and rapid, and pit initiation depends on generation of the conditions needed for a pit to be able to grow, the question then arises as to how those conditions can exist at the instant of film breakdown. Galvele suggested that a critical factor, $x \not\propto i$ is required to achieve critical pit acidification for sustained pit growth (4,5), where x is pit depth and i is current density. From Galvele's model, a critical $x \not\propto i$ value of 10^{-4} A/m was determined for the case of Fe. Others have also developed

models with a similar factor or made experimental observations that critical values of x¢i exist for pit stability, and values of 0.3-0.6 A/m for stainless steel (15,57,58) and 0.2 A/m for Al (59) have been suggested. If a freshly-initiated pit at the instant of film breakdown has a depth on the order of the passive film thickness, 2-5 nm, then extraordinarily high current densities, about 10^8 A/m^2, are required for the breakdown to stabilize. (Note that stabilization of dissolution of such an incipient pit is no guarantee that the pit would grow past the metastable stage to become a stable growing pit.) Such arguments have led some to conclude that salt films form on the pit surface at very early stages of pit growth (7). Current densities as high as 10^7 A/m^2 have, in fact, been measured on Al even in a neutral chloride-free solution immediately (a few σs) after exposure of a small area by the thin-film breaking technique (60). It is possible that the particular sites that are susceptible to pit generation have some occluded aspect, such as by being at the bottom of a scratch, so that the effective pit depth is greater than the passive film thickness. The current density required for pit growth stability would be correspondingly lower at these sites. Furthermore, as the pit develops, the occlusion associated with the pit itself and its cover, which may be the under-mined passive film, will reduce the current density requirement. Regardless, very large current densities are necessary at the instant of film breakdown, and, at least for the case of stainless steel, a high local chloride concentration would be needed to achieve such a high current density. This problem was addressed in one theory of initiation that combines film-breaking with film penetration (6). It is proposed in this theory that chloride migrates to the metal/oxide interface and forms a metal chloride phase that cracks the overlying oxide as a result of its larger specific volume. The chloride phase would then provide a ready source of chloride ions to stabilize pit growth from the very outset of pit development.

1.1.8.2 Metastable Pitting

Metastable pits are pits that initiate and grow for a limited period before repassivating. Large pits can stop growing for a variety of reasons, but metastable pits are typically considered to be those of σm size at most with a lifetime on the order of seconds or less. Metastable pits can form at potentials far below the pitting potential (which is associated with the initiation of stable pits), and during the induction time before the onset of stable pitting at potentials above the pitting potential. These events are characterized by potential transients in the active direction at open circuit or under an applied anodic current, or anodic current transients under an applied anodic potential. Such transients have been reported in stainless steels (15,57,58,61-65) and Al (59,66) for many years. Individual metastable pit current transients can be analyzed for pit current density, and stochastic approaches can be applied to groups of metastable pits. It has been shown that when stable pits are small, they behave identically to metastable pits, and in fact are metastable. Stable pits survive the metastable stage and continue to grow, whereas metastable pits repassivate and stop growing for some reason.

Shibata showed that a large ensemble of pitting potential values follows a normal distribution, suggesting random variation (48). A formalism to explain the distributions observed for pitting potentials and induction times was presented. Williams and coworkers realized that the stochastic approach set out by Shibata could be extended to describe metastable pits, since large ensembles of metastable pits can be generated easily (58,67,68). Metastable pits are assumed to nucleate randomly in time and space at a frequency ς ($cm^{-2}s^{-1}$). Each pit has a

probability σ ($cm^{-2}s^{-1}$) of dying, unless it survives beyond a critical age ϑ_t (s) at which point it becomes stable. The nucleation frequency of stable pits Θ (s^{-1}) is then given by:

$$\Theta = a\,\varsigma\,\exp(-\sigma\vartheta_t) \qquad (9)$$

where a is the sample area. Underlying this approach is the notion that there is a non-zero chance of stable pit formation if metastable pits form. Pitting potential was determined potentiodynamically, and, in a fashion similar to Shibata (48), Williams determines Θ from the survival probability at a given potential, $P_s(E)$:

$$\Theta = -\tau\,d(\ln[P_s(E)])/dE \qquad (10)$$

where τ is the potential ramp rate, and $P_s = n/(1+N)$, where N is the total number of samples studied, and n is the number of samples that had pitted at a potential of E or lower. Equation 1 simply states that the probability of forming a stable pit is equal to the probability of forming a metastable pit times the probability that the metastable pit will survive to become a stable pit. Θ and ς have the same dependence on potential (although the rates are orders of magnitude different), indicating that Equation 1 is indeed valid (58). This is an important notion, as it suggests that the stochastically-defined susceptibility of a material to the formation of stable pits can be determined by studying the frequency of metastable pits, which are more abundant, and thus easier to observe in large numbers. Such an approach should be used with caution to compare the susceptibility of different materials however, since, as mentioned above, different sites might be activated at different potentials and the behavior at a given potential might not be indicative of the material properties.

Metastable pitting events at open circuit result in potential transients with a typical shape consisting of a rapid decrease followed by a slow increase (69). Isaacs explained that such pitting events draw cathodic current from the interfacial capacitance of the surrounding passive film (70). Upon repassivation, the capacitance is slowly recharged.

1.1.8.3 Stable Pitting/Pit Growth

Pits grow at a rate that depends on material composition, pit electrolyte concentration and pit-bottom potential. The mass-transport characteristics of the pit influence pit growth kinetics through the pit electrolyte concentration. Pit stability depends upon the maintenance of pit electrolyte composition and pit bottom potential that are at least severe enough to prevent repassivation of the dissolving metal surface at the pit bottom.

In order to understand pit growth and stability, it is essential to ascertain the rate-determining factors. Pit growth can be controlled by the same factors that can limit any electrochemical reaction: charge-transfer processes (activation), ohmic effects, mass-transport, or some combination of these factors. Pit growth at low potentials below the range of limiting pit current densities is controlled by a combination of ohmic, charge-transfer, and concentration overpotential factors. At high potentials, mass transport may be rate-controlling. Ultimately,

however, mass transport determines the stability of pits even at lower potentials because the local environment controls passivation.

For any growing pit or crevice where a portion of the cathodic reaction is located on the boldly-exposed surface (or at the counter electrode of a potentiostat), the pit bottom potential will be lower than the outside potential as a result of the ohmic potential drop associated with current flowing through the pit solution of finite resistance. For systems in which the metal exhibits active/passive behavior in the bulk environment, such as iron and nickel in sulfuric acid, the ohmic potential drop can stabilize localized corrosion in a sample held at a potential nominally in the passive region by depressing the local pit potential far enough that it resides in the active region (71). Under those conditions, the pit current density is large and stabilizes the attack by creating the requisite potential drop to keep the potential of the occluded area in the active region. This is only true for alloys that exhibit an active/passive transition in the pit environment. However, if there is no active/passive transition in the pit environment, the ohmic potential drop decreases the potential available at the pit surface to drive electrochemical reactions, and thus destabilizes the pitting reaction. In these systems, the changes in local pit environment (pH and chloride concentration) are key to pit stability. The IR drop theory of localized corrosion will be covered in more detail below in the section on crevice corrosion.

1.1.8.4 Death/Pit Stifling

Despite the autocatalytic nature of pitting, large pits, which would be considered to be stable by any criterion, can stop growing or die. The stifling of pit growth has not been studied in detail, but is clearly relevant to waste packages. As mentioned above, if the conditions (environment and potential) at the dissolving wall of a pit are not sufficiently aggressive, the pit will repassivate. The potential at the pit bottom is lower than that at the outer surface as a result of the ohmic potential drop associated with current flow out of the pit. As the pit deepens, the ohmic path length and ohmic resistance increase. This tends to cause an increase in the ohmic potential drop, a decrease in the local potential and a decrease in the pit current density. The environment tends to be acidic and rich in chloride owing to hydrolysis of the dissolved metal cations and electrolytic migration of chloride into the pit. The high concentration in the pit is depleted by transport out of the pit, but is replenished by continued dissolution at the pit bottom. As the pit deepens, the rate of transport out of the pit decreases, so the pit can be stable with a lower anodic current density replenishing the environment. As mentioned, the pit current density tends to decrease with time owing to an increase in the pit depth and ohmic potential drop. Repassivation might occur if a sudden event, such as loss of a pit cover, caused a sudden enhancement of transport and dilution of the pit environment to the extent that the rate of dissolution at the pit bottom would be insufficient to replenish the lost aggressive environment.

Pits are often under cathodic control, growing as fast as cathodic current consumes the generated electrons, so pits can also die if the available cathodic current decreases to the extent that the local anodic current density decreases below that required for stability. Even though the local anodic current density tends to decrease, the total anodic current for a given pit tends to increase owing to the increase in active pit area as the pit grows. If the available cathodic current is limited, for instance by a limited number of cathodic sites, then a given pit might repassivate

after a period of growth.

1.2 Crevice Corrosion

The growth of a pit generates a morphology that is essentially a crevice, so active pits and crevices are basically identical. Both are usually acidified and rich in chloride. The cathodic reaction is typically removed to a location on the boldly-exposed surface. As mentioned above, the phenomenological aspects of pitting apply equally to crevice corrosion. The difference between pitting and crevice corrosion is in the initiation phase. The occlusion associated with a crevice provides a ready barrier to transport, so initiation of crevice corrosion is easier. Alloys are usually resistant to pitting corrosion under conditions in which they are resistant to crevice corrosion, but the inverse is certainly not true. It is likely that the WP will be much more susceptible to crevice attack since Alloy 22 resists pitting, but crevices will exist between the WP and the supporting rails, beneath surface deposits and between the Alloy 22 outer can and 316L NG inner can.

Accelerated corrosion in a crevice can initiate at potentials well below the pitting potential, and after considerable periods of exposure with no prior evidence of crevice attack. It has long been accepted that crevice corrosion involves passive dissolution followed by oxygen depletion, acidification and chloride enrichment. However, whether these phenomena are causal, directly resulting in initiation of crevice corrosion, or are simply consequences of the active crevice corrosion process is still a matter of debate. Similarly, ohmic potential drops have been shown to stabilize crevice corrosion under certain circumstances, and will likely exist in all crevices and pits. The question of causality can equally be raised for ohmic potential drops. Other mechanisms for crevice initiation have also been suggested. This section will review some of the work that has tried to quantify and predict the crevice corrosion process. Proper comparison of quantitative theories to experiments should allow determination of the real crevice initiation mechanism.

1.2.1 Critical Crevice Solution

The view of crevice corrosion initiating by the formation of a solution of critical composition was put forth by Fontana and Greene (72). In this view, crevice corrosion is initiated as a result of passive dissolution within the crevice at a low rate over a long period of time. Owing to limited transport associated with the crevice occlusion, this passive dissolution slowly creates an altered local environment that is aggressive enough to depassivate the crevice. Oldfield and Sutton developed what is probably the first realistic quantitative model for crevice corrosion of stainless steels, and it is based on the critical crevice solution concept (73). They assumed that the first step in the initiation process was consumption of the crevice oxygen at a rate equal to the passive current density. Calculations show that the time for deaeration of the crevice is small compared to crevice initiation times, so differential aeration, while important, is not the direct cause of crevice corrosion. The second stage is acidification of the crevice resulting from Cr hydrolysis. The time for the pH to drop to a certain value was determined from the Cr concentration required (based on the equilibrium constants) and the rate of Cr^{3+} production, again from the passive current. Permanent breakdown of the passive film was

assumed to occur when the crevice pH fell below a critical value. This breakdown would then lead to rapid metal dissolution and signify the initiation of true crevice corrosion. Accurate determination of the critical pH for film breakdown is the crucial part of this model.

Oldfield and Sutton used experimental observations to validate the model and determine the critical crevice pH (74). The critical crevice pH was determined by potentiodynamic polarization curves in 4 M Cl^- solutions with a range of pH values. The critical pH was arbitrarily defined as the solution that produced an active peak current density of 10 □A/cm^2. It was suggested that values of passive crevice current density and critical crevice pH would be useful quantitative predictors of alloy susceptibility. There is some question, however, as to whether pH is the critical driving force for breakdown of stainless steels.

1.2.2 IR Drop Effects

As mentioned above in relation to pitting, an ohmic potential drop will be associated any growing crevice or pit as long as at least some portion of the cathodic reaction occurs outside of the pit, i.e. at the outer surface or at a counter electrode in a potentiostatically-controlled experiment. Pickering and coworkers have published several articles explaining how this IR drop can, under certain circumstances, stabilize the localized attack by driving the potential in the occluded region below the Flade potential into the active dissolution region of the polarization curve (71,75-77). Besides separation of anodic and cathodic reactions, which is usually the case for localized corrosion, this model depends on the presence of an active/passive transition in the polarization curve for the material in the crevice solution, which may be different than the bulk environment. The IR drop theory has successfully explained many of the features of crevice corrosion of nickel in chloride-free acidic solutions, and iron in chloride-free solutions of varying pH (71,75-77). In these systems, the metal exhibits an active/passive transition in the bulk solutions.

Despite the suggestions that the IR drop theory is equally valid for any localized corrosion situation, it has not been explored fully for corrosion resistant alloys such as alloy 22 in practical environments, such as neutral chloride solutions. These systems certainly generate crevice solutions that are significantly different than the bulk solutions in terms of pH, metal ion and chloride ion concentration. Furthermore, it is not clear that these alloys exhibit active/passive transitions in their crevice solutions. As a result, the relative importance of the changes in potential and environment within a crevice for a system such as Alloy 22 in a neutral bulk environment has yet to be determined.

1.2.3 Metastable Pitting Initiation of Crevice Corrosion

The exact cause of crevice corrosion initiation has been debated. The concentrations of H^+, metal ions, chloride ions, and sulfur-containing species, as well as IR drop down the crevice, have all been implicated as the critical parameter. In order to cause initiation, the critical factors obviously should exist at the time of the initiation event. However, the experimental evidence suggests that the chloride concentration, pH, and potential in stainless steel crevices do not change appreciably until after initiation (78-80). A small amount of sulfide has been observed to

accumulate in a 304 SS crevice during the initiation stage (81,82). However, crevice experiments on alloy 825, which contains very little S, were very similar to the results on 304 SS, so S is not required for initiation (78). In that work, pitting in the crevice was also ruled out because the externally-applied potential was below the pitting potential (78).

Stockert and Bohni have suggested a mechanism that eliminates the concerns of causality vs. consequence (83). In this model, it is assumed that crevice corrosion initiates as the result of a metastable pitting event in the crevice region. In essence, the initiation of crevice corrosion is envisaged to be identical to pitting corrosion. As described above, metastable pits will initiate and grow for a limited time at potentials well below the pitting potential. Metastable pits usually repassivate when a hole forms in the passive film pit cover. This hole allows the pit solution to mix with the bulk environment, which results in repassivation. If, however, the metastable pit forms in a crevice, then it is possible for it to more-readily stabilize. When the pit cover ruptures, the pit solution mixes into the crevice region, which is itself occluded. There is a higher probability for the solution at the pit wall to maintain a critical chemistry required to prevent repassivation. The stabilized pit would then be able to develop into generalized crevice attack. In fact, Oldfield and Sutton observed small pits in the early stages of crevice initiation (74).

In this scenario, the crevice region need not enrich in acid, chloride, or metal ion before the metastable pitting event, but would do so as the metastable pit grew into a stable crevice. Similarly, the ohmic potential drop would result from the metastable pit itself, assuming that the cathodic reaction occurred primarily outside of the crevice. Of course, if the crevice were enriched in acid or chloride as a result of passive dissolution in the crevice prior to initiation, the metastable pitting rate might increase, thereby increasing the likelihood for crevice corrosion to initiate. Furthermore, it is likely that the metastable pit sites are associated with sulfide inclusions, so sulfur may still play a critical role. However, the role would not be different than that in standard pitting corrosion.

1.3 References

1. G. S. Frankel, J. Electrochem. Soc., **145,** 2186 (1998).

2. G. S. Frankel, in Passivity of Metals and Semiconductors; Vol. Proceedings Volume 99-42, edited by B. Ives, J. L. Luo, and J. R. Rodda (The Electrochemical Society, Pennington, NY, 2001), p. 445.

3. H. P. Leckie and H. H. Uhlig, J. Electrochem. Soc., **113,** 1262 (1966).

4. J. R. Galvele, Corros. Sci., **21,** 551 (1981).

5. J. R. Galvele, J. Electrochem. Soc., **123,** 464 (1976).

6. G. T. Burstein and S. P. Mattin, in Critical Factors in Localized Corrosion II; Vol. PV 95-15, edited by P. M. Natishan, R. J. Kelly, G. S. Frankel, and R. C. Newman (ECS, Pennington, NJ, 1995), p. 1.

7. T. R. Beck and R. C. Alkire, J. Electrochem. Soc., **126,** 1662 (1979).

8. T. R. Beck, J. Electrochem. Soc., **129,** 2413 (1982).

9. R. C. Alkire and K. P. Wong, Corros. Sci., **28,** 411 (1988).

10. R. C. Alkire and M. Feldman, J. Electrochem. Soc., **135,** 1850 (1988).

11. K. P. Wong and R. C. Alkire, J. Electrochem. Soc., **137,** 3010 (1990).

12. Annual Book of ASTM Standards; Vol. G61-86 (ASTM, Philadelphia, PA, 1994), p. 238.

13. B. E. Wilde and E. Williams, Electrochim. Acta, **16,** 1971 (1971).

14. B. E. Wilde and E. Williams, J. Electrochem Soc., **117,** 775 (1970).

15. G. S. Frankel, L. Stockert, F. Hunkeler, and H. Boehni, Corrosion, **43,** 429 (1987).

16. B. E. Wilde, in Localized Corrosion; Vol. NACE-3, edited by R. W. Staehle, B. F. Brown, J. Kruger, and A. Agrawal (NACE, Houston, TX, 1974), p. 342.

17. M. Yasuda, F. Weinberg, and D. Tromans, J. Electrochem. Soc., **137,** 3708 (1990).

18. N. Sridhar and G. A. Cragnolino, Corrosion, **49,** 885 (1993).

19. N. G. Thompson and B. C. Syrett, Corrosion, **48,** 649 (1992).

20. Z. Szklarska-Smialowska, Pitting Corrosion of Metals, NACE, Houston, (1986).

21. J. Horvath and H. H. Uhlig, J. Electrochem. Soc., **115,** 791 (1968).

22. H. Ogawa, H. Omata, I. Itoh, and H. Okada, Corrosion, **1978,** 52 (1978).

23. K. Hashimoto, K. Asami, and K. Teramoto, Corros. Sci., **19,** 3 (1979).

24. M. Sakashita and N. Sato, Corros. Sci., **17,** 473 (1977).

25. M. Urquidi and D. D. Macdonald, J. Electrochem. Soc., **132,** 555 (1985).

26. R. C. Newman, Corros. Sci., **25,** 341 (1985).

27. P. Marcus, in Corrosion Mechanisms in Theory and Practice, edited by P. Marcus and J. Oudar (Marcel Dekker, New York, 1995), p. 239.

28. A. J. Sedriks, in Advances in Localized Corrosion; Vol. NACE-9, edited by H. Isaacs, U. Bertocci, J. Kruger, and S. Smialowska (NACE, Houston, 1990), p. 253.

29. A. J. Sedriks, Corrosion of Stainless Steels, Wiley-Interscience, New York, (1996).

30. R. C. N. a. T. Shahrabi, Corros. Sci., **27,** 827 (1987).

31. D. C. Agarwal, in Uhlig's Corrosion Handbook, 2 ed., edited by R. W. Revie (John Wiley and Sons, New York, 2000).

32. T. E. Evans, in Corrosion; Vol. 1, 3 ed., edited by L. L. Shreir, R. A. Jarman, and G. T. Burstein (Butterworth-Heinemann, Ltd., Oxford, UK, 1994), p. 4:116.

33. R. B. Rebak and P. Crook, in Critical Factors in Localized Corrosion III, A Symposium in Honor of the 70th Birthday of Jerome Kruger; Vol. PV 98-17, edited by R. G. Kelly, P. M. Natishan, G. S. Frankel, and R. C. Newman (The Electrochemical Society, Pennington, NJ, 1998), p. 289.

34. J. Charles, J.-P. Audouard, and M. Verneau,, 1998 (NACE International).

35. P. E. Arnvig and A. D. Bisgard, Corrosion 96, **Paper No. 437,** NACE (1996).

36. P. E. Arnvig and R. M. Davison, Proc. 12th International Corrosion Congress, Houston, TX; Paper No. 209**,** 1477 (1993).

37. R. J. Brigham and E. W. Tozer, Corrosion, **29,** 33 (1973).

38. R. J. Brigham and E. W. Tozer, Corrosion, **30,** 161 (1974).

39. R. Qvarfort, Corros. Sci., **28,** 135 (1988).

40. R. Qvarfort, Corros. Sci., **29,** 987 (1989).

41. N. J. Laycock, M. H. Moayed, and R. C. Newman, in Critical Factors in Localized Corrosion II; Vol. PV 95-15, edited by P. M. Natishan, R. J. Kelly, G. S. Frankel, and R. C. Newman (ECS, Pennington, NJ, 1995), p. 68.

42. N. J. Laycock and R. C. Newman, Corr. Sci., **39,** 1771 (1997).

43. S. B. deWexler and J. R. Galvele, J. Electrochem. Soc., **121,** 1271 (1974).

44. W. Schwenk, Corrosion, **20,** 129t (1964).

45. H.-H. Strehblow and B. Titze, Corr. Sci., **17,** 461 (1977).

46. R. C. Newman and M. A. A. Ajjawi, Corros. Sci., **26,** 1057 (1986).

47. K. J. Vetter and H.-H. Strehblow, Werkst. Korros., **74,** 449 (1970).

48. T. Shibata and T. Takeyama, Corrosion, **33,** 243 (1977).

49. H.-H. Strehblow, Werkst. Korros., **27,** 792 (1976).

50. H.-H. Strehblow, in Corrosion Mechanisms in Theory and Practice, edited by P. Marcus and J. Oudar (Marcel Dekker, New York, 1995), p. 201.

51. T. P. Hoar, Corros. Sci., **5,** 279 (1965).

52. C. Y. Chao, L. F. Lin, and D. D. Macdonald, J. Electrochem. Soc., **128,** 1187 (1981).

53. L. F. Lin, C. Y. Chao, and D. D. Macdonald, J. Electrochem. Soc., **128,** 1194 (1981).

54. H. H. Uhlig, J. Electrochem. Soc., **97,** 215C (1950).

55. N. Sato, Electrochim. Acta, **16,** 1683 (1971).

56. J. A. Richardson and G. C. Wood, Corros. Sci., **10,** 313 (1970).

57. P. C. Pistorius and G. T. Burstein, Phil. Trans. R. Soc. Lond. A, **341,** 531 (1992).

58. D. E. Williams, J. Stewart, and P. H. Balkwill, Corros. Sci., **36,** 1213 (1994).

59. S. T. Pride, J. R. Scully, and J. L. Hudson, J. Electrochem. Soc., **141,** 3028 (1994).

60. G. S. Frankel, C. V. Jahnes, V. Brusic, and A. J. Davenport, J. Electrochem. Soc., **142,** 2290 (1995).

61. N. Pessall and C. Liu, Electrochim. Acta, **16,** 1987 (1971).

62. Y. Hisamatsu, T. Yoshii, and Y. Matsumura, in Localized Corrosion; Vol. NACE-3, edited by R. W. Staehle, B. F. Brown, J. Kruger, and A. Agrawal (NACE, Houston, TX, 1974).

63. H. Ezuber and R. C. Newman, in Critical Factors in Localized Corrosion; Vol. PV 92-9, edited by G. S. Frankel and R. C. Newman (ECS, Pennington, NJ, 1992), p. 120.

64. P. C. Pistorius and G. T. Burstein, Corros. Sci., **33,** 1885 (1992).

65. P. C. Pistorius and G. T. Burstein, Corros. Sci., **36,** 525 (1994).

66. G. C. Wood, W. H. Sutton, J. A. Richardson, T. N. K. Riley, and A. G. Malherbe, in Localized Corrosion, edited by R. W. Staehle, B. F. Brown, J. Kruger, and A. Agrawal (NACE, Houston, TX, 1974), p. 526.

67. P. H. Balkwill, C. Westcott, and D. E. Williams, Mat. Sci. For., **44 & 45,** 299 (1989).

68. D. E. Williams, C. Westcott, and M. Fleischmann, J. Electrochem. Soc., **132,** 1796 (1985).

69. M. Hashimoto, S. Miyajima, and T. Murata, Corros. Sci., **33,** 885 (1992).

70. H. S. Isaacs, Corros. Sci., **34,** 525 (1993).

71. H. W. Pickering, Corros. Sci., **29,** 325 (1989).

72. M. G. Fontana and N. D. Greene, Corrosion Engineering, (McGraw-Hill, New York, (1978).

73. J. W. Oldfield and W. H. Sutton, Br. Corros. J., **13,** 13 (1978).

74. J. W. Oldfield and W. H. Sutton, Br. Corros. J., **13,** 104 (1978).

75. K. Cho, M. Abdulsalam, and H. W. Pickering, J. Electrochem. Soc., **145,** 1862 (1998).

76. Y. Xu and H. W. Pickering, J. Electrochem. Soc., **140,** 658 (1993).

77. M. Wang and H. W. Pickering, J. Electrochem. Soc., **142,** 2986 (1995).

78. N. Sridhar and D. S. Dunn, Corrosion, **50** (1994).

79. B. K. Nash and R. G. Kelly, Corros. Sci., **35,** 817 (1993).

80. S. E. Lott and R. C. Alkire, Corros. Sci., **28,** 479 (1988).

81. C. S. Brossia and R. G. Kelly, in Critical Factors in Localized Corrosion II; Vol. PV 95-15, edited by P. M. Natishan, R. J. Kelly, G. S. Frankel, and R. C. Newman (ECS, Pennington, NJ, 1995), p. 201.

82. C. S. Brossia and R. G. Kelly, Corrosion, **54,** 145 (1998).

83. L. Stockert and H. Bohni, Mater. Sci. Forum, **44/45,** 313 (1989).

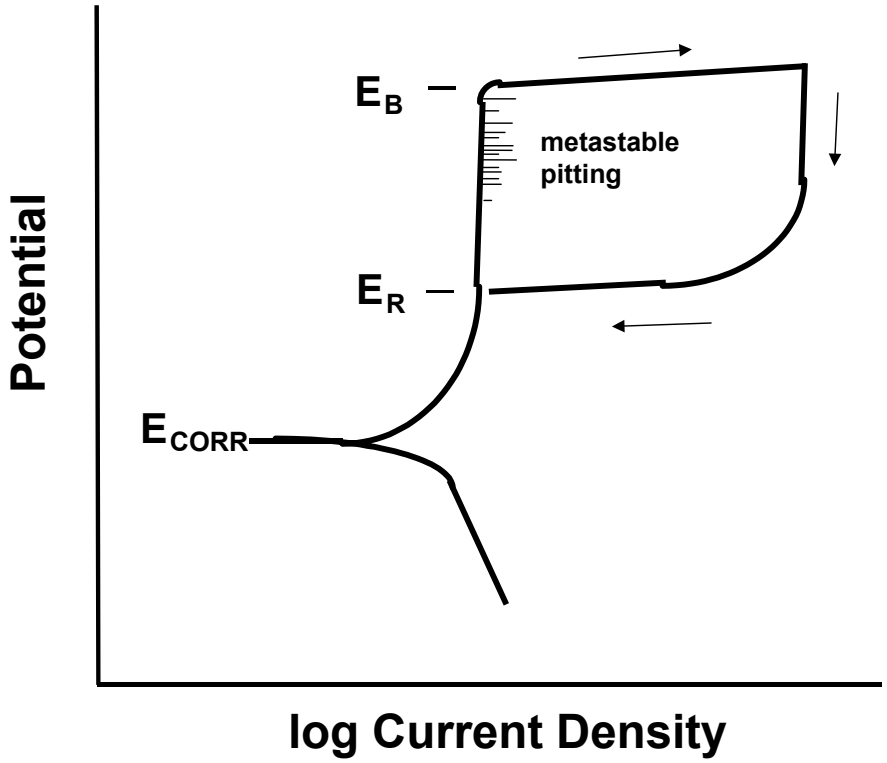

Figure 1 – Schematic polarization curve showing critical potentials and metastable pitting region (1).

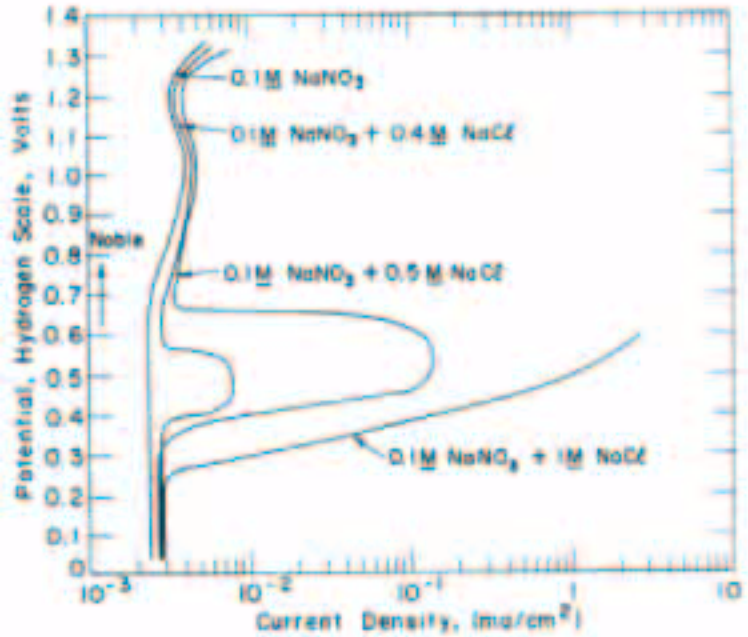

Figure 2 – Polarization curves for 17.7% Cr, 8.7% Ni stainless steel in nitrate/chloride solutions (3).

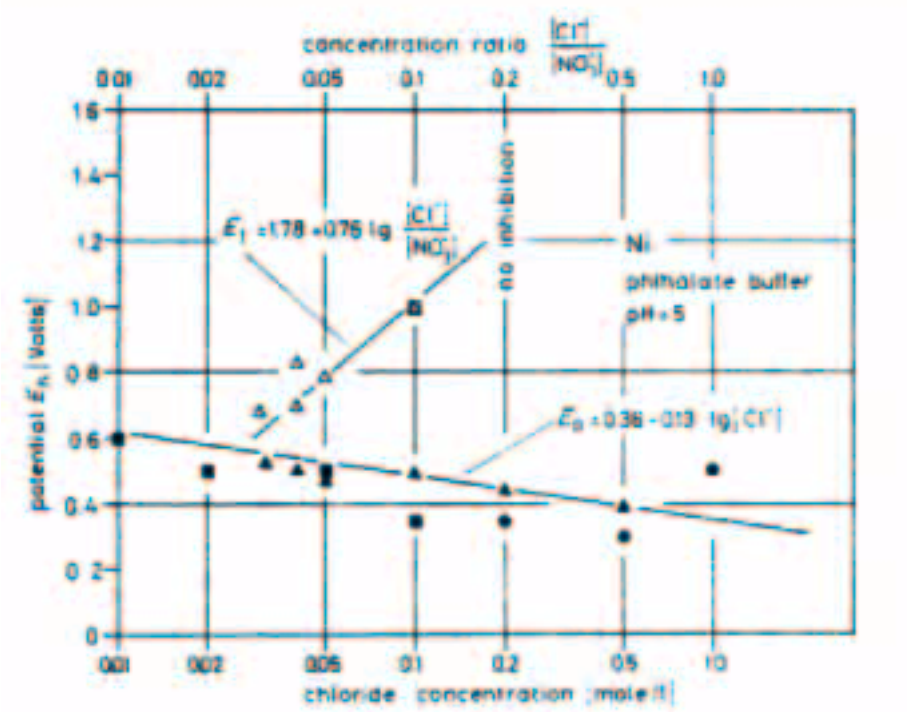

Figure 3 – Dependence of inhibition potential, E_I, on the chloride/nitrate concentration ratio and pitting potential, E_P, on the chloride concentration for nickel in pH 5 phthalate buffer. Open triangle - E_I and filled triangle - E_P for 1 M KNO_3. Open square - E_I and filled square - E_P for 0.1 M KNO_3. Filled circle - galvanostatic experiments in 1 M KNO_3. (45).

7. Water Composition within Yucca Mountain

Kathryn L. Nagy
University of Colorado
Boulder, Colorado, USA

EDITORIAL NOTE

This volume, "A Compilation of Special Topic Reports," contains a series of reports that were prepared for the Waste Package Materials Performance Peer Review Panel to use as background and input to the peer review. Summaries drawn from the reports were also presented in Section 11 of the Panel's Final Report. The Panel used the reports as background and input for its review. Any views and comments expressed in the summaries and the full reports do not necessarily reflect the opinion and findings of the Panel. Further, opinions expressed in the reports are not necessarily those of the Panel or reflected in the Panel's reports and recommendations.

Bounding Compositions of Seepage Waters

The corrosion resistance of the waste package metals will depend on the composition of the water that may come into contact with the waste package. Waters extracted from Yucca Mountain (YM) show variability in pH and elemental concentrations (Rosenberg et al., 2001), and also age (Sonnenthal and Bovardsson, 1999), all of which reflect different sources of water, flow pathways, and flow velocities. A key question, therefore, is to ask whether or not any limits can be placed on the range of water compositions expected to contact the WP. The most obvious approach to determining bounds on seepage water composition would be to analyze waters in and around Yucca Mountain (YM), including ground water, fracture water, and pore water in the unsaturated zone (UZ) and the same types of waters in the saturated zone (SZ), including perched water. Approximately 40 different water samples from within the mountain have been reported (see Rosenberg et al., 2001 for a summary in figure format); however, at least some of these analyses have been questioned because of charge imbalances and loss/gain of CO_2 on sampling which can result in changes in measured pH from in situ values. Also, the first water sampled was from a SZ well, J-13 (Harrar et al., 1990). J-13 well water has been used extensively in various experimental simulations (see Rosenberg et al., 2001), possibly in disproportion to the family of water compositions it represents at YM. J-13 well water is thought to represent perched water compositions (Rosenberg et al., 2001), which lie 100-200 m beneath the repository horizon (Fabryka-Martin et al., 2000). Only two water samples are from the pores of the welded tuff of the repository (Gdowski, 2000), highlighting the fact that these waters are the most difficult to extract. Ease of sampling is related to the degree of saturation of the pore water as well as the extractability of the water. Most water samples are from either perched water horizons in the unwelded tuff below the repository horizon or from pore waters in unwelded tuff above the repository horizon. Pore waters from above are those most likely to

Special Topic Report prepared for the Waste Package Materials Performance Peer Review. The Final Report of the Peer Review was submitted to U.S. Department of Energy and Bechtel SAIC Company, LLC on February 28, 2002.

move through fractures. It should be noted that contamination of sampled waters, particularly by sampling apparatus and the process of drilling, must be assessed particularly when considering reported trace element compositions (see below).

The major element composition of J-13 water is dominated by Na and bicarbonate/carbonate anions with a pH slightly above neutral (pH ~ 7.4). Some UZ pore waters from the Paintbrush unit of the Topopah Spring tuff above the repository horizon have higher Ca, Mg (although Mg < Ca), Cl, and SO_4, concentrations, and lower Na and bicarbonate/carbonate concentrations than the J-13 well and sampled perched waters. The UZ pore waters also have lower pH values around 5.6, suggesting equilibrium with atmospheric PCO_2. The fact that these pore waters have higher divalent cation, Cl, and SO_4 concentrations may indicate the effects of some evaporation nearer the surface. The higher concentrations also may be related to evaporation during the sampling procedure: it is difficult to extract small amounts of water from an unsaturated material. J-13 water has a lower ionic strength than the UZ waters due to its higher concentration of monovalent ions, excluding Cl^-, and possibly also the effects of evaporation of the UZ waters. Nitrate concentrations range from ~ 1 to ~ 20 mg/L in all YM waters. Dissolved silica (as $SiO_2(aq)$) is slightly higher in J-13 than in the UZ pore waters (~ 60 mg/L vs. ~ 40 mg/L). This concentration range represents approximately four to six times supersaturation with respect to quartz (Rimstidt, 1997), and also supersaturation with respect to opal-CT (Fabryka-Martin et al., 2000), which is found in YM fractures.

YM waters vary in composition within certain ranges (Rosenberg et al., 2001). Characteristics relevant to corrosivity of the waste package (excluding trace elements and silicon discussed separately below) are pH and Cl concentration. pHs of measured waters range from ~ 5.5 - 6 to ~ 9 (at deeper depths) and are controlled either by equilibrium with carbon dioxide gas at the lower end or with carbonate minerals, if present, at the higher end. In the absence of carbonate minerals, the higher pHs also may be related to exchange of protons for sodium in the tuff minerals (Fabryka-Martin et al., 2000) or equilibrium with silica phases, zeolites, and/or smectite clays and perhaps buffering by silicic acid. These pH values could evolve to values in the range of 11 – 13 upon evaporation on the WP surface (Rosenberg et al., 2001) due to attainment of equilibrium with respect to various hydrous salts. The exact pH depends on the starting ratios of cations and anions present. It would be impossible to achieve a pH < 5.5 purely by the kinds of mineral-water reactions expected at YM. Mechanisms of obtaining lower pHs include the production of organic acids by microbes, substrate dissolution and subsequent hydrolysis of dissolved metal cations, generation of acidic gases in the repository, or influx of acid rain. In the absence of any of these mechanisms, the lower limit of pH should be a pH in equilibrium with the local PCO_2. In an oxygenated unsaturated zone with little to no decaying organic matter, the PCO_2 should be close to atmospheric values, which at YM is ~ $1 \times 10^{-3.55}$ atm, yielding a pH slightly above ~ 5.6. To obtain a pH value above the upper observed limit of ~ 9, evaporation is required.

Anion concentrations (HCO_3/CO_3, Cl, and SO_4) will be controlled by reaction with PCO_2 or carbonate minerals, Cl-bearing salts, and SO_4-bearing salts. Upper limits will be determined by equilibrium with solid phases; lower values will vary according to the amount of solids available for reaction. To some extent compositions may be controlled by reaction kinetics with

solid phases, although reaction rates of salts and carbonates under ambient or near-ambient conditions are relatively fast.

UZ waters likely span a range of compositions of downward fluxing waters over the entire mountain. Vaniman et al. (2001) estimated an average major cation composition of percolating water (assuming the modern infiltration rate of 5 mm/yr) through one particular horizon in the UZ at YM for the last 10 Ma by examining the vertical distribution of zeolite compositions in zeolitized tuff. They determined an average composition of 8.2 mg/L Mg and 33.3 mg/L Ca, which falls within the range of reported water compositions (Rosenberg et al., 2001). Their work also indicated that movement of water had been only in the downward flow direction for this time period based on the occurrence of high Ca-Mg exchanged zeolites only in the upper sections of zeolitized horizons. The high Ca and Mg concentrations (relative to J-13 water) are considered to reflect a ground water that rapidly had reached equilibrium with carbonate dust (Vaniman et al., 2001) in the surface environment. Their analysis suggests that water in equilibrium with surface dust particles (or an actual recent ground water) could provide a reasonable approximation to the starting water composition that might encounter the WP. Their analysis also indicates that measured water compositions today bracket those that on average have percolated through YM for the last 10 Ma.

While the general composition of seepage waters at YM can be obtained within ranges of values, there is no specific composition that occurs uniformly throughout the UZ. In this sense, an approach that considers families of waters (in terms of cation and anion compositions), such as that used by Rosenberg et al. (2001) is appropriate. Because the primary concern is the effect on corrosion of such waters upon evaporation at the WP surface, exact initial starting compositions are not needed because these will change as evaporation proceeds. Instead, the ratios of corrosive elements are more important to determine.

An alternative approach to using actual water samples from YM is to place theoretical bounds on YM water composition taking into consideration equilibria and kinetics of relevant mineral/water reactions. For example, one bound would be provided by water in equilibrium with the proposed repository or overlying rock units under ambient conditions (including temperature and PCO_2). The closest approach to the composition of such water might be that of a measured pore water. Perched waters may approximate such water in some cases depending on recharge and discharge conditions in the perched water horizon. The initial source of any water is precipitation. Thus, a second bound on the composition of YM water might sensibly be a local relatively young ground water, which has equilibrated rapidly with dust and aerosols. A third end member, important for understanding changes in the repository after waste is emplaced, would be water in equilibrium with a suite of fracture minerals, which may have a different bulk composition from that of the tuff (e.g., Carlos et al., 1993). It is interesting to note that the reported pore water compositions from the Topopah Springs tuff are at the high end of the range of Ca plus Mg concentrations (Gdowski, 2000; Rosenberg et al., 2001), but fall within the range of pore water compositions in the Paintbrush tuff in terms of having higher Cl and SO_4 concentrations. High Cl and SO_4 has been considered to be a result of evaporation. However, high concentrations, especially in the welded tuff, may be related to volcanic gases (HCl and

H_2S) present at the time of formation of the tuff unit and either trapped in the volcanic ash via adsorption or as fluid inclusions.

Redox reactions in the bulk rocks are unlikely to be important as this is a highly oxidizing environment. Mn minerals in the fractures and tuff contain most Mn in the IV oxidation state. Fe in the minerals is also in the III oxidation state. Reducing environments could be artificially produced as a result of waste emplacement and subsequent reactions involving microbes or acidic gas generation.

Recommendations:

1. A statistical evaluation of the sampling strategy and actual samples analyzed thus far should be implemented. This might take into account distribution of rock type (welded vs. unwelded, mineralogy, etc.) in YM, distribution of sampled water in space and time, effects of sampling techniques on measured compositions, etc.

2. Water compositions should be categorized by ratios of elements that play a role in either the application of the chemical divide principle (Rosenberg et al., 2001) or directly in the corrosion process.

Effects of Fractures on Composition

Results and interpretations from many studies, both tracer and modeling (Flint et al., 2001), have indicated that water moves at the fastest rate through fractures at YM, despite the fact that many of these fractures are filled with secondary minerals (Carlos et al., 1993). Therefore, the likely scenario for dominant water movement away from and back towards the waste package during the heating and cooling cycles of the waste is through fractures. In this regard, chemical interaction of heated water and fracture material may result in new water compositions distinct from those based on current analyses, depending on the temperature of the contacting water, the rates of reaction of the fracture minerals with this water, and the time the water is in contact with the fracture minerals. Possible reactions with fracture minerals would include ion-exchange, surface sorption, dissolution, and precipitation. Secondary minerals in fault-related fractures include smectite clays, calcite, metastable silica phases, various Mn-oxides, and Fe-oxides (dominantly hematite) (Carlos et al., 1993). Fracture minerals may be an important source or sink of trace elements that can affect corrosion rates (see below). For example, Pb and U are known to be associated with the fracture-lining Mn-oxides at YM (Carlos et al., 1993). Mn-oxides, in addition to containing an important redox element (Mn), are known to take up other trace elements in their structures (Hudson-Edwards, 2000) such as Cr, Cd, Co, Ni, and Zn. Some Mn-oxides contain these trace elements in exchangeable positions and the apparent (i.e., non-thermodynamic) stabilities of the phases are sensitive to solution pH (Silvester et al., 1997; Lanson et al., 2000).

The silicate and carbonate minerals found in fractures were also observed to form upon evaporation of synthetic J-13 and UZ waters in contact with finely-ground Topopah Spring tuff

at 75°-85°C (Rosenberg et al., 2001), along with various salts. In particular amorphous silica and calcite were observed upon incomplete evaporation of synthetic J-13 water, and smectite clays upon evaporation of synthetic UZ water. This suggests that evaporation of simulated YM water may be related to the process of formation of the fracture minerals. Support for an evaporation process is provided by the reported locations of opal and calcite coatings on the lower surfaces of open-aperture fractures at YM (Fabryka-Martin et al., 2000). Conversely, fracture mineralogy that involves trace elements (Mn and Fe oxides) may be important to consider in evaporative simulation experiments.

Recommendation: Evaporation experiments should include trace elements at known or suspected natural concentrations in YM waters (see below). An approach to determining such element concentrations, in the absence of their measurement or if reported analyses are dubious, is to equilibrate a suite of minerals in masses proportional to their occurrence in fractures with water at various temperatures expected in LTOM and HTOM models of thermal evolution in the repository, and then use these solutions for subsequent evaporation experiments.

Trace Element Bounds and Analysis

In addition to chloride salts, certain trace elements can contribute to WP metal corrosion, such as mercury (Hg), lead (Pb), fluorine (F), and arsenic (As). Analysis of these elements in the YM environment should include both concentrations in sampled waters as well as concentrations in the rocks, and particularly in fracture minerals and dust particles that may settle on the WP. However, few analyses have been performed on the subsurface rocks and waters, and some of these are questionable due to either contamination (e.g., a source of dissolved Pb in the J-13 well may be from lubrication fluids) or due to inadequate analytical techniques (i.e., detection limits too high to measure actual concentrations). Some investigation of trace element concentrations in the bulk rock has been made (Castor et al., 1994; Perfect et al., 1995); however, the speciation (e.g., part of a stable mineral structure, exchangeable ion, surface-sorbed species, etc.) of these elements in the rock needs to be determined to assess how easily these elements might enter the aqueous phase.

In general, the trace elements listed above are associated with volcanic gases and ash, and may largely arise from these sources at Yucca Mountain. Hg concentrations in natural waters are typically between 0.01 to 10 ppb (Ehrlich, 1996), and a current source worldwide is from atmospheric pollutant deposition. Reported ground water concentrations at YM are below 100 ppb, the detection limit of the method used for the analyses (Perfect et al., 1995). Concentrations as low as 1×10^{-12} mol/L ($\sim 0.1 \times 10^{-9}$ g/L) can be measured using cold vapor atomic fluorescence spectroscopy, and clearly lower values within the range mentioned above are likely at YM. Dissolved Pb can be derived from the burning of fossil fuels, but more likely originates from the tuff itself. Pb is found in the fracture-lining Mn-oxide minerals, for example (Carlos et al., 1993). Pb concentration is not reported for J-13 well water (Harrar et al., 1990) and is in the 1-100 ppb range for YM waters (Perfect et al., 1995), with one evaporation pond at the Nevada Test Site containing ~ 1000 ppb Pb. The likely sources of F are the tuff and aerosols. Concentration is ~ 2 mg/L in J-13 well water (Harrar et al., 1990) and typically is not reported

for other YM water analyses. Arsenic is found in general in ground waters where its concentration can range from 1 to 10 ppb, with higher concentrations being typical in the arid western parts of the United States (Welch et al., 2000). Perfect et al. (1995) reported a concentration of ~ 1 ppb in YM ground water. Arsenic may also substitute for tetrahedrally-coordinated Si in silicate minerals, and might leach out in small amounts as these minerals dissolve at higher pHs. However, the most readily available form of As may be associated with Fe-oxide minerals in the fractures (Bowell, 1994; Welch et al., 2000).

These four trace elements could all come into contact with the WP, although to variable extents. Likely mechanisms include deposition of infiltrating water onto the WP, reaction of water with dust particles on the WP surface, and deposition of heated water from the overlying rock during the thermal evolution of the repository. It is not clear how soluble these trace elements might remain in evaporating fluid as solid phases precipitate on the WP. For example, the majority of the Pb could be precipitated as $PbCO_3$ or $PbSO_4$ solids. Arsenic or mercury, on the other hand, could remain as a relatively easily adsorbed and desorbed component of a wet mineral coating. Mercury will complex dominantly with chloride and hydroxyl ions in most well-oxygenated surface and near surface waters, with Hg-chloride complexes dominant at low pH, and $Hg(OH)_2^0$ dominant above pH ~ 6. In evaporating solutions, Hg may precipitate at the highest pHs as a mercury-oxide (HgO) if evaporation proceeds to near completion and chloride is reduced by precipitation of other phases (Martell and Smith, 1998).

Recommendations:

1. Attention should be given to measuring trace element concentrations relevant to corrosion processes in SZ and UZ waters using appropriate techniques (i.e., using techniques that can measure the lowest concentrations possible) and analytical procedures (i.e., avoidance of contamination). As many trace elements as possible should be included in such analyses for completeness.

2. Evaporation experiments on WP metals should include trace element concentrations typical of the YM waters (see section on fracture minerals above and silica and other mineral deposits below).

Likelihood of Formation of Silica Deposits on Waste Package

Passivation of the WP metal surfaces may occur if upon evaporation of drip water, thin layers of non-corrosive solids (e.g., silicates) are formed. Si concentrations of measured YM waters are above equilibrium with opal-CT the metastable silica phase in the fractures and tuff. Experiments (Rosenberg et al., 2001) have shown that precipitation of silica phases (amorphous silica and phyllosilicate clays in the smectite family) will occur upon evaporating synthetic J-13 and UZ pore water. The ratio of silicate to non-silicate mineral phases was not reported in this study. Calculations of the masses of each phase that formed upon evaporation would depend on the assumption of equilibrium, because necessary kinetic information is rare for silicate minerals. As a consequence, it is likely that incorrect proportions and an incorrect sequence of mineral

precipitation might be calculated. Thus, calculations may not simulate which mineral phase actually formed closest to the WP surface. While amorphous silica could form in a thin layer inaccessible to flowing fluids, excessive drying of such a layer could cause it to crack. Also, if phyllosilicate clays form, these will occur as small crystallites on the order of a few nanometers to micrometers in diameter. Clay layers can act as relatively impermeable membranes, but they will contain grain boundaries along which fluid can move. Clays flocculate at high pH indicating that they may settle on the WP surface as a randomly oriented aggregate of tiny crystals rather than a stacked layer of flat particles.

Recommendations:

1. Mineral precipitates formed in evaporation experiments on WP metals should be examined with high-resolution analytical techniques to determine their spatial distribution, and also to identify phases in amounts less than can be measured with powder X-ray diffraction techniques (Rosenberg et al., 2001).

2. Evaporation experiments should be conducted at rates expected for the range of LTOM and HTOM temperature gradients.

References

1. Bowell R. J., "Sorption of arsenic by iron oxides and oxyhydroxides in soils," Applied Geochemistry, **9**, 279-286, (1994).

2. Carlos B. A., Chipera S. J., Bish D. L., "Fracture-lining manganese oxide minerals in silicic tuff, Yucca Mountain, Nevada, USA. Chemical Geology," **197**, 47-69, (1993).

3. Castor S. B., Tingley J. V., and Bonham H. F., Jr., "Pyritic ash-flow tuff, Yucca Mountain, Nevada. Economic Geology," **89**, 401-407, (1994).

4. Ehrlich H. L., Geomicrobiology, Marcel Dekker, Inc., (1996).

5. Fabryka-Martin J., Meijer A., Marshall B., Neymark L., Paces J., Whelan J., and Yang A., "Analysis of geochemical data for the unsaturated zone," ANL-NBS-HS-000017, Rev. 00, Office of Civilian Radioactive Waste Management, (2000).

6. Flint A. L., Flint L. E., Bodvarsson G. S., Kwicklis E. M., and Fabryka-Martin J.,"Evolution of the conceptual model of unsaturated zone hydrology at Yucca Mountain, Nevada," Journal of Hydrology, **247**, 1-30, (2001).

7. Gdowski, G. E., "Environment on the surfaces of the drip shield and waste package outer barrier," ANL-EBS-MD-000001 Rev 00 ICN 01, Office of Civilian Radioactive Waste Management, (2000).

8. Harrar J., Carley J. F., Isherwood W. F., and Raber E., "Report of the Committee to Review the Use of J13 Well Water in Nevada Nuclear Waste Storage Investigations UCRL-ID-21867," Lawrence Livermore National Laboratory, Livermore, CA., (1990).

9. Hudson-Edwards K. A., "Heavy metal-bearing Mn oxides in river channel and floodplain sediments," in J. D. Cotter-Howells, L. S. Campbell, E. Valsami-Jones, and M. Batchelder, Eds., Environmental Mineralogy: Microbial Interactions, Anthropogenic Influences, Contaminated Land and Waste Management, **9**, Mineralogical Society, London, (2000).

10. Lanson B. Drits V. A., Silvester E. J., and Manceau A., "Structure of H-exchanged hexagonal birnessite and its mechanism of formation from Na-rich monoclinic buserite at low pH: New data from X-ray diffraction," American Mineralogist, **85**, 826-835, (2000).

11. Martell A. E. and Smith R. M., "Critically Selected Stability Constants of Metal Complexes Database Version 5.0," National Institute of Standards and Technology, (1998).

12. Perfect D. L., Faunt C. C., Steinkampf W. C., Turner A. K., "Hydrochemical data base for the Death Valley region, California and Nevada," USGS Open-File report 94-305, (1995).

13. Rimstidt J. D., "Quartz solubility at low temperatures," Geochimica et Cosmochimica Acta, **61**, 2553-2558, (1997).

14. Rosenberg N. D., Gdowski G. E., and Knauss K. G., "Evaporative chemical evolution of natural waters at Yucca Mountain, Nevada," Applied Geochemistry, **16**, 1231-1240, (2001).

15. Silvester E., Manceau, A., and Drits, V. A., "The structure of monoclinic Na-exchanged birnessite and hexagonal H-birnessite. Part 2. Results from chemical studies and EXAFS spectroscopy," American Mineralogist, **82**, 962-978, (1997).

16. Sonnenthal E. L. and Bodvarsson G. S., "Constraints on the hydrology of the unsaturated zone at Yucca Mountain, NV from three-dimensional models of chloride and strontium geochemistry," Journal of Contaminant Hydrology, **38**, 107-156, (1999).

17. Vaniman D. T., Chipera S. J., Bish D. L., Carey J. W., and Levy S. S., "Quantification of unsaturated-zone alteration and cation exchange in zeolitized tuffs at Yucca Mountain, Nevada, USA," Geochimica et Cosmochimica Acta, **65**, 3409-3433, (2001).

18. Welch A. H., Westjohn D. B., Helsel D. R., and Wanty R. B., "Arsenic in ground water of the United States: Occurrence and geochemistry," Ground Water, **38**, 589-604, (2000).

8. Localized Corrosion Chemistry and Radiolysis Effects

Alan Turnbull
National Physics Laboratory
Teddington, Middlesex, UK

EDITORIAL NOTE

This volume, "A Compilation of Special Topic Reports," contains a series of reports that were prepared for the Waste Package Materials Performance Peer Review Panel to use as background and input to the peer review. Summaries drawn from the reports were also presented in Section 11 of the Panel's Final Report. The Panel used the reports as background and input for its review. Any views and comments expressed in the summaries and the full reports do not necessarily reflect the opinion and findings of the Panel. Further, opinions expressed in the reports are not necessarily those of the Panel or reflected in the Panel's reports and recommendations.

Author's Cautionary Comment

This note will provide hopefully some useful insight and provoke discussion. However, my still limited knowledge of the details of the Yucca Mountain Project may be quite apparent. Please use what you think of value.

Optimum Conditions for Localised Corrosion

For the C22 alloy waste package material, localised corrosion will arise when the conditions are optimum for pitting or crevice attack. Crevice attack will almost always occur in less aggressive conditions than pitting corrosion because it is easier to form the local chemistry conditions conducive to passivity breakdown. The crevice geometry may be induced by physical deposition of particles or produced at the toe of a weld by inadequate welding. In principle, inspection techniques should ensure that the latter possibility is negligible.

The optimum environmental conditions for generating passivity breakdown will be high temperature, high oxidising conditions in a sufficiently conducting environment with a high ratio of chloride ions to other anions (to avoid competitive anion effects). The concept of a sufficiently conducting environment has to account not only for the solution conductivity but the thickness of the solution layer as the potential drop in a thin liquid layer may limit crevice propagation rates. In that context, the absence of a generally wetted surface would certainly limit propagation of crevice attack as the anodic and cathodic areas would not be well separated and the effective cathodic area would be small, although perhaps sufficient to initiate breakdown.

Special Topic Report prepared for the Waste Package Materials Performance Peer Review. The Final Report of the Peer Review was submitted to U.S. Department of Energy and Bechtel SAIC Company, LLC on February 28, 2002.

In crevice geometries, metal ion dissolution from the crevice wall/s associated with the passive current will tend to draw anions into the crevice building up a metal salt concentration which can be high, depending on crevice dimensions. For a significant crevice chemistry change when the passive current is very low, as for this alloy, the crevice geometry has to be very constrained. For a parallel-sided crevice, dimensionless analysis indicates that the key parameter is $l^2 i_p/h$ where l is the crevice length, i_p is the passive current density and h is the half width of the crevice (i.e. half the crevice gap). Increasing the temperature will increase the passive current density. However, long, tight crevices in the waste package, whether associated with a weld or deposits in a simple way, seem unlikely. Nevertheless, evaporation/boiling will assist in concentrating the solution when the geometrical conditions are less favourable and is likely to be critical in this system not least because in a porous salt media it may also increase the effective area of metal to volume solution ratio (the basis of the l^2/h term) and encourage the development of high metal salt concentrations with attendant acidity.

Formation of an insoluble carbonate scale is known from seawater studies to retard the cathodic reduction of oxygen. However, when the main reactant, hydrogen peroxide, can be produced within the pores at the metal surface this may not be limiting although it would depend on whether it altered the effective area of the cathode. Calcareous scales in seawater simply limit the oxygen diffusion rate without much change in the effective area.

The pH in a crevice of a corrosion resistant alloy such as C22 will fall due to hydrolysis of chromium and molybdenum cations coupled with ionic strength effects due to a high salt concentration. Although the solubility of metal ions decreases with increasing temperature, this is not so limiting when the pH is low for the temperature range of interest, the major factor being geometric parameters. In many systems, a thinning liquid layer resulting from a wetting and drying cycle may induce more oxidising conditions when the reduction of the cathodic reactant is transport limited. This is unlikely for this system in that specific context because the potential is expected to be high. However, it may influence the radiolytic products as indicated below.

From the viewpoint of localised corrosion it would be relevant to pose the question as to the envelope of conditions within which this alloy can be made susceptible to localised corrosion and to assess the likelihood of overlap with the envelope of environmental conditions associated with the waste package over some period of the relevant life of 10,000 years plus.

Source of Surface Water on Waste Package

There are two potential sources of water to the waste packages: condensation from the atmosphere associated with dust particles containing deliquescent salts with a sufficiently low critical relative humidity (i.e. the RH value at which condensation will occur) and direct dripping onto the waste packages if no drip shield is present (or if the drip shield fails). Dripping will originate from perch or pore water resulting ultimately from interconnectivity to the surface exposed to occasional precipitation As such the latter is intrinsically intermittent and of low probability but with a 10,000 year prediction in relation to climate stability there is uncertainty.

In relation to atmospheric corrosion, the temperature-RH relationship is shown in Figure 1. The highest temperature at which wetting will occur will be associated with a deposit containing a salt with the lowest CRH. Frankenthal[1] argues that *fine* particles, which contain a larger fraction of water-soluble ionic compounds with low CRH values compared with large particles, will not deposit at elevated temperature much above ambient because of thermophoretic effects, where small differences in temperature across the particles may be sufficient to give momentum to the particles away from the waste package. *Large* particles will deposit and can form physical crevices but the conditions of temperature and pH at which wetting occurs just locally in this situation needs to be established. In addition, for the reason articulated above, crevice and pitting corrosion will proceed only to a significant extent when there is a wetted surface external to the cavity. Hence, the conditions required are those for which essentially a spatially continuous liquid layer is formed. It is not obvious that we have the data to predict this. However, one possible limitation of Frankenthal's analysis is the neglect of ionising radiation on the small dust particles. Thermophoretic effects may be counterbalanced by the impact of charge on the particle induced by the radiation and subsequent attraction to the metal surface. Certainly, this factor needs consideration before dismissing the idea of fine particle deposition at elevated temperature.

Any direct dripping onto the hot surface will obviously outweigh dust considerations because the evaporation process will concentrate salts, form scale deposits and may create conditions conducive to sustained wetting at quite elevated temperature with the upper limit determined by the composition of the evaporated solution. Whilst wetting itself will have little impact on heat transfer, a wetting and drying cycle leading to developed carbonate/silicate scales would impede heat transfer.

Factors Affecting the Water Chemistry

It is imperative in our thinking that the evolution of the water chemistry over the long timescales involved is perceived to be determined by the interaction of a number of processes defined by the details of the system; i.e. thin liquid layer with deposits of some kind that may be porous and themselves contributing to the chemistry, elevated temperatures (affected possibly by the build up of deposits); radiolysis with the distribution of products of the latter being temperature and chemistry sensitive; corrosion reaction byproducts (e.g. elevated pH in cathodic regions); interaction with CO_2 of the atmosphere.

Such a statement is necessary to balance the tendency to transfer information to the waste package system from bulk solution experiments often in poorly related chemistry and temperature conditions. The challenge is to establish the best conceptual physical picture we have of the likely chemistry and to model and/or design experiments to validate our ideas and to consolidate the details.

Radiolysis

General

The range of radiolytic processes and the subsequent supplementary reactions that may occur in aqueous solutions is reasonably well established, with numerous publications[2-6]. For example, Airey points out that the rate of energy absorption in the electrochemical reaction layer can amount to twice that in the bulk solution when the radiation source is external to the electrode (i.e. the dose rate is effectively higher). Since this is likely to provide conservative conclusions, neglect of this is not critical.

The radiolysis of pure water due to gamma radiation generates primary products of H, OH, HO_2, $e^-(aq)$, H^+, H_2, H_2O_2 and secondary products of O_2, O_2^-, and additional H_2O_2. The yield of primary species from radiolysis of pure water is nearly independent of pH in the range 4 to 10 (Ref. 18 quoted in Ref. 5). Species such as $e^-(aq)$, H, H_2 are reducing agents (i.e. can be oxidised, thereby lowering the corrosion potential) and OH, HO_2, H_2O_2, O_2, and O_2^- act as oxidising agents (ie. can be reduced, thereby increasing the potential). In a single phase, pure water, closed system the net effect is neutral (with H_2, H_2O_2 being by far the dominant species, of near equal concentrations) but in an open system exposed to air, a net oxidising condition of the bulk solution is suggested by Marsh et al[6] as it is perceived that H_2 is readily lost to the atmosphere whilst other reducing species H and $e^-(aq)$ react with oxygen (see below). The ready loss of H_2 is to an extent inferred by the significant enobling of the corrosion potential of stainless steel when using an Ar gas cover.

In a practical system it will be the balance of kinetics and transport that determine the local conditions at the metal surface, and the net effect in terms of oxidising characteristics has to be determined. Also, whilst the solution would be nominally neutral it remains to be established whether the efficiency of oxidation and reduction per mole of oxidising or reducing species is equally efficient on the C22 metal surface.

This is particularly true in the presence of chloride ions because they act as a scavenger for radicals, the net effect being to increase the yield of molecular products by limiting the attack of these by radicals.

$$Cl^- + OH \Downarrow Cl + OH^- \quad (1)$$

$$e^-(aq) + Cl \Downarrow Cl^- \quad (2)$$

$$H + Cl \Downarrow Cl^- + H^+ \quad (3)$$

$$H_2O_2 + Cl \Downarrow Cl^- + H^+ + HO_2 \quad (4)$$

$$HO_2 + HO_2 \Downarrow H_2O_2 + O_2 \quad (5)$$

The regeneration of the chloride ion means that there is no net consumption.

Dissolved oxygen from exposure to air can act also as a scavenger for $e^-(aq)$ and H through the reactions

$$e^-(aq) + O_2 \Downarrow O_2^- \quad (6)$$

$$H + O_2 \Downarrow HO_2 \quad (7)$$

If the pH is much greater than about 4.9, Glass et al[5] suggest that the HO_2 ionises to produce more O_2^-.

In the absence of oxygen, these radicals would recombine with H_2O_2 limiting the amount of H_2O_2:

$$H_2O_2 + e^-(aq) \Downarrow OH^- + OH \quad (8)$$

$$H + H_2O_2 \Downarrow OH \quad (9)$$

The overall effect of oxygen is then to increase the yield of H_2O_2.

The quasi-steady products developed are going to be an important function of chloride concentration, the ready access of oxygen, the temperature, dose rate and the rate of consumption by reaction at the metal surface. In aerated solutions exposed to 2 Mrad h^{-1}, computations[7] suggest that chloride concentration has little effect on hydrogen peroxide generation below 350 ppm but between 3500 ppm and 35000 ppm the concentration of both oxygen and hydrogen peroxide increase by a factor of 5-10, with the oxygen concentration about a factor of two higher than the peroxide concentration.

An additional radiolytic process reported is that of irradiation of N_2 in the atmosphere to form nitric acid when subsequently dissolved in solution. Although, a method of calculating the concentration of nitric acid has been proposed (see ref. 5) it is limited to a sealed air-water system and should not be generalised since inevitably it will depend on the exposure details.

Thin liquid layers on surface

Here we consider a situation of a thin liquid layer (typically about 200 σm) with no significant scaling deposits, except that associated with residues of dust particles. The situation of a porous layer or a crevice is discussed below. The likely chemistry associated with absorption of water and dissolution of salts in dust particles has been described by Frankenthal but will include sulphate, acid sulphate, nitrate anions and ammonium and sodium cations with some carbonaceous residue. The likelihood of forming salt concentrations associated with absorption of water and then evaporation effects at elevated temperatures depends on resolution of the competing influence of thermophoretic effects and ionising radiation in attracting particles to the surface.

In view of the proximity of the gas-solution interface, gradients in H_2 should be minimal, the H_2 being lost readily to the atmosphere unless the dose rate is very high relative to exchange with the atmosphere. This remains to be determined but approximate calculations should be straightforward. An impact of radiolytically produced H_2 on the corrosion potential would then seem improbable and from a conservative perspective should be discounted. Hence, the water chemistry should be that associated with a highly oxidising condition. It is not evident in the reactions involving oxygen consumption (6 and 7) whether these would become supply limited (probably very unlikely) but for a thin liquid layer it should not be an issue.

The extent of production of nitric acid and the likely concentration developed in a thin liquid layer is simply unknown.

Porous Deposit

The underlying physical picture is of a surface exposed to a drying environment leading to evaporation and the development of an insoluble scaled surface with the water-filled pores rich in salts. The thickness of the porous layer is difficult to predict, as it will depend on the extent of dripping of water onto the surface and the temperature and time domains in which this might occur. The distinctive feature is that oxygen replenishment of the solution at the pore base will be constrained as oxygen may be consumed by reaction with radiolysis products as it progresses along the pore. This again requires quantitative modelling, accounting for the salt concentration also, but the net effect might be expected to be essentially towards a more benign situation compared to the thin liquid layer scenario described above as the concentration of reducing species at the metal-solution interface could be higher because of the reduced oxygen level. However, it may be prudent to ignore any beneficial effect.

The chemistry of the groundwater that will drip onto the surface can reasonably be characterised (e.g. Glass et al[5]). However, if we adopt the dripping scenario, there may be a washing away of products from radiolysis in the initial stages before a scale is formed and prediction of the chemistry would be difficult. It is in the later stages when a scale is formed and water filled pores are present that are not so readily washed out that may prove to be most important. The pH of the groundwater when concentrated can be predicted. The pH developed at the base of a pore in a scale and the efficiency of the possible buffering processes when there are various reaction processes including electrochemical and radiolytical is harder to predict without detailed modelling.

Crevice Solution

The situation in a crevice as far as radiolysis should have parallels with deposit pore chemistry to an extent since oxygen depletion in the crevice solution will occur readily. If coupling to the external surface were put aside, the chemistry would be essentially neutral from the viewpoint of radiolytic factors being typical of an oxygen-free situation. When considering coupling to the external surface the latter should be perceived as a spatially continuous or semi-continuous wetted surface. If a porous scale deposit were present then the driving force may be less than for a thin liquid layer for the reason indicated. The interesting question is to consider

the worst case which is that of a thin but very conducting liquid layer with highly oxidising conditions – what is the influence of internal radiolytic processes on the chemistry and potential in the crevice and does it mitigate or increase the severity of the conditions. Again, the high chloride will play an important role but there is evidence to suggest that in oxygen-free situations there is no impact on the relative concentrations of oxidising and reducing species.

Experimental evidence from crevice studies in stainless steels[8] imply that the main impact of radiolysis is on the external potential with little evidence of mitigating internal cavity chemistry. Nevertheless, it is instructive to consider the impact of oxidising and reducing environments in the crevice separately. The impact on crevice chemistry of introducing a more efficient cathodic process inside a crevice was considered by Turnbull[9]. Prior to passivity breakdown, the net effect is to minimise the potential drop in the crevice but to elevate the pH, which is to be expected conceptually. Of course the potential is high so that the kinetics of reduction are constrained to some extent. Nevertheless, on the basis of a critical solution composition for passivity breakdown based on achieving a sufficient acid pH, the implication is that crevice attack would be prevented. When reducing species (H_2, H or e^-(aq)) are generated directly in the crevice and the oxidation conditions are favourable, the crevice pH will tend to become more acidic but the potential drop in the crevice will be greater, as the net anodic current to be supported by cathodic reactions on the external surface is now greater. This would mean an increase in potential drop in the crevice solution and outside the crevice. Nevertheless, the low pH may be enough to render the passive film unstable.

When both oxidising and reducing species are considered together in the crevice (because of high chloride the quantities will be high also), the net effect will depend on the efficiency of the electrochemical reactions and the impact of coupling to the external surface. Prediction requires specific electrochemical data relevant to the substrate. However, since the potential associated with the external surface exposed to aerated solution should be higher with little H_2 around, there should be a net oxidation of reducing species in the crevice leading to enhanced acidification.

Impact of Water Chemistry And Radiolysis on the Bulk Corrosion Potential

Since the water chemistry of relevance is a complex function of radiolysis, temperature and exposure history simple statements are usually not possible but it is legitimate to ascertain what species/reactions are most important in determining the potential, at what concentrations do these become significant relative to behaviour in unirradiated solutions and what set of conditions will yield the highest potential at a specific temperature. For C22 alloy, the corrosion potential will most likely be determined by a redox potential as the passive current is expected to be very small.

Most studies have been conducted using 304L SS or 316L SS and involved tests with radiation sources (although external to the working electrode) or with a solution chemistry modified by addition of H_2O_2. Although various studies on Pt have been carried out, this ignores

the importance of the substrate characteristics in determining the electrochemical kinetics and will not be referred to.

Glass et al[5] consider the important cathodic reactions on austenitic stainless steel to be described by

$$OH_{ads} + e- \div OH- \quad (10)$$

$$O_2 + 2H_2O + 4e^- \ \& \ 4\ OH^- \quad (11)$$

$$O_2^- + H_2O + e^- \ \& \ HO_2^- + OH^- \quad (12)$$
(small contribution)

$$HO_2^- + H_2O + e^- \ \& \ 3OH^- \quad (13)$$
(very small contribution)

They suggest various metal dissolution reactions (of Fe, Cr and Ni) as providing the anodic reactions but a redox process may be more likely to control the corrosion potential on a more corrosion resistant alloy of very low passive current density. An example would be oxidation of hydroxyl ions, the reverse of reaction (10), but also carried to completion, or oxidation of chloride ions which is more feasible in restricted geometries :

$$4\ OH^- \ \& \ O_2 + 2H_2O + 4e^-$$

$$2Cl^- \ \& \ Cl_2$$

The absence of H_2O_2 from the above scheme (equations 10-13) is not to suggest it is unimportant; rather it is involved in the initial formation of adsorbed OH atoms either by a dissociation process or by reduction.

The corrosion potentials attained in irradiation tests do not respond markedly to increase in dose rate (albeit at relative low dose rates overall) as shown in Table 1. In practice this lack of dependence on dose rate is known to extend up to 10000 Gy h^{-1}.

Herbert et al argue that this follows from the lack of dependence of corrosion potential on H_2O_2 concentration once the level exceeds about 0.5 ppm (1.5×10^{-5} M), Figure 2, and considered to be associated with the requirement to achieve a surface coverage of adsorbed OH. Increasing the peroxide concentration beyond that has then little impact. In the latter figure, the data relate to tests on 304L SS in aerated solutions containing 100 ppm Cl^- at ambient temperature.

TABLE 1
Effect of ν Radiation on the Corrosion Potential of Stainless Steel
(Work by Marsh reported by Herbert et al[8])

Dose rate / Gy h^{-1}	Potential / mV SCE
0	-150 to 80
10	250 to 300
200	250 to 300
1000-2000	260 to 380

Note: 1 Gy = 100 rad

Note inserted by Panel: *To put this into perspective, the following are the expected gamma radiation levels in the repository. The waste package and surrounding environment will be subjected to a flux of neutrons and gamma rays from the stored radioactive waste. The peak gamma flux is about 1000 rad/hr at the time of emplacement of waste packages. This gamma flux decreases by a factor of 100 to 10 rad/hr after about 200 years and another factor of 100 to 0.01 rad/hr after about 400 years. Based on data above, the radiolysis effect has not been sufficiently studied or analysed at the lower gamma fluxes that will exist after the initial emplacement. Radiolysis effects on the environment will only occur when surfaces are wet.*

Marsh et al[6] suggest that the irradiation induced rise in corrosion potential is not determined by H_2O_2 but by other oxidising species such as O_2^- and OH radicals. However, the tests were conducted in an oxygen-free atmosphere. They indicate that in an air atmosphere higher levels of H_2O_2 are obtained, typically 5-7 ppm compared with 0.01-1.1 ppm with an Ar cover gas, although the corrosion potentials were not much different (about 320 mV SCE). These tests were conducted for a 304L SS with a ν-radiation dose rate of $2x10^3$ Sv h^{-1} (0.2 Mrem h^{-1}) in 300 ppm Cl^- at 40∀C. The authors noted that there was some inhibition of initiation of localised corrosion when the breakdown potential was below about 500 mV SCE but not at potentials above 600 mV SCE. The authors postulate that certain radiolytic species adsorb on the metal surface and influence the passive film. They discount an enhanced cathodic process causing a high pH at the metal surface. They did not consider the possibility of radiolysis affecting local chemistry changes in metastable pits.

Irrespective, Herbert et al[9] were able to demonstrate enhanced crevice propagation rates in 304L SS by ν-irradiation, as measured by ZRA, by switching the source on and off. They emphasise that whilst initiation would not be perceived to be too sensitive to the concentration of oxidising species, the propagation rate would be.

In the work of Glass et al[5] a ν-radiation dose rate of 3 Mrads h^{-1} ($3x10^4$ Gy h^{-1}) resulted in a shift in corrosion potential of 316L SS from about –105 mV SCE to about 116 mV SCE in 600 ppm Cl^- at 30∀C with no effect on the breakdown potential. The value of 600 ppm Cl^- represents a 100-fold concentration of J-13 well water.

In both this work and that of Marsh et al[6], there is indication of a change in the passive film characteristics such that when the oxidising source was removed the corrosion potential did not recover to the initial un-irradiated value.

Impact of Scale Formation on Surface Temperature

An important issue is the extent to which the surface temperature of the waste packaging can rise due to formation of a surface film which at one level is just a thin liquid layer but when dripping occurs for a period of time may be a relatively thick scale. This is simply the solution of a heat transfer problem in which definition of the heat transfer coefficient (U) between the fluid and the heat transfer surface is required. This is usually written as

$$\frac{1}{U} = R_f + \frac{1}{h}$$

where R_f is the thermal resistance of the deposit and h is the coefficient of heat transfer between the deposit at its interface and the fluid, usually taken to be that of the metal in the absence of deposit. R_f is often written as $(m_d/\psi)/k_f$ where k_f is the thermal conductivity of the deposit, m_d is mass per unit area and ψ is the density.

Solution to the heat transfer problem in the absence of a deposit but with a thin liquid layer[10] suggests that the presence of a layer up to 500 σm thick (at which thickness water will probably stream) has little impact on the heat transfer coefficient. However, no calculations were made assuming a deposit.

Conclusions

The products of the radiolysis process are sensitive to temperature, oxygen and chloride concentration and dose rate. An assessment of the impact of these variables on the corrosion potential of C22 alloy when exposed to ν-irradiation is required.

Such data that exist for stainless steels tend to be limited to near ambient temperature conditions but there is a clear enobling of the corrosion potential although the extent varies between 304L SS and 316L albeit based on results from different experimenters and conditions. For these alloys there appears little impact on the pitting breakdown potential.

More experimental studies for crevice geometries are recommended.

The possibility of ionising radiation counteracting the thermophoretic effect in relation to dust particle settlement should be assessed. Is it a viable process that could be important?

There is little useful relevant information to predict the chemistry and electrode potential associated with the deposits which may form on a waste package container in relation to the

interactive effects of radiolysis and chemical and electrochemical reaction. Modelling of the behaviour in porous layers and in crevice geometries is required. Despite the limitations of such models, they can provide a test bed for assessing the relative impact of different processes and their interactive effect.

The possibility of enhanced acidification in a crevice due to oxidation of radiolytically produced reducing species in the crevice solutions should be considered.

Dripping corrosion tests in the absence of radiolysis will have limitations, as radiolysis will also determine the development of the chemistry in the porous deposit.

The heat transfer problem for a layer deposit should be solved theoretically to ascertain the extent of possible surface temperature elevation over time.

References

1. R. Frankenthal. Discussion Note, 2001.

2. P.L.Airey, Radiation Research Reviews, **Vol. 5**, 341-371, 1973.

3. J O'M Bockris and L.F. Oldfield, Trans. Faraday Soc., **Vol. 51**, 249, 1955

4. W.G. Burns and P.B. Moore, Radiation Effects, **Vol. 30**, 233, 1976

5. R.S. Glass et al, Corros. Sci., **Vol. 26** (8), 1986, 577-590.

6. G. P Marsh et al, **Vol. 26** (11), 971-982, 1986.

7. W.G. Burns et al, "Water radiolysis under bottled fuel conditions," AERE Report R 9063, June 1979.

8. D. Herbert, G. O. H. Whillock and S.E. Worthington, "Zero-resistance ammetry- its application in preventing the corrosion of stainless steel in cooling waters," in Electrochemical methods in Corrosion Research, Material Science Forum, **Vols. 192-194** (1995), 469-476.

9. A Turnbull, Corrosion, **Vol 55** (2), 206, 1999.

10. M. Baklouti et al, "Atmospheric corrosion in interim storages", Eurocorr 2000.

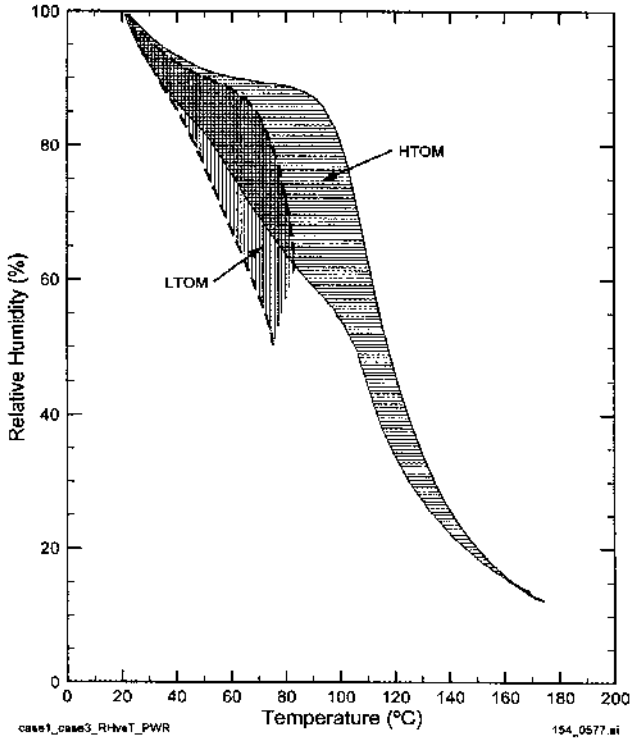

Figure 1 – RH vs Drift Wall Temperature for Two Operating Modes under Consideration

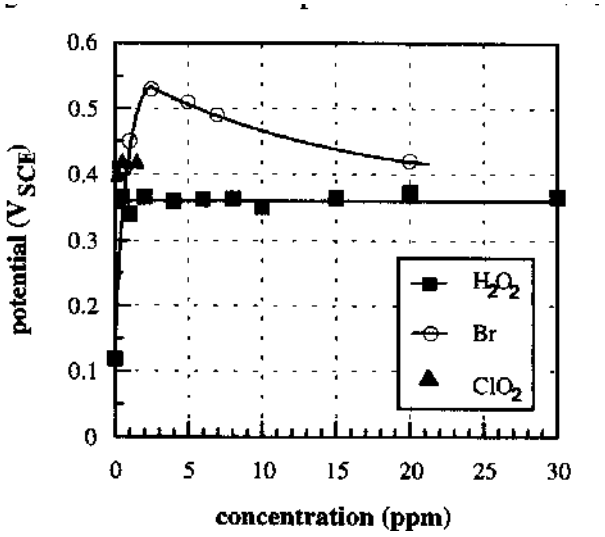

Figure 2 – Effect of Oxidising Species on Corrosion Potential of 304L SS[8]

9. Issues Relevant to the Uniform Corrosion Resistance of Alloy22

Thomas M. Devine, Jr.
University of California, Berkeley
Berkeley, California, USA

EDITORIAL NOTE

This volume, "A Compilation of Special Topic Reports," contains a series of reports that were prepared for the Waste Package Materials Performance Peer Review Panel to use as background and input to the peer review. Summaries drawn from the reports were also presented in Section 11 of the Panel's Final Report. The Panel used the reports as background and input for its review. Any views and comments expressed in the summaries and the full reports do not necessarily reflect the opinion and findings of the Panel. Further, opinions expressed in the reports are not necessarily those of the Panel or reflected in the Panel's reports and recommendations.

Four major topics are covered in this report on uniform corrosion of Alloy 22: (1) the structure and composition of the passive film formed on Alloy 22 in aqueous solutions, (2) the uniform corrosion of Alloy 22 in the passive state, (3) the uniform corrosion of Alloy 22 in the transpassive state, and (4) measurement of the uniform corrosion rate of Alloy 22.

1.0 Passive Film of Alloy 22

1.1 Structure and Composition of the Passive Films Formed in Aqueous Solutions

Overview. The generally excellent resistance of Alloy 22 to uniform corrosion is entirely due to the protective nature of its passive film. Even though this uniform corrosion resistance is expected to persist for thousands of years, the passive film itself is amazingly thin.

The passive films that form on other corrosion resistant nickel-base alloys and stainless steels are also extremely thin. For example, the thickness of the passive film formed on a 15Ni-16.7Cr-4.28Mo austenitic stainless steel in 0.1M HCl + 0.4M NaCl was less than 15Å. The thickness of the passive film increased from 10 to 15 Å with increasing potential in the passive range (Olefjord et al., 1985). Similarly, the thickness of the passive films formed on four nickel-base superalloys [**] in a mildly acidic acetate buffer were measured to be 15±5 Å (Pound and Becker

[**] Inconel 718 (nominal composition: 19 Cr 16Fe 5 (Nb+Ta) 3Mo, bal Ni), Incoloy 925 (nominal composition: 29Fe 22Cr 3Mo 2(Nb+Ta), bal Ni), and MP35N (20Cr 10Mo, 33Co 35 Ni).

(1991)). In close agreement, the TOFSIMS measurements by Lloyd et al. (2001) indicate the thickness of the passive films of Alloy 22 in 0.1M H_2SO_4 + 1M NaCl are in the range of 14-16Å.

Given the extreme thinness of the passive films, it is surprising that many of the films consist of at least two layers. Passive films with layered structures are formed on nickel-chromium binary alloys (Boudin et al. 1994; Bojinov et al. 2001), stainless steels (Clayton et al. 1986, Brooks et al. 1986), iron-chromium binary alloys (Kumai and Devine, 2000), and pure iron (Davenport et al., 1995 and Schroeder and Devine, 1999). The passive film formed on Alloy 22 in an acidic solution (pH–1) also exhibits two layers (Lloyd et al. 2001) as does the passive film formed on Alloy 59 (23Cr 16Mo 1Fe bal Ni) (Rajeswari et al., 2001), which is similar in composition to Alloy 22.

It is instructive to compare the structure and composition of the passive film of Alloy 22 with the structures and compositions of the passive films formed on nickel, nickel-chromium binary alloys, and nickel-chromium-iron ternary alloys.

Structure and Composition of Passive Films of Nickel. Cowan and Staehle investigated the passive film of pure nickel and found that at 22∀C, the passive film consisted of a single species whose identity was dependent on the pH of the solution. Film identification was performed by passivating the sample potentiostatically for 30 minutes and then shutting the potentiostat off and measuring the decay in the open circuit potential with time. In pH 1.3, 3.4 and 6.3, only one potential arrest was observed indicating that the film consisted of a single species. The value of the potential arrest in pH 1.3 and 3.4 was slightly less than the Ni/Ni_3O_4 equilibrium potential. In pH 6.3 the value of the potential arrest was slightly less than the Ni/NiO and $Ni/Ni(OH)_2$ equilibrium potentials.

The passive film that forms on nickel in mildly alkaline, borate buffer (pH=8.4) was investigated by *in situ* surface enhanced Raman spectroscopy (SERS) (Oblonsky and Devine, 1995). The passive film consisted of a single species: amorphous/microcrystalline $Ni(OH)_2$; NiO was not detected. The presence of $Ni(OH)_2$ and the absence of NiO are consistent with the Pourbaix diagram for nickel in water, which indicates that $Ni(OH)_2$ is thermodynamically stable in neutral or slightly alkaline solutions and that $Ni(OH)_2$ is more stable than NiO (Pourbaix, 1974).

Structure and Composition of Passive Films on Ni-Cr and Ni-Cr-Fe Alloys. While the passive film formed on nickel in acidic and neutral pH solutions consists of a single species (Ni_3O_4 in pH 1.3 and 3.4; NiO or $Ni(OH)_2$ in pH 6.3; $Ni(OH)_2$ in pH 8.4), the passive films formed on nickel-chromium alloys consist of two layers. Passive films formed on nickel-chromium binary alloys (7.1-31.6 a/o Cr) by anodic polarization for 2 hrs. at +0.2V (SCE) in borate buffer (pH=9.2) were determined by Auger electron spectroscopy (AES) depth profiling to be 15-21Å thick and bi-layered (Boudin et al., 1994). The outer layer consisted of nickel oxide/hydroxide with some chromium hydroxide and bound water. The inner layer contained anhydrous Cr_2O_3. For alloys with more than 15 a/o chromium, the inner layer consisted of 4-5 monolayers (– 8-10Å) of pure Cr_2O_3. For alloys with more than 15 a/o chromium, the overall composition of the passive film is chromium-rich. For alloys with less than 15 a/o chromium the overall composition of the passive film is nickel rich.

The passive films formed on nickel-chromium-iron ternary alloys consisted of three layers. The innermost and outermost layers of the passive films formed on nickel- (15.5 and 34.o a/o) chromium – 8 a/o iron by anodic polarization for 2 hrs. at +0.2V (SCE) in borate buffer (pH=9.2) were investigated by AES depth profiling and found to be similar to the inner and outer layers of the passive films formed on nickel-chromium binary alloys of similar chromium concentrations (Boudin et al.). That is, the innermost layer of the passive film of nickel-chromium-iron ternary alloys is largely chromium oxide and the outermost layer is a mixture of nickel oxide, nickel hydroxide and a relatively small amount of chromium hydroxide. The passive films of nickel-chromium-iron ternary alloys also contain an intermediate layer, which is largely iron oxide.

The tri-layered passive film formed on nickel-chromium-iron alloys in borate buffer (Boudin et al.) and described in the previous paragraph was also observed on Inconel 600 in near neutral chloride solutions (Lorang et al.). Specifically, the passive film formed on Inconel 600 that was anodically polarized for 2 hrs. at –200 mV/SCE in 0.5M NaCl had an inner layer of chromium oxide, an intermediate layer of iron oxide and an outer layer of nickel oxide/hydroxide.

Structure and Composition of Passive Films on Alloy 22. As already mentioned, the passive film of Alloy 22 consists of two layers (Lloyd, et al.). The investigations of the passive films of Alloy 22 and other nickel-chromium-molybdenum alloys have primarily been conducted on films formed in acidic solutions. This is in contrast to the studies discussed above of the passive films formed on nickel-chromium and nickel-chromium-iron alloys. The studies of nickel-chromium and nickel-chromium-iron alloys were conducted in neutral and mildly alkaline solutions. The differences between the structures and compositions of the passive films formed on nickel-chromium-molybdenum alloys in acidic solutions and the structures and compositions of the passive films formed on nickel-chromium and nickel-chromium-iron alloys in neutral and mildly alkaline solutions can be attributed to differences in alloy composition as well as differences in solution composition. As discussed in the next section, entitled “Formation of a Layered Passive Film,” solution pH appears to have a significant effect on the composition of the outer layer of the passive films formed on nickel-chromium binary and nickel-chromium-iron and nickel-chromium-molybdenum ternary alloys.

The inner layer of the passive film on Alloy 22 in acidic chloride (Lloyd et al., 2001) is enriched in chromium, which is similar to the films formed on nickel-chromium and nickel-chromium-iron alloys in mildly alkaline solution. However, whereas nickel-chromium and nickel-chromium-iron with > 15 a/o chromium in neutral and mildly alkaline pH have an inner layer that is essentially pure chromium oxide, the inner layer of the passive film of Alloy 22 in acidic chloride also contains appreciable amounts of nickel.

The outer layer of the passive film on Alloy 22 in acidic chloride (Lloyd et al., 2001) is enriched in chromium plus molybdenum and significantly depleted of nickel. This is in marked contrast to the passive films of nickel-chromium and nickel-chromium-iron alloys that form in mildly alkaline solution (Boudin et al.). The outer layers of these films consist almost completely of nickel hydroxide.

AES depth profiling of the passive film formed on Alloy C4 (Ni-18 a/o Cr and 10 a/o % Mo) during anodic polarization for 2 hrs. at –200 mV/SCE in 0.5M NaCl indicates the passive film consists of two layers: an inner layer that is enriched in chromium and an outer layer that is enriched in nickel. This is similar to the passive films formed on nickel-chromium alloys in mildly alkaline solutions.

Collectively, analyses of the passive films of C4 in neutral chloride solutions and of the passive films of Alloy 22 in acidic chloride solutions and of nickel-chromium binary alloys and nickel-chromium-iron ternary alloys in mildly alkaline solutions suggests that the solution pH has a significant effect on the structure and composition of the passive films. In neutral and mildly alkaline solutions, the passive films on nickel-chromium, nickel-chromium-iron and nickel-chromium-molybdenum alloys have an inner layer that is rich in chromium and an outer layer that is rich in nickel. In acidic chloride, the passive film that forms on Alloy 22 has an inner layer that is rich in chromium, but contains significant amounts of nickel, and an outer layer that is rich in molybdenum and chromium.

The results of investigations into the structure and composition of the passive films on nickel, nickel-chromium binary alloys, and nickel-chromium-iron and nickel-chromium-molybdenum ternary alloys are summarized in Table I.

While the results summarized in Table I suggest that the pH of the solution has a major influence on the structure and composition of passive films of nickel-chromium binary alloys and nickel-chromium-iron and nickel-chromium-molybdenum ternary alloys, there is also evidence that the exact composition of nickel-chromium-molybdenum alloys has a significant effect on the structure and composition of the passive film. For example, in acidic chloride the passive film formed on Alloy C276 (nominal composition of Alloy C276 = 15.5 Cr and 16 Mo) is distinctly different from the passive film that forms on Alloy 22 (nominal composition of Alloy 22 = 22 Cr and 13 Mo). In particular, the passive film on Alloy C276 is not layered and consists of a molybdenum (especially) and chromium enriched nickel oxide (Lloyd et al., 2001). The passive film of Alloy C276 does begin to approach the composition and structure of the passive film of Alloy 22 at very high potentials (e.g., 700 mV vs Ag/AgCl). The results of Lloyd et al. clearly indicate that the resistance of Alloy 22 to uniform corrosion is strongly related to the protectiveness of the inner layer of the passive film, which is directly related to the high chromium concentration of Alloy 22, and only indirectly related to the molybdenum concentration. According to Lloyd et al. the indirect effect of molybdenum on the protectiveness of the inner layer appears to result from MoO_4^{-2} in the outer layer causing deprotonation of the inner layer, making more O^{-2} available for the formation of Cr_2O_3, which is largely responsible for the protectiveness of the inner layer.

Table I
Structure and Composition of Passive Films on Ni, Ni-Cr, Ni-Cr-Fe, and Ni-Cr-Mo

Alloy	Solution	pH	Analytical Technique	Film	Reference
Ni	0.1N K_2SO_4	1.3 3.4 6.3	Potential arrest during galvanostatic reduction of film	Ni_3O_4 Ni_3O_4 NiO or $Ni(OH)_2$	Cowan
Ni	Borate buffer	8.4	Surface enhanced Raman Spectroscopy (SERS)	$Ni(OH)_2$	Oblonsky
Ni-7-31Cr	Borate buffer +200mV_{SCE}/2h	9.2	Auger electron spectroscopy (AES) depth profiling	bi-layered: Outer Layer: NiO/$Ni(OH)_2${Cr_2O_3}* Inner Layer: Cr_2O_3	Boudin
Ni-15Cr-8Fe Ni-34Cr-8Fe	Borate buffer +200mV_{SCE}/2h	9.2	Auger electron spectroscopy (AES) depth profiling	bi-layered: Outer Layer: NiO/$Ni(OH)_2$ {Cr_2O_3}* Inner Layer: Cr_2O_3	Boudin
Inconel 600	0.5M NaCl -200mV_{SCE}/2h	neutral	AES depth profiling	tri-layered: Outer Layer: NiO/$Ni(OH)_2$ {Cr_2O_3}* Mid Layer: Fe_xO_y Inner Layer: Cr_2O_3	Lorang
Alloy C4	0.5M NaCl -200mV_{SCE}/2h	neutral	AES depth profiling	bi-layered: Outer Layer: Ni-rich Inner Layer: Cr-rich	Lorang
Alloy C22	1M NaCl +0.1M H_2SO_4	1	TOF-SIMS	bi-layered: Outer Layer: Cr/Mo-rich,Ni Inner Layer: Cr-rich, Ni	Lloyd
Alloy C276	1M NaCl +0.1M H_2SO_4	1	TOF-SIMS	Single layer: Mo-rich, Cr, Ni	Lloyd

N.B.: {Cr_2O_3}* => small amount of Cr_2O_3

Table I (Continued)
Structure and Composition of Passive Films on Ni, Ni-Cr, Ni-Cr-Fe, and Ni-Cr-Mo

Summary of Films on Alloys with ∅Critical Chromium Concentration – 15-20 a/o

Alloy	Alkaline Solution	Acidic Solution
Ni-Cr	Outer Layer: Ni-rich Inner Layer: Cr-rich	
Ni-Cr-Fe	Outer Layer: Ni-rich Mid Layer: Fe-rich Inner layer: Cr-rich	
Ni-Cr-Mo	Outer Layer: Ni-rich Inner Layer: Cr-rich	Outer Layer: Cr, Mo-rich Inner Layer: Cr-rich

The greater uniform corrosion resistance of Alloy 22 compared to Alloy C276, which appears to be the result of the higher chromium concentration of Alloy 22 (and, possibly, the chromium/molybdenum ratio of Alloy 22), illustrates the importance of the chromium concentration (and, possibly, the chromium/molybdenum ratio) and raises the question as to whether or not the composition (specifically the chromium and molybdenum concentrations) of Alloy 22 is optimized for uniform corrosion resistance. Results of Lloyd et al. suggest that the critical concentration of chromium is – 20% and the results of Boudin et al. indicate the critical concentration of nickel-chromium and nickel-iron-chromium is greater than 15 a/o chromium. A critical chromium concentration between 10 and 20 a/o is supported by the study of Bojinov et al. (2001), who investigated the passive films formed on nickel-chromium binary alloys in 0.1 M $Na_2B_4O_7$ using contact electric resistance and electrochemical impedance spectroscopy. The passive film formed on Ni-10Cr was similar to the passive film formed on pure nickel. The passive film formed on Ni-20Cr resembled the passive film of pure chromium.

The major difference in passive behavior of Alloy 22 and Alloy C276 is also illustrated by the different effect that increasing temperature has on the passive dissolution rates of the two alloys (Lloyd et al.). The passive dissolution rate of Alloy C276 increases with increasing temperature at an applied potential of 350 mV. The passive dissolution rate of Alloy 22 was only weakly dependent on temperature.

Summary. In summary, results to date indicate that the passive film of Alloy 22 in acidic solutions is thin (Ω 20 Å) and bi-layered. The passive films that form on iron-chromium and other nickel-chromium alloys are also thin and bi-layered. Investigations of the passive films formed on nickel-chromium-molybdenum alloys in acidic solutions and nickel-chromium and nickel-chromium-iron and nickel-chromium-molybdenum alloys in neutral and mildly alkaline solutions indicate the compositions of the passive films are strong functions of the composition of the alloy and the pH of the solution. In acidic solutions, the outer layer of the passive film is depleted of nickel. In neutral and mildly alkaline solutions, the outer layer of the passive film is enriched in nickel. For excellent uniform corrosion resistance, a nickel base alloy must contain a critical minimum concentration of – 20 a/o chromium. The inner layer of the passive films of

alloys with greater than or equal to the critical chromium composition is nearly pure chromium oxide. The inner layer of passive films of alloys with less than the critical concentration of chromium is a mixed nickel-chromium oxide, which is less protective than pure chromium oxide.

1.2 Mechanism(s) of Formation of a Layered Passive Film

The processes that lead to the formation of the duplex structure of the passive film of Alloy 22 are not completely understood. For guidance, it is instructive to consider a small subset of what is known about the formation of the passive films on ferrous alloys. Specifically, the method of formation of the layered passive films that form on stainless steels and iron in high-temperature (288°C) water.

Formation of Bi-Layered Passive Films on Iron and 304 Stainless Steel in 288°C Water. The passive films formed in 288°C water are considerably thicker than those that form at room temperature. Because of their greater thickness, the films that form at high temperatures are easier to analyze.

At potentials below the passivation potential in 288°C water, an M_3O_4 film forms on stainless steel and a film of Fe_3O_4 forms on iron (Kumai et al.). The films of M_3O_4 and Fe_3O_4 exhibit a duplex structure consisting of a thin, inner layer that is conformal with the underlying metal substrate and an outer layer that is composed of relatively large (up to several microns in diameter), faceted particles. Gold particles, which were approximately 500 nm in diameter, were deposited on the metal surface before the start of the experiment and served as surface markers. The inner layer of M_3O_4 lie underneath the gold particles, whereas the gold particles were often buried by the outer layer of faceted particles of M_3O_4. The gold marker experiments indicate the inner layer of M_3O_4 grows at the metal/film interface, and much, if not all, of the outer layer of particles of M_3O_4 precipitate from the aqueous phase. Passivation occurred in two steps. First, passivation began with the removal of defects, such as porosity, in the layer of M_3O_4. Second, passivation was completed by the formation of an outer layer of M_2O_3 that completely covered the layer of M_3O_4. That is M_2O_3 covered both the inner, conformal layer of M_3O_4 and the outer layer of particles of M_3O_4. In the case of iron, the outer layer is ζ-Fe_2O_3. In the case of 304 stainless steel the outer layer consists of ν-M_2O_3.[**]

The outer layer of M_2O_3 of the passive films of iron and 304 stainless steel in 288°C water is formed by the oxidation of M_3O_4 and not by the precipitation of M_2O_3 onto the surface of M_3O_4

[**] A word of caution is in order. Even though the vibrational spectrum (Schroeder et al.) and XANES (Davenport et al.) of the passive film formed on iron in borate buffer (pH 8.4) at room temperature suggest the passive film contains Fe_3O_4 and Fe_2O_3, the electrical and optical properties of the passive film of iron are markedly different from the electrical and optical properties of mixtures of Fe_3O_4 and Fe_2O_3 (Schmuki et al.). Fe_3O_4 and Fe_2O_3, as they exist in the passive film, would seem to contain a very high concentration of defects (e.g., point defects and electronic defects). Consequently, it is better to think of the passive films of iron and stainless steel as mixtures of species that resemble M_3O_4 and I $_2O_3$ rather than as mixtures of M_3O_4 and I $_2O_3$. A similar situation might exist for the passive films that form on Ni-Cr, Ni-Cr-Fe and Ni-Cr-Mo alloys.

(Kumai et al. 2000). The oxidation of M_3O_4 starts at the M_3O_4/water interface and progresses into the M_3O_4 layer.

General Comments on the Formation of Bi-Layered Passive Films on Nickel Base Alloys. The outer layer of a bi-layered passive film is sometimes stated without proof to form by precipitation of metallic cations from the aqueous solution. However, when considering possible mechanisms of formation of the multi-layered passive films that form on nickel-chromium binary and Ni-Cr-X ternary alloys, it is worth bearing in mind that there are other possible mechanisms of formation of the outer layer. For example, as described in the previous paragraph, the outer layer (M_2O_3) of the passive films of iron and stainless steel in 288°C water forms by oxidation of the layer of M_3O_4, starting at the M_3O_4/solution interface. A similar mechanism of formation of a layered passive film might occur in Alloy 22 in acidic solutions at room temperature. The results of Bellanger and Rameau (1996) indicate the existence of a film on the surface of Alloy 22 at potentials below the passivation potential in a mildly acidic solution (pH=3). [**] This prepassive film might serve as the inner layer of a layered passive film, as was the case for iron and stainless steel in 288°C water (Kumai, 2001). That is, a mixed nickel-chromium-molybdenum oxide might initially form and then the outer layer of the oxide might be depleted of nickel due to the high solubility of nickel in acidic solutions. Alternatively, a chromium and molybdenum rich film might initially form due to the higher oxygen affinities of chromium and molybdenum. Subsequent transport of H_2O or O^{-2} to the film/metal interface might then result in the formation of an inner layer containing nickel-chromium-molybdenum. In either case, the result is a bi-layered film with an outer layer depleted in nickel and an inner layer with a higher nickel concentration.

In the case of the passive film formed on Alloy 22 in acidic solutions, the compositions of the inner and outer layers are different. This is in contrast to the bi-layered passive film of iron (and, possibly, of stainless steel in 288°C water) in which the composition of the cations in the inner and outer layers are identical (except for change in oxidation state). The more protective layer of the passive film of Alloy 22 is thought to be the inner layer. In contrast, the more protective layer of the passive films in 288°C water of iron and 304 stainless steel is the outer layer. The outer layer of the passive film in acidic solutions of Alloy 22 might form, in part, as the result of the preferential dissolution of nickel (in particular) and chromium. At potentials above +0.261 V (SHE) at pH 1 the outer layer of the passive film is expected (based on thermodynamics) to be enriched in MoO_3 (Pourbaix, 1974)

Formation of Bi-layered Passive Films on Ni-Cr Binary Alloys and Ni-Cr-Fe Ternary Alloys. The structure and composition of the multi-layered passive films that form on nickel-chromium and nickel-chromium-iron alloys strongly suggest that the process of film formation in neutral and mildly alkaline solutions is different from the process of film formation on iron and stainless steel in 288°C water. There are three characteristics of the passive films of nickel and nickel chromium alloys that inform on the mechanism of the film formation in nickel-chromium binary and nickel-chromium-iron/molybdenum ternary alloys. (1) The passive film of nickel in

[**] Caution is in order. Although the authors identify an active region in the anodic polarization curve of Alloy 22, the evidence for the existence of an active region of Alloy 22 is not strong.

acidic, neutral pH, and mildly alkaline solutions consist of a single species. (2) The passive films of binary nickel-chromium alloys in neutral and mildly alkaline solutions consist of two layers: a chromium-rich inner layer and a nickel-rich outer layer. (3) The passive films of nickel-chromium-iron alloys in neutral and mildly alkaline solutions consist of three layers: a chromium rich innermost layer, an iron rich middle layer and a nickel rich outermost layer. (4) The composition of the metal layer underneath the passive films in nickel-chromium alloys and nickel-chromium-iron alloys is depleted of chromium and enriched in nickel.

Collectively, the four characteristics listed in the previous paragraph strongly suggest that the passive films of nickel-chromium binary and ternary alloys form by chromium being preferentially oxidized to form a chromium-rich layer. Subsequent oxidation occurs by chromium, nickel, and iron moving through the chromium oxide layer to form a middle layer of iron oxide and an outer layer of nickel oxide and to increase the thickness of the inner layer of chromium oxide. The multi-layered structure and composition of the passive film is controlled by the relative oxygen affinities of chromium, nickel and iron (Cr>Fe>Ni) and the relative rates of transport of chromium, nickel, and iron through chromium oxide (Fe>Ni>Cr).

The same factors of relative oxygen affinity and rate of transport through chromium oxide plus a third factor, the relative solubilities in aqueous solutions of iron, nickel, chromium, and molybdenum species, could also figure prominently in the formation of the bi-layered passive film of Alloy 22 in acidic solutions.

Concentrations of Nickel and Molybdenum in the Outer Layer of the Passive Film of Alloy 22. The nickel depletion of the outer layer of the passive film of Alloy 22 in acidic chloride is undoubtedly due to the high solubility of nickel-oxide, -hydroxide, and –oxyhydroxide species in acidic solutions (Pourbaix).

That the outer layer of the passive film formed on Alloy 22 in acidic solutions is enriched in molybdenum is not surprising. The enrichment of molybdenum could be due to either an increase in the amount of molybdenum and/or a decrease in the amount of chromium. In either case, the relatively high ratio of the concentration of molybdenum to the concentration of chromium in the outer layer is consistent with the lower solubility of species of molybdenum, compared to the solubility of species of chromium, in acidic solutions at potentials in the passive region of Alloy 22 (Pourbaix, (1974)). The following comparison of MoO_3 and Cr_2O_3 illustrates the higher solubility of chromium species in acidic solutions. Dissolving MoO_3 in pH 1.5 water until a saturated solution is obtained will yield a solution with $10^{-2.2}$ g.at./L Mo (Pourbaix, (1974)). Decreasing the pH of the solution will decrease the amount of dissolved MoO_3. In contrast, dissolving Cr_2O_3 in pH 1.5 water until a saturated solution is obtained will yield a solution with $10^{+0.1}$ g.at./L Cr (Pourbaix, (1974)). Decreasing the pH will increase the amount of dissolved Cr_2O_3. Consequently, in strongly acidic solutions, the outer layer of the passive film of Alloy 22 is expected to have a relatively high value of the ratio of molybdenum concentration to chromium concentration. Based on the solubilities of MoO_3 and Cr_2O_3 in aqueous solutions, the ratio of molybdenum concentration to chromium concentration in the passive film is expected to be relatively low in neutral and mildly alkaline solutions.

Molybdenum in the passive film of Alloy 22 exhibits a number of valencies (+4, +5 and +6) (Lloyd et al. 2001). At relatively low passive potentials the +4 state of molybdenum is dominant, suggesting molybdenum exists in the passive film as MoO_2. The equilibrium potential of the oxidation of MoO_2 to MoO_3 is 0.261 V (SHE) at pH 1. Based on the relatively low solubility of molybdenum species in low pH solutions (Pourbaix), a significant amount of MoO_3 would remain in the passive film.

There is another scenario that would explain the higher ratio of molybdenum concentration to chromium concentration in the outer layer of the passive film formed on Alloy 22 in acidic solutions. Rather than MoO_2 in the passive film being oxidized to MoO_3, MoO_2 might be oxidized to $HMoO_4^-$. The equilibrium potential of the oxidation of MoO_2 to soluble $HMoO_4^-$ is 0.1634 V (SHE) at pH 1, which is much lower than 1.062 V (SHE), the equilibrium potential of the oxidation of Cr_2O_3 to highly soluble CrO_4^{-2} at pH1 (Pourbaix, 1974). It is possible that MoO_2 is oxidized to $HMoO_4^-$ (rather than MoO_3), which is then adsorbed onto the surface of the oxide and later incorporated into the outer layer of the oxide.

Summary. The mechanism of formation of a multi-layered passive film on Alloy 22 is expected to be a strong function of solution pH. In acidic solutions, the outer layer of the passive film of Alloy 22 is rich in molybdenum and chromium. The outer layer forms by the preferential dissolution of nickel in acidic solutions. The enrichment of molybdenum in the outer layer is a consequence of the relatively low solubility of molybdenum in acidic solutions.

No investigations have been conducted on the formation of passive films on Alloy 22 in neutral and mildly alkaline solutions. However, examinations of films formed on nickel-chromium and nickel-chromium-iron alloys and C4 (Ni-18Cr-10Mo) in mildly alkaline solutions suggest that a multi-layered film will form on Alloy 22 in mildly alkaline solutions and that the inner layer of the film will be enriched in chromium and the outer layer of the film will be enriched in nickel. The high nickel concentration of the outer layer appears to be the result of the faster mobility of nickel through the inner layer. The distribution of molybdenum in the film will depend on the relative mobility of molybdenum in the inner layer film and the solubility of molybdenum species in water.

1.3 Effect of Air-Formed Oxide Film

For the first several hundred years in the repository, the temperature of the waste package will be too high for water to come into contact with the waste package. By the time an aqueous phase contacts the waste package, the surface of Alloy 22 will be covered with an air-formed oxide film. The oxide film on the surface of Alloy 22 will primarily be the result of oxidation that occurs during the thermomechanical processing of the waste package. Included in the thermomechanical processing is a thermal treatment intended to introduce a residual stress pattern in the waste package that will increase resistance to stress corrosion cracking. The favorable residual stress distribution is to be created by an isothermal heat treatment at 1150°C / 3.5 hours. followed by a water quench of the entire Alloy 22 waste package (Gordon, 2002). After the canister is filled with nuclear waste and closed, a favorable residual stress pattern will

be introduced in the vicinity of the final closure welds by either an induction anneal (1000∀C - 1100∀C /–30 sec. and cooled to 600°C in less than 10 min.) or laser peening (Gordon, 2002).

The amount of metal loss that Alloy 22 might sustain during high temperature heat treatments is expected to be negligible. This estimation is based on the high temperature oxidation behavior in air of nickel-chromium alloys and Inconel 600. As summarized in the textbook by G.Y. Lai (pg. 24), the oxidation resistance at 980°C of iron-nickel-chromium alloys with 15-25% Cr is dramatically increased by raising the nickel concentration of the alloy to above 32%. In particular, the results indicate that Inconel 600 and a Ni-20 Cr binary alloy did not sustain any change in weight during over 500 hrs. of exposure to cyclic oxidation in air at 980°C (15 min. heating – 5 min. cooling). The oxidation resistance is attributed to the formation of a protective scale of Cr_2O_3.

Iron-chromium binary alloys with > 20 wt.% Cr form a continuous protective scale of Cr_2O_3 when oxidized in 0.13 atm. O_2 at 1000°C (Lai, pg. 22). In general, iron-chromium, nickel-chromium, and cobalt-chromium alloys with greater than 15-30% chromium form a protective scale of Cr_2O_3. Consequently, a scale of Cr_2O_3 is expected to form on Alloy 22 during oxidation in air at high temperatures.

An indication of the high temperature oxidation resistance expected of Alloy 22 is provided by the oxidation behavior of Inconel 600 exposed at high temperatures to flowing air for 1008 hrs. The amount of metal loss increased with temperature as shown in the following Table.

Table II*
Oxidation Behavior of Inconel 600 during 1008 hrs. in High Temperature, Flowing Air

Temperature	Amount of Metal Loss
980°C	7.5 μm
1095°C	28 μm
1150°C	43 μm
1205°C	130 μm

* Data in this Table were extracted from results presented in Lai, pg. 33.

As the temperature exceeds about 1000°C, Cr_2O_3 begins to convert to volatile CrO_3 and is no longer protective. Nevertheless, based on the above results for Inconel 600, the amount of metal lost by oxidation of Alloy 22 during 3.5 hrs. at 1150°C is expected to be less than 1 μm.

For comparison, Table III summarizes the oxidation behavior of a Nickel-20% Chromium alloy in air at temperatures from 700°C to 1102°C. The results indicate a greater loss of metal than in the tests on Inconel 600 reported in Table II.

Table III*
Oxidation Resistance of Ni-20Cr in Air at Temperatures of 700°C – 1102°C

Temperature	Weight Increase (g/m^2hr)
700°C	0.35
785°C	0.70
895°C	2.0
998°C	4.0
1102°C	8.0

* Data in this Table were extracted from results presented in Friend, pg. 166.

Other tests indicate that Inconel 600 has good resistance to oxidation in air at temperatures up to about 1090°C and for times as long as 80 hrs. However, tests at 1204°C resulted in significant corrosion accompanied by subsurface oxidation and void formation within about 50 μm of the surface (Friend, pg. 166).

It is worth noting that the 15% molybdenum contained in Alloy 22 will not contribute to high temperature oxidation resistance as MoO_3 melts at 795°C.

Based on the performance of Inconel 600 and Ni-20 Cr binary alloy, Alloy 22 is expected to have good oxidation resistance in air at temperatures as high as – 1100°C. For this reason, it might be advisable to keep the high temperature annealing treatment (for residual stress improvement) of Alloy 22 at or below 1100°C, even though the time at temperature will be very short (Ω3.5 hrs.).

The influence of the oxide formed at high temperature on the corrosion resistance of Alloy 22 in aqueous solutions at Ω100°C is not known. However, preliminary results suggest that the film formed on Alloy 22 in air at room temperature is as protective against aqueous corrosion as is the passive film. Results by Lloyd et al indicate that the air formed film on Alloy 22 is largely unchanged following immersion in an acidic chloride solution at 200 mV (vs Ag/AgCl). Furthermore, the uniform corrosion rate at 200 mV in acidic chloride of Alloy 22 covered with an air-formed film remained acceptably low as the temperature was raised every 10-12 hours in increments of 10°C to a maximum of 85°C. This preliminary result suggests that the uniform corrosion resistance of the Alloy 22 outer layer of the waste package will not be adversely affected by the formation of an air-formed film.

2.0 Uniform Corrosion Rate of Alloy 22 in the Passive State

The passive film that covers the surface of Alloy 22 is responsible for its corrosion resistance in aqueous solutions. It is for this reason that the composition and structure of the passive film are of great interest. Ultimately, it is important to know the rate of uniform corrosion in order to confirm that the waste package of Alloy 22 will resist uniform corrosion for thousands of years. A two-step procedure for establishing confidence in the prediction that the waste packages will not fail by uniform corrosion is as follows. First, correlate an acceptably low uniform corrosion rate with a particular passive film (structure, composition). Second, demonstrate that this particular passive film will remain stable over the life of the waste package.

In this section, the factors of solution chemistry and alloy composition that might adversely affect the uniform corrosion resistance of Alloy 22 in the passive state are discussed.

2.1 Influence of Solution pH on Time-dependent Changes

The corrosion currents that are measured on samples of Alloy 22 anodically polarized in the passive state decrease with time at a rate that is dependent on potential and temperature. Lloyd et al. found that most of the passive current in a solution of pH 1 was the result of the dissolution of the alloy. Very little of the current went into thickening of the passive film. In contrast, Bellanger and Rameau (1996) found that in pH 3, most of the passive current went into thickening of the passive film. Assuming that the results of Lloyd et al. and Bellanger and Rameau are both correct indicates that the uniform dissolution of Alloy 22 is dependent on pH and that the dissolution rate increases as the pH is decreased. However, even in pH 1, the dissolution rate of Alloy 22 in the passive state decreases rapidly with time, as was the case in pH 3.

The combined results of Lloyd et al. and Bellanger and Rameau indicate that (1) the decrease in corrosion rate with time in pH 3 is the result of thickening of the passive film and (2) the decrease in corrosion rate with time in pH 1 is the result of changes in the film's composition and/or structure.

Regardless of their cause(s), the time dependent changes of the passive film of Alloy 22 are important because of their effect on the alloy's uniform corrosion rate and the long-term performance of the waste package.

The results of potentiostatic corrosion tests conducted by Lloyd et al. in 0.1M H_2SO_4 + 1.0M NaCl indicate there is little influence of temperature (in the range of 25°C-85°C) on the uniform corrosion rate of Alloy 22 at potentials Ω300 mV vs Ag/AgCl. After 48 hrs. of immersion, the corrosion rate of Alloy 22 at +300 mV vs Ag/AgCl was – 2.5 x 10^{-7} amps/cm^2 and was still decreasing with time. A corrosion rate of 2.5 x 10^{-7} amps/cm^2 is equivalent to a uniform penetration rate of 2 cm in – 7,500 yrs.

At an applied potential of +500 mV vs Ag/AgCl, the uniform corrosion rate of Alloy 22 was temperature dependent and ranged from – 2.4 x 10^{-7} amps/cm^2 at 25°C to 3.3 x 10^{-7} amps/cm^2 (–2 cm in – 4,300 yrs.) at 85°C.

At an applied potential of +700 mV vs Ag/AgCl, the uniform corrosion rate of Alloy 22 exhibited greater temperature dependency than at lower potentials and ranged from – 2.8 x 10^{-7} amps/cm^2 at 25°C to 13 x 10^{-7} amps/cm^2 (–2 cm in – 1,400 yrs.) at 85°C. Keep in mind that these tests were conducted in a more corrosive solution than is expected to contact the waste package in the repository and that the steady state corrosion rates will be less than the rates measured after 48 hrs. of testing. Nevertheless, the results do indicate that the uniform corrosion rate of Alloy 22 might be unacceptably high under the combined effects of high temperature, high potential, and low pH.

The waste package could be exposed over long periods of time to temperatures that are high enough to cause unacceptably high rates of corrosion if the corrosion potential is also high. In the high temperature operating mode of the repository, the temperature of the waste package could decrease from 100°C to 85°C over a period of approximately 900 years (Mon, 2002). Thus, the waste package could experience, for a considerable length of time, temperatures higher than those evaluated in the study of Lloyd et al.

It is possible for the corrosion potential of Alloy 22 to reach values high enough that, in conjunction with high temperatures (e.g., between 100°C and 85°C for – 1,000 years), will result in high rates of uniform corrosion. Making use of information generated by the Project and discussed in section 6.2, the corrosion potential of coupons of Alloy 22 immersed in simulated acidified water at 90°C for 4.5 years was found to have risen to +400 mV vs Ag/AgCl.

The high value of 400 mV vs Ag/AgCl of the corrosion potential might not indicate a high rate of uniform corrosion. A high corrosion potential of a passive alloy can be the result of either the passive corrosion rate decreasing or the reduction reaction rate increasing. The former case would not result in significant uniform corrosion of the waste package. The latter case would cause significant uniform corrosion. The cause(s) of the increase in corrosion potential of Alloy 22 in simulated acidified water at 90°C in the Long-Term Corrosion Test Facility, at Lawrence-Livermore National Laboratory, is (are) not completely known. This issue is discussed in more detail in section 7.2.2 of the Final Report of the Waste Package Materials Performance Peer Review Panel (J. Payer et al, 2002).

Radiation emitted by the nuclear waste contained in the package could increase the corrosion potential of Alloy 22 in a manner that results in an increase in the uniform corrosion rate of Alloy 22. Measurements of Glass et al. (1986) indicate that gamma irradiation increases the oxidizing power of aqueous solutions causing an upwards shift of 150-250 mV in the corrosion potentials of 304L and 316L. Similar increases might occur in the corrosion potential of Alloy 22.

High concentrations of Fe^{+3} in the water contacting the waste package would also increase the corrosion potential of Alloy 22 in a manner that results in an increase in the uniform corrosion rate of Alloy 22. Corrosion of steel components that will surround the waste package in the repository could develop relatively high concentrations of Fe^{+3} in the water that contacts the waste package.

In summary, Fe^{+3} from corrosion of steel components in the vicinity of the waste package in the repository and gamma irradiation might raise the corrosion potential of Alloy 22 to values high enough to cause high rates of uniform corrosion of the waste package in the passive state.

It is worth pointing out a matter of secondary importance that is related to the passive corrosion rate and the structure and composition of the passive film. Time-dependent changes in the structure and composition of the passive film and in the passive corrosion rate might be used to judge the validity of different models of passivity and the passive films of Alloy 22. Models that can predict short time changes in the passive film and in the passive corrosion rate can be extrapolated with greater confidence to predict the uniform corrosion rate at times much greater than those that can be tested in laboratory experiments.

2.2 Influence of Surface Segregation

The uniform corrosion rate of Alloy 22 might be adversely affected by the segregation to the surface of elements such as phosphorus and sulfur (Briant, 2002).

In general, there have been relatively few studies of surface segregation. In contrast, there are a large number of studies of grain boundary segregation. It is not always possible to assess the likelihood of surface segregation based on studies of grain boundary segregation. This is because elements that segregate to the surface might not segregate to grain boundaries (Briant). Reasons for the difference in the tendency of an element to segregate to grain boundaries and to a free surface are listed by Briant, who cites factors such as the difference in the energies of binding an element to the free surface and to grain boundaries.

Sulfur in nickel-chromium alloys is an example of an element that shows a strong tendency to segregate to a free surface, but little tendency to segregate to grain boundaries. While sulfur segregates to the grain boundaries of unalloyed nickel, chromium in a nickel-base alloy prevents the grain boundary segregation of sulfur. Phosphorus is the most important grain boundary segregant of nickel-chromium alloys.

Surface segregation of sulfur in nickel-chromium alloys is a strong function of the temperature and time of heat treatment. Briant and Luthra (as cited in Briant, 2002) reported on the surface segregation of sulfur in a Ni-23Co-20Cr-12Al alloy. Heat treating at 1100°C for five – 60 minutes resulted in coverage by sulfur of 10% of the surface. A heat treatment of 6 hours at 900°C resulted in a sulfur concentration at the surface of 13 a/o. Heat treatments for up to 30 hrs. at 800°C did not produce significant surface concentrations of sulfur.

The amount of sulfur that segregates to the free surface will depend on the amount of sulfur present in the alloy.

Based on studies of the effects of surface segregation of sulfur on the uniform corrosion of unalloyed nickel and nickel-base alloys, the segregation of only a monolayer of sulfur to the surface of nickel and nickel base alloys can cause large increases in the uniform corrosion rate of

the alloy (Chaung et al.; Marcus). The sulfur is thought to enhance the rate of nickel dissolution by forming nickel-sulfur bonds that weaken nickel-nickel bonds. In addition, the presence of a monolayer of sulfur undermines the formation of protective passive films. In enhancing the rate of anodic dissolution and in inhibiting the formation of passive films, the sulfur acts in a catalytic manner, meaning it is not consumed in the dissolution and film inhibition activities. Consequently, a monolayer of sulfur increases the uniform corrosion rate of nickel alloys to an extent that is completely disproportionate to the amount of sulfur present in the alloys.

In considering the likelihood of sulfur segregation to the free surface of the outer layer of Alloy 22 waste canisters, it is important to note two important facts. (1) There are two mechanisms by which sulfur can segregate to the free surface of nickel base alloys: thermal treatments (Briant; Chaung et al.) and anodic oxidation (Marcus). (2) While sulfur segregates to nickel and nickel-alloy free surfaces, significant amounts of sulfur do not segregate to a metal/oxide interface (Briant).

According to the second fact stated above, thermally-driven sulfur segregation to the surface of Alloy 22 will only be significant if the surface is not covered by an oxide film. Based on the discussion in section 1.1, "Passive Film of Alloy 22," it is clear that waste canisters of Alloy 22 will be covered by an oxide film. Consequently, thermally-driven sulfur segregation to the free surface will only occur if vacancies are created at the passive film/metal interface. There are at least two processes by which vacancies can be created at the interface between Alloy 22 and the oxide or passive film that covers the alloy's surface: high temperature air-oxidation and aqueous corrosion at low temperatures. Each of these possibilities is discussed below.

As discussed in section 1.1, heat treating Alloy 22 in air at temperatures below ~ 1100°C should result in the formation of a protective film of Cr_2O_3, which limits the amount of oxidation of the alloy. However, at temperatures above ~ 1000°C, Cr_2O_3 starts to lose its protectiveness and significant amounts of oxidation can occur at temperatures above ~1100°C, resulting in the formation of grain boundary voids in the vicinity of the alloy's surface. The amount of oxidation increases with increasing temperature and increasing time at temperature. As noted in the previous section, sulfur will segregate to the surface of the voids.

Thus, if waste canisters of Alloy 22 are heat treated at temperatures above 1100°C then grain boundary voids that are covered with a monolayer of sulfur might be formed just below the surface of the canister. If the surface of the canister comes into contact with aqueous solutions in the repository, uniform corrosion will occur and the corrosion might expose the sulfur-coated voids to the aqueous solution. The presence of the monolayer of sulfur will locally prevent the formation of a protective passive film. If there is a significant amount of voids, then there would be a significant increase in the uniform corrosion rate. However, it is unlikely that the waste canisters will be heat treated at high enough temperatures for long enough periods of time for significant amounts of sulfur coated voids to form. By keeping annealing temperatures below 1100°C this potential problem can be avoided entirely.

As mentioned above, aqueous corrosion is a second process that might create voids at the interface between Alloy 22 and its passive film or thermal oxide coating. According to the Point

Defect Model (Macdonald, 1999) of passivity, it is possible for growth conditions to be such that vacancies condense and voids develop at the passive film/metal interface. However, according to studies by Rapp (2001) and others (as cited in Rapp, 2001) of corrosion product films grown during gaseous oxidation at high temperatures, vacancies are annihilated at metal/film interfaces. If such mechanisms of vacancy annihilation are operative at the interface between Alloy 22 and its passive film at the relatively low temperatures (–Ω160°C) in which an aqueous environment might be in contact with the waste package, then thermally-driven sulfur segregation to the surface of Alloy 22 will not occur. Even if corrosion creates voids at the passive film/alloy interface, the segregation of sulfur to the surface of the void should be small given the relatively low temperatures present in the repository. For example, the analysis by Briant suggests that the amount of phosphorus segregation to the surface will reach a saturation value of – 40 a/o after 220 years at 250°C. The saturation value is only 6 a/o at 180°C and is reached after 450 years at 180°C. The saturation value is a mere .012 a/o at 85°C and is reached after 720 years.

In addition to a – monolayer of sulfur developing at the film/alloy interface by sulfur segregating to the surface of voids formed underneath the surface by either thermal oxidation or aqueous corrosion, another mechanism by which sulfur might segregate to the surface of Alloy 22 is anodic oxidation. This process is possible if sulfur in the alloy is not oxidized when it comes into contact with the aqueous solution. As successive layers of metal are oxidized, the concentration of unreacted sulfur at the surface increases. The amount of sulfur segregated at the surface will depend on the concentration of sulfur in the alloy and on the uniform corrosion rate. In the case of nickel doped with 50 ppm of sulfur and immersed in 1N H_2SO_4, P. Marcus demonstrated that a monolayer of sulfur was quickly created on the nickel surface. This monolayer prevented the formation of a passive film, resulting in a seven-fold increase in the maximum corrosion rate of nickel in the active state and many orders of magnitude increase in the dissolution rate at potentials above the potential at which nickel would form a protective passive film if the monolayer of sulfur were not present.

A back-of-the-envelope calculation indicates that anodic segregation of sulfur is a potential problem for Alloy 22. Because of the relatively high bulk concentration of sulfur in Alloy 22 (400 ppm), the uniform corrosion of 1 μm of Alloy 22 can produce a monolayer of sulfur at the alloy's surface. If Alloy 22 is uniformly corroding at the low rate of 0.01 $\mu A/cm^2$ (= 0.7mm/10,000yr.), a monolayer of sulfur can be formed at the alloy's surface in approximately 10 years.

In summary, surface segregation of sulfur to the free surface of Alloy 22 can result in significantly high uniform corrosion rates of the waste canisters. The surface segregation of sulfur can occur during the high temperature treatments used to improve the residual stresses in the canisters. Anodic segregation is a second process by which sulfur might segregate to the surface of waste canisters of Alloy 22. The probability of sulfur segregation occurring as a result of heat treatment can be minimized and possibly reduced to zero by reducing the bulk sulfur concentration of the alloy and/or keeping the temperature of heat treatment below – 1100°C, which will reduce the likelihood of formation of voids to which sulfur can segregate. The probability of sulfur segregation occurring as a result of anodic segregation can be minimized and possibly reduced to zero by reducing the bulk sulfur concentration of the alloy.

3.0 Uniform Corrosion Rate of Alloy 22 in the Transpassive State

At potentials Ó500 mV (vs. Ag/AgCl) and at temperatures between 25°C and 85°C, the passive dissolution rate of Alloy 22 in 1M NaCl + 0.1M H_2SO_4 increases with increasing potential and temperature (Lloyd et al.). This is due to the transpassive corrosion of Cr(III) to Cr(VI). Very little Cr(VI) is found in the passive film, indicating that all of the Cr(VI) is leached out of the film and into the solution as soluble CrO_4^{-2}. At an applied potential of 700 mV (vs Ag/AgCl) the passive dissolution rate of Alloy 22 reaches a quasi steady state value of – 1 $\mu A/cm^2$ after 10 hrs. at 65°C (Lloyd et al.). This corresponds to a uniform penetration rate of 2 cm in – 2,800 years. While failure of the waste package by uniform corrosion is thought to be unlikely, a likely cause of failure of the waste package by uniform corrosion might be transpassive corrosion.

Potentials high enough to equal or exceed the transpassive potential of Alloy 22 might be established as a result of the ennoblement of the corrosion potential of Alloy 22. Ennoblement has been observed in samples of Alloy 22 tested in simulated acidified water at 90°C in the Long-Term Corrosion Test Facility (Lian et al., 2002). The protective, inner layer of the passive film of Alloy 22 primarily consists of a species that is/resembles Cr_2O_3. Consequently, transpassive dissolution of Alloy 22 will not occur until the corrosion potential is high enough to cause oxidation of chromium (III) to chromium (VI), which is highly soluble in water. To date, the ennoblement of the corrosion potential of Alloy 22 in simulated acidified water at 90°C has not raised the corrosion potential high enough to cause oxidation of Cr(III) to Cr(VI). It is possible (although not yet completely proven) that the ennoblement of the corrosion potential of Alloy 22 in simulated acidified water is caused by the low rate of corrosion in the passive state (see section 7.2.2 of the Final Report of the Waste Package Materials Performance Peer Review Panel (J. Payer et al, 2002)). If so, the rate of the reduction reaction at these high values of corrosion potential is too low to support high rates of uniform corrosion in the transpassive state.

High corrosion potentials of Alloy 22 will develop if Fe^{+3}, which was produced by corrosion of steel structures in the vicinity of the waste package, makes contact with the waste package. Fe^{+3} has very limited solubility in mildly alkaline and neutral pH solutions. Consequently, only if very acidic solutions (e.g., pHΩ1) are developed on the waste package will the concentration of Fe^{+3} be high enough to significantly raise the corrosion potential of Alloy 22. Even in the case of acidic solutions with high concentrations of Fe^{+3}, it is not likely that the corrosion potential of Alloy 22 will be high enough to cause transpassive dissolution of chromium.

Transpassive potentials might develop as a result of radiolysis of the water that comes into contact with the waste package (Glass et al., 1986). Turnbull (2001) has indicated that oxidizing potentials are particularly likely to develop as a result of radiolysis of water if the water is present as a thin film. This is exactly the quantity of water that is likely to be on the surface of the waste package.

Transpassive conditions can be initiated at relatively low oxidizing potentials by a combination of events that starts with an increase in corrosion potential leading to localized transpassive

corrosion of regions enriched in chromium and/or molybdenum. The products of this localized corrosion are oxidizing (e.g., MoO_4^{-2} and CrO_4^{-2}) and can lead to the lateral spreading of the transpassive corrosion of the remaining alloy. This is an example of an unusual process in which localized corrosion leads to uniform corrosion. Although unusual, just such a process is described by Bellanger and Rameau, who reported on the initiation of transpassive dissolution of Alloy 22 at local sites, possibly chromium-rich and molybdenum-rich precipitates. The experiments of Bellanger and Rameau were conducted at very high temperatures (360°C) in highly oxidizing (0.48 M oxygen), highly acidic (0.05M HCl) solutions. These test conditions are more corrosive than those expected in the repository. Nevertheless, the results of Bellanger and Rameau demonstrate how transpassive dissolution, begun on a local scale, can spread across the surface and lead to uniform corrosion.

Another example of uniform, transpassive corrosion that began at local sites is provided in a study by P. Kritzer et al. (March, 2000), who reported on transpassive corrosion that initiated at grain boundaries in nickel, Alloy 625 (Ni-22Cr-9Mo) and chromium. This result suggests that transpassive dissolution might initiate at grain boundaries that are enriched in sulfur, phosphorus, and silicon as a result of equilibrium segregation.

In summary, radiolysis of the water is the only process that is capable all by itself of raising the oxidizing power of the solution to values high enough to cause transpassive dissolution of Alloy 22. However, it is not known if the amount of radiolysis that will occur in water on the surface of the waste package is sufficient to raise the corrosion potential of Alloy 22 into the transpassive region. Other than radiolysis of the water, combinations of phenomena are required to raise the corrosion potential of Alloy 22 to values high enough to cause transpassive corrosion. For example, a combination of (1) Fe^{+3} ions, (2) a low pH, (3) a small amount of radiolysis of the water, and (4) the presence of chromium-rich precipitates or grain boundary segregation of sulfur or phosphorus, might result in localized transpassive corrosion, which could spread to more uniform transpassive corrosion.

In brief, uniform corrosion of Alloy 22 by transpassive corrosion in the repository is unlikely but cannot be completely ruled out at this time.

4.0 Measurement of Uniform Corrosion Rate

The change in weight of a test coupon can provide a measure of the coupon's average corrosion rate. However, the formation of solid corrosion products as well as the precipitation of solid phases on the surface of the test coupon will mask the true weight-loss of the sample. Consequently, it is necessary to rid the test coupon of solid products before measuring its change in weight. The solid products are often removed mechanically (e.g., by brushing) and sometimes electrochemically. In either case, it is necessary to confirm the removal of solid products by examining the surface of the coupon with an optical microscope.

For several reasons, measurement of the uniform corrosion rate by weight loss measurement is not as informative of the corrosion behavior of the material as is measurement of the corrosion

rate by electrochemical techniques, in particular, the linear polarization resistance technique. First, measurements of weight loss provide a measure of the average corrosion rate. Oftentimes, it is more important to know the instantaneous corrosion rate. Second, as already mentioned, the formation of solid corrosion products complicates the determination of the weight-loss caused by corrosion. Third, our ability to measure the small change in weight caused by a small amount of corrosion is not as great as our ability to measure the low electrical currents associated with small corrosion rates. Consequently, the corrosion rate of a corrosion resistant material is more accurately measured by electrochemical techniques such as the linear polarization resistance technique.

Linear polarization resistance measurements of the corrosion rate are also subject to errors. For example, the measured current may be difficult to relate to the corrosion rate of the metal if electrochemical reactions, in addition to the oxidation of the metal, are occurring on the surface of the metal. An example of an electrochemical reaction that would complicate the measurement of an alloy's corrosion rate is the breakdown of water. Oxidation of O^{-2} in water may occur at a significant rate on Alloy 22 at the high values of corrosion potential that are reached during the ennoblement that has been observed in simulated acidified water at 90°C.

Care must be exercised in the measurement of corrosion rate by linear polarization resistance. In linear polarization resistance, the external current is measured in an electrochemical cell consisting of the sample, which is the working electrode, and a counter and reference electrodes. The external current is measured as a function of the change in voltage between the sample and the reference electrode. The curve of voltage vs. current will be non-linear for a proper electrochemical corrosion reaction. The measurement of the corrosion rate comes from the measurement of the slope of the current versus voltage plot at zero cell current. For a good definition of the slope at zero cell current, the slope must be measured over a narrow range of voltage that typically should not exceed a few millivolts.

The proper procedure for linear polarization resistance measurement of corrosion rate and the major factors that contribute to errors in measurement of corrosion rate by linear polarization resistance are described in a number of publications (Barnartt, 1969; Oldham, 1971; Mansfeld, 1971; Mansfeld, 1973; Leroy, 1973; Mansfeld 1981; Macdonald, 1979; Townley, 1991; Scully, 2000).

References

S. Boudin, J.-L. Vignes, G. Lorang, M.Da Cunha Belo, G. Blondiaux, S.M. Mikhailov, J.P. Jacobs and H.H. Brongersma, "Analytical and Electrochemical Study of passive Films Formed on Nickel-Chromium Alloys: Influence of the Chromium Bulk Concentration," Surface and Interface Analysis, **v. 22**, p.462 (1994).

G. Lorang, N. Jallerat, K.Vu Quang and J.P. Langeron, "AES Depth Profiling of passive Overlayers Formed on Nickel Alloys," Surface and Interface Analysis, **v. 16**, p.325 (1990).

B.G. Pound and C.H. Becker, "Composition of Surfcae Films on Nickel Base Superalloys," Journal of the Electrochemical Society, **v. 138**, p. 696 (1991).

A.C. Lloyd, D.W. Shoesmith, J.J. Noel and N.S. McIntyre, "Effects of Temperature and Anodic Potential on the Passive Corrosion properties of Alloys 22 and C276," submitted for publication in Journal of the Electrochemical Society.

G. Bellanger and J.J. Rameau, "Behavior of Hastelloy 22 Steel in Sulphate Solutions at pH 3 and Low temperatures," Journal of Materials Science, **v. 31**, p. 2097 (1996).

M. Bojinov, G. Fabricius, P. Kinnunen, T. Laitinen, K. Makela, T. Saario and G. Sundholm, "Electrochemical Study of the passive Behavior of Ni-Cr Alloys in a Borate Solution – A Mixed Conduction Model**,"** Journal of Electroanalytical Chemistry, **v. 504**, p. 29 (2001).

Gerald Gordon, "Waste Package Residual stress Mitigation Approach and Status," Presentation at Lawrence Livermore National Laboratory, January 23, 2002.

G.Y. Lai, High Temperature Corrosion of Engineering Alloys, ASM International, Materials Park, OH (1990).

W.Z. Friend, Corrosion of Nickel and Nickel-Base Alloys, The Electrochemical Society, John Wiley & Sons, NY (1980).

P. Kritzer, N. Boukis and E. Dinjus, "Review of the Corrosion of Nickel-Based Alloys and Stainless Steels in Strongly Oxidizing Pressurized High temperature Solutions at Subcritical and Supercritical Temperatures," Corrosion, **v. 56**, p.1093 (2000).

P. Kritzer, N. Boukis and E. Dinjus, "Transpassive Dissolution of Alloy 625, Chromium, Nickel, and Molybdenum in High Temperature Solutions Containing Hydrochloric Acid," Corrosion, **v. 56**, p.265 (2000).

S. Rajeswari, K. Suresh Kumar Danadurai, T.M. Sridhar and S.V. Narasimhan, "Surface Characterization and Pitting Behavior of High Cr-Ni-Mo Alloys in Simulated White Water Environemnt," Corrosion, **v. 57**, p.465 (2001).

M. Pourbaix, Atlas of Electrochemical Equilibria in Aqueous Solutions," NACE, Houston, TX (1974).

R.L. Cowan and R.W. Staehle, "The Thermodynamic and Electrode Kinetic Behavior of Nickel in Acid Solution in the Temperature Range 25°C to 300°C," Journal of the Electrochemical Society, **v. 118**, p.557 (1971).

L.J. Oblonsky and T.M. Devine, "Surface Enhanced Raman Spectra from the Films Formed on Nickel in the Passive and Transpassive Regions," Journal of the Electrochemical Society, **v. 142**, p. 3677 (1995).

V. Schroeder and T.m. Devine, "SERS during the Galvanostatic Reduction of the Passive Film on Iron," Journal of the Electrochemical Society, **v. 146**, 4061-70 (1999).

I.Olefjord, B. Brox, and U. Jelvestam, "Surface Compossition of Stainless Steels during Anodic Dissolution and Passivation Studied by ESCA," Journal of the Electrochemical Society, **v. 132**, p.2854 (1985).

C.R. Clayton and Y.C. Lu, "A Bipolar Model of the Passivity of Stainless Steel: The Role of Molybdenum Additions," Journal of the Electrochemical Society, **v. 133**, p.2465 (1986).

A.R. Brooks, C.R. Clayton, K. Doss and Y.C. Lu, "On the Role of Cr in the Passivity of Stainless Steel," Journal of the Electrochemical Society, **v. 133**, p.2459 (1986).

C.S. Kumai and T.M. Devine, "Oxidation of Iron in Oxygen-Containing Water at 288°C," Corrosion 2001, Paper #01149, NACE, Houston, TX (2001).

C.S. Kumai and T.M. Devine, "Oxidation of Fe-Ni-Cr Alloys in Oxygen-Containing Water at 288°C," Corrosion 2001, Paper #01150, NACE, Houston, TX (2001).

A.J. Davenport, J. A. Bardwell, C. M. Vitus, J. Electrochemical Society, **v. 142**, 721 (1995).

H. Chaung, J.B. Lumsden and R.W. Staehle, "Effecct of Segregated Sulfur on the Stress Corrosion Susceptibility of Nickel," Metallurgical Transactions A, **v. 10A**, p.1853 (1979).

D.A. Vermilyea, C.S. Tyedmon and D.E. Broecker, "Effect of Phosphorus and Silicon on the Intergranular Corrosion of a Nickel-Base Alloy," Corrosion, **v. 31**, p.222 (1975).

C.L. Briant, "Interfacial Segregation in Nickel Base Alloys: A Report to the Yucca Mountain Peer Review Panel," January 21, 2002 (Waste Package Materials Performance Peer Review: A Compilation of Special Reports, Section 20, May 2002)

A.Turnbull, "Localized Corrosion: Chemistry and Radiolysis Effects," Waste Package Materials Performance Peer Review: A Compilation of Special Reports, Section 8, May 2002.

K. Mon, "Waste Package Degradation Studies at the Yucca Mountain Potential High-level Nuclear Waste Repository," YMP Senior Materials Science Panel Meeting, LLNL, January 24, 2002.

R.S. Glass, G.E. Overturf, R.A. Van Konynenburg and R.D. McCright, "Gamma Radiation Effects of Corrosion – I. Electrochemical Mechanisms for the Aqueous Corrosion Processes of Austenitic Stainless Steels Relevant to Nuclear Waste Disposal in Tuff," Corrosion Science, **v. 26**, p.577 (1986).

D.D. Macdonald, "Passivity: The Key to Our Metals-Based Civilization," Pure and Applied Chemistry, **v. 71**, p.951 (1999).

R.A. Rapp, "High Temperature Corrosion Perspectives on Alloy Corrosion in the Burial of Radioactive Waste," Subject Matter Report, November 1, 2001 (Waste Package Materials Performance Peer Review: A Compilation of Special Reports, Sections 5 and 19, May 2002).

T. Lian, J. Estill, G. Hust, D. Fix, C. Orme and J. Farmer, "Evolution of Corrosion Potential," YMP Senior Materials Science Panel Meeting, LLNL, January 24, 2002.

S. Barnartt, "Linear Corrosion Kinetics," Corrosion Science, **v. 9**, p.145 (1969).

F. Mansfeld and K.B. Oldham, "A Modificatiion of the Stern-Geary Linear Polarization Equation," Corrosion Science, **v. 12**, p. 434 (1971).

F. Mansfeld, "Tafel Slopes and Corrosion Rates from Polarization Resistance Measurements," Corrosion, **v. 29**, p.397 (1973).

D.D. Macdonald, "An Impedance Interpretation of Small Amplitude Cyclic Voltammetry," Journal of the Electrochemical Society, **v. 125**, p.1443 (1978).

R.L. Leroy, "The Range of validity of the Linear polarization Method for Measurement of Corrosion Rates," Corrosion, **v. 29**, p.272 (1973).

K.B. Oldham and F. Mansfeld, "On the So-Called Linear Polarization Method for Measurement of Corrosion Rates," Corrosion, **v. 27**, p.434 (1971).

F. Mansfeld and M. Kendig, "Concerning the Choice of Scan Rate in Polarization Measurements," Corrosion, **v.37**, p.545 (1981).

D.W. Townley, "Determination of aximum Scan Rtae for Linear Polarization Measurements," Corrosion, **v. 47**, p.737 (1991).

J.R. Scully, "Polarization Resistance Method for Determination of Instantaneous Corrosion Rates," Corrosion, **v. 56**, p.199 (2000).

Summary of Recent Alloy 22 Corrosion Potential Data, Preliminary Predecisional Draft, June 21, 2001.

C.Y. Chao, L.F. Lin and D.D. Macdonald, "A Point Defect Model for Anodic Passive Films, I. Film Growth Kinetics," Journal of the Electrochemical Society, **v. 128**, p. 1187 (1981).

L.F. Lin , C.Y. Chao and D.D. Macdonald, "A Point Defect Model for Anodic Passive Films, II. Chemical Breakdown and Pit initiation," Journal of the Electrochemical Society, **v. 128**, p. 1194 (1981).

C.Y. Chao, L.F. Lin and D.D. Macdonald, "A Point Defect Model for Anodic Passive Films, III. Impedance Response," Journal of the Electrochemical Society, **v. 129**, p. 1874 (1982).

M. Urquidi-Macdonald and D.D. Macdonald, "Transients in the Growth of passive Films on High Level Nuclear Waste Canisters," Proc. Int. Workshop Pred. Long-Term Corros. Behav. Nucl. Waste Systs., Cadarache, France, Nov. 26-29, 2001.

10. Inhibition of Localized Corrosion by Non-Halide Anions

Roger C. Newman
UMIST, Corrosion and Protection Centre
Manchester, UK

EDITORIAL NOTE

This volume, "A Compilation of Special Topic Reports," contains a series of reports that were prepared for the Waste Package Materials Performance Peer Review Panel to use as background and input to the peer review. Summaries drawn from the reports were also presented in Section 11 of the Panel's Final Report. The Panel used the reports as background and input for its review. Any views and comments expressed in the summaries and the full reports do not necessarily reflect the opinion and findings of the Panel. Further, opinions expressed in the reports are not necessarily those of the Panel or reflected in the Panel's reports and recommendations.

Summary

Localized corrosion of stainless steels or nickel-base alloys is inhibited by non-halide anions (except aggressive sulfur compounds) according to well-defined rules. A number of anions will inhibit pitting if their concentration is comparable with that of chloride. A few appear to be relatively ineffective, such as bicarbonate. Hydroxide anions are more effective owing to their higher mobility in corrosion sites and perhaps also their simple mode of action (neutralization of the acidic local solution). When the temperature is increased or a crevice is introduced, the required amount of inhibitor increases.

The most persuasive explanation of these inhibitor effects is based on Galvele's pitting theory and involves competitive electromigration of anions into a dissolving pit nucleus.

Nitrate, in particular, shows inhibition of pitting over a range of potentials. Artificial-pit studies show that nitrate only stifles pit dissolution when an anodic salt film has been precipitated, i.e. at high potentials. To some extent, sulfate shows analogous behavior, but only in a critical range of concentration. Since there is a large amount of nitrate in Yucca Mountain, this kind of phenomenon is very important for the corrosion assessment.

Lack of discrimination between possible crevice-corrosion initiation mechanisms (metastable pitting or passive dissolution) is hindering the crevice corrosion assessment in this area.

It should not be assumed that fluoride is an aggressive anion. It may be an inhibitor of localized corrosion.

Special Topic Report prepared for the Waste Package Materials Performance Peer Review. The Final Report of the Peer Review was submitted to U.S. Department of Energy and Bechtel SAIC Company, LLC on February 28, 2002.

Localized corrosion can be inhibited very effectively if the oxygen reduction reaction is shut off. This may occur naturally in Yucca Mountain.

HISTORY AND GENERAL CONSIDERATIONS

Electrochemical investigation of the localized corrosion of stainless steels was undertaken much earlier than is commonly believed. In 1939 Uhlig and Wulff [1] already showed clearly that pitting occurred above a critical potential, explored the effects of Mo alloying, and compared different halide ions. The electron theory of passivity was already used to interpret the results. In the same period, Uhlig was aware of inhibiting effects, at least for OH^- and NO_3^- , but comprehensive study of these had to wait until the late 1960s.

Other classic studies of pitting followed in the 1950s, notably the work of Streicher [2] who devoted some effort to the effect of nitrate as an inhibitor of pitting. He stated:

The nitrate probably does not completely prevent breakdown of the surface but acts to heal rapidly and effectively all points which are beginning to break down and, thereby, prevents the formation of pits.

This strikingly modern interpretation contrasts with that proposed by Uhlig himself in the 1960s. According to Leckie and Uhlig [3], passivity was due to an alteration of the surface electronic configuration of the metal, pitting was due to adsorption of Cl^- on this oxide-free surface (replacing what he called "oxygen", or OH), and inhibition of pitting was due to occupation of those same sites by the inhibiting anion. Such interpretations can still be found in the literature of the last decade, though usually it is admitted that a passive film exists on the metal surface, and the competitive adsorption is believed to occur on the surface of this oxide film. But in 1976 Galvele had already provided a quantitative theory of pitting and its inhibition, which was developed further over the next decade [4-10]. According to this very testable theory, pit "initiation" or "nucleation" is the result of an anodic dissolution process occurring at a pre-existing flaw in the passive film, and a sufficient condition for pit stability (at least initially) is that the dissolution rate (determined by the metal composition, applied potential, IR drop, anions, temperature, etc.) is enough to produce a sufficient degree of acidification in the cavity. Pit inhibitors provide an important test of Galvele's pitting model. Most of his corroborative experimental work was done using inhibitors that act directly upon the pH: OH^- , or weak-acid anions like borate. But even in 1976 he discussed the competitive enrichment, by electromigration, of anions within a rapidly dissolving pit nucleus, and speculated that doubly charged anions would be particularly effective inhibitors, using sulfate as an example. Although Galvele preferred to talk in terms of lowering of pH rather than enrichment of aggressive halides in a pit, it was clear that he knew a high enrichment of sulfate, relative to chloride, would have a passivating tendency. We shall return to this point later in this review.

Actually sulfate is a buffer anion, since the pH of a pit on stainless steel or aluminium is lower than the pK_a value for sulfate/bisulfate (1.9), but Galvele was not working with the

assumption of extremely low pH values in pits – he assumed initially that pits would be stable if the equilibrium concentration of dissolved metal cations was greater than 10^{-6}M, which for Cr would be about pH 3 or 4. Perchlorate is an interesting case examined by Leckie and Uhlig – a strong-acid anion that inhibits pitting. Perhaps the normally electro-inactive perchlorate becomes reducible within an anodic salt film, in which case it resembles nitrate rather than sulfate.

Log-Log Relationships for Pitting Inhibition and Their Interpretation

Inhibitors of pitting were reviewed by Smialowska in her 1986 book on pitting corrosion [11]. Unfortunately the presentation of this topic was marred by typographical or algebraic inconsistencies, with the coefficients *a* and *b* in the following kind of equation being used in two different ways in tables and text:

$$\log C_{ag} = a \log C_i + b$$

where C_{ag} is the maximum concentration of aggressive anion tolerated at a concentration of inhibiting anion C_i. When defined as above, it is found that *a* is about 1 and *b* is about 0 for a number of anions at room temperature - that is, the concentration required to inhibit pitting effectively is about the same as the chloride concentration . Sulfate is an example of this kind of anion. Other anions are rather more effective, such as nitrate which has a positive value of *b*, and hydroxide which has a *b* value between 1 and 2 - that is, less than a tenth of the molar concentration of hydroxide is required to inhibit pitting, compared with a common-or-garden anion like sulfate (an accurate value is about 1/30). A number of studies have been done showing that stainless steel is more tolerant of chloride than carbon steel in high-pH solutions or cements [12,13], and the effects of pH on pitting have been used constructively by a number of authors, either to make corrosion assessments or to suggest inhibition procedures [14].

The fact that carbon steel and stainless steel behave similarly with respect to inhibition in high-pH solutions or cements is one of many pieces of evidence that one need not take elaborate account of the nature of the passive film on stainless steel when predicting localized corrosion. Smialowska also reviews the inhibition of carbon-steel corrosion by anions such as nitrite, chromate, phosphate, benzoate, and so on, and displays the similarities between this behavior and that of stainless steel. All these inhibitors act upon the pitting process that initiates passivity breakdown, but in the case of carbon steel there is the additional factor that the metal has an active dissolution peak in neutral solution; the same compounds may enable an initially film-free surface to passivate, usually via slightly different rules (for example, benzoate is less good at suppressing the anodic active peak than at maintaining the repair of a pre-existing air-formed oxide).

At higher temperatures, more inhibitor is required as we would expect, and important work has been done on this topic, showing that whilst high potentials may induce pitting even at low chloride levels, useful elevations in pitting potential still occur at about the same ratios of chloride to inhibiting anion as those that suppress pitting at ambient temperature [15-17]. Obviously this subject is not exhausted, and some systematic data development for a simple Ni base alloy in the range 0-100^{o}C would be helpful. Doing this on the C-22 alloy would require

autoclaves and may not give any more information, since crevices are more relevant than pits for C-22.

The general form of the inhibition equation does not change for different stainless alloys.

The utility of generalized inhibitor-chloride relationships has been demonstrated by a number of authors. Disappointingly, there appears to be no really clean study of the effect of temperature on the inhibition criteria for a variety of anionic inhibitors, but there are several useful studies of the effects of sulfate as a function of temperature, e.g. by Hakkarainen whose context was papermaking [18-20]. Those developing neural network approaches for the prediction of localized corrosion are working with reasonable but limited databases at present. The data for basic grades of stainless steel from 20 to 60^{o}C are fairly densely packed and permit adequate predictions [21].

The inhibition equation says different things to different people. It is very understandable that those convinced of the importance of anion adsorption in the pitting process will see the equation as evidence of a competitive adsorption mechanism. However similar equations arise naturally from Galvele's reaction-transport approach to pitting. A pit is a net anode with a concentrated anolyte, and anions in the bulk solution migrate into the pit in proportion to their concentration and mobility. In this respect, the high value of *b* for OH^- is a natural consequence of its higher mobility compared with an anion like sulfate or chloride, though clearly since D_{OH} is less than five times D_{SO4}, some modeling will be required to show that the 30x increase in efficiency is reasonable.

A number of citations suggesting competitive adsorption on the passive film as the basis of inhibition are also included, even though the present author considers this to be a blind alley for interpretation of the inhibition problem [22,23]. Some very eminent corrosion scientists have gone down this path, extending the well-known behavior of iron or carbon steel in neutral solutions containing inhibiting and aggressive anions (which has also been ascribed to competitive adsorption), but it is extremely likely that the Galvele approach will prove to be the right one for all these systems - carbon steel and stainless steel, and for that matter aluminum. Rather than attempt a comprehensive analysis, we simply suggest that any system showing a *similar effect of an inhibitor on pit repassivation to its effect on pit initiation* should be classed in the "Galvele" category. "Similar" in this context means "analogous" - we do not expect the repassivation potential to be equal to the pitting potential, or the critical environments to be equal. Rather, we expect that deeper cavities will always be harder to inhibit and will show lower critical potentials or temperatures, or high amounts of required inhibitor.

Careful experimentation by French authors [24] gave results that were considered to support, potentially, a variety of inhibition mechanisms including effects on oxide-surface adsorption and diffusion through the passive film. In this and other work related to adsorption effects, the authors did not consider the Galvele model at all, perhaps understandably because Galvele really only considered pH effects, and it is not immediately obvious how anions such as sulfate, perchlorate and nitrate achieve this. One might also speculate that some scientists are unwilling to abandon the idea of the passive film as an intact entity that has to be 'broken down'

by chloride, ignoring effects of non-metallic inclusions whose dissolution will lead eventually to exposure of metal in any case.

It has been very popular to compare the effect of alloyed Mo with the effect of dissolved MoO_4^{--} [e.g. ref 25], even though molybdate is no more effective than a variety of other inhibiting anions that have no analog within the alloy. One conclusion reached by a number of authors is that MoO_2 may be an important solid stifling compound, as shown beautifully by Wanklyn some 20 years ago [26].

An unresolved issue in Galvele's approach is the actual kinetics of the metal in the localized environment. Galvele assumes that once the dissolved metal ion is more stable than solid species, dissolution can proceed at an arbitrarily high rate - and this rate does need to be very high to sustain pitting, certainly on the order of A/cm^2. For aluminium, or for Cr alloys such as stainless steel, the affinity of the metal for oxygen is such that the dissolution rate can only reach this kind of value in highly acidified, concentrated chloride solutions [27]. An important aspect of this is the steep increase in mean ionic activity coefficient as the metal salt concentration increases in the range of one to a few molal, which enhances the drop in pH and facilitates the replacement of surface OH by Cl. In most case this means that a correction would be required to Galvele's model that would require a more concentrated local solution (and thus a higher product of pit nucleus depth and anodic current density, Galvele's *"x.i"* criterion). The easiest way to rationalize this is to propose that real metal surfaces have much deeper and/or tighter micro-crevices than were assumed by Galvele in the accompanying text to his papers on his pit model. Pitting of very flat surfaces such as sputtered thin films is an important way to resolve such issues.

When the amount of inhibitor is insufficient to inhibit pitting at all potentials, there is a relationship between pitting potential and buffer anion addition (or OH^- addition) at constant chloride concentration, along the lines of

$$E_{pit} = A + B \log [C_i]$$

Galvele showed that such a relationship arose naturally from his pitting model. Other authors have not realized that such a relationship exists, and have carried out pitting studies in buffered solutions as a function of chloride concentration [e.g. refs 28,29]. This is bound to be misleading if it involves the assumption that the buffer anion was simply controlling the bulk pH and had no inhibition role in competition with chloride.

Role of Anodic Salt Films

Galvele was not able to model the effect of sulfate or nitrate, but as mentioned earlier, he hinted that the operative mechanism involved a large accumulation of the non-chloride anion. In this case we are in similar territory to that discussed in the accompanying review on temperature effects: the trajectory of the pit pH might not be greatly altered by the presence of the other anion, but we introduce a strong tendency for passivation if and when an anodic salt film is precipitated, especially if this film is dominated by the iron salt of the non-chloride anion. Such

phenomena were demonstrated by Ezuber some years ago [30] for 304SS in chloride/sulfate solutions. When sulfate was injected into a growing pencil electrode (artificial pit), dissolution was stable if the potential was *high* enough (an interesting difference from nitrate, as mentioned below). Upon reducing the potential, passivation occurred directly from the salt-covered state above a certain level of added sulfate. The amount required to cause this effect would not be the same in a small pit nucleus dissolving at a much higher rate, but by extrapolation one could rationalize the critical chloride/sulfate ratio for pit initiation, at least qualitatively. Recently Pistorius and Burstein [31] studied the properties of the anodic salt films formed in chloride/sulfate media and confirmed that they had a mixed character; Ernst [32] has also shown differences in diffusion-controlled pit growth rate and pit repassivation and undercutting behavior due to sulfate addition.

A result of some generality emerges from the study of sulfate effects and temperature effects: that the anodic $FeCl_2$ salt film formed in a pit can become an intermediary in passivation (rather than a stabilizing factor in pitting) upon reducing the temperature or adding a competing anion. The more the situation under the salt film resembles that of iron in sulphuric acid, the more likely it is that the result will be the same, i.e. salt precipitation followed by passivation by reaction with water under the salt film. According to Beck [33] this kind of protection occurs because H_3O^+ ions migrate out of the salt film faster than they are replenished by diffusion from the pit solution, thus neutralizing the pore solution within the salt film and facilitating passivation.

A very surprising result emerges when the pitting of a high-alloy steel (904L) is studied in chloride/sulfate mixtures as a function of temperature [34]. Sulfate actually *lowers* the critical pitting temperature (CPT), provided this is defined in a sufficiently subtle way. In the presence of sulfate, pitting that initiates at intermediate potentials and would normally be metastable becomes exceptionally stable, giving rise to a smooth peak in anodic current. If the CPT test is carried out at very high potential, no difference is seen between chloride and chloride/sulfate solutions, but if the test is carried out in the region of the current hump, stable pitting only occurs in the presence of sulfate. It was shown that the stable pits occurring in this region were growing under the metal surface in an exceptionally occluded way. A pitting inhibitor, by challenging the stability of pitting, can "force it underground" leading to a slow rate of opening of the pit mouth and a stable propagation. A similar observation was made by Ernst [32], and she also speculated that under certain conditions pitting stability might show an inverse dependence on temperature, though the practical significance of this is not clear.

Nitrate Effects

Nitrate is a fascinating inhibitor for pitting of stainless steel, with apparently bizarre behavior that nevertheless can be incorporated into a rational overall model of the inhibition process. It is a very important component of the Yucca Mountain environment. At this point we consider nitrate as unique in its behavior and in the depth with which it has been studied, but there may be other reducible anions (molybdate, nitrite, even perchlorate) with similar inhibition mechanisms.

Streicher established some of the features of nitrate inhibition in 1956 [2], but the first systematic study was that of Leckie and Uhlig [3]. The present author is confused by a historical point hereabouts. Leckie showed beautifully that chloride/nitrate mixtures exhibited pitting over a *range of potentials*, with this range contracting as the nitrate concentration was increased: eventually pitting vanished at all potentials. This observation raises a number of theoretical and practical points:

> Why did Uhlig maintain his adsorption-based model of pitting inhibition (Cl^- versus OH^- ["oxygen"] versus X^-) when it must have been apparent that pits in nitrate solution, once initiated at low potential, would repassivate upon the application of a higher potential? In other words, when passivity has already broken down and the metal is dissolving at some A/cm^2, pitting can be arrested by increasing the potential. This surely argues for a mechanism based on local reaction and transport in the special pit environment, albeit adsorption might be involved in some way, but certainly not the *same* way as in the initiation stage from a pristine passive surface.
>
> Depending on the definition of critical potentials for pitting, and on the test procedure applied, one might come to radically different conclusions about the effect of nitrate. For example, a highly oxidizing environment might more benign than a mildly oxidizing one. This was illustrated by Herbsleb and Schwenk [35,36] who showed that anodic galvanostatic tests (giving very high anodic potentials) required only a trace of nitrate to inhibit pitting.
>
> There is an opportunity to unify the effect of nitrate with that of temperature, noting that a similar peak in pitting activity at intermediate potentials occurs below the CPT for high-alloy steels [37-39]. Such behavior indicates that the metal is adopting an anodic active-passive transition in the local environment of the pit: in fact this is a natural type of behavior, and perhaps it surprising that this is not seen more often in localized corrosion situations (it is well known for titanium but obscure for stainless steel).

Like many other aspects of localized corrosion, the nitrate effect yields some of its secrets when investigated by the artificial pit or pencil electrode technique [40]. This study initially showed that 304SS at room temperature was not unconditionally stable when undergoing diffusion-controlled anodic dissolution in a pit with a bulk solution of 0.1M NaCl. This had not been observed before, e.g. by Tester and Isaacs [41], because those workers had used much thicker wires to make their pencil electrodes. Irregular oscillatory behavior was observed, and later shown by Laycock to involve period doubling and other interesting dynamic features [42]. When the temperature was increased to 55^oC, the oscillations disappeared. The oscillations were interpreted as reversible passivation events under the salt film. For nitrate/chloride molar ratios up to 0.4, no passivation by nitrate was ever observed on a surface free from a salt film, but nitrate stabilized the passivation tendency that was already present without nitrate. A pit could be grown stably at low potential, irrespective of the nitrate concentration, with a current density of 80-100% of the anodic diffusion limit, but upon increasing the potential, passivation would either occur immediately from the supersaturated state upon salt precipitation (at the higher

nitrate levels) or would occur at a somewhat higher potential from the salt-covered state (for the lower nitrate levels).

These observations of Ajjawi clearly show that the nitrate problem reduces to one of passivation under an anodic salt film. It was speculated that whilst nitrate lacks electroactivity in ordinary aqueous solutions (at least at ambient temperature), it becomes much more reactive in the low water activity of the salt film environment. Thus a redox reaction occurs between nitrate and ferrous ions, leading to a rise in pH and solid products that stifle pitting (whether this constitutes true passivation is an interesting issue - in Ajjawi's work a residual anodic current was often observed for a long time after adding an inhibiting amount of nitrate).

While nitrate has its own special passivation mechanism, we should not lose sight of the common features of nitrate and sulfate inhibition: passivation under a salt film, and competitive electromigration with chloride.

The peculiar nature of nitrate inhibition lends itself to galvanostatic methods of evaluation, or at least flexible methods, since potentiostatic methods can be misleading [43].

Special Features of Nickel Base Alloys

Generally nickel base alloys appear to behave the same as stainless steel in response to inhibiting anions, even in complex electrolytes [44,45].

At high temperatures and pressures, nickel becomes able to reduce sulfate ions, and the reduction products such as sulfide can catalyse nickel corrosion [46-48]. This is well known in the nuclear power industry but not always cited in work on waste issues. Whether this is relevant to the Yucca Mountain repository remains to be seen.

Otherwise nickel base alloys behave like stainless steel as would be expected if the Galvele model were to be operating [49]

The interest in nickel base alloys as steam generator tubing materials has prompted research on their pitting behavior (since ingress of traces of chloride and copper ions used to cause occasional failures in PWR steam generators) [17], and often such studies have used mixtures of chloride and sulfate [50], but no systematic study is available on different chloride/sulfate ratios.

Crevice chemistry studies have shown promising inhibiting effects of sulfate in chloride-rich media [51], but this must be balanced against the general feeling in the nuclear power industry that sulfate is an aggressive anion because of reduction to sulfide.

Ineffective Anionic Inhibitors

In principle, bicarbonate should be just as effective as sulfate or any other buffering type of inhibitor (we include sulfate as a buffer because the pK_a of sulfate/bisulfate is 1.9, which is well above the pH of a pit on stainless steel). In fact bicarbonate is a rather bad inhibitor. Not much has been published on this topic, but it appears from the literature, and from unpublished work by Ezuber at UMIST, that the bicarbonate/chloride ratio for effective inhibition may be at least 3 [52-54]. This may be due to the special kinetics of the CO_2/water system. It is well known that the hydration of CO_2 is a slow reaction, compared with the fast processes that are involved in pit initiation, and it may be that the consumption of protons by bicarbonate is also slow in that it will become limited by accumulation of carbonic acid that only slowly dehydrates to yield CO_2. This deserves attention from those more qualified than the present author.

It has been reported that bicarbonate, because of its relatively inert nature, can actually enhance pitting of stainless steel welds, perhaps by increasing the solution conductivity [55].

Crevice Corrosion Inhibition

The inhibition of crevice corrosion is a somewhat treacherous field, since it is probably even more dependent on crevice geometry than the other properties of crevice corrosion, such as critical temperature or critical potential. However we can attempt some generalizations, and there are some useful data in the literature.

In high temperature water the anion enrichment processes are subtle, yet some of the most distinguished work in the field of crevice chemistry was done in such environments [56].

It is frequently found that 304SS is unsuitable for chloride levels in the range of a few hundred ppm, such as those in paper machines. When upgrading to 316SS, it is important to be aware of possible crevice effects that may nullify the advantages of the more highly alloyed material. Fortunately, paper-machine white water contains significant levels of sulfate, and this provides just enough inhibition to qualify 316SS for most situations that might be encountered. In the course of investigating this issue, it was found that the sulfate to chloride ratio required for complete inhibition of crevice corrosion, at all potentials, was higher than for pitting; however modest levels of sulfate gave a good elevation in critical potential. This highlights the fact that we may not need to inhibit localized corrosion at *all potentials* to get a sensible improvement in alloy performance. In principle, it is sufficient to elevate the critical potential for crevice corrosion above the long-term corrosion potential. The difficulty is that one has little confidence in the long-term (10^4 years) meaning of the critical potentials!

It is difficult to assess the current state of knowledge for crevice corrosion initiation in complex electrolytes, since there is a poorly publicized crisis in basic crevice corrosion theory. Different schools consider that crevice corrosion is initiated by, on the one hand, metastable pitting occurring at special locations in the crevice, and on the other, passive dissolution occurring in the crevice. Both are supposed to lead to active dissolution by injecting acid into the crevice. These are very different theories, and there is very little concrete evidence to distinguish

between them. The passive-dissolution theory has difficulty explaining the potential dependence of crevice corrosion, or the existence of long initiation times that are hundreds or thousands of times the characteristic time for diffusion into the crevice (in concentrated solutions where one cannot ascribe this time to the completion of a migration process). There is also little evidence for gradual acidification in crevices on stainless steel. The metastable pitting theory has some supporting evidence, but its predictions are unclear especially for complex electrolytes.

Some studies of crevice corrosion inhibition have emerged from the nuclear waste programs in several countries. At the Southwest Research Institute a theoretical and experimental approach was developed to handle mixed-electrolytes, based on empirical measurements of kinetics [57,58].

Good progress was made by Brossia and Kelly using their solution-analysis approach for nitrate inhibition of crevice corrosion [59], and similar work is continuing. They noted that sulfate operated by a "supporting electrolyte" effect (restricting chloride enrichment), while nitrate had a more complex, reactive role. Other work on nitrate inhibition of crevice corrosion or deep pitting has shown that rather large amounts of nitrate may be required for inhibition [60].

If we assume for the moment that crevice corrosion always initiates by metastable pitting, then it is easy to rationalize the lower critical temperatures and critical potentials compared with stable pitting, since metastable pitting occurs at much lower temperatures and potentials than stable pitting. This is especially noticeable for alloys such as 904L which will crevice-corrode at 15^{o}C. When we add a non-chloride anion, the situation becomes quite confusing. According to work done in the 1980s in UMIST [61], the addition of an inhibitor selectively suppresses the faster-growing metastable pits, but the meaning of this observation was and is unclear. To initiate crevice corrosion, a metastable pitting event needs to be in a special location and not to be especially fast. Following this argument to its logical conclusion, we cannot be confident of immunity to crevice corrosion until there are no metastable pitting events at all. For the C-22 alloy at temperatures around 80^{o}C, this may be a realizable result; alternatively it may be possible to show that crevices initiated at some higher temperature cannot propagate at the temperature of interest. In either case, it is of the utmost importance to be alert to the possibility that localized corrosion may be favored within a *range of potential*, not just above some "critical" potential. For nitrate this does not need emphasis, but even for sulfate there is evidence of similar behavior, as outlined earlier.

It is precisely in the borderline conditions of temperature, anionic content and potential that the greatest care needs to be taken to ensure that no region of localized corrosion susceptibility has been missed. It is exactly those conditions that are most likely to lead to active-passive transitions *within the crevice environment*. We also need to be alert to the possibility that inhibited (nitrate-chloride) mixtures may cause unusually slow but persistent localized corrosion.

Fluoride

The groundwater at Yucca Mountain contains a significant concentration of fluoride ions. Many scientists would identify this as an aggressive species, but this is not at all certain for

localized corrosion of stainless steel. Since HF is a weak acid, fluoride may act as an inhibitor of pitting, Whether it will truly have a beneficial action, taking all factors into account, is not certain - for example, it may stabilize peroxide by chelating heavy-metal ions, enhancing the effect of radiolysis on the corrosion process, and it can cause a certain level of uniform corrosion of titanium.

Organic Inhibitors

It is often stated that organic compounds, when added in a concentration low compared with that of chloride, have no effect on the pitting potential. This is entirely reasonable, although one might have anticipated that certain inhibitors might affect the dissolution of manganese sulfide inclusions and hence the likelihood of pitting. Sometimes such inhibitors are stated to have affected the rate of pit growth, as assessed (usually) by the rate of increase of current above the pitting potential. It is not always clear whether the number of pits has been separated from the rate of individual pit growth when such statements are made.

Some of this work is interesting [62-64] and would repay further investigation, but probably the most important aspect of organic compounds is their ability to affect the oxygen reduction reaction.

Cathodic Inhibitors

Corrosion scientists working on stainless steel or aluminum often ignore the cathodic reaction, especially (paradoxically) those trained in electrochemistry. But if we take a long view and take account of recent advances in surface chemistry, reliable inhibition of localized corrosion in industrial systems is likely to emerge from the inhibition of the oxygen reduction reaction. This in turn may well involve the science of self-assembled monolayers. Whilst such compounds are unlikely to be used in Yucca Mountain, we must pay particular attention to the long-term kinetics of oxygen reduction, and it would be folly not to exploit to the full the samples that have been immersed for periods of years in various actual or simulated YMP environments.

In the present author's opinion, it is entirely possible that localized corrosion will be self-inhibited in the long term because oxygen reduction will cease as the passive film thickens or substances are deposited on top of it. This possibility may deserve some attention.

Inorganic cathodic inhibitors such as rare earth salts have been investigated in both pre-treatment and addition modes [65-67]. This field seems to be rather competitive, and some of the findings give no clue as to the long-term performance of such treatments. However this type of treatment deserves attention, if only because substances naturally present in the Yucca Mountain environment may have similar effects.

Evaporative Environments

This review has not considered one of the most important aspects of the Yucca Mountain corrosion problem - that of corrosion in thin liquid layers. The contractors working on the DOE program have much of this in hand, and sporadic literature is available from the 1980s and early 1990s [68].

Much depends on the fate of inhibitive anions in these thin liquid layers, and as the physical chemistry of this situation is quite complex, directed experimentation using simplified model electrolytes is essential.

Conclusions

1 For pitting at smooth surfaces, there is a well-defined log-log relationship between inhibiting anion and chloride concentrations for complete inhibition of pitting at all potentials.

2 This relationship is consistent with either an adsorption or a mass transport (electromigration) process as the critical factor in inhibition, but other evidence overwhelmingly supports the latter interpretation -for example, the results of metastable pitting studies.

3 Not much is known about mixed-inhibitor systems.

4 Bicarbonate is a poor inhibitor, probably because of slow solution-phase reactions involving carbonic acid.

5 When moderate concentrations of a pitting inhibitor are present, one should not be surprised to see pitting or even crevice corrosion occurring over a range of potentials. This has important implications for testing.

6 There are cases documented where addition of an “inhibitor” has promoted localized corrosion of stainless steel.

7 In general, crevice corrosion requires a higher concentration of inhibitor than pitting, to eliminate corrosion at all potentials, but the concentration required for reasonable inhibition at realistic potentials may be accessible.

8 If the cathodic reaction ceases on the oxidized metal surfaces exposed in Yucca Mountain, so will corrosion.

References

1. H.H. Uhlig and J. Wulff, Trans AIMME, **135**, 494 (1939).

2. M.A. Streicher, J. Electrochem. Soc., **103**, 375 (1956).

3. H.P. Leckie and H.H. Uhlig, J. Electrochem. Soc., **113**, 1262 (1966).

4. J.R. Galvele, J. Electrochem. Soc., **123**, 464 (1976).

5. J.R. Galvele, Corros. Sci., **21**, 551 (1981).

6. A.D. Keitelman and J.R. Galvele, Corros. Sci., **22**, 739 (1982).

7. J.R. Galvele, in Pitting Corrosion, in Treatise on Materials Science and Technology. **Vol. 23**. Corrosion: Aqueous Processes and Passive Films, pp. 1-57, Academic Press, London (1983).

8. A.D. Keitelman, S.M. Gravano and J.R. Galvele, Corros.Sci., **24**, 535 (1984).

9. S.M. Gravano and J.R. Galvele, Corros. Sci., **24**, 517 (1984).

10. M.G. Alvarez and J.R. Galvele, Corros. Sci., **24**, 27 (1984).

11. S. Szklarska-Smialowska, Pitting Corrosion of Metals, NACE, Houston (1986).

12. L. Bertolini, F. Bolzoni, P. Pedeferri and T. Pastore, Br. Corros. J., **31**, 218 (1996).

13. Z. Chaudhary, Dissertation Abstracts International, **52**, no. 11, p. 336, May 1992.

14. G. Bellanger and J.J. Rameau, Corros. Sci., **40**, 1985 (1998).

15. H. Yashiro, A. Oyama and K. Tanno, Corrosion, **53**, 290 (1997).

16. H. Yashiro, H. Kami, T.Kosaka and K. Tanno, Zairyo-to-Kankyo (Corrosion Engineering), **42**, 152 (1993).

17. G. Cragnolino, "A Review of Pitting Corrosion in High-Temperature Aqueous Solutions," in Advances in Localized Corrosion, pp 413-431, NACE, Houston (1990).

18. T.J. Hakkarainen, "Stainless steels in chlorine dioxide environments - predicting the possibility of pitting," Paper #588, Corrosion/2000, NACE, Houston (2000).

19. T.J. Hakkarainen, "Conditions of growth of open corrosion pits in stainless steels--electrochemical experiments on model pits," Paper #310, Corrosion/98, NACE, Houston (1998).

20. T.J. Hakkarainen, "Use of artificial pits to investigate conditions for the growth and repassivation of open macroscopic corrosion pits in stainless steels," in Proceedings of Electrochemical Methods in Corrosion Research VI, Materials Science Forum (Switzerland), **vol. 289-292**, 955 (1998).

21. J. Gartland, G. Owen, R.A. Cottis and M. Turega, "Neural network methods for the prediction of pitting potentials," Paper #238, Corrosion/99, NACE, Houston (1999).

22. G. Trabanelli, Corrosion, **47**, 410 (1991).

23. Y. Kuznetsov, Zashch. Met., **31**, 229 (1995).

24. C. Lemaitre, B. Baroux and G. Beranger, "Role of oxyanions in the improvement of passivity," in Passivity of Metals and Semiconductors, Proc. Sixth Int'l. Sym. on Passivity--Part 1, pp 24-28, eds N. Sato and K. Hashimoto; Corros. Sci., **31**, 585 (1990).

25. S. Maximovitch, G. Barral, F. Le Cras and F. Claude, Corros. Sci., **37**, 271 (1995).

26. J.N. Wanklyn, Corros. Sci., **21**, 211 (1981).

27. R.C. Newman, Corrosion, **57**, 1030 (2001).

28. D.D. Macdonald, "Probing (and understanding?) the passive state," in Critical Factors in Localized Corrosion, eds G.S. Frankel and R.C. Newman, pp 1-35, The Electrochemical Society, Pennington, NJ, USA (1992).

29. K.-S. Lei, D.D. Macdonald, B.G. Pound and B.E. Wilde, J. Electrochem. Soc., **135**, 1625 (1988).

30. H. Ezuber, A.J. Betts and R.C. Newman, "Electrochemical Kinetics in Localized Corrosion Cavities," in Electrochemical Methods in Corrosion Research (conference, Zurich, 1988), Mater. Sci. Forum, **44-45**, pp. 247-258 (1989).

31. P.C. Pistorius and G.T. Burstein, Corros. Sci., **33**, 1885 (1992).

32. P.Ernst and R.C. Newman, Corros. Sci., **44**, 927 and **44**, 943 (2002).

33. T.R. Beck, J. Electrochem. Soc., **129**, 2412 (1982).

34. M.H. Moayed and R.C. Newman, Corros. Sci., **40**, 519 (1998).

35. W. Schwenk, Werkstoffe und Korros., **19**, 741 (1968).

36. G. Herbsleb and W. Schwenk, Werkstoffe und Korros., **24**, 763 (1973).

37. N.J. Laycock, M.H. Moayed and R.C. Newman, J. Electrochem. Soc., **145**, 2622 (1998).

38. G. Riedel, H. Werner and C. Voigt, Materials and Corrosion (Germany), **47**, 383 (1996).

39. J.M. Sykes and L.F. Garfias Mesias, Corros. Sci., **41**, 959 (1999).

40. R.C. Newman and M.A.A. Ajjawi, Corros. Sci., **26**, 1057 (1986).

41. J.W. Tester and H.S. Isaacs, J. Electrochem. Soc., **122**, 1438 (1975).

42. N.J. Laycock and R.C. Newman, "The use of pitting transients to test microscopic models of localized corrosion," Electrochemical Methods in Corrosion Research V, proceedings of conference, Sesimbra, Portugal, 1994, Materials Science Forum, **192-194**, 649-662 (1995).

43. V.I. Lomovtsev, A.P. Gorodnichii and A.B. Bykov, Protection of Metals, **29**, 28 (1993).

44. E.L. Hibner, "Laboratory Investigations on the Effect of calcium, magnesium, sulfite, sulfate, fluoride and Fly Ash on the Resistance of Nickel Alloys to Localized Corrosion in SO_2 Scrubber Environments," Corrosion/84, Paper #298, NACE, Houston (1984).

45. W. Bogaerts, P. Vanslembrouck and A. Van Haute, "Influence of bicarbonate, phosphate and sulfate on Localized Corrosion Phenomena in Hot Water Systems, in Industrial Water Treatment and Conditioning (conference, Liege, Belgium, 25-27 May 1983)," Editions CEBODOC, pp. 123-135, 1983 (also available from NACE, Houston).

46. T. Shibata and S. Fujimoto, Corrosion, **46**, 793 (1990).

47. D.A. Jones and J.P.N. Paine, "Corrosion and Electrochemistry of Alloy 600 in Organic Salts and Other PWR Secondary Water Contaminants, in Environmental Degradation of Materials," in Nuclear Power Systems--Water Reactors (Conference, Traverse City, Michigan, 1987), pp. 183-189, The Metallurgical Society/AIME, Warrendale, PA (1988).

48. P. Kritzer, N. Boukis and E. Dinjus, Corrosion, **54**, 689 (1998).

49. M.-Y. Chang and G.-P. Yu, Journal of Nuclear Materials, **202**, 145 (1993).

50. G.S. Was and D. Choi, D, Corrosion, **48**, 103 (1992).

51. I.-J. Yang, Corros. Sci., **33**, 25 (1992).

52. K. Zhou, H. Zhang and Y. Qiu, Materials Protection (China), **32**, 20 (1999).

53. J.J. Park, S.-I. Pyun, W.-J. Lee and H.-P. Kim, Corrosion, **55**, 380 (1999).

54. M. Drogowska, L. Brossard and H. Menard, J. Appl. Electrochem., **28**, 491 (1998); J. Appl. Electrochem., **27**, 169 (1997).

55. H. Wakahiro, N. Mitsuaki, A. Toshiro and N. Toshiro, "Corrosion resistance of stainless steel piping for water and hot water supply," Nisshin Steel Technical Report (Japan), **vol. 77**, pp. 25-40 (1998).

56. D.F. Taylor and C.A. Caramihas, J. Electrochem. Soc., **129**, 2458 (1982).

57. N. Sridhar, G.A. Cragnolino, J.C. Walton and D. Dunn, "Prediction of Localized Corrosion Using Modeling and Experimental Techniques," in Application of Accelerated Corrosion Tests to Service Life Prediction of Materials, pp 204-223, ASTM STP 1194 (1994).

58. G.A. Cragnolino and N. Sridhar, Corrosion, **47**, 464 (1991).

59. C.S. Brossia and R.G. Kelly, Corrosion, **54**, 145 (1998).

60. D. Herbert, G.O.H. Whillock and S.E. Worthington, "Zero resistance ammetry--its application in preventing the corrosion of stainless steel in cooling waters," in Electrochemical Methods in Corrosion Research V (conference, Sesimbra, Portugal, 1994), Materials Science Forum (Switzerland), **192-194**, #1, pp 469-476 (1995).

61. R.C. Newman and H. Ezuber: "Growth-rate distributions of metastable pits," Critical Factors in Localized Corrosion, G.S. Frankel and R.C. Newman, eds., pp 120-133, The Electrochemical Society, Pennington, USA (1992).

62. Z.-L. Tang, S.-Z. Song and Y.-K. Guo, Journal of Chinese Society for Corrosion and Protection (China), **18**, 168 (1998).

63. Z. Tang and S. Song, Corros. Sci., **34**, 1607 (1993).

64. X.J. Chen and M. Zhang, Mater. Prot. (China), **26**, 4 (1993).

65. A. Aballe, M. Bethancourt, F.J. Botana, M. Marcos, J. Perez and M.A. Rodriguez, "Green inhibitors, Rare earth based systems" [Inhibidores de escaso impacto medioambiental. Sistemas basados en tierras raras.], Revista de Metalurgia (Spain), **33**, 363-369 (1997).

66. C.B. Breslin, C. Chen and F. Mansfeld, Corros. Sci., **39**, 1061 (1997).

67. Y.-C. Lu and M.B. Ives, Corros. Sci., **37**, 145 (1995).

68. M.H. Wilde and B.E. Wilde, Corros. Sci., **34**, 433 (1993).

11. Passivity-Induced Ennoblement

Gerald S. Frankel
The Ohio State University
Columbus, Ohio, USA

Robert G. Kelly
University of Virginia
Charlottesville, Virginia, USA

EDITORIAL NOTE

This volume, "A Compilation of Special Topic Reports," contains a series of reports that were prepared for the Waste Package Materials Performance Peer Review Panel to use as background and input to the peer review. Summaries drawn from the reports were also presented in Section 11 of the Panel's Final Report. The Panel used the reports as background and input for its review. Any views and comments expressed in the summaries and the full reports do not necessarily reflect the opinion and findings of the Panel. Further, opinions expressed in the reports are not necessarily those of the Panel or reflected in the Panel's reports and recommendations.

According to the well-established mixed potential theory of corrosion, the corrosion potential or open circuit potential (OCP) is determined by the principle of charge-conservation; it is the potential at which the sum of the anodic (or oxidation) currents over the electrode area equals the sum of the cathodic (or reduction) currents. The corrosion rate is given by the rate of the corrosion reaction (i.e., metal oxidation) at the OCP. Figure 1 shows a schematic Evans diagram for the case in which only one oxidation reaction and one reduction reaction act on the surface, and both are activation-controlled. The figure shows a generic reduction reaction involving O and R, which represent oxidized and reduced forms of some species. O_2 reduction will likely be the dominant cathodic reaction on waste packages in the repository environment, but hydrogen evolution might be dominant in acidified test solutions. The intersection of the lines representing the two reactions gives the OCP and corrosion rate. Figure 1 shows that these values are influenced by both thermodynamics, through the reversible potentials for the two half reactions, and kinetics, through the exchange current densities and Tafel slopes. Figure 1 represents the situation at an instant in time. As corrosion proceeds, the environment or electrode surface can change in ways that change the thermodynamic or kinetic parameters, and thus the OCP and corrosion rate.

For a spontaneously and ideally passive material, the dissolution kinetics can be represented by a vertical line in the Evans diagram, Figure 2. In this case, the corrosion rate is given by the passive current density, and the OCP is determined by the cathodic reaction kinetics, as shown schematically in Figure 2. It is common that a passive film will improve with

Special Topic Report prepared for the Waste Package Materials Performance Peer Review. The Final Report of the Peer Review was submitted to U.S. Department of Energy and Bechtel SAIC Company, LLC on February 28, 2002.

time, either by thickening or by a reduction in the number of defect sites. This improvement leads to a decrease in the passive current density, and thus a decrease in corrosion rate. Commonly, the passive current density varies inversely with time. If it is assumed that the cathodic kinetics do not change with time, the improved passivity will lead to a decrease in corrosion rate and an increase in corrosion potential, from points 1 to 4 in Figure 2. Many passive materials reach a steady state condition where the rate of film formation at the/metal film interface equals the rate of film dissolution at the film/environment interface. The limiting corrosion rate is then given by the rate of film dissolution in the environment.

Note that it is possible that the cathodic kinetics will be affected by the improvement in the passive film or other environmental effects. For example, passive film thickening might lead to a decrease in the exchange current density for the cathodic reaction, which would shift the cathodic curve in Figure 2 to the left, thereby counteracting to some extent the tendency for ennoblement.

Passive alloys were discovered less than 100 years ago. As a result, details of their long-term behavior (on the order of centuries or millennia) have not been studied. It is possible that an extremely passive metal, such as Alloy 22, when exposed to a relatively mild environment, such as the waters in Yucca Mountain, will exhibit a continually improving passivity, perhaps as a result of a continually thickening passive film. In this case, the OCP should continue to rise with time, albeit at a rate that might vary inversely with time. This phenomenon will be called passivity-induced ennoblement. The purpose of this document is to consider the implications of passivity-induced ennoblement for an alloy that exhibits a critical potential in the given environment.

A critical potential is the potential at which the current increases rapidly, either as a result of breakdown associated with localized corrosion, or as a result of transpassivity. In solutions with a high chloride-to-oxyanion concentration ratio, and at high temperatures, Alloy 22 can exhibit crevice corrosion, a form of localized corrosion above a critical potential. Under other conditions, Alloy 22 exhibits transpassive dissolution at high potentials during which the dissolution current increases as a result of oxidation of Cr(III) in the passive film to the soluble Cr(VI) state. If the potential is sufficiently high, oxygen gas evolution from the oxidation of water is possible, which can lead to high anodic currents. The critical potentials associated with chromate formation are likely thermodynamic in nature and independent of passive film characteristics or time. A considerable overpotential is usually required for oxygen evolution. To determine whether the current increase associated with a critical potential in a polarization curve is caused by localized corrosion, transpassive dissolution, or oxygen evolution (or a combination of two or more), it is necessary to examine the surface of the sample for evidence of localized attack, analyze the solution for corrosion products, and collect evolved gas. Oxygen evolution alone on a surface with a good passive film does not typically lead to degradation of the material. However, higher potentials are required for oxygen evolution than for transpassive dissolution of Cr(III) to Cr(VI), and so oxygen evolution often occurs in parallel with transpassive dissolution.

Consider first an alloy that dissolves transpassively at potentials above the transpassive potential, Figure 3. If the passive film were to improve continuously, the OCP would increase with time, eventually reaching the transpassive potential after a very long period. This potential, point 5 in Figure 3, would pose an upper limit to the OCP, and the limiting corrosion rate would be given by the rate of the cathodic reaction at the transpassive potential. In potentiostatically-controlled experiments where the potentiostat supplies whatever current is required, it is possible for the alloy to dissolve at high rates at potentials equal to and above the transpassive potential. At open circuit, however, high rate transpassive dissolution is only possible under oxidizing conditions in which a cathodic reaction is available to consume the electrons at an equally high rate. However, it was assumed that the cathodic reaction was unchanged during the potential ennoblement. Furthermore, at the high transpassive potentials, the rate of the cathodic reaction would tend to be small, because the rates of cathodic reactions decrease as the potential increases. For example, an alloy that exhibits a passive current density of 10^{-7} A/cm^2 upon immersion and then ennobles by 400 mV as a result of passivity improvement, the resultant corrosion rate of the aged alloy would be 4-6 orders of magnitude lower, assuming a cathodic Tafel slope of 60-100 mV/dec. If an alloy exists at the transpassive potential, but the dissolution current density is only 10^{-12} A/cm^2, then it is questionable whether the alloy is truly in a transpassive state. Any oxidation of Cr(III) to chromate, even at a very low rate, would decrease the passivity of the alloy, perhaps resulting in an increase in the passive current density. However, if the cathodic kinetics remain unchanged, then a higher passive current density would lead to a decrease in potential out of the transpassive region. The OCP might oscillate near the transpassive potential, but the rate of dissolution would remain low.

This condition of passivity-induced ennoblement to the transpassive potential, however, would be very susceptible to enhanced dissolution if a new oxidizing cathodic reaction were to develop, represented by the dashed lines in Figure 3. In the purely passive condition, dissolution is rate-limited by the anodic reaction, regardless of the oxidizing power of the solution, as represented by points 1 to 3'. After ennoblement to the transpassive potential, however, the rate of dissolution would be limited by the cathodic reaction and any added oxidizing reaction would result in an increase in dissolution rate, as represented by points 4' and 5' in Figure 3.

The considerations are somewhat different for the case in which the alloy is susceptible to localized corrosion. As described in the contribution to this volume by Frankel on localized corrosion, initiation of localized corrosion is associated with a breakdown potential, Figure 4. As in the case of transpassivity, passivity-induced ennoblement would be limited to the breakdown potential, point 4 in Figure 4. Localized corrosion growth at open circuit would require sufficient cathodic current, and this might limit the extent of growth, especially since the increasing area associated with growing localized corrosion requires increasing amounts of current. However, because localized corrosion is a local phenomenon by definition, it is possible that cathodic current from a large exposed passive area could be used to consume the current produced by localized attack at a much smaller area. This means that a low cathodic current density across the surface of a sample could be accompanied by a relatively high rate of anodic attack if the anodic area were small. On the other hand, sustained localized corrosion growth would likely depend on the development and maintenance of an oxidizing cathodic reaction to consume the electrons at a high rate. The potential of a sample that is undergoing localized

corrosion tends to decrease upon initiation of the attack as a result of the activation of a part of the surface. This activation brings the potential to values where the cathodic reaction rate is increased. However, the simple Evans diagrams shown in this report are no longer valid once localized corrosion initiates because of the physical separation of the locations of the anodic and cathodic reactions and the differences in solution composition at the anodic and cathodic regions. The physical separation leads to an ohmic potential drop between the anode and cathode, and thus a difference in the local potential. Nonetheless, it is possible that localized corrosion, once initiated, can drive the potential to values at which sufficient cathodic reaction would be possible to allow sustained attack.

The repassivation potential might be considered as the critical potential for designing against localized corrosion using the ΔE criterion. Since the repassivation potential is below the breakdown potential, it is more likely that passivity-induced ennoblement will drive the potential above the repassivation potential. This condition would be considered to be a failure according to the criteria used by the DOE Yucca Mountain Project, in that ΔE would be negative. Any initiated localized corrosion might continue to propagate at a potential above the repassivation potential. However, if the cathodic kinetics were unchanged, the problem remains as to how localized corrosion could propagate to any considerable extent under open circuit conditions.

It is clear that any mixed potential model for the corrosion potential and corrosion rate must carefully consider the cathodic kinetics. It is possible that cathodic kinetics could change with time. The exchange current density reflects the catalytic properties of the surface. With time, the improved passivity might result in a decrease in the catalytic nature of the surface. If the exchange current density for the cathodic reaction were to decrease, or the cathodic Tafel slope were to increase, the OCP would tend to decrease, counter to the effects of passivity-induced ennoblement. Equally important is the development of new oxidizing cathodic reactions, as described above.

It is possible that the OCP might be limited to a potential below any critical potential by a redox reaction involving solution species. If a redox reaction existed in the environment at a potential below the critical potential and with an exchange current density on the passive metal surface that was large relative to the passive current density, then the redox reaction would pin the potential at the reversible potential, Figure 5. This situation would be the most effective means of keeping the potential below any critical potential under open circuit conditions.

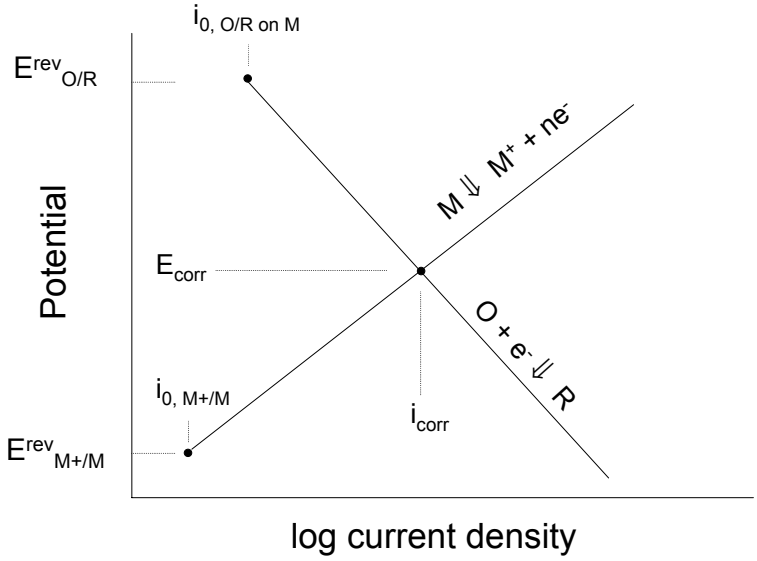

Figure 1. Schematic Evans diagram showing metal oxidation and a generic reduction reaction on a metal surface.

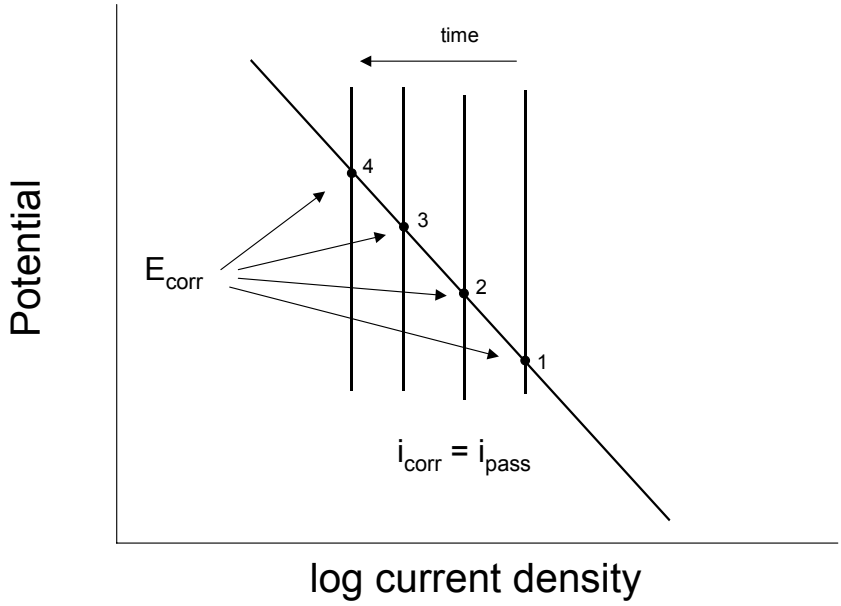

Figure 2. Schematic Evans diagram showing the effect of a decreasing passive current density on the corrosion potential.

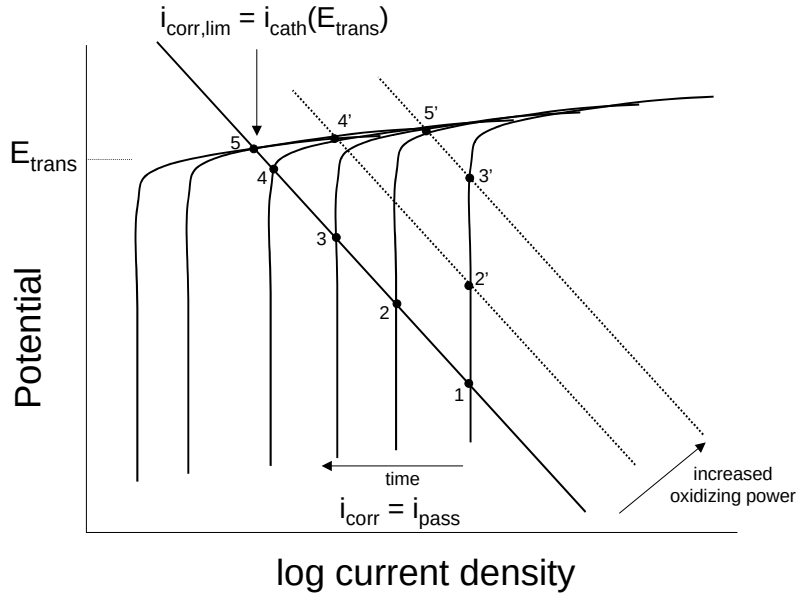

Figure 3. Schematic Evans diagram showing the effect of transpassivity on limiting passivation induced ennoblement, and the effect of increased oxidizing power.

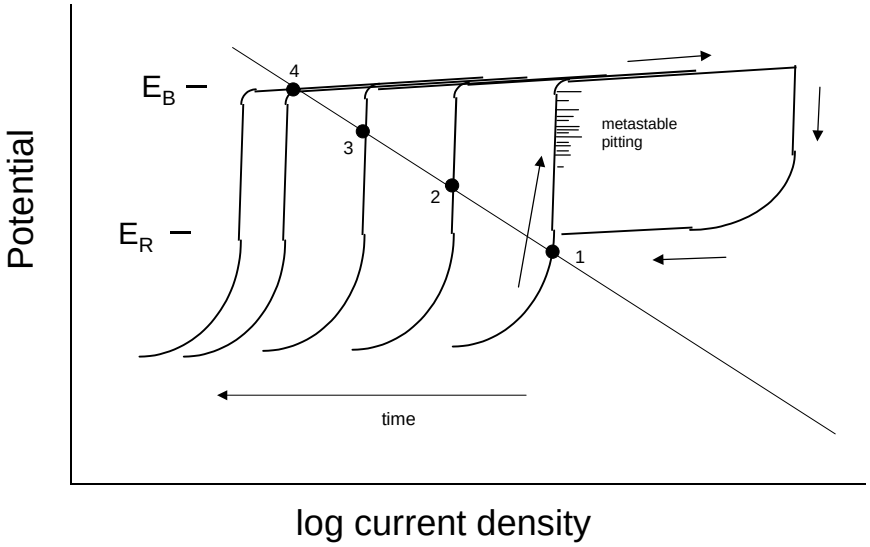

Figure 4. Schematic Evans diagram showing the effect of localized corrosion on limiting passivation induced ennoblement.

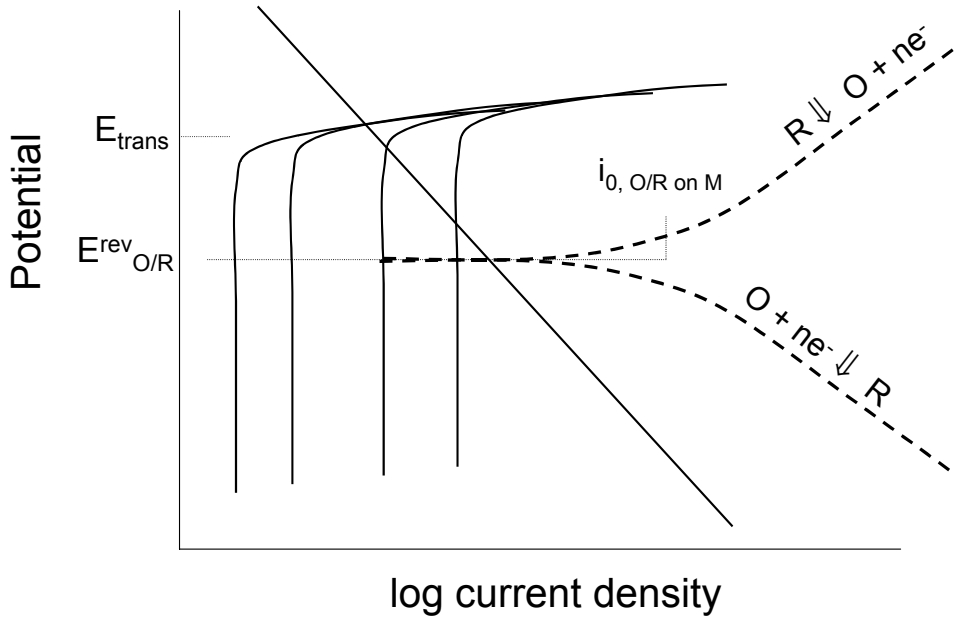

Figure 5. Schematic Evans diagram showing the effect of a redox reaction on limiting passivation induced ennoblement.

12. Temperature Effects in Localized Corrosion

Roger Newman
UMIST, Corrosion and Protection Centre
Manchester, UK

EDITORIAL NOTE

This volume, "A Compilation of Special Topic Reports," contains a series of reports that were prepared for the Waste Package Materials Performance Peer Review Panel to use as background and input to the peer review. Summaries drawn from the reports were also presented in Section 11 of the Panel's Final Report. The Panel used the reports as background and input for its review. Any views and comments expressed in the summaries and the full reports do not necessarily reflect the opinion and findings of the Panel. Further, opinions expressed in the reports are not necessarily those of the Panel or reflected in the Panel's reports and recommendations.

Summary

Localized corrosion of stainless steels and nickel base alloys shows a remarkable dependence on temperature. For pitting, a critical temperature exists (the critical pitting temperature or CPT) below which pitting vanishes at all potentials. For well-prepared surfaces of modern alloys the CPT can be reproduced to within 1^{o}C, and does not depend on the chloride concentration, at least in the range 1 to 5M. The CPT does show some dependence on the surface finish, being up to ten degrees higher for polished than for rough-ground surfaces.

There has not been much progress in general testing philosophy for temperature effects since the pioneering work of Brigham in the 1970s. The main advance has been the recognition of the importance of specimen design and avoidance of crevice corrosion in CPT measurements. Alloy manufacturers have made many of the important refinements in this area, and given that unwanted crevice corrosion can lower the CPT by 40 degrees, one can certainly understand their motivation for remaining at the forefront of this subject.

The deterministic nature of the CPT transition requires a deterministic explanation, and there is evidence that this lies in the anodic kinetics of the metal in the local pit environment. Passivation occurs below the CPT, even in the most aggressive local environment, preventing the attainment of the necessary current densities (ca. 10 A/cm^2) for pit stabilization. Probably this passivation occurs beneath a freshly precipitated salt film. Metastable pitting occurs well below the CPT.

Pitting in inhibited solutions, for example chloride plus sulfate, tends to propagate under the metal surface. For certain solution compositions and potentials, this leads to enhanced pit

Special Topic Report prepared for the Waste Package Materials Performance Peer Review. The Final Report of the Peer Review was submitted to U.S. Department of Energy and Bechtel SAIC Company, LLC on February 28, 2002.

stability and a lowering of the CPT, even though the pitting potential above the CPT is inhibited by sulfate in the normal way. This observation by Moayed requires further investigation in view of the anions present in the Yucca Mountain environment.

Above the CPT, the gradual decrease of the pitting potential with increasing temperature has been ascribed mainly to the enhanced dissolution kinetics of the metal (increase in corrosion current density in the pit environment). However in deep pits or crevices there will also be effects on the critical environmental conditions.

Crevice corrosion in a standard geometry also shows a critical temperature or CCT. This cannot be reproduced as well as the CPT; however it does have value especially for shallow crevices, where corrosion initiates by metastable pitting. In deep, tight crevices there may be a different initiation mechanism of the passive-dissolution type, though this has yet to be demonstrated. The effects of surface deposits on the critical conditions for localized corrosion have not been studied in detail, but are likely to be as severe (at least) as those of conventional crevices.

Deleterious phase transformations or segregation effects can be quantified by CPT measurements according to the literature. It is not clear how conservative such evaluations are in view of the narrow regions that are subject to depletion in Cr or Mo. There is also a need for spatial mapping of the reduction in localized corrosion resistance due to such metallurgical effects.

Background and Early Work

Some of the author's views on this topic may be found in two recent review articles [1,2].

The effects of temperature on pitting or crevice corrosion of stainless alloys may be classified into two kinds: gradual variation, generally associated with 300-series austenitic steels, and discontinuous variation, generally associated with high-alloy materials. The recognition of discontinuities in pitting behaviour led to the concept of the critical pitting temperature (CPT).

The definition of the CPT is:

A characteristic temperature for a given alloy and surface finish, below which stable pitting will never occur from a free surface, no matter how oxidizing the potential.

This may be qualified by noting that the chloride content is assumed to be on the order of one to a few molar (easier pitting occurs at very high chloride content, and pit stability is very dubious at low chloride content unless some kind of surface deposit is present). However the exact chloride content should not affect the definition.

Even today, there are corrosion specialists who regard the CPT as an engineering convenience and would be surprised to learn that it truly is a discontinuous transition,

reproducible to within one degree. Figure 1 shows data from my own laboratory (M.H Moayed, unpublished) that illustrate this point quite spectacularly (there was no selection of data here – these were the only tests conducted for this condition).

Several factors delayed the realization that the temperature dependence of pitting in stainless alloys was more interesting than a gradual variation. First, the amount of electrochemical work on high-alloy materials (more alloyed than basic 300-series grades) was very limited prior to 1975. Second, the materials used in early work were quite 'dirty' and pitted too easily below room temperature. Nowadays we know that good-quality 316SS should have a CPT of 20 or even 25^{o}C. Similar evolution in quality has been reported for duplex steels [3]. Third, it is very likely that unreported crevice corrosion affected many early measurements, especially close to the CPT. Fourth, academic corrosion scientists have taken little interest in the CPT, and until recently always worked on basic 300-series grades of steel (or laboratory alloys).

Temperature was one of the variables studied in classic work on pitting carried out in Uhlig's laboratory at MIT [4,5]. 304SS showed a gradual increase of pitting potential as the temperature was reduced below room temperature, with an indication of a steep increase near 0^{o}C. Surprisingly, 316SS was reported to be worse than 304SS at 0^{o}C. There are several possible explanations for this observation. Most likely, the 316SS had a more damaging number, size or state (interface integrity) of manganese sulfide inclusions. One could, however, speculate that the relative stability of pitting in different alloys might show reversals around the CPT, as suggested by the thin-foil experiments of Ernst [6]. Near the CPT pits tend to grow under the metal surface in a more convoluted manner. Crevice corrosion is also a possibility (the measures taken to ensure this was absent are not entirely clear in Uhlig's papers).

The Work of Brigham and Consequences for Testing Methods; Origins of the PRE Index

The true nature of the CPT was discovered by Brigham in the 1970s [7]. He and his co-authors did not propose any fundamental theory, but their work provided the foundation for all the methods by which the CPT is now determined [8]. These are, essentially:

- Gradual increase in temperature for samples immersed in an oxidizing solution such as ferric chloride, with visual examination at each removal of the sample.

- Anodic polarization scans at different temperatures.

- Increase of temperature while holding the potential at a constant, oxidizing value [9].

To this list we should probably add the electrochemical measurement of pit initiation by zero-resistance ammetry of coupled samples immersed in ferric chloride solution and subjected to at temperature ramp [10]. This is particularly useful for the evaluation of welds or crevice effects, in which case only one of the two samples would have the weld or crevice. Another possibility, not reported to our knowledge, is the coupling of two different grades of steel to determine the CPT of the less resistant grade. Galvanostatic polarization with a temperature ramp may also have value as a relatively fast method [11]. The authors used current densities in the 50

to 200 σA/cm^2 range. Some authors believe that nickel alloys should be tested differently from stainless steels [12].

Techniques for determining the CPT have been standardized, starting with a temperature dependent version of the ASTM G-48 ferric chloride test (take the sample out each day, look at it[1], then increase the temperature and put it back). More recently there has been a focus on electrochemical variants via ASTM G-150-97 which has been subject to round-robin testing [13]. This standardization process is not yet complete and has proceeded largely without academic input (not that this is necessarily a bad thing). The ferric chloride test has probably been subject to more scrutiny (because it does not involve any confusing electrochemistry) and various refinements have been proposed [14] to produce more reproducible results.

The essence of the CPT, as defined by Brigham and Tozer, was that it was a potential-independent transition. At high anodic potentials such as +600 mV (SCE), the value of the CPT does not depend on potential changes on the order of ±150 mV. Of course higher values of "CPT" can be determined by using lower, more "realistic" potentials, but in that case one is just measuring the temperature at which the pitting potential is equal to the applied potential. A number of authors have reported convincing correlations of CPT values with industrial performance [e.g. 15], but for seawater service it is widely believed that the CPT or even CCT is an over-conservative criterion [16,17], and "CPT" or "CCT" values have been determined at potentials such as 300 mV (SCE) instead. The terms "CPT" or "CCT" should *not* be used for such data as this is very confusing and downgrades the true significance of the CPT as a deterministic transition. On the other hand, there are powerful examples of the use of CPT and CCT data to qualify alloys for particular applications (albeit these are often published by steel companies and academic scientists might think these are subject to commercial bias; this would be a narrow-minded view) [18].

Brigham and Tozer were the first to show that the CPT was independent of chloride concentration within a wide range, provided enough time was allowed for pit initiation at the lower chloride levels. This immediately showed that classical theories of pitting would have difficulty with the CPT, and perhaps that is why passive-film specialists have tended to ignore it. The Avesta scientist Qvarfort confirmed in the 1980s that the CPT was independent of chloride concentration over the range 1-5 M NaCl, and also that the CPT could be reproduced to within 1∀C [19]. He used the "Avesta Cell" to prevent crevice corrosion; this device prevents crevice corrosion by injecting de-ionized water around the perimeter of a flat sample whose active area is defined by an O-ring [20-24]. Avesta scientists recently published a painstaking demonstration that the CPT did not depend on the origin of a particular seawater [25], which seems a rather obvious observation in view of Qvarfort's earlier work. At very high chloride concentrations the CPT decreases, since the pits can now acquire extremely high chloride activity [26].

Early in the history of the CPT, it was realized that it provided an opportunity to generate empirical equations expressing the effects of alloying elements on pitting. Brigham and Tozer [7] initially showed that for a set of austenitic alloys, the CPT was given by:

[1] And poke it with a needle in case the pits are under the surface.

CPT (^{o}C) = 5 + 7 (wt.% Mo)

Modern steels do a little better than this, and other authors have reported slightly different correlations [27] but this equation remains broadly valid, and any theory of the CPT will eventually have to explain such powerful correlation equations. Many authors have incorporated nitrogen alloying, while others have included a variety of other elements such as Mn (detrimental), W (beneficial) and so on [8,28]. Others have studied duplex steels, either on an average-composition basis [29] or with consideration of the compositions of individual phases [30]. In all cases the aim was to produce a pitting resistance equivalent or PRE number that varied linearly with the CPT. Mn-based austenitic steels have also been studied on this basis [31]. It is possible that nitrogen alloying changes the form of the dependence on other elements, a so-called synergistic effect. Weld metal shows systematically lower CPT values than parent metal, and the CPT can be used for weld procedure development [32-36]. This shows for example that high-speed laser welding gives relatively good properties [34,35], because the alloy element segregation profiles are either narrower or less deep (probably the former). For high-alloy cladding, dilution from the carbon steel substrate can be quantified using CPT values [37]. The use of nitrogen atmospheres (to increase the N content of weld metal) can be evaluated neatly using CPT values [38]. Post-weld heat treatment can also be studied [39]. Deleterious phase transformations (apparently not relevant to Alloy 22 at <500^{o}C) have also proved amenable to quantification using CPT values [40-42].

Needless to say, some authors vehemently disagree with the slavish use of PRE numbers, citing supposed errors of judgement leading to expensive failures in plant, but in the presence of deposits and varying plant conditions this is not surprising [43]. It is not the fault of the developers of the PRE index that it is sometimes misused for systems containing crevices, deposits and welds.

Some Considerations Relevant to Nickel Base Alloys Such As C-22

A good source for work up to 1987 is the review by Sridhar [44]. There are also a number of reviews covering the general properties of these materials [e.g. 45,46].

Nickel base alloys such as C-22 have very high CPT values in ferric chloride solution, above 100^{o}C. This is due to the very high Mo content, a fact drastically illustrated by carrying out similar tests in bromide solution, where Mo is much more soluble and the CPT plummets to room temperature, or even lower in the case of the C-276 alloy which has only 16% Cr. The unfavourable interaction between bromide and molybdenum was known already in 1939 [47] and studied electrochemically by Streicher as early as 1956 [48]; recently it has been rationalized kinetically by artificial pit studies [2,26].

It is not clear[2] why highly concentrated chloride solutions were not used to bring the CPT of nickel alloys (such as C-22) below 100°C in order to investigate issues such as thermal ageing and welding. The CPT decreases significantly above 5M chloride concentration. Instead, authors from Haynes International and other alloy companies report the use of acidic solutions such as "green death", a copper containing mixture [49]. Recently Avesta have started to use strong chloride and even bromide solutions, and to face up to the complications therein (such as the fact that Mo alloying does not have much if any benefit in bromide media). More fundamental study of these issues is recommended. The effects of pH and chloride concentration have been studied, but in a rather conservative way [50].

Crevice Corrosion

In the context of Yucca Mountain, conventional pitting is not to be expected, but crevice or underdeposit corrosion is much more likely and the applicable temperatures are much lower. Crevice corrosion occurs at lower temperatures, as well as potentials, compared with pitting. If care is taken to provide a repeatable crevice, the temperature dependence of crevice corrosion is also very steep, leading to the concept of a critical crevice corrosion temperature (CCT) as proposed by Brigham [51]. Caution is necessary in using this quantity for predictive purposes, since it is so dependent on geometry. Its fundamental meaning will be discussed later. Good correlations with service performance have been reported [52].

Specifically, for Alloy C-22, data are available that suggest a steep decline in crevice corrosion susceptibility below 90°C [53]. Comparisons with the well-studied Alloy 625 have been valuable in this work. The 625 alloy shows rather easy crevice corrosion from tight crevices, which may be partly due to its residual elemental segregation in many of its product forms, but this is an unresolved issue.

Ultimately one is liable to arrive at a dilemma – crevice corrosion will propagate if initiated artificially (e.g. by increasing the temperature temporarily), but its propensity to initiate will remain uncertain.

A few authors have presented comprehensive PRE-type equations covering both pitting and crevice corrosion [54]. A common feature of all these studies (for stainless steels) is the weak effect of nickel [55].

[Warning: it would not be correct to take as a generalization the statement by Russell and Covino [56] that CCT values are 10 to 30°C below CPT values. There are examples that are much more extreme than this (or at any rate, 30°C is much more likely to be correct than 10°C). In our own work on the 904L alloy the difference was at least 40 degrees.]

[2] at least to this author

Critical Issues Connected with the CPT and CCT

The fundamental basis of the CPT was little discussed until recently. A basic priority is to determine whether the CPT is a true initiation threshold or a growth/stability threshold. Several facts, already known in the 1980s, indicated that the latter was much more likely. First, authors who reported potentiodynamic determinations of the CPT often showed metastable pitting at lower temperatures, although this was rarely mentioned. Second, it was known from studies of laser surface melting [57] that refinement or elimination of the sulfide inclusions in 300-series stainless steels could vastly improve the pitting resistance[3]. If pits always initiate at inclusions, it is hard to imagine that variations in alloy composition could change the critical temperature for pit initiation. Third, in order for the CPT to be a true initiation threshold (and presumably if one held this view one would also believe that the pitting potential was an initiation threshold), one would have to believe that initiation thresholds can be stochastic or deterministic in character, dependent or independent on chloride concentration, and dependent or independent on potential[4].

The first attempt to incorporate metastable pitting into the description of the CPT was made by Salinas Bravo and Newman, as already mentioned [10]. The observations were made in the context of technique development (trying out a novel ZRA technique), so not much analysis of the data was attempted; however it was clear that metastable pitting occurred far below the CPT - possibly as much as 30 degrees for the super-duplex steel under investigation. Later a key observation was made by Moayed et al. [58]. Moayed worked with the Avesta 904L alloy, which has 4.5% Mo and a CPT of around 60^{o}C. Below the CPT, metastable pitting occurred in potentiodynamic scans, but showed a peak in intensity at intermediate potentials – Figure 2. By carrying out potential step experiments on fresh surfaces, it was shown that this was a genuine effect and not an artifact of site exhaustion. A similar observation had been made by Garfias and Sykes [59], and by Riedel et al., [60] but without much interpretation. This effect recalled an earlier study by Liew [61] who was developing an artificial pit (pencil electrode) method for ranking high-alloy materials by their repassivation temperature (T_r)[5]. When Liew increased the constant applied potential in the 500 to 800 mV range, he expected to obtain equal or decreasing values of T_r, but was surprised to obtain higher values at higher potentials – in other words, the alloys were more resistant to pit propagation at higher potentials. In Liew's case this could be unambiguously associated with repassivation occurring under an anodic salt film, since the experiment was carried out in a one-dimensional geometry and it was easy to determine when the salt film was or was not present. In Moayed's case, extensive studies were done [58,62] to test the idea that the apparent disappearance of pitting at high potentials (below the CPT) was due to anodic passivation occurring before the current transients due to pitting had become detectable. The simplest view would be that passivation ensued immediately upon precipitation of the anodic salt film. A numerical reaction-diffusion-passivation model showed good

[3] So long as the surface was refinished mechanically after laser treatment, without removing the melted layer.
[4] But it might not be correct to argue that "the passive film cannot suddenly change at a particular potential which is different for every alloy", which used to be the author's view. The CPT could be an initiation threshold, yet dependent on the relative kinetics of two or more processes, such as point defect creation, transport and annihilation. In that case there might not be a change in any measurable property of the passive film on traversing the CPT, or at least the change would be subtle.
[5] These temperatures were much lower than CPTs but possibly similar to CCTs.

qualitative agreement with the experimental data. This was the first demonstration of a new kind of metastable pitting in which repassivation is deterministic with little or no random element[6].

Deterministic repassivation of metastable pits mediated by salt precipitation (like iron in sulphuric acid) [58] is a refinement of the model proposed by Salinas Bravo and Newman [10], in which there is no essential role of the salt film – simply a critical current density for passivation (i_{crit}) that varies more steeply with temperature than the limiting anodic current density (i_L) for a characteristic size of cavity. The CPT on that basis corresponds to ($i_{crit} = i_L$). The two models are hard to distinguish, but they do have slightly different implications for the effect of surface finish and the tightness of the distribution of measured CPTs. The salt-film model is "more deterministic" than the Salinas model. In unpublished work [62], Moayed came to the conclusion that the CPT is intimately bound up with the onset of lacy metal cover formation over the pit; the first undercutting event needed to create a stable pit occurs at the boundary between passive and active areas and requires an enormous local current density; any hindrance of the passage of this current will allow repassivation of the pit. Some evidence for this interpretation comes from cross-sectional studies of pits in foils, where undercutting is hindered in more dilute chloride solutions [6].

The CPT does depend on surface finish, even though for a single surface finish it is extremely reproducible. This appears somewhat contradictory, but the effect is not large – for the 904L alloy the CPT varies by about 9 degrees over a range of grit sizes – Figure 3 [62,63]. This may indicate that the range of micro-crevice geometries created by a particular grit size is not as large as might be supposed, or perhaps that outlying (deep/tight) crevice geometries are unlikely to contain a suitable inclusion. Since polished surfaces give more reproducible results than abraded ones, it may be suggested that the pit size at which the pit experiences its stability crisis is larger than the fine relief on a polished surface, but becomes smaller than the relief on successively coarser abraded surfaces. This subtle geometrical effect may be contrasted with the effect of a tight macro-crevice, which reduces the critical temperature to below 15^{o}C for this alloy. Pickling has been reported to increase the CPT, and Avesta and other companies have extensive data on commercial finishes, but one has to doubt whether any of these effects are really fundamental or just time-dependent. Oxidation due to welding has profound effects on localized corrosion that have not been investigated to their deserved depth (another fault of academic scientists, or their funding structure), but it is possible to use CPT values to quantify such effects [64,65]. Various other surface effects have been studied by authors from steel companies [66,67].

One of the most paradoxical results obtained in the field of temperature effects was Moayed's demonstration [68] that sulfate addition could *lower* the CPT of the 904L alloy. In potentiodynamic experiments, an extremely smooth (quiet) anodic current feature occurred below the transpassive transition and below the normal CPT value. Inspection of the metal surface initially showed nothing, but on probing with a pin, pits growing beneath the surface

[6] Other than the effect of nitrate addition, which appears identical in effect though not in detailed mechanism. According to Newman and Ajjawi (Newman, RC; Ajjawi, MAA, Corros. Sci., 26, 1057 (1986)), nitrate undergoes redox and/or electroreduction reactions within the salt film environment that are sluggish in a normal aqueous acid solution, thus explaining why it inhibits pitting above a particular potential where the salt film is present.

were detected. SEM examination showed that the pits formed with sulfate had much finer holes in the lacy metal covers that retained their contents. The result may be rationalized by suggesting that the critical stage in pit stability is the formation of the first re-entrant hole in the metal surface resulting from the first undercutting event. If this hole is extremely fine (because of easier passivation occurring with sulfate present), then the pit will be more, not less stable. The effect was quite dramatic, with reduction of the CPT from 55 to less than 40^{o}C at certain sulfate concentrations. Above the CPT, sulfate had its normal inhibiting effect (i.e. increase in the pitting potential).

The CCT, with the precautions mentioned earlier regarding geometry, is a very useful concept. Its mechanistic basis is not so clear. According to the view that crevice corrosion initiates by metastable pitting, the CCT would simply be the critical temperature (if one exists) for metastable pitting. Even on this basis, one can anticipate that tighter crevices will be able to take advantage of smaller metastable events to initiate stable crevice corrosion. In any event, the longer diffusion length associated with a crevice makes it easier (lower potential; lower temperature) to initiate localized corrosion, because a lower anodic current density is needed in the cavity to sustain an appropriate local chemistry.

If one believes that crevice corrosion initiates by passive dissolution leading to a critical local chemistry, then extremely tight and deep crevices will be able to initiate slow corrosion at very low temperatures, but ultimately the rate of crevice corrosion will be no faster (because of the ohmic limitation) than ordinary passive dissolution. At least, this would be the normal way of looking at it. But for the Yucca Mountain project one can visualize propagation of crevice corrosion at, say, 0.001 mm/year (ca. 0.1 σA/cm^2 in electrochemical language) under conditions where the passive current would have fallen to values two or three orders of magnitude lower than that. So we still would have localized corrosion, at a rate that may eventually perforate a waste container.

Dependence of Pitting on Temperature above the CPT

Little of a quantitative or predictive nature was published on this topic until Laycock's work in UMIST [69], which showed that the pitting potential variation with temperature above the CPT could be divided into effects of increased dissolution kinetics and reduced IR potential drop[7]. Recently he has published a more quantitative treatment of this issue [70]. Essentially, there is a good agreement with pitting potential data using artificial pit kinetics treated so as to extract the salt-film precipitation potential as a function of pit depth. Further analysis of the overpotential contributions shows that the kinetic factor is the most important.

For crevice corrosion, the Laycock treatment would not be appropriate, since it is clear that the crevice chemistry required to stabilize crevice corrosion is much more dilute than for initiation of pitting. Crevice corrosion initiation is not well understood, since we do not know the relative

[7] recognising that critical chemistry within the pit nucleus and cation diffusivity also vary with temperature, but weakly

contributions of metastable pitting and passive dissolution. Indeed, in this author's opinion it has never been demonstrated that passive dissolution is capable of initiating crevice corrosion.

Conclusions and Future Priorities

1 The CPT is a deterministic pitting transition.

2 The CCT depends on crevice geometry but is more well-defined than is generally realized.

3 Surface deposits in Yucca Mountain will create at least as aggressive a condition as a conventional crevice (recognising that a thin-film electrolyte is in itself less aggressive).

4 "Inhibiting" anions may promote pitting below the normal CPT, by causing sub-surface pit propagation.

5 More work is required on:

- ∉ Non-chloride anion effects on pit stability
- ∉ Corrosion product effects
- ∉ Crevice corrosion initiation
- ∉ Long-term crevice and pit stability criteria
- ∉ Welding and HAZ performance (possible non-conservative nature of the normal CPT test).

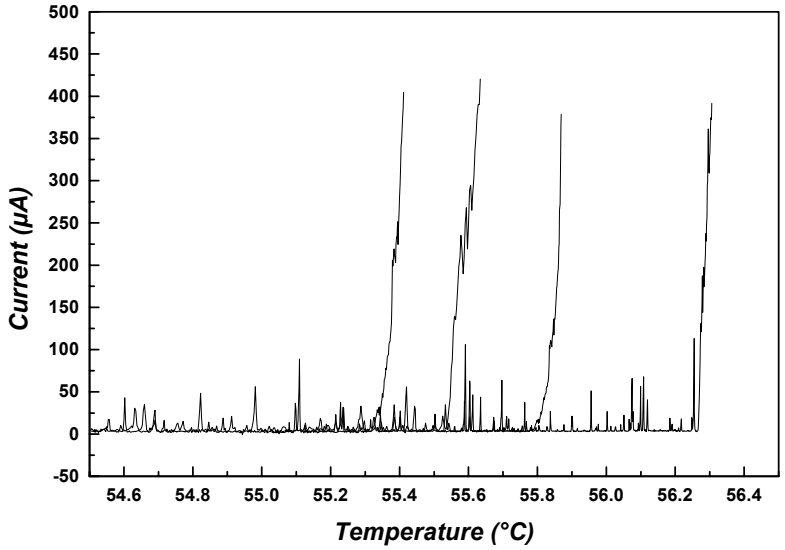

Figure 1 – Response of 904L SS in four identical temperature-ramp tests at +750 mV (SCE) in 1M NaCl, showing reproducibility to better than 1°C when a 3 σm diamond paste finish is applied (M.H. Moayed, unpublished).

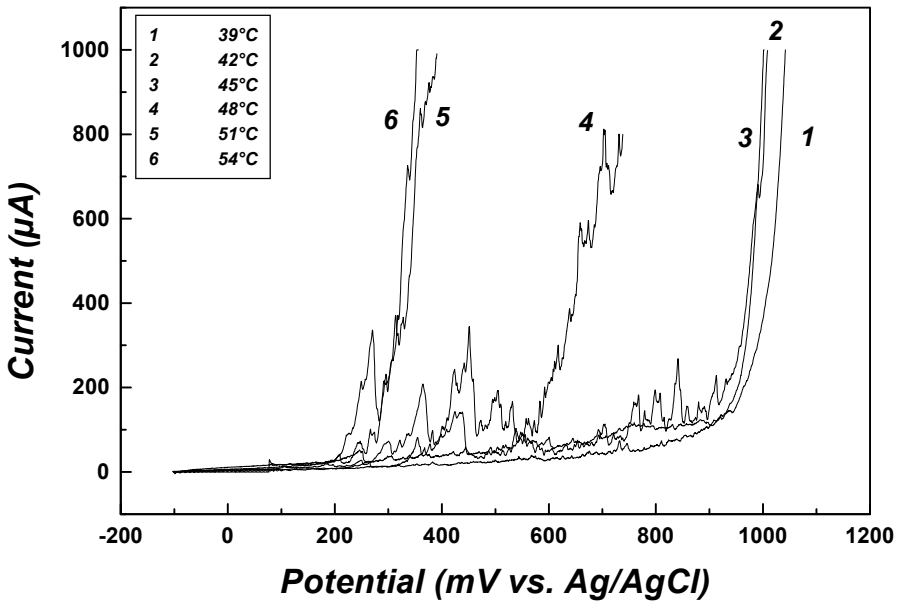

Figure 2 – Potentiodynamic polarization scans for 904L SS at different temperatures in 1M NaCl, showing metastable pitting occurring over a range of potentials below the CPT (M.H. Moayed, unpublished).

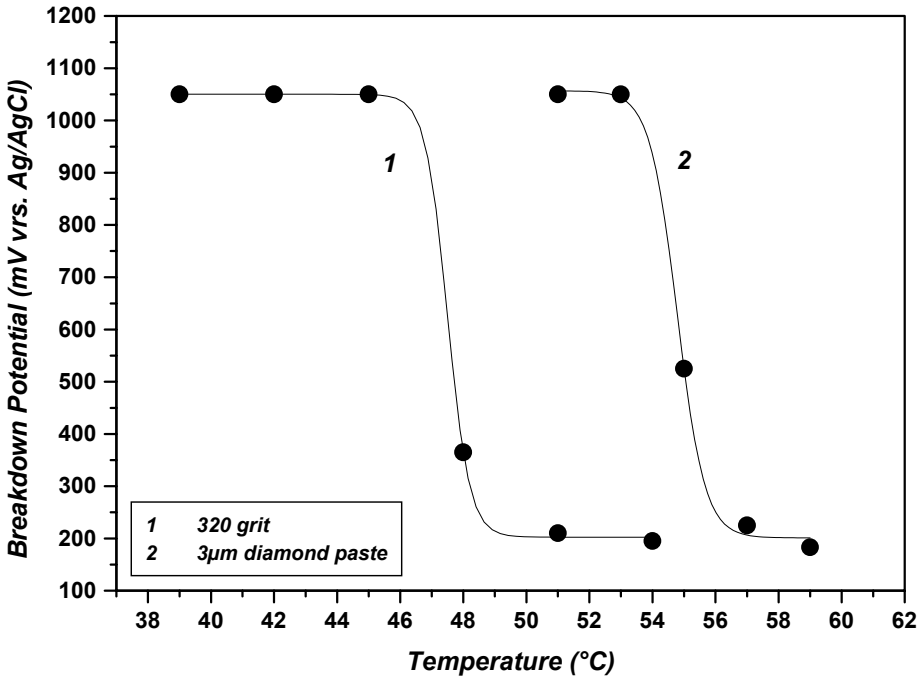

Figure 3 – Breakdown potentials for two different surface finishes of 904L SS in potentiodynamic polarization tests using 1M NaCl (M.H. Moayed, unpublished).

References

1. R.C. Newman, "Prediction of localized corrosion of stainless steel", Plenary Lecture, Proc. 14th International Corrosion Congress (Cape Town, 1999), Corrosion Institute of Southern Africa, Kelvin, SA (1999).

2. R.C. Newman, Corrosion, **57**, 1030 (2001).

3. E. Alfonsson and R. Qvarfort, "Duplex Stainless Steels of Yesterday and of Today--a Pitting Corrosion Investigation," in Duplex Stainless Steels '91, **Vol. 2**, pp. 839-845, Les Editions de Physique, Les Ulis (1992).

4. H.P. Leckie and H.H. Uhlig, J. Electrochem. Soc., **113**, 1262 (1966).

5. J. Horvath and H.H. Uhlig, J. Electrochem. Soc., **115**, 791 (1968).

6. P.Ernst and R.C. Newman, Corros. Sci, **44**, 927 and **44**, 943 (2002).

7. R.J. Brigham, Corrosion, 28, 177 (1972); R.J. Brigham and E.W. Tozer, Corrosion, 29, 33 (1973); Corrosion, 30, 161 (1974); J. Electrochem. Soc., **121**, 1192 (1974).

8. J. Flyg and R.F.A. Jargelius-Pettersson, "Electrochemical evaluation of crevice corrosion in stainless steels," in Electrochemical Methods in Corrosion Research VI. II, Trento, Italy, 25-29 Aug. 1997 [Materials Science Forum (Switzerland), **vol. 289-292**, no. 2, pp. 1067-1072, 1998]

9. J. Kolts and N. Sridhar, Temperature Effects in Localized Corrosion, in Corrosion of Nickel-Base Alloys, pp 191-198, ASM (1985).

10. V.M. Salinas Bravo and R.C. Newman, Corros. Sci., **36**, 67 (1994).

11. K.V. Quang, P.L. Guevel, N. Jallerat and J.C. Bavay, Corros. Sci., **28**, 423 (1988).

12. E.L. Hibner, "Modification of Critical Crevice Temperature Test Procedures for Nickel Alloys in a Ferric Chloride Environment," Mater. Perform., **26**, 37 (1987).

13. L. Wegrelius, "Round robin comparison of critical pitting temperatures determined according to ASTM G 150-97," in Proc. International Congress Stainless Steel '99 (Sardinia,1999), **Vol. 3**: Properties and Performance, pp. 91-99, Associazione Italiana di Metallurgia, Milan (1999).

14. M. Renner, U. Heubner, M.B. Rockel and E. Wallis, Werkst. Korros., **37**, 183 (1986).

15. W.L. Silence, S.M. Corey and J. Kolts, "Alloy Ranking for Corrosion Resistance: Laboratory Tests vs. Field Exposures", in The Use of Synthetic Environments for Corrosion Testing, pp 120-131, ASTM STP 970, ASTM. Philadelphia (1988).

16. U. Steinsmo, T. Rogne and J. Drugli, Corrosion, **53**, 26 and **53**, 955 (1997).

17. J.-P. Audouard, D. Thierry, D. Feron, C. Compere and V. Scotto, "Crevice corrosion resistance of stainless steels in natural seawater", Stainless Steel World, **8**, 37 (1996).

18. M.B. Rockel, W. Herda and U.Brill, "Two New Austenitic Special Stainless Steels With High Molybdenum Content and Nitrogen Additions", in Stainless Steels '91, **Vol. 1**, Iron and Steel Institute of Japan, Tokyo (1991).

19. R. Qvarfort, Corros. Sci., **29**, 987 (1989).

20. R. Qvarfort, "Avesta Cell--a New Tool for Studying Pitting," ACOM, no. 2-3, pp. 2-5 (1988).

21. P.-E. Arnvig and A.D. Bisgard, "Determining the potential independent critical pitting temperature (CPT) by a potentiostatic method using the Avesta cell," ACOM, vol. 3, pp. 1-12 (1996).

22. H. Andersen, C. Olsson and L. Wegrelius, "Critical pitting temperatures in sodium chloride and ferric chloride solutions - determined using the 'Avesta Cell'," in Electrochemical Methods in Corrosion Research VI (Trento 1997), Materials Science Forum (Switzerland), **vol. 289-292**, no. 2, pp. 925-931.

23. P.E. Arnvig and A.D. Bisgard, "Determining the potential independent CPT by a potentiostatic method using the Avesta cell," Corrosion/96, Paper #437, NACE, Houston (1996).

24. P E Arnvig and R M Davison, "Pitting of steels using the Avesta Cell – experiences and new applications," in Proc 12th International Corrosion Congress (Houston 1993), Paper #209, NACE Houston (1993).

25. B. Wallen, "Critical pitting temperatures of UNS S31600 in different seawaters," in European Federation of Corrosion Publications (UK), **vol. 33**, pp. 19-25, 2001, Institute of Materials, London (2001).

26. P. Ernst, PhD thesis, UMIST (1999).

27. J. Kolts, J.B.C. Wu, P.E. Manning and A.I. Asphahani, "Highly Alloyed Austenitic Materials for Corrosion Service," Corros. Rev., **6**, no. 4, pp. 279-326 (1986); also Met. Prog., **124**, pp. 25-29, 32-36 (Sept. 1983).

28. E. Alfonsson and R. Qvarfort, "Applicability of the PRE Index for Stainless Steels," Acciaio Inossid., **59**, 22 (1992) ;E. Alfonsson and R. Qvarfort, "Investigation of the Applicability of Some PRE Expressions for Austenitic Stainless Steels," in Electrochemical Methods in Corrosion Research IV (Espoo, Finland, 1991), Mater. Sci. Forum, **vol. 111-112**, pp. 483-491 (1992); also ACOM, no. 1, pp. 1-5, 1992.

29. R.D. Kane, S.M. Wilhelm and D.R. McIntyre, "Application of the Critical Pitting Temperature Test to the Evaluation of Duplex Stainless Steel," in Corrosion Testing and Evaluation: Silver Anniversary Volume, pp 298-302, ASTM STP 1000, Philadelphia (1990).

30. H. Vannevik, J.-O. Nilsson, J. Frodigh and P. Kangas, "Effect of elemental partitioning on pitting resistance of high nitrogen duplex stainless steels," ISIJ International (Japan), **36**, 807 (1996).

31. B. Vicentini, G. Rondelli and A. Cigada, Werkstoffe und Korrosion, **46**, 628 (1995).

32. A. Garner, Corrosion, **35**, 108 (1979).

33. B.J. Gunn, "Effect of welding variables on the pitting resistance of autogeneous welds in UNS S31245 high alloy austenitic steel tube," TWI Journal, **vol. 4**, no. 4, pp. 541-564 (1995).

34. J.I. Leitonen, S.A. Jarvenpaa and L.P. Karjalainen, "Pitting Corrosion Properties of Autogenous TIG and Laser Welds in a 20Cr--22Ni--6Mo--N Steel," in Stainless Steels '91. **Vol. 1**, pp 373-378, Iron and Steel Institute of Japan, Tokyo (1991).

35. M. Vilpas, R. Karppi, M. Kuronen and A. Kyrolainen, "Pitting corrosion resistance of austenitic stainless steels welded by high-speed laser process," in Proc. Stainless Steel '99 (Sardinia, 1999), **Vol 3**, pp 111-120, Associazione Italiana di Metallurgia, Milan (1999).

36. K.-K. Baek, C.-S. Lim and H.-J. Sung, "Evaluation of pitting corrosion resistance of high-alloyed stainless steels welds for FGD plants in Korea," Stainless Steel World, **10**, 28-31 (1998).

37. M.F. Gittos and T.G. Gooch, Br. Corros. J., **31**, 309 (1996).

38. S. Pak and L. Karlsson, Scand. J. Metall., **19**, 9 (1990).

39. R. Francis and G.R. Warburton, "Effect of post weld surface treatments on the corrosion resistance of super duplex stainless steel welds in seawater," Corrosion/2000, Paper #630, NACE, Houston (2000)

40. R.B. Rebak and N.E. Koon, "Localized corrosion resistance of high nickel alloys as candidate materials for nuclear waste repository. Effect of alloy and weldment aging at 427 deg C for up to 40,000 h," Paper #153, Corrosion/98, NACE, Houston (1998).

41. M. Kohler and D.C. Agarwal, "Thermal stability and microstructural changes of some Ni-Cr-Mo alloys as detected by corrosion testing," Paper #313, Corrosion/98, NACE, Houston (1998).

42. H.M. Tawancy and A.I. Asphahani, "Ordering Behavior and Corrosion Properties of Ni--Mo and Ni--Mo--Cr Alloys," in High-Temperature Ordered Intermetallic Alloys, pp 485-494, Materials Research Society, Pittsburgh (1985).

43. J.H. Cleland, "What does the pitting resistance equivalent really tell us?," Engineering Failure Analysis, **3**, pp 65-69 (March 1996).

44. N. Sridhar, "Effect of Alloying Elements on Localized Corrosion Resistance of Nickel-Base Alloys," in Advances in Localized Corrosion, pp 263-269, NACE, Houston (1990).

45. J.N. Visser, "History and Development: The Hastelloy Family," Stainless Steel Europe, **4**, no. 21, pp.54-57 (October 1992).

46. Hastelloy Alloy C-22 (Nickel--Chromium--Molybdenum Alloy), Alloy Dig., pp. 2, July 1985.

47. H.H. Uhlig and J. Wulff, Trans AIMME, **135**, 494 (1939).

48. M.A. Streicher, J. Electrochem. Soc., **103**, 375 (1956).

49. K.-K. Baek, H.-J. Sung, C.-S. Im, I.-P. Hong and D.-K. Kim, "Evaluation of pitting corrosion resistance of high-alloyed stainless steels welds for FGD plants in Korea," Paper #474, Corrosion/98, NACE, Houston (1998).

50. A. Pardo, E. Otero, M.C. Merino, M.D. Lopez, M.V. Utrilla and F. Moreno, Corrosion, **56**, 411 (2000).

51. R.J.Brigham, Corrosion, **30**, 396 (1974); Mater. Perform., **24**, 44 (1985), Mater. Perform., **13**, 29 (1974).

52. C W Kovach and J D Redmond, "Correlations between the CCT, PRE number and long-term crevice corrosion data for stainless steels," Corrosion/93, Paper #267, NACE, Houston (1993).

53. B.A. Kehler, G.O. Ilevbare and J.R. Scully, "Comparison of the crevice corrosion resistance of alloys 625 and 22 in concentrated chloride solution from 60 to 95 deg C,"

Corrosion 2000, paper #182, NACE, Houston (2000); R.S. Lillard and J.R. Scully, J. Electrochem. Soc., **141**, 3006 (1994).

54. N. Suutala and M. Kurkela, "Localized Corrosion Resistance of High Alloy Austenitic Stainless Steels and Welds," in Proc. Stainless Steel '84, (Goteborg 1984), pp 240-247, Institute of Metals, London (1984).

55. M. Kobayashi, S.-I. Akiyama, S. Kiya, T. Matsuda, T and H. Uno, "Effect of Chromium, Molybdenum and Nitrogen Contents on the Critical Pitting Temperature of Stainless Steels," Nippon Stainless Tech. Rep., no. 19, pp. 23-46 (1984).

56. J.H. Russell and B.S. Covino, "Critical temperatures for crevice corrosion of high-nitrogen stainless steels," Paper #695, Corrosion/98, NACE, Houston (1998).

57. J. Stewart and D.E. Williams, Corros. Sci., **33**, 457 (1992).,

58. N.J. Laycock, M.H. Moayed and R.C. Newman, J. Electrochem. Soc., **145**, 2622 (1998).

59. G. Riedel, H. Werner and C. Voigt, Materials and Corrosion (Germany), **47**, 383 (1996).

60. J.M. Sykes and L.F. Garfias Mesias, Corros. Sci., **41**, 959 (1999).

61. R.C. Newman and K.H. Liew, Corrosion, **43**, 58 (1987).

62. M.H. Moayed, PhD thesis, UMIST (1999).

63. M.H. Moayed, N.J. Laycock and R.C. Newman, "Effect of surface finish on the critical pitting temperature," Corros. Sci., submitted (2002).

64. A. Elhoud, MPhil thesis, UMIST (1999).

65. S. Strom and H. Li, "Oxide Induced Corrosion on the Welded Stainless Steels SS 2352 and 2353," Korrosionsinstitutet Rapport (Sweden), pp. 26, 1991 (KI Rapp. 1991:1).

66. P. Gumpel, T. Vollmer, M. Blaise and W. Racky, "Effect of surface condition on corrosion resistance of stainless steels," Stainless Steel Europe, **7**, 47-49, (1995).

67. M.B. Rockel and W.R. Herda, Werkstoffe und Korrosion, **43**, 354 (1992).

68. M.H. Moayed and R.C. Newman, Corros. Sci., **40**, 519 (1998).

69. N.J. Laycock and R.C. Newman, Corros. Sci., **40**, 887 (1998).

70. N.J. Laycock and S.P.White, "Influence of temperature on pitting corrosion of stainless steels," in Corrosion & Prevention-2000 (Auckland, 2000), Paper #43, Australian Corrosion Association (2001).

13. Development in the Concept of Repassivation Potential as a Measure of Crevice Corrosion Susceptibility

Toshio Shibata
Fukui University of Technology,
Fukui, Fukui Prefecture, JAPAN

EDITORIAL NOTE

This volume, "A Compilation of Special Topic Reports," contains a series of reports that were prepared for the Waste Package Materials Performance Peer Review Panel to use as background and input to the peer review. Summaries drawn from the reports were also presented in Section 11 of the Panel's Final Report. The Panel used the reports as background and input for its review. Any views and comments expressed in the summaries and the full reports do not necessarily reflect the opinion and findings of the Panel. Further, opinions expressed in the reports are not necessarily those of the Panel or reflected in the Panel's reports and recommendations.

1. Introduction

Various electrochemical methods for evaluating the corrosion resistance of stainless steels have been developed and standardized in various industrial standards such as JIS, ASTM, ISO and others. Pitting potential is most popularly used for evaluating the pitting corrosion resistance of stainless steels and/or for evaluating the exact performance in the industrial applications. Tests for the potentials associated with crevice corrosion formation or repassivation have been not standardized because crevice corrosion depends not only on solution chemistry and alloy composition, but also on the crevice geometry. Various crevice electrode assemblies for the electrochemical tests have been proposed and polarization methods were used for identifying crevice generation and repassivation behavior (1-3). In Japan, Shiobara found a large decrease in the generation and repassivation potential for localized corrosion on creviced electrodes compared with nominally uncreviced titanium (4) and stainless steel (5) electrodes. Suzuki reported that crevice corrosion of stainless steels in the field could be effectively suppressed by maintaining the potential below a critical protection potential (6). In the 1970's, it was recognized that there are three characteristic potentials relating to crevice corrosion of passive metals; generation, repassivation and protection potentials. In 1980, Tsujikawa reported that the protection potential could be evaluated by measuring a critical potential for stopping crevice growth under appropriate electrochemical and geometrical conditions (7). This critical potential was called repassivation potential for crevice corrosion, $E_{R,CREV}$.

Special Topic Report prepared for the Waste Package Materials Performance Peer Review. The Final Report of the Peer Review was submitted to U.S. Department of Energy and Bechtel SAIC Company, LLC on February 28, 2002.

Through the 80's and 90's, research committees organized by the Japanese Society of Corrosion Engineering (JSCE) published a series of progress reports, including case histories of field failures due to crevice corrosion, round robin tests, and a proposal for standardization of the measurement of $E_{R,CREV}$. Based on the accumulation of a sufficient database for the measurement of E_{RCREV}, a JIS committee decided to standardize a method. "Method of determining the repassivation potential for crevice corrosion of stainless steels" will be published in 2002 (8).

2. Concept of Repassivation Potential for Crevice Corrosion

It is well accepted that the possibility for the initiation and development of localized corrosion could be judged by comparing the open circuit potential, E_{op}, with the critical potential, E_{crit}, as shown in Fig.1. For the waste package, WP, this criterion could be used successfully. However, whereas the open circuit potential can be easily determined by conventional methods, there are still many discussions about how to determine the critical potential for the localized corrosion, especially for crevice corrosion. Pitting potential is well accepted as a characteristic potential for generation of pitting on a free surface.

Accumulated field experience, however, indicates that crevice corrosion, which is formed under deposits or at contacts between flanges, is a more important failure mode than pitting corrosion. Stress corrosion cracking, which is the other important failure mode of localized corrosion, is more likely to initiate after crevice corrosion. It is required to assess crevice corrosion behavior more definitely and to establish a measure for characterizing crevice corrosion. Many people from academia and industry in Japan have been studying the mechanism of crevice corrosion since the beginning of the 1980's. Tsujikawa played a major role in understanding the basic mechanism of crevice corrosion and proposed a concept of repassivation potential for stopping a growing crevice, providing a conservative and unique measure for crevice corrosion resistance.

As shown in Fig. 2, the initiation potential for crevice corrosion, E_1, can be seen in an anodic potentiodynamic polarization curve by using the working electrode with an intentionally-formed crevice. The same test provides the value of E_2, the potential at which the anodic current approaches to zero in the reverse scan. Tsujikawa found that E_2 depends on the depth of the crevice and scanning conditions. His detailed analysis on the conditions of growing and stopping crevices around E_2 showed that a critical potential called repassivation potential for crevice corrosion, $E_{R,CREV}$, could provide a conservative and reliable measure for evaluating the susceptibility of passive alloys to crevice corrosion. No occurrence of crevice corrosion below $E_{R,CREV}$ was observed in a large amount of data including the round robin tests. He showed that the crevice formation proceeds by a two-stage process. The first stage occurs near the edge of the crevice at a higher dissolution rate with little dependence on potential and alloy composition. This is followed by the second stage, which occurs at greater depths and depends largely on potential and alloy composition. The second stage is the step at which a stable crevice forms (9). This is the reason why the method described below requires that a crevice at least 40 σm deep must be confirmed after the measurement.

3. Standardized Method to Measure $E_{R,CREV}$

An electrochemical method can be used for determining the repassivation potential, $E_{R,CREV}$, with a conventional potentiostat, an electrochemical cell and a specimen electrode with a tight crevice as shown in Fig. 3 (8). A metal/metal crevice is formed at the contact interface between two plates with different areas that are fastened by a titanium washer and bolt. The contact area is 20 x 20 mm. Before the measurement, the surface of both specimens should be polished with #600 paper and rinsed with distilled water or alcohol, followed by assembling two plates into the electrode in a wetted condition using the test solution. The test solution in the standard uses sodium chloride solution containing 200 ppm Cl^- at 50°C.

Crevice corrosion in the specimen with a tight crevice is initiated by anodic potentiodynamic polarization over E_1. The sample is then held galvanostatically to grow the crevice to a sufficient size. The potential is then stepped downward to determine the critical potential to stop the crevice growth. The actual procedure to measure $E_{R,CREV}$ is shown in Fig. 4 (8). The plate specimen with the tight crevice is immersed in dearated sodium chloride solution, and polarized in the anodic direction from the open circuit potential by a constant sweep rate of 30 mV/min until 0.2 mA anodic current is observed. At this potential, the potentiostat switches modes to control the anodic current at a constant value of 0.2 mA for 2 hours to ensure formation of a deep crevice. After the 2 h galvanostatic treatment, the potential of the specimen is stepped down by 10 mV under potentiostatic control, during which the anodic current is monitored. After every 10 mV step down, the anodic current decreases at first, but again increases if the crevice is active. The potential at which no increase in the anodic current is observed during 2 hours, indicating death of the active crevice, corresponds to $E_{R,CREV}$. After the measurement, it is required to confirm the formation of the crevice, the depth of which should be more than 40 σm. If the depth of crevice was not found to reach 40 σm, the data has to be discarded.

4. Examples and Remarks

Some examples of the measurements on Type 304 stainless steel are shown in Fig. 5 (10), in which $E_{R,CREV}$ (10mV/2h) measured by the standardized method described above is plotted as a function of chloride concentration with other characteristic potentials of $V'_{C,CREV}$(30mV/min) and $E_{R,CREV}$(10mV/min), which are the initiation and repassivation potentials, respectively, for crevice corrosion determined by the potentiodynamic method instead of the standardized method. The discrepancy between $E_{R,CREV}$(10mV/2h) and $E_{R,CREV}$(10mV/min) becomes larger with decreasing chloride concentration. $E_{R,CREV}$ (10mV/2h) is more reliable because a quasi steady state of the solution chemistry within crevice could be maintained due to longer term holding. Another example obtained by the round robin test is shown in Fig. 6 (11), which demonstrates that crevice generation on a creviced electrode kept at a constant potential requires some incubation time above $E_{R,CREV}$, but no crevice is formed when the potential is below $E_{R,CREV}$.

The usefulness and reliability of this method proposed by Tsujikawa (7) has been discussed for years in Japan. Industrial engineers hesitate to standardize the Tsujikawa method, because they believe that $E_{R,CREV}$ determined by this method is too severe and conservative. It was claimed that $E_{R,CREV}$ of common stainless steels like Type 304 is sometimes less noble than the open circuit potential in ordinary environments in which the steel even could be utilized. This situation might be judged to be in the incubation stage shown in Fig. 6. If stainless steel is used in this condition, we could expect the generation of a crevice after some incubation time. At present we have no definite model or reliable theory to predict the incubation time, and this material should be replaced one with higher $E_{R,CREV}$ if long time performance is required.

Because of its conservative nature, I would like to recommend $E_{R,CREV}$ for evaluating the long-term crevice corrosion behavior of candidate WP materials. If $E_{R,CREV}$ of the candidate alloy is above the open circuit potential in the repository environment, we could have a confidence to use the material for the WP for long term without crevice corrosion. Another important point which should be discussed is how to assume the environmental condition for the candidate alloy in the repository site because $E_{R,CREV}$ depends on the environmental conditions.

Acknowledgment

I would like to express sincere thanks to Dr. M. Akashi who made a great contribution for preparing the draft of the JIS of the repassivation potential.

References

1. I. L. Rosenfeld and I. K. Marshakov, Corrosion, **20**, 115t (1964).

2. B. E. Wilde, Corrosion, **28**, 283 (1972).

3. E. A. Lizlovs, J. Electrochem. Soc., **117**, 1335 (1970).

4. K. Shiobara and S. Morioka, Trans. Japan Inst. Metals, **33**, 581 (1969).

5. K. Shiobara and S. Morioka, Trans. Japan Inst. Metals, **36**, 385 (1972).

6. T. Suzuki and Y. Kitamura, Corrosion, **28**, 1 (1972).

7. S. Tsujikawa and T. Hisamatsu, Boshoku Gijutsu (Corrosion Engineering), **29**, 37 (1980).

8. Draft of the JIS on "Method of Determining the Repassivation Potential for Crevice Corrosion of Stainless Steels," which will be published in 2002.

9. T. Shinohara, S. Tsujikawa, and N. Masuko, Boshoku Gijutsu (Corrosion Engineering), **39**, 238 (1990).

10. M. Akashi and S. Tsujikawa, Zairyo-to-Kankyo (Corrosion Engineering), **45**, 106 (1996).

11. T. Fukuda, Summary of the Round Robin Test, Proc. of the115th Corrosion and Protection Symposium, JSCE, p.38 (1997)

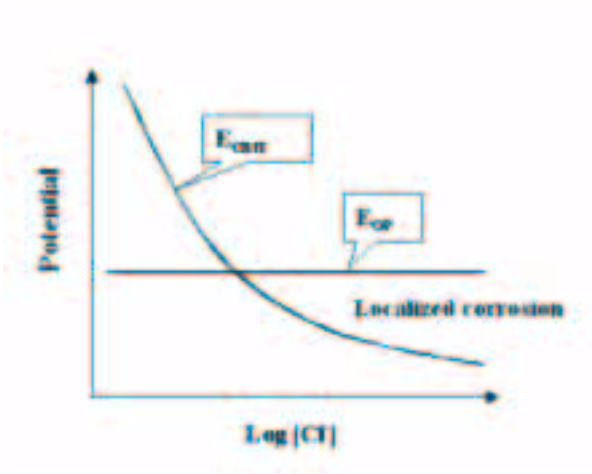

Fig.1 – Localized corrosion is possible to occur at Ecrit <Eop.

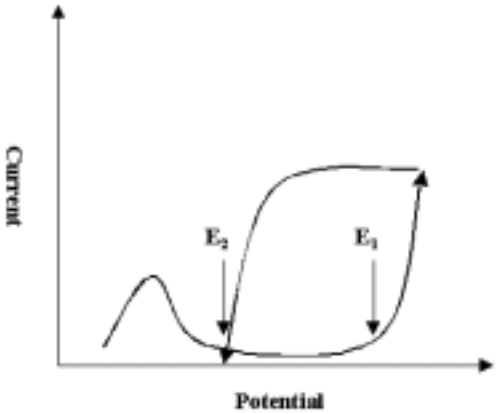

Fig. 2 – Initiation and Termination of Crevice Growth at E_2 and E_1

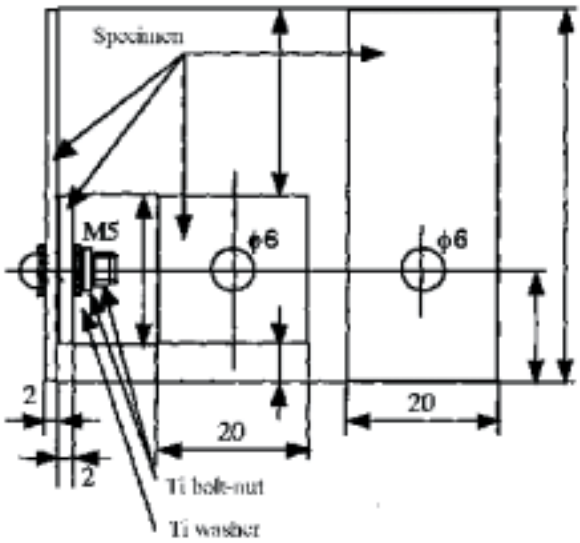

Fig.3 – Specimen Electrode with a Crevice

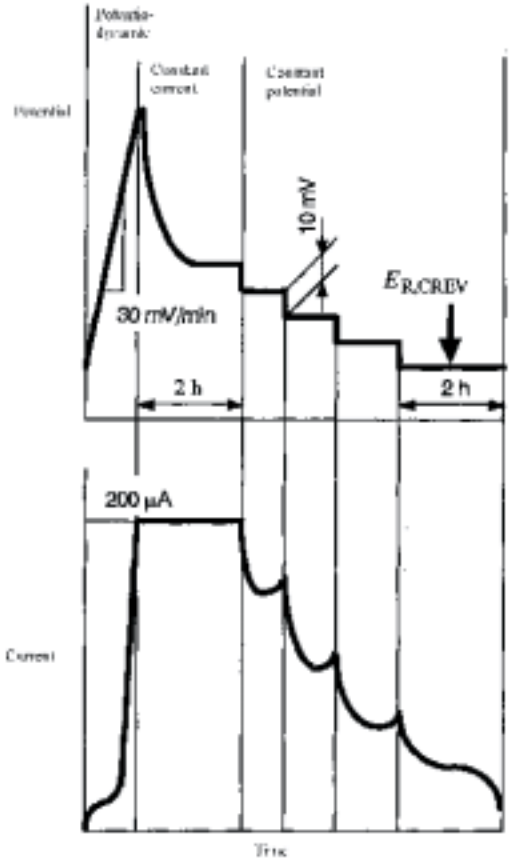

Fig. 4 – Polarization Procedure for Measuring $E_{R,CREV}$

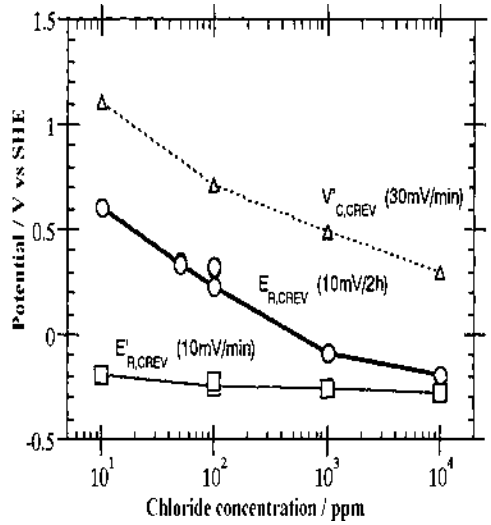

Fig. 5 – $E_{R,CREV}$ as a function of [Cl^-] for Type 304 SS at 328 K (10).

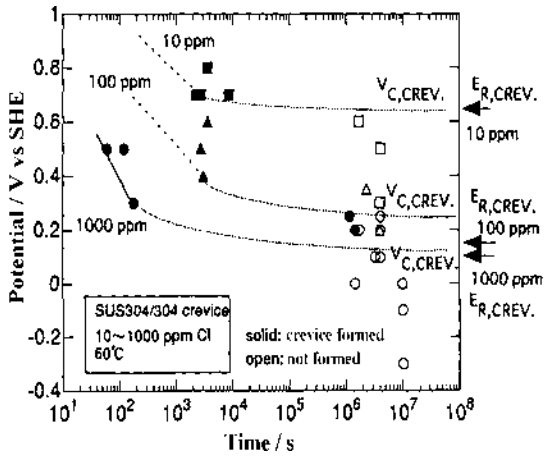

Fig. 6 – Crevice Generation Time Depending on Potential and Chloride Concentration

14. The Critical Potential for Localized Corrosion

Masatsune Akashi
Ishikawajima-Harima Heavy Industries Co., Ltd. (IHI)
Research Laboratories
Tokyo, JAPAN

EDITORIAL NOTE

This volume, "A Compilation of Special Topic Reports," contains a series of reports that were prepared for the Waste Package Materials Performance Peer Review Panel to use as background and input to the peer review. Summaries drawn from the reports were also presented in Section 11 of the Panel's Final Report. The Panel used the reports as background and input for its review. Any views and comments expressed in the summaries and the full reports do not necessarily reflect the opinion and findings of the Panel. Further, opinions expressed in the reports are not necessarily those of the Panel or reflected in the Panel's reports and recommendations.

Special Topic Report prepared for the Waste Package Materials Performance Peer Review. The Final Report of the Peer Review was submitted to U.S. Department of Energy and Bechtel SAIC Company, LLC on February 28, 2002.

The Critical Potential for Localized Corrosion

- There exists a critical potential for each form of localized corrosion, V_C.

- The safety usage domain can be quantitatively defined on the comparison of V_C to the steady-state corrosion potential, E_{SP};

  $E_{SP} \geq V_C$:
  possibility of the localized corrosion

  $E_{SP} < V_C$:
  immunity to the localized corrosion

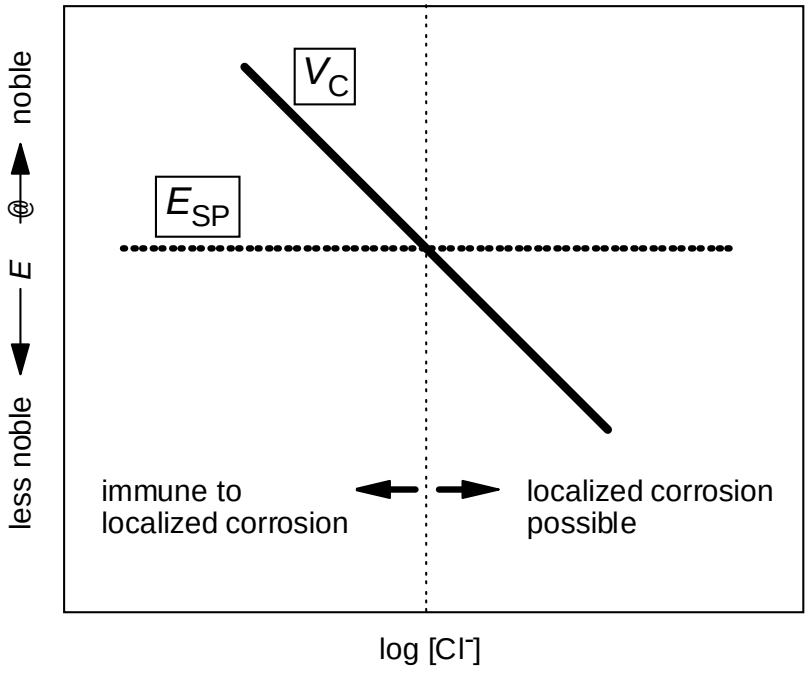

Corrosion Potential vs. Time

The free-corrosion potential, E_{corr}, changes with time, becoming higher as the time elapses, and attaining the steady-state corrosion potential, E_{SP}, after a few months of time.

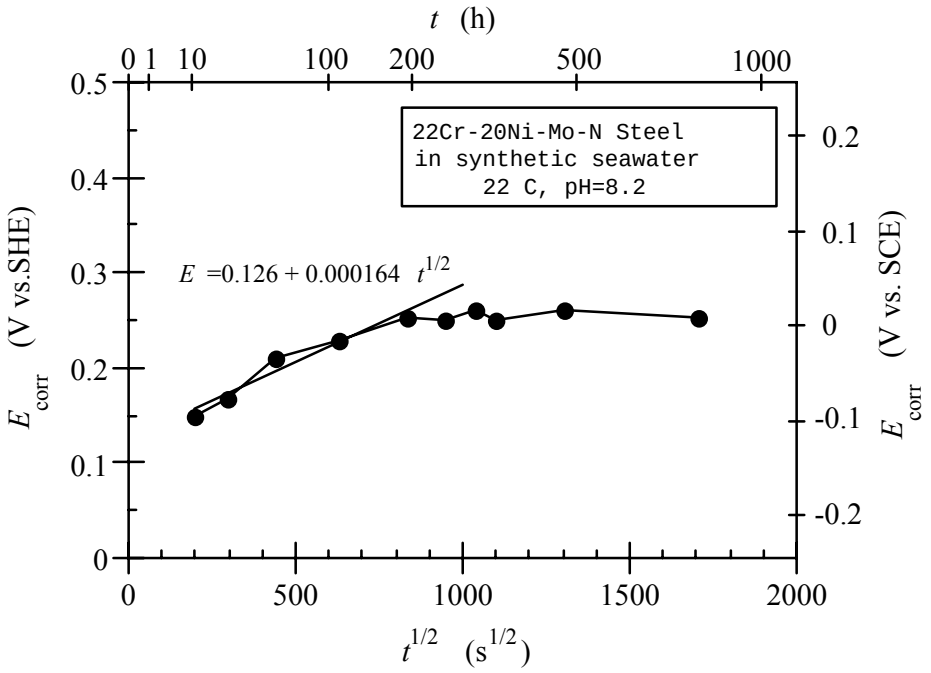

E_{SP} vs. pH

- No difference between the stainless steel and the titanium.
- Small temperature dependency.
- E_{SP} = +0.32 V vs. SHE at pH = 7.

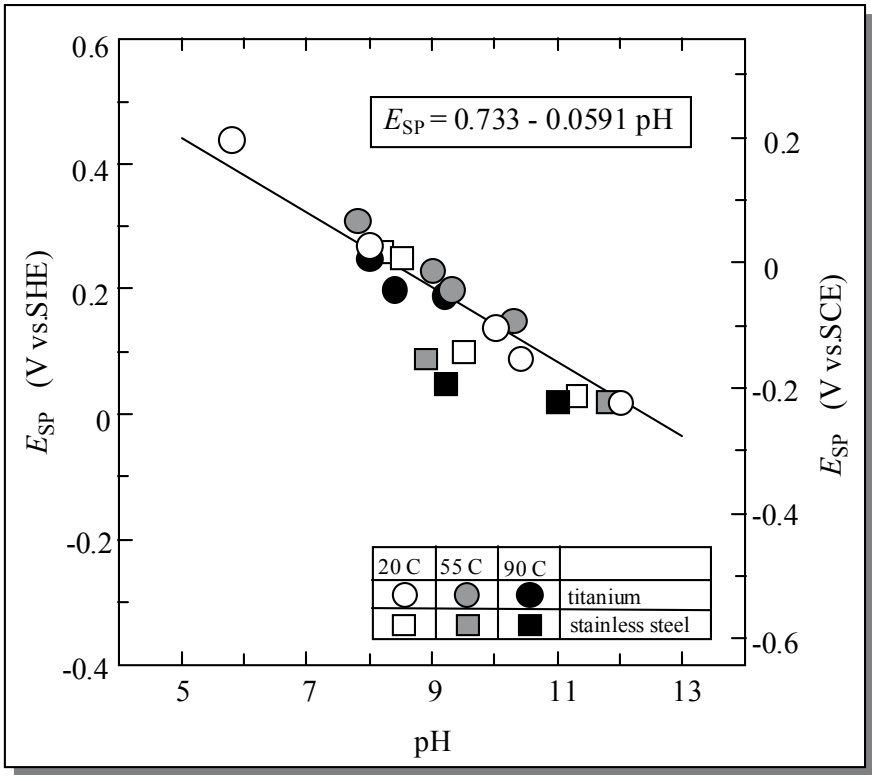

Determination of E_{SP}

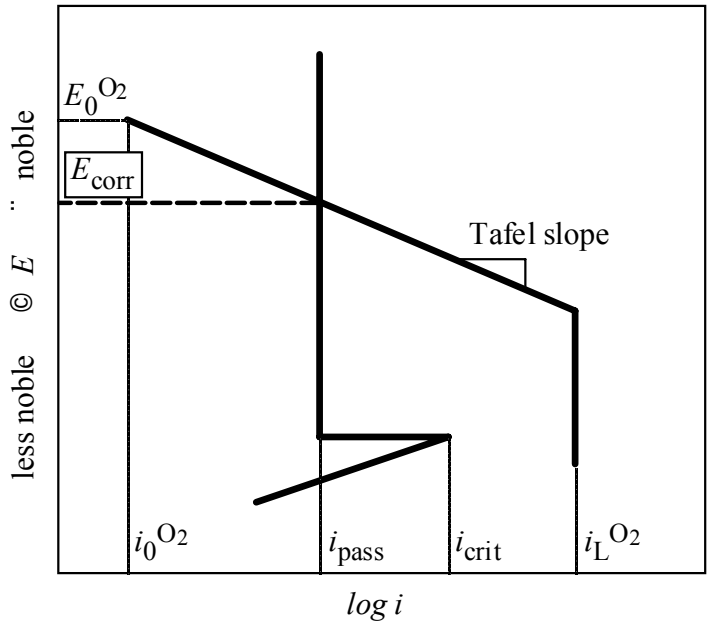

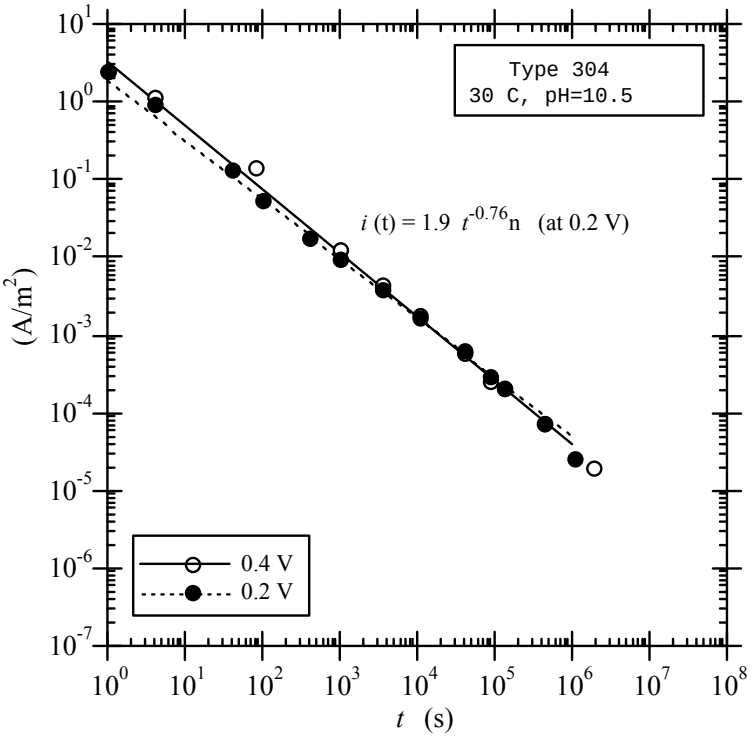

The Critical Potential for Localized Corrosion

The critical potential for localized corrosion, V_C, is defined as the lowermost potential at which the concerned localized corrosion has taken place in the potentiostatically holding test. This means that determining a V_C in literal accordance with this definition calls for a great number of specimens and a great deal of time. Therefore, development of a simpler way of determination has been an industrial request.

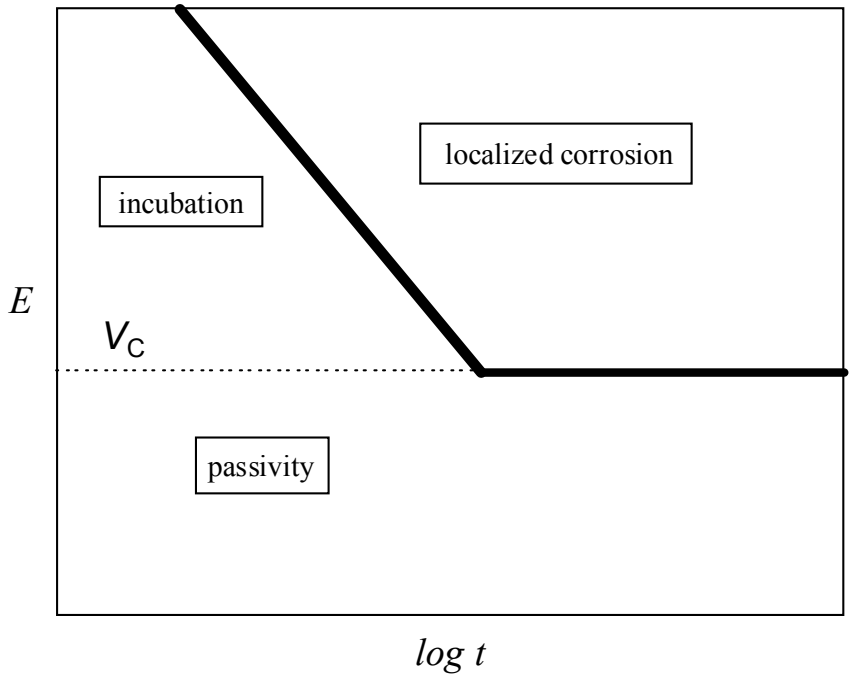

V'_C as determined by the potentiokinetic polarization

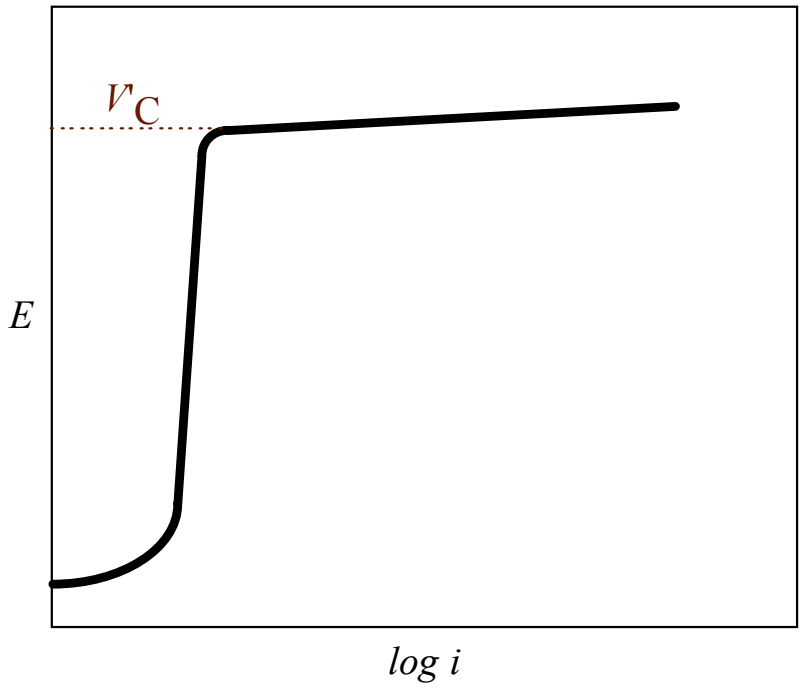

Pitting Corrosion

Since the $V'_{C,PIT}$ as determined by the potentiokinetic polarization test agrees approximately with $V_{C,PIT}$, the use of $V'_{C,PIT}$ for $V_{C,PIT}$ has been a universal practice.

Crevice Corrosion

The $V'_{C,CREV}$ as determined by the potentiokinetic polarization test is higher, often by as much as several hundred mV, than $V_{C,CREV}$.

The Critical Potential for Crevice Corrosion

This trouble has been remedied by Tsujikawa and Hisamatsu (1980) when they have demonstrated that the corrosion-crevice repassivation potential, $E_{R,CREV}$, which is to be determined by the cycling polarization test with a creviced specimen.

[Ref] S. Tsujikawa, Y. Hisamatsu: Corr. Eng. (Jpn.), **29**, 37 (1980).

$E_{R,CREV}$: Corrosion-Crevice Repassivation Potential (Tsujikawa method)

- The specimen electrode potential is potentiostatically varied in the noble direction so as to initiate the corrosion crevice.
- When the corrosion current has reached 200 σA, the current is galvanostatically held at this level for 2 hours so as to allow the corrosion crevice to progress further.
- Then the electrode potential is reduced by 10 mV, and potentiostatically held for some time to see if the corrosion current takes an upward turn, in which case it is reduced further by 10 mV.
- This step is repeated until the increase in corrosion current no longer recognized after 2 hour's holding, and the noble-most potential that brings about this situation is taken as the corrosion-crevice repassivation potential, $E_{R,CREV}$.

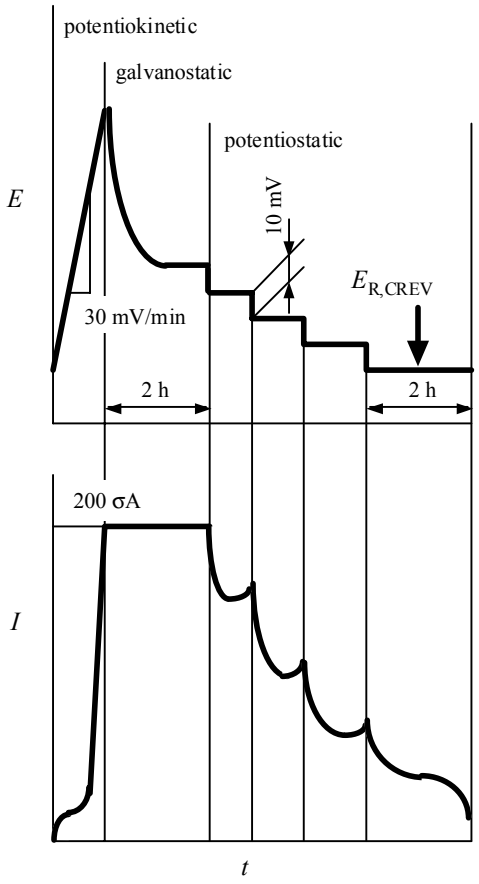

Special Topic Report prepared for the Waste Package Materials Performance Peer Review. The Final Report of the Peer Review was submitted to U.S. Department of Energy and Bechtel SAIC Company, LLC on February 28, 2002.

$E_{R,CREV}$ vs. $V_{C,CREV}$

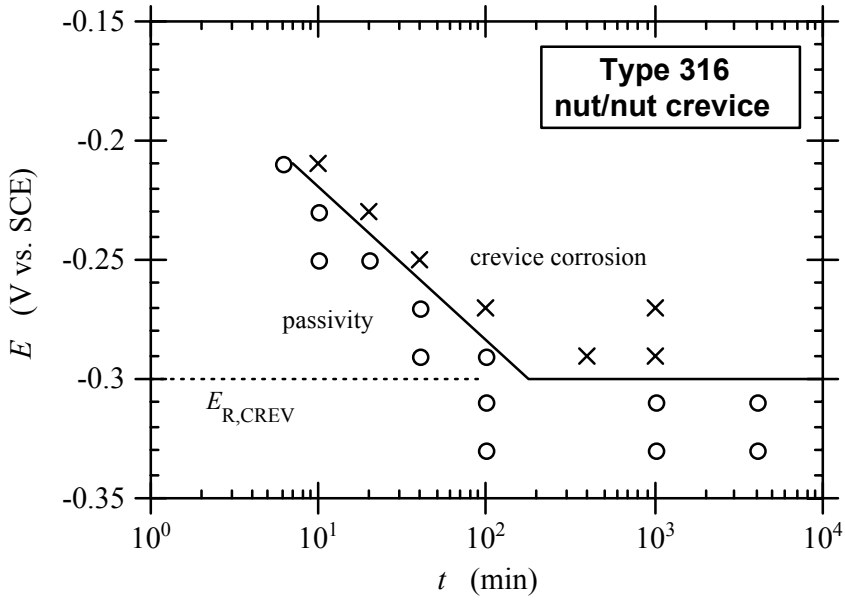

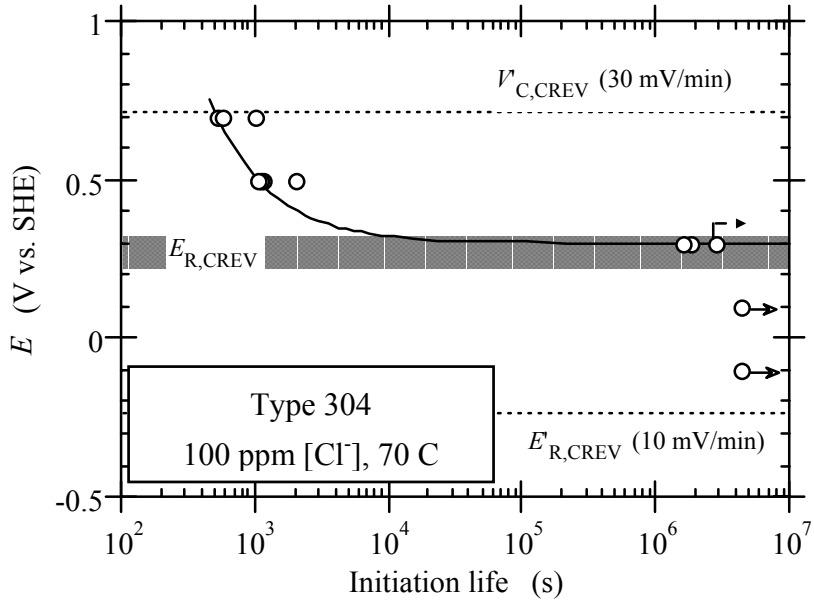

$E_{R,CREV}$ agrees with $V_{C,CREV}$

[Ref] S. Tsujikawa, Y. Hisamatsu: Corr. Eng. (Jpn.), **29**, 37 (1980).

M. Akashi, G. Nakayama, T. Fukuda: CORROSION/98, Paper No. 98158 (1998).

"Low-Rate Stepwise Polarization"

- It must be emphasized that the most important technical point in determining $E_{R,CREV}$ resides in "the stepwise polarization rate should be set slow enough near $E_{R,CREV}$," for failure of observing this rule can result in obtaining outrageous $E_{R,CREV}$'s.

- The use of the continuous potentiokinetic polarization method (*i.e.*, the so-called "dynamic" method) for its simplicity instead of authentic low-rate stepwise polarization method (*i.e.*, the "steady" method), which is admittedly awkward and time-consuming, is all and utterly wrong.

- As a proof for this statement, the author offers next figure, where the $E_{R,CREV}$'s determined by the dynamic method (at 10 mV/min) are compared to their counterpart $E_{R,CREV}$'s (10 mV/(2 hr) stepwise for currents less than 50 σA), both as determined for a Type 304 stainless steel in [NaCl] solution environments at 55 C

[Ref] M. Akashi, G. Nakayama, T. Fukuda: CORROSION/98, Paper No. 98158 (1998).

$E_{R,CREV}$ *vs.* $E'_{R,CREV}$

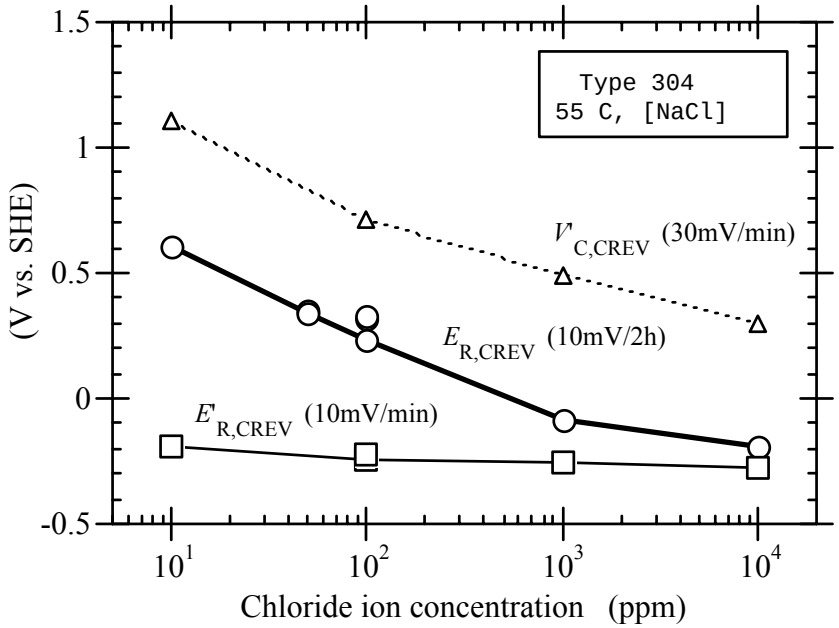

- The two can agree with each other only when [Cl^-] concentration is unusually high.
- It is to be noticed here also that the values of the dynamically determined (30 mV/min) critical potential for corrosion-crevice initiation, $V'_{C,CREV}$, shown in the figure as a reference, all run far higher.

[Ref] M. Akashi, G. Nakayama, T. Fukuda: CORROSION/98, Paper No. 98158 (1998).

$E_{R,CREV}$ *vs.* $V_{C,CREV}$

- The $E_{R,CREV}$ determined by the steady method coincides correctly with the potentio-statically determined $V_{C,CREV}$, whereas the $E'_{R,CREV}$ lies far low, and the $V_{C,CREV}$ far high, to it.

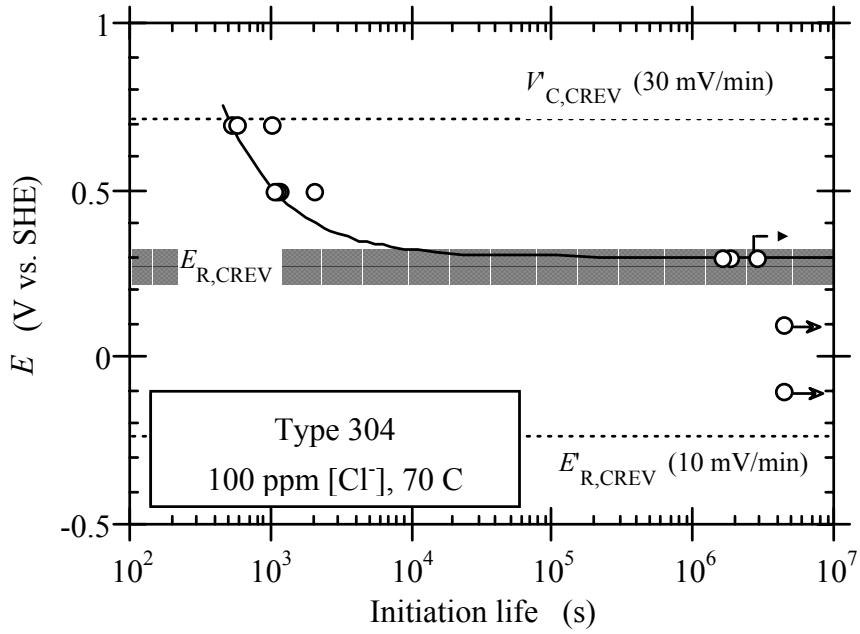

[Ref] M. Akashi, G. Nakayama, T. Fukuda: CORROSION/98, Paper No. 98158 (1998).

$E_{R,CREV}$ *vs.* $E'_{R,CREV}$ *(2)*

- While it is true enough that the $E'_{R,CREV}$ does approach $E_{R,CREV}$ with decreasing scan rate, the discrepancy is quite appreciable even at 1 mV/min.

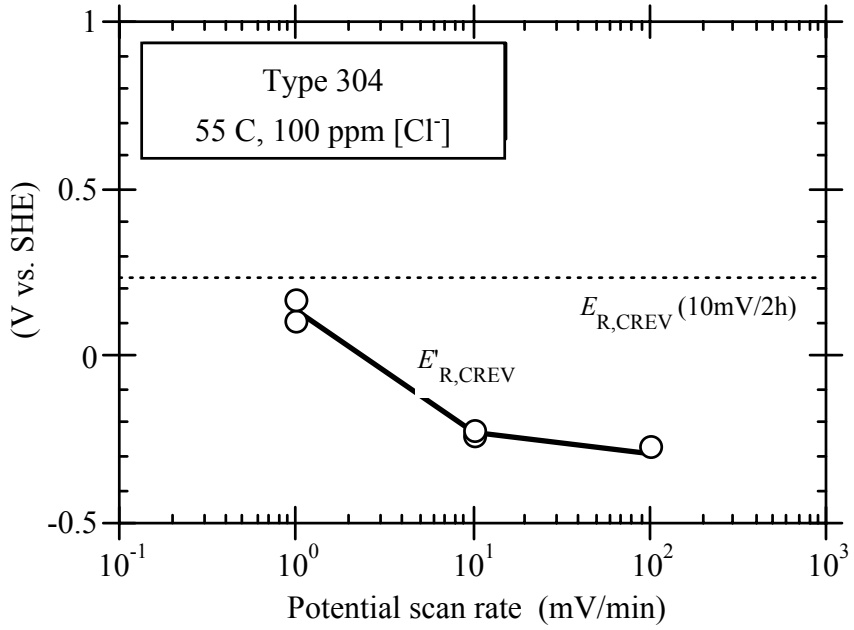

[Ref] M. Akashi, G. Nakayama, T. Fukuda: CORROSION/98, Paper No. 98158 (1998).

Conclusions

It can be concluded that the $E_{R,CREV}$ can be a sufficient substitute for the $V_{C,CREV}$, with the proviso that the stepwise polarization rate be held slow enough, at least near the $E_{R,CREV}$, and that neither the $E'_{R,CREV}$ nor the $V'_{C,CREV}$ should be used as a feature value.

Safety Usage Limits for Type 304 stainless steel

- This figure gives the safety usage limits for Type 304 stainless steel pertaining to crevice corrosion on the rule that a metal should be immune to it whenever $E_{R,CREV} > E_{SP}$ (=+0.32 V vs. SHE at pH=7, as shown earlier).
- According to this diagram, the critical [Cl^-] concentration for an operation temperature of 70 to 80 C range is approximately 20 ppm, a prediction that perfectly tarries with the practical experiences.

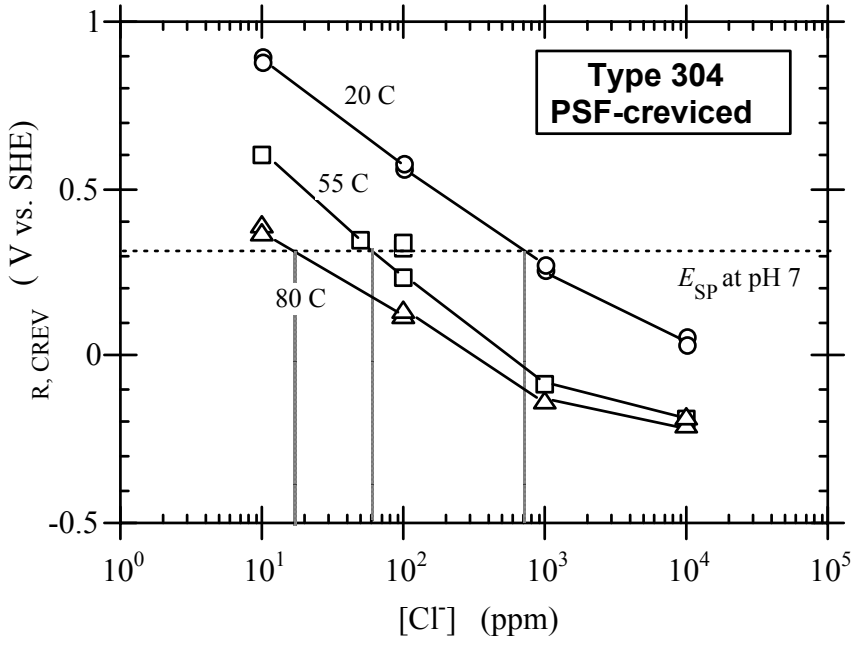

[Ref] M. Akashi, G. Nakayama, T. Fukuda: CORROSION/98, Paper No. 98158 (1998).

Safety Usage Limits

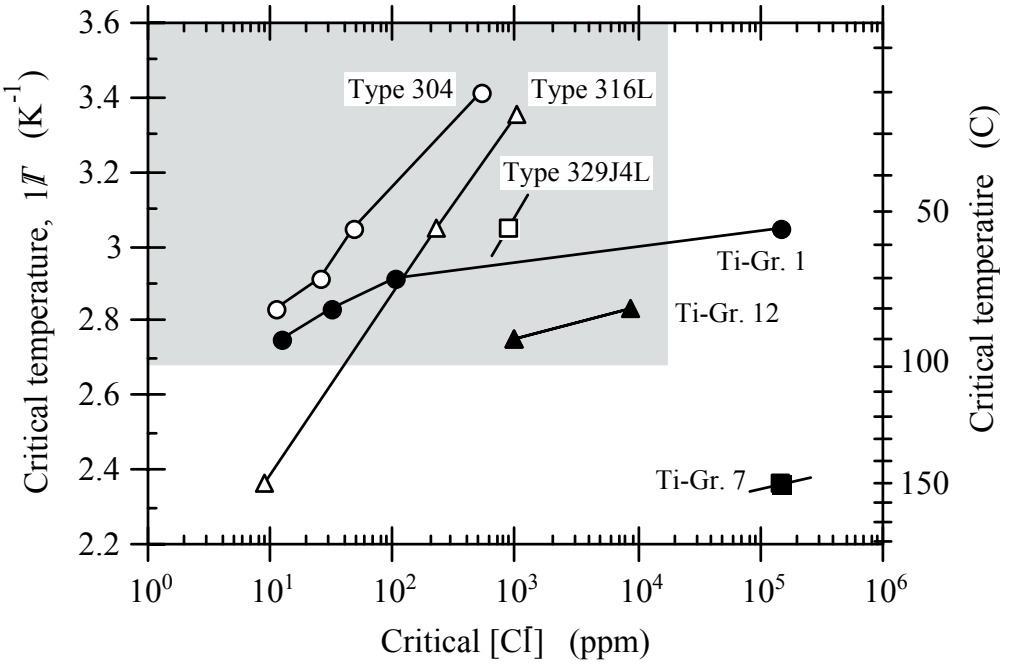

[Ref] M. Akashi, G. Nakayama, T. Fukuda: CORROSION/98, Paper No. 98158 (1998).

15. Formation of an Aqueous Environment from Condensation in Dust Layer

Robert P. Frankenthal
Basking Ridge, New Jersey, USA

EDITORIAL NOTE

This volume, "A Compilation of Special Topic Reports," contains a series of reports that were prepared for the Waste Package Materials Performance Peer Review Panel to use as background and input to the peer review. Summaries drawn from the reports were also presented in Section 11 of the Panel's Final Report. The Panel used the reports as background and input for its review. Any views and comments expressed in the summaries and the full reports do not necessarily reflect the opinion and findings of the Panel. Further, opinions expressed in the reports are not necessarily those of the Panel or reflected in the Panel's reports and recommendations.

This report deals with the formation of the aqueous environment on waste package and drip shield surfaces. The source of water is condensation with no contribution from direct seepage or dripping.

Origin, Size Distribution, and Composition

The typical environment while the repository is open and, in particular, during construction will contain all the components present in outdoor environments, such as gases derived from fossil fuel combustion processes, sulfur dioxide (SO_2) and nitrogen oxides (NO_x), particulate matter, and microbes (1). It will also contain components derived from indoor sources, such as outgassed vapors from paints, plastics, operational activities, smoking, office equipment, appliances, etc. (2) The factors likely to affect the environment include, temperature, relative humidity, electric fields, air velocity, mechanical stresses, and thermal shock (2).

Particulates present in the environment are distinguished by a bimodal size distribution (2). Most of the particulate mass exists in the size range 0.1 to 15 σm. Particles 2.5 to 15 σm in size, usually referred to as coarse particles, are largely derived from natural materials and are largely mineralogical in composition. They typically form from the erosion of soils and rock due to wind and rain or are the result of human activity such as mechanical processes.

Particles in the size range of 0.1 to 2.5 σm, usually called fine particles, are mostly derived from anthropogenic sources such as fossil fuel combustion (2). Geological and volcanic activity may also contribute to their origin. Fine particles are formed by a complex sequence of chemical and photochemical reactions in which SO_2 and NO_X , products of fossil fuel combustion, are oxidized further over periods of hours and days to sulfuric acid and nitric acid.

Special Topic Report prepared for the Waste Package Materials Performance Peer Review. The Final Report of the Peer Review was submitted to U.S. Department of Energy and Bechtel SAIC Company, LLC on February 28, 2002.

The two acids are neutralized to varying extents, depending on the environment, by ambient NH_3, ammonia, which is the result primarily of animal and human activity. The particles, at first smaller than 0.1 σm, rapidly grow through condensation on carbonaceous nuclei acting as seed particles to the stable size range of fine particles, i.e. 0.1 to 2.5 σm. These seed particles are also largely a product of fossil fuel combustion.

The corrosivity of dust particles is largely the result of the water-soluble ions they contain. The higher the fraction of these ions, the higher the corrosivity is likely to be. Coarse particles, due to their origin, tend to have a much lower water-soluble ion content than fine particles. As a result, coarse particles are generally much less corrosive than fine particles. The composition of the coarse particles at the Yucca Mountain site will be determined primarily by the composition of the local soils and rocks. Inside the repository, the origin of coarse particles will be the local rock formations and also external sources brought in with fresh air by ventilation processes.

As shown by Sinclair and coworkers (3), fine particles contain principally ammonium (NH_4^+), sulfate (SO_4^{2-}), acid sulfate (HSO_4^-), and nitrate (NO_3^-) ions. In most cases the salts contained in coarse particles have a much higher critical relative humidity (CRH) than the salts in fine particles. The CRH of the coarse particles is usually greater than 80%, while the CRH of salts in fine particles are in the range of 40% (NH_4HSO_4) to 81% [$(NH_4\}_2SO_4$]. Other salts commonly found in fine particles include NH_4NO_3 (CRH 65%) and NaCl (CRH 70%), the latter only in marine environments. CRH is a function of temperature. The values given above are for a temperature of 24°C (4,5).

Deposition rates on surfaces depend on particle concentration and migration rates (2). Relevant factors affecting the migration rate include particle size, velocity, temperature, and surface configuration. Electric fields, if present, would also be a factor. Coarse particles are sufficiently large to deposit by gravitational settling. They most frequently deposit on top horizontal surfaces unless air velocities are very high and the surface is tacky. The sticking coefficient is almost always unity. The residence time of typical coarse particles suspended in air of an ordinary room is a maximum of a few minutes, i.e., these particles settle on surfaces rapidly. The migration of fine particles, on the other hand, is controlled by convective diffusion. They can remain in the air for hours and even days, depending on the ambient air exchange rate. They deposit with equal likelihood on all surface configurations and can penetrate narrow spaces and crevices more easily than coarse particles.

A most relevant factor determining deposition for the Yucca Mountain project is the thermophoretic effect (6,7). Particles are attracted to surfaces colder than the particles and are repelled from surface that are warmer. The thermophoretic force and velocity are both proportional to the thermal gradient, ⊆T. The implication of this is that fine particles, i.e., the corrosive particles, are not likely to deposit on the containers until they cool to ambient temperature. By that time, presumably, all activities generating corrosive fine particles, i.e., combustion processes will have ceased for hundreds or thousand of years and the particles will have been deposited elsewhere.

In addition to the intrinsically corrosive dust, that is dust that absorbs moisture from the atmosphere to form an electrolyte solution, dust may be indirectly corrosive, absorbing moisture and corrosive agents from the atmosphere or being conductive and serving as a cathode, or it may be essentially harmless, but on occasion produce a geometry conducive to crevice corrosion. Fine particles contain a larger fraction of water-soluble ionic compounds, while coarse particles could form crevice geometries.

Recommended Experimental Program

1. Sampling air for particulates
2. Analysis of particulates
3. Corrosion test of relevant alloys in presence of dust

1. Sampling

Sampling of airborne particles and of dust on equipment surfaces should be conducted at numerous representative locations including outside the mouth of the repository and at several locations in each branch. This should preferably be done at different times of the year to account for seasonal variations. Sampling of airborne particles may be performed with any one or more of several devices: (a) dichotomous samplers, for example, Sierra Automatic Dichotomous Samplers Model No. 245, that separate fine (< 2.5 σm) and coarse (2.5-15 σm) particles for collection on pre-cleaned and weighed Teflon filters (3); (b) portable pumps, e.g., Bios AirPro 6000D and Teflon filters mounted in sampling devices suitable for collecting airborne particles, e.g., plastic cassettes (8); (c) Gilian personal sampling pumps equipped with sampling cassettes (9). Additional fine particle samples may be collected on Teflon filters with an impactor, such as the Model 200 Personal Environmental Monitor (PEM) made by MSP Corporation (9). A reasonable sampling period is 4 weeks. At the end of the sampling period, the filters are reweighed to determine the mass of collected particles and the particulates are analyzed. Larger quantities of dust may be collected from larger filters placed in a plastic bag in front of a fan. This dust can be used to measure its corrosivity in laboratory experiments.

Dust that has settled onto relevant surfaces, i.e., the waste package or drip shield, may be extracted using filter paper wet with deionized water (3).

2. Analyses

Particles should be checked for their water-soluble ionic content. This is best done by ion chromatography following water extraction of the Teflon filters or filter papers (3,10). Separate anion and cation analyses should be performed, as described in the references.

The ability of particulates to absorb moisture from the air and form an electrolyte solution and the relative humidity at which this commences may be determined gravimetrically (11) or by electrical conductivity measurements of the dust as a function of relative humidity (1,2,8). The gravimetric method permits the determination of the critical relative humidity of individual salts and other materials as well as of mixtures of these. Electrical conductivity measurements are

more relevant to degradation problems in the electronics and communications industry but may also be useful for assessing the tendency of salts to ionize and, hence, be more corrosive. These measurements are made using an interdigitated test pattern on an insulating substrate with solder-coated copper conductors that are 12 mils wide and separated by 50 mils. The dust sample is applied to the test pattern by placing approximately the same volume each time in the center of the test pattern covering a circular area about I cm in diameter. 400 V is then applied between conductors and the surface resistance is monitored as the relative humidity is increased from 30 to 90% over a period of 120 minutes (8).

3. Corrosion Tests

Corrosion testing of the relevant alloys must be performed with deposited dust as a function of time, temperature, and relative humidity. Dust particles may be collected as described above and uniformly distributed over the alloy surface either with a brush, through a sieve, or with a salt shaker. A synthetic dust, chemically resembling the analyzed dust or the reactive components of it, may be prepared and applied (12). The preparation of this dust involves mechanically grinding the salts into a powder that typically has a relatively large particle size of several microns or more. A specific salt found in the dust may be applied as described by Lobnig et al. (13 and references therein). Here, fine particles are prepared by atomizing a dilute solution of the salt, drying the aerosol in a stream of hot nitrogen or air, separating the particles into several size fractions with a cascade impactor (California Measurements, Inc., Model MPS 4G1) and depositing the desired size fraction on a metal coupon. This method is best when heavy deposits are desired but results in a non-homogeneous pattern of the deposit. For lesser quantities of particles deposited more homogeneously, the cascade impactor was used to separate out the desired particle fraction that was then deposited by the thermophoretic effect by heating the particle-gas mixture and cooling the metal coupon.

The metal coupons with salt deposits should then be exposed in an environmental test chamber at relative humidities corresponding to a few percent below the critical relative humidity of the deposited salt, its critical relative humidity, and a relative humidity 10-20% above the critical relative humidity. These tests should be run at a minimum of two temperatures, the steady state temperature of the repository and a high temperature, for example, 85-90\°C. Specimens should be pulled periodically and examined after cleaning for the type and extent of any corrosion by usual means, that is optical and electron microscopes, atomic force microscopy, etc. The composition of any corrosion products can be determined by X-ray or electron diffraction, Auger electron spectroscopy, X-ray photoelectron spectroscopy, etc. Other methods may be found in Ref. 13. . Exposure times probably should range from times as short or shorter than 1 day to many months. This will allow for the determination of possible induction times for pitting or crevice corrosion, as well as for collection of sufficient data to determine (a) whether the metal corrodes under the given conditions, (b) the rate of corrosion, (c) whether the corrosion rate decreases with time and the rate approaches zero indicative of passive film formation, and (d) whether passivity is maintained for an extended period of time. Experiments to look for possible crevice corrosion can be done by building an artificial crevice into the metal coupon before deposition of salt particles.

References

1. J. D. Sinclair, "Indoor Atmospheres", in "Corrosion Tests and Standards: Application and Interpretation", R. Baboian, Ed., ASTM Manual 20, American Society for Testing and Materials, Philadelphia, PA, 1995.

2. R. B. Comizzoli, R. P. Frankenthal, and J. D. Sinclair, "Corrosion Engineering of Electronic and Photonic Devices", in Corrosion and Environmental Degradation, **Vol. II**, M Schuetze, Ed., Wiley-VCH Verlag, Weinheim, Germany, 2000.

3. J. D. Sinclair, L. A. Psota-Kelty, C. J. Weschler, and H. C. Shields, "Measurement and Modeling of Airborne Concentrations and Indoor Surface Accumulation Rates of ionic Substances at Neenah, Wisconsin", Atmospheric Environment, **24A**, 627 (1990).

4. G. O. Nelson, Controlled Test Atmospheres, Ann Arbor Science Publishers, Inc., Ann Arbor, MI, 1972.

5. D. R. Lide, Handbook of Chemistry and Physics, 71st Ed., CTC Press, Inc., Cleveland, OH.

6. W. C. Hinds, Aerosol Technology: Properties, Behavior, and Measurement of Airborne Particles, 2nd Ed., J. Wiley & Sons, Inc., New York, 1999.

7. J. H. Seinfeld and S. N. Pandis, Atmospheric Chemistry and Physics: From Air Pollution to Climate Change, John Wiley & Sons, Inc., New York, NY, 1998.

8. R. B. Comizzoli, C. A. Jankoski, G. A. Peins, L. A. Psota-Kelty, D. J. Siconolfi, and J. D. Sinclair, "Reliability of Electronics in Harsh Environments: Electrical Leakage and Corrosion Caused by Hygroscopic Pollutant Particles", in Corrosion and Reliability of Electronic Materials and Devices, R. B. Comizzoli, R. P. Frankenthal and J. D. Sinclair, Eds., PV 99-29, The Electrochemical Society, Inc., Pennington, NJ, 1999.

9. J. D. Sinclair, L. A. Psota-Kelty, G. A. Peins, and A. O. Ibidunni, Atmospheric Environment, **26A**, 871 (1992).

10. J. D. Sinclair, "Paper Extraction for Sampling Inorganic Salts on Surfaces," Analyt. Chem., **54**, 1529 (1982).

11. J. D. Sinclair, "An Instrumental Gravimetric Method for Indexing Materials, Contaminants, and Corrosion Products According to Their Hygroscopicity," J. Electrochem. Soc., **125,** 734 (1978).

12. R. B. Comizzoli and J. D. Sinclair, "Electronic Components and Assemblies: Reliability and Testing," in Encyclopedia of Applied Physics, **Vol. 6**, VCH Publishers, Inc., 1993.

13. R. Lobnig, R. P. Frankenthal, C. A. Jankoski, D. J. Siconolfi, J. D. Sinclair, M. Unger, and M. Stratmann, "Corrosion and Protection of Metals in the Presence of Submicron Dust Particles," in Corrosion and Reliability of Electronic Materials and Devices, R. B. Comizzoli, R. P. Frankenthal, and J. D. Sinclair, Eds., PV 99-29, The Electrochemical Society, Inc., Pennington, NJ, 1999.

16. Statistical and Stochastic Aspects of Corrosion Life Predictions

Toshio Shibata
Fukui University of Technology
Fukui, Fukui Prefecture, JAPAN

EDITORIAL NOTE

This volume, "A Compilation of Special Topic Reports," contains a series of reports that were prepared for the Waste Package Materials Performance Peer Review Panel to use as background and input to the peer review. Summaries drawn from the reports were also presented in Section 11 of the Panel's Final Report. The Panel used the reports as background and input for its review. Any views and comments expressed in the summaries and the full reports do not necessarily reflect the opinion and findings of the Panel. Further, opinions expressed in the reports are not necessarily those of the Panel or reflected in the Panel's reports and recommendations.

1. Introduction

Candidate materials for the waste package (WP) canisters are required to survive more than ten thousand years and reliable assessment of the canister design is required. For this assessment, corrosion life predictions have to be made. Two different approaches can be applied to predict corrosion failure life. The first approach is deterministic and corrosion life can be estimated based on the exact corrosion rate measured by laboratory and/or field tests. A theoretical model to predict the failure life of a passive metal based on a deterministic approach was proposed by Macdonald [1] who developed the point defect model for the passive film breakdown. Reliable assessment of the long lifetime in the repository, however, should be based on the exact corrosion rate or be supported by complementary data from a natural analog.

The other approach [2,3], which is stochastic, describes corrosion life as the probability of occurrence. Corrosion failure statistics show that the major corrosion mode for passive alloys exposed to the repository environment, which is near-neutral and mildly oxidizing with aggressive halogen ions, is not general corrosion, but rather localized corrosion such as pitting, crevice corrosion and stress corrosion cracking. In the case of localized corrosion, the probability of occurrence plays a decisive role for deciding the corrosion failure life, as pointed out by Evans [4]. He stated that the knowledge of corrosion rate is less important than ascertainment of the statistical risk of localized corrosion initiation for predicting corrosion failure in actual field environments. Thus stochastic concepts and reliability assessment are necessary for the assessment of long-term corrosion life in the repository.

Special Topic Report prepared for the Waste Package Materials Performance Peer Review. The Final Report of the Peer Review was submitted to U.S. Department of Energy and Bechtel SAIC Company, LLC on February 28, 2002.

Various types of the probability distribution functions (pdf) have been observed for corrosion data, as shown in Table 1 [5]. The normal distribution is most familiar, and data having an average and standard deviation can be properly analyzed by a normal probability distribution. In corrosion phenomena, however, extreme values including the largest or the smallest value are often more important than the average, so that extreme value distributions such as the Gumbel and Weibull distribution are useful for analyzing corrosion data. In this report, the important types of pdf's for reliability assessment are discussed for pitting corrosion, crevice corrosion and stress corrosion cracking. Life assessment based on reliability concept is also discussed.

2. Corrosion Probability and Poisson Type Probability Distribution

The concept of corrosion probability was introduced by Evans [6], who demonstrated that the corrosion loss of mild steel covered with a water droplet under controlled gas atmosphere had a maximum at about 20% O_2. The maximum was caused by a combination of increasing trend of corrosion rate and decreasing trend of corrosion probability with increase in the O_2 partial pressure. The increase in the corrosion rate with the O_2 partial pressure could be rationalized based on the electrochemical theory of corrosion, but the decrease in the corrosion probability needs another explanation, such as a decrease in the corrosion site distribution with accumulated corrosion film. Corrosion site distributions are simply deduced from a Poisson process, which comes from the Bernoulli trial consisting of a series of go/no-go events. Evans showed that the two dimensional distribution of pits on a surface obeys the Poisson distribution. A rating number (RN) is popularly used for assessing the degree of rusting or pitting of the corroded surface of stainless steels after an exposure test. RN is decided by comparison to reference figures, with patterns that surely come from the Poisson distribution [5]. Thus, even standard evaluations of pitting corrosion resistance tacitly use the concept of corrosion probability.

3. Pit Generation as a Stochastic Process

Pitting potential is a standard measure for assessing the pitting corrosion resistance of passive alloys. The electrochemical procedure to measure pitting potential is standardized, but its random scattering and stochastic nature has not been studied much. The stochastic theory of pitting corrosion [7-9] was proposed to rationalize the probability distribution of pitting potential shown in Fig 1 [7], which is measured by the potential sweep method and the probability distribution of the pit generation time, which is recorded at a constant potential.

The stochastic theory of pitting corrosion [2,9] assumes that the probability associated with the pitting process is related to pit birth and death according to:

$$dP(t)/dt = -\varsigma P(t) + \sigma(1-P(t)) \qquad (1)$$

where ς and σ are the rates for transition from the non-pit state to the pit generated state and back, being equivalent to the pit generation rate and repassivation rate, respectively. Integration

of Eq. 1 assuming that P = 1 when t equals the t_0, the incubation time, gives

$$P(t) = \sigma/(\varsigma+\sigma) + \varsigma/(\varsigma+\sigma)\exp(-\varsigma(t-t_0)) \quad (2)$$

Experimental data for pit generation time can be fitted to Eq. 2 as shown in Fig. 2 [9] from which ς and σ are determined. As shown in Fig. 3 [7], the pit generation rate, ς, is an increasing function of applied potential, while σ is not dependent on applied potential. It is emphasized that pit generation takes place above the critical potential, E_{pit}, because the pit generation rate, ς, prevails over the pit repassivation rate, σ.

When the applied potential increases and reaches a condition of $\varsigma >> \sigma$, that is, pit generation prevails, Eq.(1) reduces to:

$$dP(t)/dt = -\varsigma P(t) \quad (3)$$

and Eq.(2) reduces to:

$$P(t) = \exp(-\varsigma(t-t_0)) \quad (4)$$

Thus the probability function of pit generation time can be described by a simple exponential function.

Failure probability for actual life can be predicted by the left side tail of the distribution, which is controlled by t_0 and ς. Neither parameter can be obtained by a theoretical approach, but they can be evaluated by data accumulated in experiments and field failures.

It is interesting that the same exponential probability function is found for the distribution of incubation time for crevice generation [10,11], indicating that random occurrence of crevice corrosion obeys the same Poisson process.

4. Extreme Value Analysis to Predict the Maximum Pit Depth

It is important to predict the maximum pit depth formed on the canister surface based on laboratory or field tests because the maximum depth, not the average depth, decides the failure life. With increasing surface area of the canister, the maximum depth increases. Transfer of laboratory data using a small area sample to engineering design data for the larger surface canister [12] can be accomplished by extreme value analysis.

Extreme value theory [13] shows that the Gumbel probability distribution:

$$F(x) = \exp(-\exp(-(x-\varsigma)/\zeta) \quad (5)$$

can be applied to analyze the distribution of pit depth data as a function of surface area. Experimental data for small area samples is analyzed to estimate the parameters of the distribution,

that is, ς and ζ. The maximum pit depth, x_{max}, of the larger surface area canister, S, can be estimated by using ς and ζ and the return period, T:

$$x_{max} = \varsigma + \zeta \ln(T) \quad (6)$$

T is given by T=S/s, where s is surface area of the small area samples. Time evolution of x_{max} is interesting for predicting failure life, examples of which can be seen in the literature [12].

5. Statistical Distribution of Stress Corrosion Cracking

A recent review given by Staehle [15] describes how the Weibull distribution:

$$F(t) = 1-\exp(-((t-\nu)/\xi)^m) \quad (7)$$

can be applied for analyzing the statistical distribution of SCC failure life. The parameters ν, ξ, and *m* in Eq. 7 are the location, scale and shape parameters. It was pointed out [15] that the average time is not suitable for the reliable assessment of failure life, but the initiation time deduced at a lower percent cumulative probability is more important for failure, and the difference in the failure probability becomes larger when the shape parameter is larger than unity.

Akashi [16] found that the SCC failure life distribution can be fitted to the exponential distribution function which is derived from the Weibull distribution at m=1. If the exponential function can be applied, the analysis is simplified, which is beneficial for engineering use.

6. Quantitative Assessment of SCC Failure by the Reliability Concept

It is desired to prove the reliability or to predict failure life by laboratory testing for systems or materials that require a high reliability [5]. For this purpose, Post and others [17] developed a statistical procedure by assuming that the failure life of sensitized Type 304 stainless steel due to IGSCC in a BWR simulated environment obeys a log normal distribution. The above assumption was verified by the analysis of failure data in the laboratory as well as in the field. Fig. 4 [17] is a schematic illustration for the procedure to verify the SCC susceptibility of a newly developed alloy or an alternating welding method relative to a given reference alloy by using an accelerated test. If the distributions for both the reference and alternate alloys obey a log normal distribution with the same variance ($\omega_X^2 = \omega_A^2$), the improvement factor, F, is defined as:

$$\ln(F) = \sigma_A - \sigma_X \quad (8)$$

where σ_A and σ_X are the mean failure times of the alternative alloy A and the reference alloy X, respectively. The factor F depends on testing time, t, the number, n, of specimens tested, and the level of reliability, η, according to:

$$\ln(F) = \ln(t) - \sigma_X - \omega_X(K_{1nA} + \eta(1/n_X + K_{2nA}^2)^{1/2}) \quad (9)$$

where K_{1nA}, K_{2nA} are the coefficients to describe the mean and standard deviation of the smallest value distribution of sample size, n, and their numerical value could be found in the rankit table.

The same equation could be applicable to determine the acceleration factor, L, of a laboratory test relative to field failures:

$$\ln(L) = \sigma'_A - \sigma'_X \qquad (10)$$

where σ'_A and σ'_X are the mean failure times of alloys A and X in the actual field.

In case of the Weibull distribution, a similar procedure could be used for comparing two distributions with the same shape parameter ($m_A = m_X = m$):

$$\ln(F) = \ln(t) - \sigma_X + (1/m)\ln(n_A - \ln\ln(1-\eta)) \qquad (11)$$

Akashi [16] found that the distribution of SCC failure time in the laboratory exhibits an exponential distribution and the ratio of ζ to ς is almost constant. For this case, the condition of ($\zeta_A/\varsigma_A = \zeta_X/\varsigma_X = \zeta/\varsigma$) is fulfilled and the following equation can be used for evaluating the improvement factor, F:

$$\ln(F) = \ln(t) - \ln(\varsigma_X) - \ln(1-(\zeta/\varsigma/n_A)\ln(1-\eta)) \qquad (12)$$

In the above three cases, the parameters of the distribution have to be known and data accumulation on the probability distribution of failure life is required. Little data on the distribution of failure life exists compared to the corrosion rate data based on the deterministic approach.

Accumulation of the failure life distribution data for the candidate materials by an accelerated test or in the actual field is required for assessment of the reliability of the candidate materials.

References

1. D. M. Macdonald and M. Urquidi-Macdonald, Electrochem. Acta., **31**, 1079, 1986. J. Electrochem. Soc., 134, 41, 1987.

2. T. Shibata and T. Takeyama, Corrosion, **33**, 7, 243-251, 1977.

3. T. Shibata, Corrosion Sci., **31**, 413-423, 1990.

4. U. R. Evans, Proc. Localized Corrosion, Ed, by B. F. Brown, J. Kruger and R. W. Staehle, p.144, NACE, Houston, 1974.

5. T. Shibata, Uhlig's Handbook, Second Edition, Edited by R. Winston Revie, John Wiley & Sons, Inc. New York, pp.367-392, 2000.

6. M. Mears and U. R. Evans, Trans. Faraday Soc., **30**, 527, 1934.

7. T. Shibata, Trans. ISIJ , 23, 785-788, 1983.

8. T. Shibata and T. Takeyama, Corrosion, **33**, 7, 243-251, 1977.

9. T. Shibata and T. Takeyama, Proc. 8th Int. Conf. Metallic Corrosion, ECHEMA, 146-151, 1981.

10. S. Tsujikawa, Z. Heng and Y. Hisamatsu, Boshoku Gijutsu, **32**, 149, 1983.

11. S. Fujimoto, T. Shibata, M. Minamida and S. Udaka, Corros. Sci., **36**, 1575-1583, 1994.

12. P. J. Laycock, R. A. Cottis and P. A. Scarf, J. Electrochem. Soc., **137**, 64, 1990.

13. C. C. Nathan and C. L. Dulaney, Proc. Localized Corrosion, Ed, by B. F. Brown, J. Kruger and R. W. Staehle, p.184, NACE, Houston, 1974.

14. T. Shibata, J. Res. Natl. Inst. Stand. Technol., **99**, 4, 327-336, 1994.

15. R. W. Staehle, Proc. Chemistry and Electrochemistry of Corrosion and Stress Corrosion Cracking: A Symposium Honoring the Contributions of R. W. Staehle, edited by R. H. Jones, TMS, K-1, (2001).

16. M. Akashi, Localized Corrosion, Ed. by F. Hine, K. Komai and K. Yamakawa,

17. Elesevier Applied Science, p.175, 1988.

18. R. Post and J. Lemair and W. Walker, Proc. Seminar on Countermeasuires for Pipe.

19. Cracking in BWR's, EPRI Workshop Report, No.WS-79-174, Vol.1, Paper No.15, 1980.

20. T. Shibata, Localized Corrosion, Ed. by F., Hine, K. Komai and K. Yamakawa, Elesevier Applied Science, p.197, 1988.

TABLE 1
Probability Distribution Observed in Corrosion[5]

Probability distribution	Examples in corrosion
Normal distribution	Pitting potential,
Log-normal distribution	SCC failure time,
Poisson distribution	Two dimensional distribution of pits,
Exponential distribution	Induction time for pit generation, SCC and HE failure time
Extreme value distribution	
Gumbel distribution	Maximum pit depth
Weibull distribution	SCC failure time
Generalized extreme value Distribution	Maximum pit depth, Fatigue crack depth

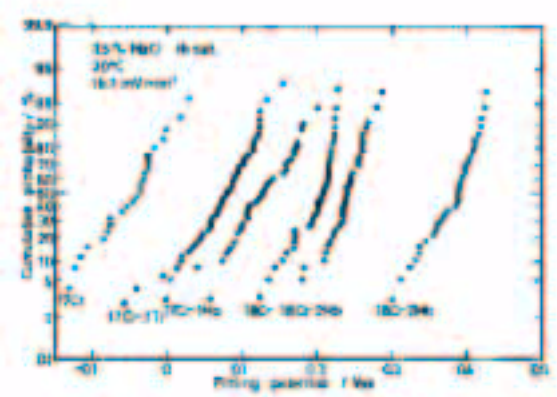

Fig.1 – Probability Distribution of Pitting Potential of Various Ferritic Stainless Steels Plotted on Normal Probability Paper [7]

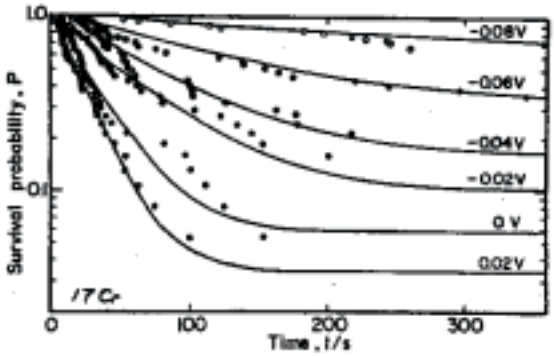

Fig.2 – Survival Probability as a Function of Time at Various Potentials

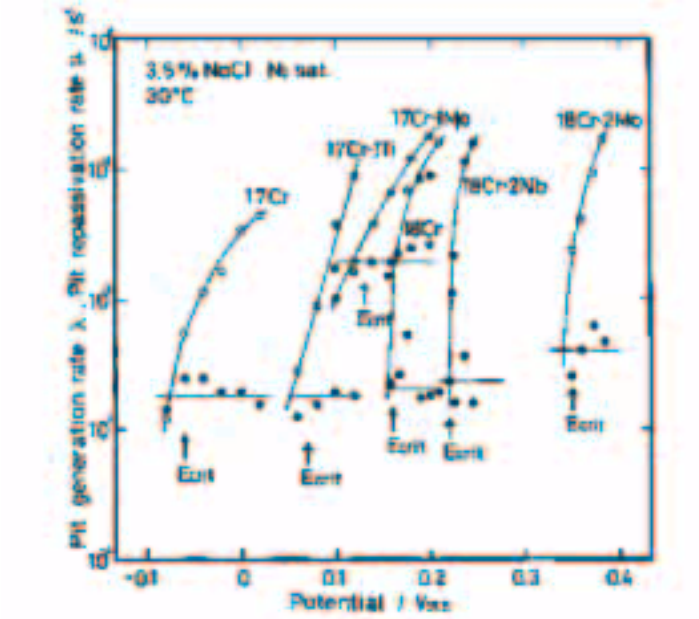

Fig.3 – Pit Generation Rate and Repassivation Rate as a Function of Applied Potential

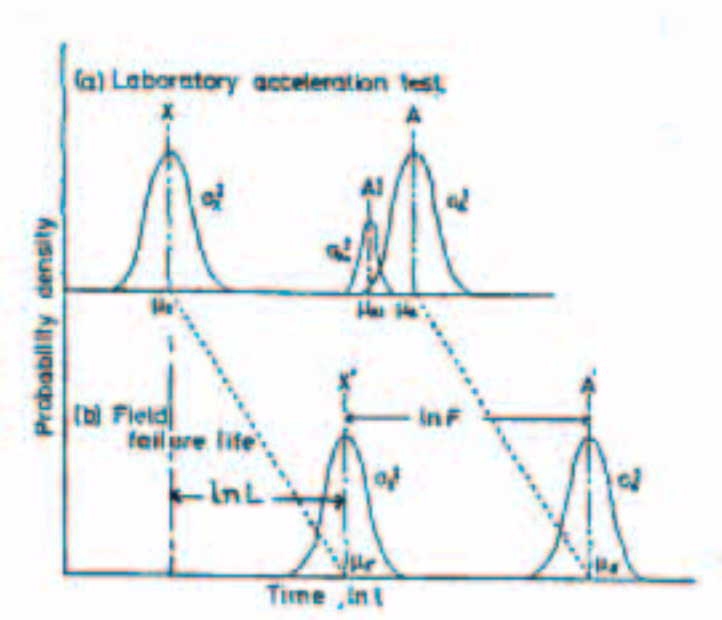

Fig.4 – Schematic Illustration of Reliable Test Based on the Acceleration Test and Field Test

17. Microbiologically Influenced Corrosion

Stephen C. Dexter
University of Delaware,
Newark, Delaware, USA

EDITORIAL NOTE

This volume, "A Compilation of Special Topic Reports," contains a series of reports that were prepared for the Waste Package Materials Performance Peer Review Panel to use as background and input to the peer review. Summaries drawn from the reports were also presented in Section 11 of the Panel's Final Report. The Panel used the reports as background and input for its review. Any views and comments expressed in the summaries and the full reports do not necessarily reflect the opinion and findings of the Panel. Further, opinions expressed in the reports are not necessarily those of the Panel or reflected in the Panel's reports and recommendations.

The primary concern of research dealing with the microbiologically influenced corrosion (MIC) issue in the YM Project is to determine whether or not MIC will introduce a serious flaw into the design. Given the desired lifetime for the waste packages and the inherent adaptability of the microbial community over that time period, the question can never be fully answered. No matter how many experiments are done, it will never be possible to conclude that MIC poses no danger to waste package integrity.

The goal of the YM Project to calculate all effects, and to put bounds on those effects for which the calculations cannot be done adequately is perhaps achievable for the inanimate structural, geological and chemical systems involved. It must be realized, however, that the goal of doing so for the effects of the living, changeable, adaptable, microbial community can never be fully achieved for a period of 10,000 years. Microorganisms are especially noted for their ability to adapt when they are put under stressful conditions, as they will be in the repository environment at Yucca Mountain. There is no guarantee that the population of microbes in the repository 1000 years from now will be the same as the population being studied today.

Having said that, however, it behooves us to do everything possible to minimize the risk that the presence of microbes may pose to the integrity of the waste packages (WP) and drip shields (DS). It is with this purpose in mind that the MIC research to date and future plans are being reviewed. The state of knowledge of the YM environment with respect to the MIC question will be considered first, followed by an identification of the worst case MIC scenarios. This will be followed by a brief consideration of several related issues, a review of current and completed Project experiments, and a recommendation for future experiments.

Special Topic Report prepared for the Waste Package Materials Performance Peer Review. The Final Report of the Peer Review was submitted to U.S. Department of Energy and Bechtel SAIC Company, LLC on February 28, 2002.

A. The Yucca Mountain Environment

The Project seems to have a good understanding of the physical, chemical and thermal YM environments as they relate to the possibility of microbial effects on corrosion. The only environmental issue that will be identified as being in need of additional investigation is the availability of bulk liquid water.

A.1) Availability of Bulk Liquid Water. Most of the known cases in which microbes have been able to initiate corrosion, change the form of corrosion from general to localized, or markedly accelerate the corrosion rate have been in the presence of bulk liquid water or water saturated soil. The Project has developed an excellent database for predicting the presence of condensed water and dripping water on WP surfaces. By far the most serious condition, however, would be that in which the WP became immersed in bulk liquid water. The types of MIC that would then become possible could result in the premature compromising of WP integrity on a large scale.

Next consider what is meant by the term "bulk liquid water." This means that there is enough water that the aqueous phase never becomes saturated with, nor depleted of a constituent that is corrosion rate limiting. For the anode reaction, this means that there is enough water available to remove saturated corrosion products, avoiding concentration polarization at the anode. For the cathode reaction, this means that the oxidized species for the reduction reaction can be delivered to the metal surface at the rate demanded by the diffusion limit for the hydrodynamics of flow. This condition is probably not met by a film of water condensed onto the WP surface from humid air. Under those condensed film conditions, the rate of the corrosion reaction, with or without organisms present, will be limited to the rate at which the oxidized specie can be delivered. The condition may be met in some cases by continuous dripping of water onto a portion of the WP surface. It is most likely to be met if the drift became flooded and the WP became immersed. Since that is the most serious condition for both microbial and abiotic corrosion, it needs to be evaluated.

According to previous Project reports, flooding of the drift is considered highly unlikely, but it has not been ruled out according to the following quote:

> **"All this having been said, it is still prudent to allow for the possibility that some packages may be contacted by bulk water for some period of time. This might result from draining of the "condensation halo" near the edge of the repository, for example, or from an isolated case of fracture flow, or from the unanticipated case of repository inundation."**
>
> Source: "Selection of Candidate Container Materials for the Conceptual Waste Package Design …" R.A. Van Konynenburg, et. al., LLNL Report UCRL-ID-112058, 1993, p. 11

One of the most widely studied cases of MIC involving welded stainless steel was reported by Kobrin (1986). Victoria, Texas well water sitting stagnant after hydrotesting caused bacterial mounds over the welds in 304L and 316L SS piping, resulting in multiple perforations

of the 1/4 inch wall thickness in just a few months. Even though Alloy C22 should be much more resistant than 304 and 316, the possibility of stagnant bulk water poses a very risky situation that must be avoided. The point in raising this issue is not to determine how bulk water might flood the drift, but rather to focus attention on how the water level might be controlled. Water filling the drift is not in itself the problem. The serious MIC situation would arise only if that water became trapped and sat stagnant in contact with the WP surface for several months.

If a way can be devised to keep the water level below the welded WP surface, then how it might get in becomes irrelevant. If one can show that even a catastrophic flooding of the drift to half its diameter would immerse the WP surface for less than a few weeks, then one can eliminate the most damaging MIC scenario as a matter of concern. It is only if the water could sit trapped in contact with the WP surface that one would need to be concerned about that form of MIC attack.

From a MIC point of view then the critical question is: Can the engineered drift system be designed in such a way as to handle a sudden large input of bulk water without immersing the welded WP surface for more than two weeks and without releasing water to the biosphere? If that could be achieved, then the probability of any catastrophic MIC problems would seem to be quite low. If, on the other hand, any portion of the WP - especially the welds - could sit in bulk water for 2 months or more, then rapid penetrations might be possible based on data in the published literature (e.g., see Dexter, 1986; Kobrin, 1993).

Purposely designing the drift to keep water away from the WP in such a case would eliminate this possibility. As a matter of fact, the drift is already designed in such a way as to handle some bulk water. A partial flood could already be handled by the invert structure acting as a dry well, thus keeping water away from the WP. This feature of the invert structure is mentioned in the Water Drainage Model (2000). Any increase in the capacity of the invert to handle water without releasing it to the biosphere would increase the level of confidence that the worst MIC cases can be avoided. Again, the report on the Water Drainage Model mentions the possibility of adding additional tuft filled bore holes to act as dry wells.

Initial calculations from the Water Drainage Model (2000) indicated that it would take about 10 years for bulk water to drain out of a drift once it became suddenly flooded. This would be very dangerous from a MIC point of view. Subsequent models for which the work is just now being completed, however, show much faster drainage rates, on the order of one week (Salmon and Sassani, 2002). This is an issue that needs to be clarified with the utmost urgency. If drainage will really take 10 years, then our ability to guarantee that the worst forms of MIC will not occur during the confinement period will only be as good as our confidence that bulk water will never flood the drift. In that case, the utmost should be done to increase the capacity of the invert structure, or to mount the WPs higher in the drift. If, on the other hand, the new calculations are correct, then we can conclude that the most catastrophic forms of MIC are of no concern to the YMP.

A.2) Microbes Present in YM Environment. The Project has identified the main classes of microorganisms making up the microbial community in the present YM environment

(Horn and Meike, 1995; Davis, et al., 1998; Horn, et al., 2002). They also have correctly assessed that: 1) the organisms within that community posing the highest risk of MIC of the WP and DS materials are those capable of acid production and those involved in various aspects of the sulfur cycle, and 2) some representatives or mutants of those organisms will survive the harsh initial environment, becoming able to colonize the WP and DS surfaces at some later time when condensed water becomes available. Moreover, they allow that other microbes, not indigenous to the YM environment will be introduced into the drifts during the construction and waste emplacement processes.

The class of organisms thought to be responsible for the most severe cases of stainless steel penetration discussed above include the iron and manganese metabolizers, ***Gallionella*** and ***Siderocapsa***. These organisms have not been included in the MIC research program to date because they have not been identified in the drift or rock environments of the YM site. According to the Project assessment, however, it will be prudent to assume that these organisms (as well as others relevant to MIC) will be introduced to the drift environment during construction and waste emplacement. It will be recommended below that these organisms should be added to those already under investigation.

A.3) Survivability and Viability of Microorganisms in Radiation Fields. It has been asserted repeatedly by Project scientists that a significant portion of the microbes in the natural YM environment will survive the radiation field, high temperature and desiccation of the initial portion of the confinement period (Davis, et al., 1998; Horn, et al., 2002). The Project also concludes that these organisms will eventually recolonize the DS and WP surfaces, thus, MIC cannot be ruled out. Similar conclusions were reached by the attendees of the "Workshop on Microbial Activity at YM" held in April, 1995 at Lafayette, CA (Horn and Meike, 1995). Moreover, the participants of that Workshop made several summary conclusions of relevance to the subject matter of this section:

> "Microbes alter their own environments and have extensive abilities to adapt to harsh conditions beyond their normal range of growth conditions."
>
> "Microbial activity can be limited by insufficient water, temperature extremes, ionizing radiation and pH extremes. These specific boundaries vary, however, depending on the microbial species and habitat under consideration."
>
> "After cessation of biological activity due to exposure to extreme environmental conditions, dormant cells can revive, and the region may be repopulated by migration of organisms when conducive conditions arise."
>
> "Radioactive flux could conceivably generate microorganisms with an increased potential to both survive and impact the repository facility."

These are not alarmist conclusions, as they are in harmony with the general microbiological literature of the past several decades. The Workshop participants' judgment that microbes will be able to survive the initially high temperature, high radiation fields of the YM environment is corroborated by the experience at Three Mile Island (TMI). Booth (1987) and Hofstetter and Ausmus (1989) described how river water containing microorganisms entered the

reactor building at the time of the accident in 1979 and then became "dispersed throughout most of the accident-generated water inventory." Iron- and sulfate-reducing bacteria were identified at TMI-2 in late 1981. However, they did not cause a problem until 1985 when a microorganism "bloom" reduced the underwater visibility in the spent fuel pools to a few feet, and ultimately to zero. Microscopic examination at that time revealed the presence of *euglena* and some filamentous algae. These microbes had lain dormant until 1985 presumably due to the lack of light, oxygen and nutrients in the closed environment of the spent fuel pools. The radiation level was reported as ~ 1 MCi in the reactor vessel coupled with very high boron levels. It was felt that the bloom occurred in 1985 as cleanup operations introduced light, oxygen and nutrients in the form of hydrocarbons from spilt hydraulic fluids.

This sequence of events took place over a period of 6 years, with the microbial activity all happening during the last year when conditions changed. It is interesting to note that all of the published reports agree that the organisms encountered at TMI-2 did not cause microbiologically influenced corrosion. This may have been due to the relatively short time period of the bloom, which was eliminated by an aggressive program of treatment with hydrogen peroxide. The various reports admit that TMI did have a MIC problem, but that it was all in the service water systems outside the reactor vessel.

The TMI environment was quite different from that at YM. First, it covered a relatively short time period. Second, it involved bulk liquid water in the spent fuel pools and reactor vessel. Third, the organisms introduced at the time of the accident were indigenous to a lighted, oxygenated river environment with abundant nutrients. Nevertheless, these organisms were able to survive the sudden change to a hostile environment, including the presence of a high radiation field, and a subset of the microbial population became active again upon a modification of the environment. Thus, the published TMI experience is consistent with the contention of Project scientists that microbial corrosion is possible in the YM environment.

Additional evidence has also been sought from experts having personal knowledge of the TMI situation. Dr. Patrick Pinhero, INEEL Research Center, concludes that "biocorrosion of the Yucca Mtn. Waste package is certainly possible" (personal communication, 2002). Dr. Pinhero goes on to say:

> "We are in the process of preparing a couple of manuscripts that demonstrate the radiotolerance of microbes to large fields of gamma radiation. The first study examines microbial gamma/UV radiation sensitivities using artificial sources and the second looks at radiation sensitivity/biofilm formation on actual cladding hulls from Experimental Breeder Reactor (EBR-II) driver rods. …we have documented proof of biofilm formation in radiation rich fields, and we also have observed biocorrosion of coupons after 2+ years. Therefore, biocorrosion of materials under high radiation conditions is indeed possible."

This directly supports the contention by Project scientists that organisms at YM will eventually go on to colonize the WP and DS surfaces.

Evidence has also been provided by Mr. Russ Green, Program Engineer responsible for MIC at TMI (personal Communication, 2002). Mr. Green supported the published reports in that there was a microbial bloom in the TMI-2 reactor vessel environment, but no MIC. He then goes on to relate that:

> "We have a very significant problem with MIC at TMI but that problem does not extend to our primary systems. Our MIC problems are principally confined to our service water systems. One exception was when I found active nodules in our low temperature condensate system. This was quite astounding because this location was after our polishing system and should be as nutrient free as possible for any large volume flow. The makeup water to this system is from our demineralized water system which is well water that has been processed through an RO membrane. … I have found high bug counts in radioactive systems that have low energy conditions, e.g. waste gas compressors cooling water. In general, we do not have a (significant) problem with any of our radioactive systems, but that is because the inoculum and nutrients are low or not present at all. The radioactivity would not have a significant effect on a biological colony."

In all of this experience where microbes were active, bulk liquid water was present and nutrients were either plentiful naturally, or they were added through human activities. Note Mr. Green's opinion, based on years of experience with the TMI system, that "radioactivity would not have a significant effect on a biological colony."

In addition to surviving radiological environments, microbes as a group are noted for being able to survive at extremes of temperature, pH and chemical concentrations. As noted in Horn and Meike (1995), most organisms have optimal growth rates in the temperature range of 20 to 40 degrees C. The upper temperature limit of 150 C for microbial viability seems to be that of the microbes observed in hydrothermal vent environments. It must be realized, however, that the water in that environment was kept from boiling by the pressure of the deep-sea environment. At the pressure of the YM drift environment the upper temperature for viability should be taken as the lower of the boiling point of a condensed, salt saturated water at that pressure, or the temperature to denature proteins in that environment.

Most microorganisms become inactive at pH values above 9. The Project is correct, however in pointing out that some microbes can thrive at pH 10-11. Moreover, some are known to tolerate extremes of temperature, pH and radiation all at the same time. The Project also reports that even under the most extreme YM environments, there will always be microniches where the conditions are more favorable, and indigenous organisms may be able to survive.

Two other published reports by Pitonzo, Amy and Rudin (1999a, 1999b) are of interest because they involve the effects of ν radiation on microbes indigenous to the YM site. In the first report (1999a) they found that a significant portion of the YM microorganisms tested were able to survive ν radiation at dosages realistic for WP surfaces at YM in a "viable but nonculturable" condition. In the second report (1999b) they found a partial recovery of metabolic capability with time in all samples tested. At all radiological doses tested, some of the microbes that had been rendered nonculturable (no metabolic capacity) became culturable again after 2 months.

Under the HTOM scenario, it seems reasonable to conclude that organisms will be of no consequence to corrosion until after the temperature at the WP surface falls below the point mentioned above, and liquid water is present in the environment. Under the LTOM scenario, it would be more prudent to assume that some microbes will be present, and potentially able to interact with corrosion at all times.

The sum of this information is not sufficient to conclude whether or not there will be significant MIC on the WP and DS during the YM confinement period. However, it does support the contention that MIC cannot be ruled out because of the harsh initial environment. The TMI experience also supports the contention expressed above that bulk liquid water needs to be avoided. Due to the tendency of the microbial community to change and adapt by mutations, especially under harsh conditions, it would seem to be a very difficult task to place any reliable, quantitative bounds on when microbes will exist, or under what conditions they will effect corrosion.

B. Identification of Worst Case and New MIC Possibilities

The purpose of trying to identify the most serious conditions under which the WP integrity might be compromised by the action of microbiologically influenced corrosion is to devise sound engineering ways of preventing such attack.

B.1. Rapid Penetration at the Welds. The worst cases of MIC on stainless steels known to industry are those cases identified above where the welded metal is immersed in bulk liquid water in the presence of some combination of *Gallionella,* Sulfate Reducing Bacteria, Acid Producing Bacteria and *Thiobacillus.* These are the conditions under which the common ordinary 300 series stainless steels become penetrated at the welds within a few months. Thus, even though the DS and WP materials of construction are known to be considerably more resistant to this type of attack than the lower grade stainless steels, this is a condition that it would be prudent to avoid. This type of attack will be of no consequence to the YMP if the new drainage calculations can be verified.

B.2. Integrity of the Welds. In any case that welded stainless steels are subjected to possible MIC, the condition of the welds is critical. The importance of sound welds to WP integrity has already been recognized by the Project (YM Science and Engineering Report, 2001, Section 3.4.2) in the context of crevice corrosion and stress corrosion cracking. Very high standards have already been set by the Project for welding the closures of the WP. The MIC concerns being discussed here just add further support to the idea that those welding standards must be enforced rigorously during the construction and emplacement phases. Microorganisms are well known in the literature for taking advantage of any defects introduced by poor welding practice.

B.3. Localized Attack at Welds and Crevices. The next most serious condition is likely to be where the hygroscopic rock dust in the YM environment collects at sharp changes of

geometry and crevices, trapping water against the WP surface at those locations. Such a location would be where the WP contacts the invert structure. This would create a geometrically shielded, crevice type area in which penetration of the WP might be supported under some conditions. The probability for meaningful corrosion at such a site would be related to several factors. The first would be whether or not the water trapped in the dust could be refreshed, and at what rate. The second would be the effective size of the cathode area that was able to remain in electrochemical contact with the potential anode. The size of the cathode area would in turn be related to the thickness of the water film on the WP surface away from the crevice and the conductivity of the water phase in that film. These statements would be true whether or not microorganisms were part of the corrosion reaction. In the case of MIC, however, the water would have an additional task, that of delivering nutrients to the organisms. Thus, a small saturated dust patch isolated on an otherwise dry surface is not going to have the capacity to either supply the electrochemical reaction or deliver the nutrients needed to sustain meaningful corrosion. The same patch in contact with a continuously refreshed film of water over a large area of the WP surface, however, might cause a serious problem.

B.4. Effect of Microbes on Corrosion Initiation and Propagation. Initiation of corrosion on a hydrated, WP surface depends on the relation between the open circuit potential, Ecorr, and the critical potential for that type of attack. In the discussions among Project scientists about putting bounds on the electrochemical potential of an interface, the effect of microbes has not been considered. Of the reversible potentials listed for candidate cathodic reactions (oxygen reduction, ferric ion reduction, nitrate reduction and peroxide reduction) the one with the most noble potential is oxygen at Er = 1.23 – 0.059pH VSHE.

The cathodic reaction now believed to be responsible for the high open circuit potentials of a variety of stainless steels in fresh and marine waters is reduction of manganese (Dickinson and Lewandowski, 1996; Braughton et al., 2001). Manganese chemical species from the water phase become concentrated in the biofilm. Reduced manganese species are then reoxidized by the organisms, thus, increasing the overall cathodic kinetics without depleting the species being reduced (Ruppel, et al., 2001).

The Pourbaix Atlas lists the reversible potential between Mn^{+2} and Mn^{+3} as being Er = 1.509 V SHE, considerably higher than that of oxygen. The reversible potential between Mn^{+2} and MnO_2 is 1.228 – 0.1182pH, while that between Mn^{+3} and MnO_2 is 0.984 – 0.2364pH. Marine biofilms, presumably using this manganese dioxide battery mechanism have been shown to be able to sustain elevated corrosion rates (i.e., elevated cathodic kinetics) for months at a time in both crevice corrosion (Zhang and Dexter, 1995b; Dexter, 1996) and galvanic corrosion (Dexter and LaFontaine, 1998).

This type of reaction has not been considered by the YM project. Dissolved manganese has not been found as a measured component of J-13 well water. It is listed, however, as a component of the bulk rock composition at Yucca Mountain (Horn, et al., 2002). Therefore, if manganese-metabolizing organisms are present in the YM environment, or if they are introduced at a later time, these reactions could occur.

B.5. Effect of Microbes on pH in Biofilms. The effect that microorganisms might have on the pH at the metal surface under a distributed biofilm or a localized biodeposit should be considered. Chandrasekaran measured the pH within marine biofilms using microelectrode techniques. He found the pH to be highly variable from place to place along the metal surface with values ranging from 7 down to as low as 2 in spite of the buffering capacity of seawater (Dexter and Chandrasekaran, 2000).

C. Related Issues

C.1) Rock Faces of the Drift. Based on what is already known about the rate of deterioration of antiquities in warm humid environments (Saiz-Jimenez and Arino, 2001; Saiz-Jimenez, 2001), the microorganisms present in the Yucca Mountain environment may be capable of accelerating the deterioration of the rock faces of the drift. The work that has been done on biodeterioration of both modern building materials and the rocks of ancient structures, shows such deterioration. The main difference between the environments in which biodeterioration of rock surfaces has been studied and the YM environment will be the availability of sunlight. Thus, it is not certain what the effect or the rate of the effect might be in the YM repository.

Given the uncertainty, it is suggested that the Project first address the question of whether a gradual collapse of the drift tunnel itself would pose an unacceptable risk to WP integrity. If that would not compromise WP integrity, then it is recommended that this issue can be ignored. If such a gradual collapse of the drift tunnel would be a problem, however, then someone with the proper expertise should evaluate this situation.

C.2) Carbon Steel Rock Bolts. With the rock face in compression, the carbon steel rock bolts might fail in such a way as to impact the DS and WP. This issue has already been addressed in design of the WP. According to Table 3-1 on p. 3-6 of the Yucca Mountain Science and Engineering Report (DOE/RW-0539) the WP was designed to withstand the impact of a "valve stem being ejected at the surface facility." The design criterion was that the WP should withstand the impact of a valve stem weighing 0.5 kg, ejected under a pressure of 2.1 MPa with a velocity of 5.7 m/s.

Thus, it is recommended that the maximum energy that could be released by a corrosion induced rock bolt failure should be determined to see if it is within the design specifications. If that is true then this is another issue that is of no consequence.

C.3) Carbon Steel Rails and Invert Structure. The carbon steel rails and invert support structures are not corrosion resistant in humid atmospheres. Moreover, they are particularly susceptible to MIC from a variety of organisms. Integrity of the rails is important during the monitoring period of about 100 years, during which the WP could be removed if a problem developed. It is considered highly unlikely that the structural functionality of the rails and the invert structure would be compromised by corrosion with or without microorganisms during that 100-year period provided they are not sitting in bulk liquid water. In the worst known cases of anaerobic corrosion (See Dexter, 1986; Kobrin, 1993; Stoecker, 2001) the rails might be

rendered unusable in less than 5 years. However, this would require them to be sitting in an anaerobic, water-saturated soil rich in decaying organic matter with sulfate reducing bacteria. Such an environment does not exist at Yucca Mountain. Moreover, if enough water got into the drift to flood it to the level of the rails during the monitoring period, it could presumably be safely pumped off, thus mitigating the problem.

After the 100 year monitoring period, it should be assumed that the carbon steel invert structure and rails will gradually deteriorate, becoming structurally unsound part way into the designed confinement period. The rails are not important after the monitoring period. That is less obvious for the invert support structure. If deterioration of this support structure would not pose a problem for WP integrity, then this issue also can be ignored. Alternatively, the date of unacceptable deterioration could be delayed by using more corrosion resistant materials for the invert structure.

D. Review of Work on MIC by Project Personnel

D.1. Some Issues Regarding MIC Modeling. The primary issue of concern in MIC modeling is the propensity of the microorganisms involved to change and adapt with time by mutations, especially under the stressful conditions they will encounter in the YM environment. Thus, the organisms now being used for the MIC measurements may bear little resemblance to those that eventually recolonize the WP and DS surfaces. The modeling efforts in all other phases of the YM Project do not face this same level of uncertainty. Those efforts are based on basic physical, mechanical, geological and chemical principles that will still be the same at the end of the confinement period as they are now. In contrast, the eventual population of recolonizing organisms may or may not produce effects similar to those being measured today.

Based on this argument, one must conclude that the output of any MIC model, using data measured with the current population of YM organisms, will be valid only in the presence of that same population. Conversely, one must realize that it is not reasonable to expect those same model results to be quantitatively applicable to the prediction of WP integrity for the next 10,000 years under a population of organisms that may be quite different.

The purpose in making this argument is not to say that the MIC modeling effort should be abandoned. That effort is the best way to determine what effects the current population of organisms could have on WP integrity. Rather, the purpose is to emphasize that there will always be uncertainty in predicting the future when one is dealing with the effects of a living system. Even with the best model, the most appropriate experiments and the most extensive database, the projections for the effects of MIC will have limited applicability over the full length of the confinement period. The best one can do is to characterize and quantify the effects of the present suite of microorganisms.

In the FY01 Supplemental Science and Performance Analyses Report, Part 1, Section 7.2.4, on Microbiologically Influenced Corrosion, it states that MIC effects can be modeled by adjusting Ecorr, Ecrit, pH and sulfide levels. This approach may have some merit for modeling

the initiation of localized attack. Biofilms are well known in the literature for changing these parameters (Scotto, et al., 1985; Zhang and Dexter, 1995a; Dexter and Chandrasekaran, 2000). In order to use this type of data in modeling, however, measurement of those parameters must be done under realistic biofilm conditions expected on the WP surface in the repository. Experiments have been done on how these parameters change when a sterile cell containing a metal coupon immersed in microbial growth medium is inoculated with a culture of a single microorganism. These experiments produce data on the capabilities of that organism under a well-defined set of conditions. Such data are scientifically interesting, but they are not useful for modeling the action of consortia of microorganisms in the actual EOWP during the desired YM confinement period. In Section 7.3.4 of the Supplemental Report, it says that only H_2 and O_2 have been considered in models of passive film breakdown. It is important to recognize in the modeling effort that colonies of microorganisms can produce localized concentrations of many ions, including H_2O_2 and sulfides as well as H_2 and O_2.

Later in Section 7.2.4 it talks about using a "rate enhancement factor" for MIC between 1 and 2 based on measured current densities for abiotic vs. inoculated samples. It further states that: “The analysis assumes conservatively that when the relative humidity condition is met, microbial activity is at such a level that the biofilm covers the entire surface of all the waste packages and drip shields.” If by the conservative assumption it is meant the most damaging one, such a statement reveals either an unacceptable oversimplification in the modeling effort, or a fundamental misunderstanding of the effects microorganisms usually have on corrosion. The most prevalent effect of MIC is to turn a slow, general, predictable corrosion rate into one that is highly localized and unpredictable. Thus, the true conservative assumption would be that the biofilm exists in spotty coverage, leading to a large degree of heterogeneity in the electrolyte chemistry from point to point along the metal surface. That heterogeneity, in turn, leads to the initiation of localized forms of attack with relatively rapid penetrations perpendicular to the surface.

This type of an effect cannot be modeled by a simple “rate enhancement factor” applied to the whole surface. Such an “enhancement factor” approach to accounting for MIC might have some validity for the hypothetical case where MIC merely contributed to general (or uniform) attack. However, the effect that is of the most consequence to WP integrity is the more usual one in which the microbes turn general corrosion (or none at all) into localized attack.

The Project research program has identified some possible contributions of MIC to general attack on alloy C22 (Horn, et al., 1999, 2000). While these data indicate that some organisms present in the YM environment may have an effect on alloy C22, they are not suitable for use in Project modeling efforts. First, the data obtained show very low corrosion rates, which are difficult to measure and interpret. The LPR technique used works well for ordinary corrosion rates of plain carbon steel in aerated aqueous solutions. For the very low corrosion rates associated with maintenance of passive films on stainless steels, however, data from the LPR technique are less reliable. Thus, before such data could be used in modeling, its variability and reliability would have to be well characterized. This would require a much larger database with data measured by more than one technique. Second, the data available to date were measured for cultured organisms in various growth media. Thus, the electrochemical environments as well as

the microbial communities in those tests were not representative of those expected in the waste package environment during the actual confinement period.

In order for such data to be useful in making predictions of relevance to integrity of the DS and WP materials, three things in addition to establishing their variability and reliability will be necessary. First, they need to be made in realistic EOWP environments, including the geometry and hydrodynamics of flow expected on WP and DS surfaces in the repository. Second, they need to include realistic consortia of organisms, rather than pure cultures. Third, some way must be found to determine how the measured numbers relate to real long-term corrosion rates. The work currently under way and planned for the future by Dr. Horn's group is moving in that more realistic direction. These efforts should be accelerated.

D.2. Experimental Measurements. The research on MIC in the YM environment by Dr. Horn's group (Horn and Meike, 1995; Horn, 1996, Horn and Lian, 1997; Lian, et al., 1998, 1999; Horn, et al., 1999, 2000, 2001) has recognized that the usual mode of MIC attack is localized. They have looked not only at how the microbes might enhance the slow passive wastage of the materials, subject to the qualifications noted above, but also at what corrosion reactions the microbes and their metabolic by-products might initiate.

Microbes indigenous to the Yucca Mountain environment have been cultured and identified. The investigators have recognized that only about 10% of the organisms existing at any given location will be "culturable." Thus, all the organisms present at YM have not been identified. To identify a higher percentage of the total organisms at the site would require a much larger research program with a substantially greater budget. This is probably not necessary. The organisms that have been identified have also been characterized as to their conditions for growth and survivability.

In order to identify what effects these organisms might have on corrosion, batch experiments have been done using pure cultures of the various microbes with coupons of the candidate YM containment materials immersed in various microbial growth media. The results of these experiments have been used as screening tests to see which microbes warrant further testing. As already noted above, this approach has some serious limitations. The environments used were highly favored for the organisms, but they are not at all realistic for what is expected in the repository during the confinement period. Moreover, the effects noted in these tests are unlikely to be predictive of what the same organisms will do in consortia with other microbes (rather than in pure culture) and in a more stressful environment. The more realistic conditions may cause a given organism to become more aggressive toward corrosion of the candidate materials, or less so. While these experiments have served to give the investigators experience in working with the various organisms and candidate materials, they have provided little data of direct use for predicting microbial corrosion.

D.3. Some Issues with Accelerated Testing. The concept of "accelerated testing" for prediction of WP or DS service life under MIC conditions is mentioned in several of the Project reports. It should be noted that "accelerated testing" can only be made quantitative to the degree that the accelerated test results can be calibrated against actual service environment exposures.

For example, atmospheric corrosion resistance of various materials can be "predicted" by accelerated tests in salt spray cabinets only when the results can be compared to long term exposures in the real environment. For 10 to 20 year service life applications, this can and has been done successfully. In the YMP case, however, we are talking about a service life on the order of 10,000 years. Over this time period, the relationship of short-term laboratory tests to what may happen during actual YM exposures is pure guesswork. Thus, the existence of data showing that accelerated corrosion takes place under some controlled laboratory conditions does not necessarily mean it will happen during real YM service. Likewise, the lack of corrosion in lab tests does not necessarily mean the same material will remain corrosion free in YM service.

The occurrence of any form of localized corrosion at non-trivial rates requires that the anode reaction be coupled with a cathode reaction having sufficiently rapid kinetics. The net kinetics of the cathode reaction is dependent on geometrical as well as chemical and thermal factors. If the volume of water is too small, or the refreshment rate is too slow, to carry away reaction products from the anode, or to supply oxidized chemical species for the cathode, then the rate of corrosion will be limited. That is, the reaction will be limited by concentration polarization of either the cathode or anode reaction. For this reason it is vital that future experiments in the MIC evaluation program use realistic geometrical configurations and hydrodynamics of flow as well as realistic water chemistries.

E. Recommended Experiments

Three of the results obtained to date are of great potential importance to the Project. These are:

1. The hint of pitting on alloy C22 surfaces (Horn, et al., 2000),
2. The selective leaching of chromium and nickel (Horn, et al., 2000) and
3. Surface roughening of the Titanium Gr7 DS material (Horn, et al., 2001).

Biological effects on the chromium content of passive films on Type 316 stainless steel have also been noted by Beech, et al. (2000) in marine environments. In order for these results to be useful to the project, more work needs to be done. First, many more tests must be done to see if the results are reproducible and to determine the degree of variability. Second, the tests need to be done over longer time periods. Any one of these results could have serious consequences for the Project if they are born out by further work. The highest priority should be placed on clarifying the importance of these findings.

There also is a vital need to accelerate the schedule for the performance of more realistic tests. Several types of such tests have been proposed by the investigators, and some of these are now under way. Two of the initial changes to more realistic conditions involve:

1. The use of flow through systems, rather than batch experiments, and

2. The use of simulated J-13 well water containing YM rock dust for the electrolyte, rather than culture media.

Other tests that are vitally needed are either just starting or in the planning stages. These include tests using:

1. Consortia of organisms, including ***Gallionella*** and ***Siderocapsa***,
2. More realistic testing geometries, including:
    a) Water film electrolytes
    b) Realistic hydrodynamics and flow rates
    c) Dripping water systems, and
    d) Crevices, including those formed by hygroscopic dust and scales.
3. Welded samples with the surface condition as specified in the YM Science and Engineering Report, 2001, Section 3.4.2.
4. Measure the open circuit and pitting potentials of alloy C22 in the presence of multi-species biofilms composed of YM organisms.

The second highest priority, including the necessary funding, should be given to these tests. It is considered that quantitative modeling of microbial corrosion effects must await the results of these more realistic tests if it is to be of any benefit to the YM Project.

A third priority for experimental time and funding should be placed on research to identify:

1. The consortia of organisms that might develop within biofilms on WP, and
2. What chemical substances these consortia might make that could impact SCC.

F. Overall Conclusions:

1. As a matter of first priority, the latest calculations for drainage of the drift need to be clarified. If it can be verified that even large quantities of bulk water can be drained sufficiently within two weeks that WP surfaces are not in contact with bulk liquid water, then the most damaging known MIC scenario can be dismissed. If that proves to be impossible, then the possibility of increasing the "dry-well" capacity of the drift, as has been suggested by Project personnel, should be considered.

It should be emphasized that the reliability of this conclusion is tied directly to the reliability with which one can determine that the WP surface, especially that portion containing a weld, will not encounter a bulk liquid water environment during the design confinement period.

2. Highest priority for Project resources should also be placed on accelerating the schedule for experiments to:

    a) Clarify the initial findings of incipient pitting and dealloying of Alloy C22, and surface roughening of Ti Gr7.

    b) Obtain microbial corrosion data under chemical, hydrodynamic, metallurgical and biological conditions more representative of those expected for the environment in the repository during the confinement period.

3) The MIC data measured so far are not suitable for use in modeling. Modeling of real benefit to the Project must await data from the measurements in more realistic environments. This work has started, and it should be accelerated.

4) The most vulnerable locations on waste package and drip shield surfaces are at welds and crevices. Integrity of the welds, as specified in the YM Science and Engineering Report, 2001, Section 3.4.2., will be critical for resisting the effects of microorganisms.

5) The "rate enhancement factor" approach to modeling the effects of MIC is unsuitable in most cases because:

    a) MIC often changes not only the rate, but also the mode of corrosion from uniform to localized, and

    b) The living microbial community is adaptable by mutations, especially under the stressful conditions expected in the repository.

6) Accelerated testing will be very difficult to employ for the purpose of getting MIC data for modeling. The reason is that the organisms may not behave the same in short-term accelerated lab tests as in the real YM environment.

7) Experience with microorganisms in the radiation field at Three-Mile Island supports the contention that MIC cannot be ruled out for the YM Project because of the harsh initial environment. The TMI experience also supports the contention that bulk liquid water needs to be avoided during the YM confinement period.

8) MIC and other forms of corrosion may lead to deterioration of the rock faces of the drift, the carbon steel rock bolts and the carbon steel invert structure. Deterioration of these latter structures should be evaluated to see if this would pose a threat to WP integrity. If such corrosion would not compromise WP integrity, then it is recommended that these effects may be ignored.

G. References:

Beech, I.B., V. Zinkevich, L. Hanjangsit, R. Gubner, R. Avci, 2000, "The Effect of *Pseudomonas* NCIMB 2021 Biofilm on AISI 316 Stainless Steel," Biofouling, **Vol. 15**(1-3) pp. 3-12.

Booth, W., 1987, "Postmortem on Three Mile Island," News and Comments Section, Science, **Vol. 238**, December 1987, pp. 1342-1345.

Broughton, K.R., R.L. Lafond, Z. Lewandowski, 2001, "Influence of Environmental Factors on the Rate and Extent of Stainless Steel Ennoblement Mediated by Manganese-Oxidizing Biofilms," Biofouling, **Vol. 17**(3), p.241.

Davis, M.A., S. Martin, A. Miranda, J.M. Horn, 1998, "Sustaining Native Microbial Growth with Endogenous Nutrients at Yucca Mountain," LLNL Report No. UCRL-JC-129185.

Dexter, S.C., Ed., 1986, Proceedings: Biologically Induced Corrosion, NACE, Houston, TX.

Dexter, S. C. 1996. "Effect of biofilms on crevice corrosion," Proc. COR/96 Topical Research Symposium on Crevice Corrosion, NACE, Houston, TX, pp. 367-383.

Dexter, S. C. and J. P. LaFontaine. 1998. "Effect of natural marine biofilms on galvanic corrosion," Corrosion, **Vol. 54**, No. 11, p. 851.

Dexter, S.C., and P. Chandrasekaran, 2000, "Direct Measurement of pH Within Marine Biofilms on Passive Metals," Biofouling, **Vol. 15**(4), pp. 313-325.

Dickinson, W.H., Z. Lewandowski, 1996, Biofouling, **Vol. 10**, pp. 79-93.

Green, Mr. R., Program Engineer at TMI responsible for MIC, Personal Communication (through Dr. R. Kelly, UVa), Jan. 15, 2002.

Hofstetter, K. J. and B.S. Ausmus, 1989, "The Identification and Control of Microorganisms at Three Mile Island Unit 2," Nuclear Technology, **Vol. 87**, pp. 837-844.

Horn, J.M., B.A. Masterson, A. Rivera, A. Miranda, M.A. Davis and S. Martin, 2002, "Bacterial Growth Dynamics, Limiting Factors and Community Diversity in a Proposed Geological Nuclear Waste Repository Environment," For submission to Geomicrobiology Journal.

Horn, J.M. and A. Meike, Eds., 1995, Report from the Workshop: "Microbial Activity at Yucca Mountain, Part I: Microbial Metabolism, Adaptation and the Repository Environment," LLNL Report No. UCRL-ID-122256.

Horn, J.M, and T. Lian, 1998, "Predicting Microbiologically Influenced Corrosion of Metal Barriere at Yucca Mountain," EMCR, V. 2, MIC Task Input, May, 1998.

Horn, J.M., 1996, "The Potential for Microbiologically-Influenced Corrosion of Metal Barriers at Yucca Mountain," Draft Preliminary Analyses, 1995-1996.

Horn, J.M., S. Martin, B. Masterson, T. Lian, 1999, "Biochemical Contributions to Corrosion of Carbon Steel and Alloy 22 in a Continual Flow System," LLNL Preprint No. UCRL-JC-136521.

Horn, J.M., S. Martin, A. Rivera, P. Bedrossian, T. Lian, 2000, "Potential Biogenic Corrosion of Alloy 22, A Candidate Nuclear Waste Packaging Material, Under Simulated Repository Conditions," CORROSION/2000 Paper No. 00387, NACE, Houston, TX.

Horn, J.M., S. Martin and B. Masterson, 2001, Evidence of Biogenic Corrosion of Titanium after Exposure to a Continuous Culture of *Thiobacillus ferrooxidans* Grown in Thiosulfate Medium," CORROSION/2001 Paper No. 01259, NACE, Houston, TX.

Kobrin, G., 1986, "Reflections on Microbiologically Induced Corrosion of Stainless Steels," in: Biologically Induced Corrosion, S.C. Dexter, Ed., NACE, Houston, TX, pp. 33-46.

Kobrin, G., 1993, "A Practical Manual on Microbiologically Influenced Corrosion," NACE, International, Houston, TX.

Lian, T. D. Jones, S. Martin, J. Horn, 1998, "A Quantitative Assessment of Microbiological Contributions to Corrosion of Candidate Nuclear Waste-Packaging Materials," LLNL Preprint No. UCRL-JC-131555.

Lian, T., S. Martin, D. Jones, A. Rivera, J. Horn, 1999,Corrosion of Candidate Container Materials by Yucca Mountain Bacteria," CORROSION/1999 Paper No. 476, NACE, Houston, TX.

Pinhero, Dr. P.J., Materials Dept. Technical Group Leader, INEEL Research Center, Idaho Falls, ID, Personal Communication (through Dr. R. Kelly, UVa), Jan. 4, 2002.

Pitonzo, B.J., P.S. Amy and M. Rudin, 1999a, "Effect of Gamma Radiation on Native Endolithic Microorganisms from a Radioactive Waste Deposit Site," Radiation Research, Vol. 152, pp. 64-70.

Pitonzo, B.J., P.S. Amy and M. Rudin, 1999b, "Resuscitation of Microorganisms after Gamma Irradiation," Radiation Research, **Vol. 152**, pp. 71-75.

Ruppel, D.T., S.C. Dexter and G.W. Luther, III, 2001, "Role of Manganese Dioxide in Corrosion in the Presence of Natural Biofilms," Corrosion, **Vol 57**(10) pp. 863-873.

Saiz-Jimenez, C., 2001, "The Biodegradation of Building Materials," in: A Practical Manual on Microbiologically Influenced Corrosion, Volume 2, J.G. Stoecker, Ed., NACE, International, Houston, TX, p. 4.1.

Saiz-Jimenez, C. and X. Arino, 2001, "Microbial Corrosion of Cultural Heritage Stoneworks," in: A Practical Manual on Microbiologically Influenced Corrosion, Vol. 2, J.G. Stoecker, Ed., NACE, International, Houston, TX, p. 11.25.

Salmon, D. and D. Sassani, 2002, Personal Communication, January 30, 2002.

Scotto, V., R. Di Cintio, G. Marcenaro, 1985, Corrosion Science, **Vol. 25**, p. 185.

Stoecker, J.G., Ed., 2001, A Practical Manual on Microbiologically Influenced Corrosion, Vol. 2, NACE, International, Houston, TX.

WATER DRAINAGE MODEL (E0070), 2000, Document Number: ANL-EBS-MD-000029, Revision: 0 ICN 1, Effective Date: 07/05/2000, Accession #: MOL.20000705.0095, DC #: 25700.

Yucca Mountain Science and Engineering Report, 2001 (May), DOE/RW-0539, U.S. Department of Energy, Yucca Mountain Characterization Office, North Las Vegas, NV.

Zhang, H-J., S.C. Dexter, 1995a, "The Effect of Biofilms on Critical Pitting Potentials for Stainless Steels S30400 and S31600 in Seawater," Proc. 1995 International Conference on MIC, P. Angel, et.al., Eds., NACE, International, Houston, TX, p. 70/1.

Zhang, H-J., S. C. Dexter. 1995b. "Effect of biofilms on crevice corrosion of stainless steels in coastal seawater," Corrosion, **Vol. 51**, No. 1, 1995, pp. 56-66.

18. Radiation Effects

Russell H. Jones
Battelle-Northwest
Richland, Washington, USA

EDITORIAL NOTE

This volume, "A Compilation of Special Topic Reports," contains a series of reports that were prepared for the Waste Package Materials Performance Peer Review Panel to use as background and input to the peer review. Summaries drawn from the reports were also presented in Section 11 of the Panel's Final Report. The Panel used the reports as background and input for its review. Any views and comments expressed in the summaries and the full reports do not necessarily reflect the opinion and findings of the Panel. Further, opinions expressed in the reports are not necessarily those of the Panel or reflected in the Panel's reports and recommendations.

Summary of Issues

The waste canister and surrounding environment will be subjected to a flux of neutrons and gamma rays from the stored radioactive waste. These fluxes can cause the following damage: 1) neutrons will produce atomic displacement damage in the metal and the passive film, and 2) gamma rays will cause electron-hole pairs in the passive film and radiolysis of the surrounding environment. The peak neutron flux has been calculated to be about 5×10^{4} n/cm^2-s (Van Konynenberg). The total neutron fluence, taking the most conservative estimate with no nuclear decay of the waste, will be 1.5×10^{16} n/cm^2 in 10,000 yrs. The peak gamma flux is about 1000 rad/hr at the time of emplacement (DOE Report-Dose calculation); decreases to approximately 10 rad/hr after 200 years; and decreases to approximately 0.1 rad/hr after 400 years. Radiolysis from gamma radiation is only a factor in the environment on the waste package surfaces when the waste packages are wet.

There is no evidence that neutron fluxes emanating from the waste will induce any mechanical property changes in the canister material within 10,000 years. This conclusion is based on available data on low-temperature irradiation of metals ($< 0.2\ T/T_m$) that produces black spot damage, faulted loops and network dislocations as shown schematically in Figure 1. Over a limited range of temperature, the density of these defects is relatively temperature insensitive and their densities saturate with fluence (Zinkle et al, 1993). This type of radiation damage can produce significant changes in mechanical properties and damage begins to accumulate upon exposure to neutrons. However, where careful hardness or strength measurements have been made, measureable changes in properties do no occur until a significant neutron fluence accumulates. For example, high-purity copper irradiated at 20 C with high energy T(d,n) neutrons did not show any strength increase until a fluence of 3×10^{16} n/cm^2

Special Topic Report prepared for the Waste Package Materials Performance Peer Review. The Final Report of the Peer Review was submitted to U.S. Department of Energy and Bechtel SAIC Company, LLC on February 28, 2002.

(Mitchel, 1978), as shown in Figure 2. A similar threshold was found for nickel irradiated with high energy neutrons (Jones et al., 1979). In austenitic stainless steels, the density of faulted loops begins to increase at low fluences when irradiated at 375-400 C (upper end of the low temperature regime), but saturation occurs at about 5 x 10^{21} n/cm^2. These data clearly suggest that radiation hardening is not expected in Alloy 22 at a fluence of 1.5 x 10^{16} n/cm^2 for the following reasons: 1) high purity metals show radiation effects at lower fluences than alloys so the threshold fluence for an increase in strength of alloy 22 will be greater than it is for Ni, 2) high-energy T(d,n) neutrons produce more damage (dpa's) per neutron than the lower energy neutrons that will be emitted from the waste package and 3) the flux from the waste package was assumed constant but in reality the flux will decrease with time such that the actual fluence will be less than 1.5 x 10^{16} n/cm^2.

Based on a limited amount of data, there is no evidence that displacement damage or ionizing radiation effects alter the properties of passive films. The corrosion resistance of alloy 22 depends totally on the protective properties of the passive film. Passive films are complex and difficult to characterize but in general they are hydrated oxides. Radiation damage to this film may occur by atomic displacements, as in the underlying metal, and from ionizing radiation effects. Saito et al. (1997) has measured the OCP of Type 304SS in the presence of gamma irradiation and found no shift at either 10^5 R/hr or 10^7 R/hr when compared to water containing H_2O_2. This result suggests that the production of H_2O_2 by radiolysis is the primary cause of a shift in the OCP and the shift is not caused by displacement or ionizing radiation damage to the film. Direct studies of the properties of irradiated passive films have not been conducted but Shikama et al. (1998) have measured the effects of irradiation on the electrical conductivity of Al_2O_3. While the passive film on alloy 22 will be a Cr rich oxide, the results for Al_2O_3 provide information about the behavior of insulators in a radiation environment. Shikama et al (1998) found no electrical breakdown in a set of polycrystalline and single crystal Al_2O_3 samples to which either 0 or 150 V was applied when irradiated to a neutron fluence of 3 x 10^{21} n/cm^2 in a gamma flux of 10^5 rad/hr to a total gamma dose of 6 x 10^{12} rad. Shikama et al. (1998) noted a 10^4 times increase in the in situ electrical conductivity but this increase was transient and decreased to the starting value with increasing dose. The cause of this transient change was not determined. Both the neutron fluence and gamma flux in the Shikama et al. (1998) study are well above those that the waste package will experience yet they are consistent with the conclusion of Saito et al. (1997).

The gamma flux emanating from the waste package can cause the radiolytic production of nitrogen oxides, nitrogen acids and ammonia in a moist air environment (Reed and Van Konynenberg) and H_2O_2 in a condensed water environment. Nitrogen compounds when mixed with condensed water will cause a shift in the pH of the water but their production rate will be low when condensed water is present. Radiolytic production of H_2O_2 has been shown in many studies to produce a shift in the OCP of metals and is expected to do likewise in alloy 22 but no studies have been conducted. Glass et al. (1986) found a 150 to 250 mV shift in the open circuit potential (OCP) of Type 304 and Type 316 SS exposed to J-13 well water in the presence of gamma radiation. A shift in the OCP affects the localized corrosion model based on the ÷E between the OCP and the breakdown potential. Stress corrosion cracking is also dependent on the oxidizing potential of the environment so a shift in the OCP is also likely to affect the stress

corrosion cracking behavior. Fujita et al. (1981) found that the susceptibility of sensitized Type 304 SS to intergranular stress corrosion was greater in air saturated water at 250 C when exposed to a flux of 4.5 x 10^4 R/hr of gamma rays as compared to tests in the absence of gamma irradiation. They concluded that gamma irradiation increased the production of H_2O_2 and hence increased the oxidation potential of the environment which led to increased stress corrosion cracking susceptibility.

Assessment of Current Project Data

Radioactive decay will reduce the primary and secondary gamma and neutron fluxes substantially within the first 500 years of storage (DOE Report-Dose Calculations). The primary gamma flux will decrease by four orders of magnitude during that period while the neutron flux will reduce by a factor of over ten during that period. Radiation damage to the metallic canister material and the passive film and radiolytic changes to the moist air and water chemistry are the processes by which radiation could affect waste canister performance. There is no evidence to suggest that radiation damage to the waste package canister material will alter its mechanical properties; therefore, radiation damage studies of alloy 22 are not warranted and have not been conducted by the Project. Also, there is no evidence that radiation damage of the passive film will alter its protective properties; although, this is based on studies by Saito et al. (1997) of Type 304 SS at 280 C. There are differences in the passive film formed on the iron based Type 304 SS at 280 C and the lower temperature (< 170 C) film formed on the nickel based alloy 22. The Project has not measured the effects of radiolysis on the corrosion properties of alloy 22 and therefore, affects on film stability are unknown. Based on the results of Shikama et al. (1998), displacement damage is not likely to alter the conductivity of the passive film but it is recommended that an evaluation of the film stability in the presence of ionizing radiation, such as a gamma flux, be conducted.

Nitrogen oxide, nitrogen acids and ammonia production during the period when the waste package is exposed only to moist air has been calculated by the program (DOE Report, Reed and Van Konynenberg. Also, little consideration has been given to the effect of radiolysis in condensed water and its affect on the corrosion behavior of alloy 22. Glass et al. (1986) have measured the effect of radiolysis of J-13 well water on the corrosion behavior of Type 304 and Type 316 SS and found a 150 to 250 mV shift in the OCP. Gamma radiation effects have not been conducted on alloy 22 although an approximation of these effects have been conducted by measuring the OCP as a function of H_2O_2 concentration in both SAW and SCW (DOE Report, Analysis/Model). These measurements were made at 25∀C and a shift in the OCP of about 225 mV was noted for SAW and about 300 mV for SCW at an H_2O_2 concentration of 72 ppm. The critical issue is the actual concentration of H_2O_2 expected in the repository environment, at the time that liquid water is formed, and the corresponding shift in the OCP.

Approach, Analysis, Methods and Plans to Support Long Term Performance

The gamma flux will decrease substantially prior to closure of the waste repository and the formation of liquid water (DOE Report-Analysis/Model). However, shifts in the OCP will continue at very low fluxes as evidenced by the results reported in the Analysis/Model DOE Report where shifts in the OCP of alloy 22 were measured as a function of H_2O_2 concentration. The OCP shifts/concentration of H_2O_2 were greatest at dilute concentrations and decreased with increasing concentration. Also, data for stainless steel (Herbert et al.) shows that most of the shift in the OCP occurs between 0 and 10^3 rad/hr but no results were given for gamma fluxes less than 10^3 rad/hr. Therefore, it is recommended that the program complete the following analysis: 1) perform a calculation of the H_2O_2 concentration expected in the repository water, 2) measure the OCP at the repository relevant H_2O_2 concentration, 3) directly measure the shift in the OCP of alloy 22 in the presence of gamma irradiation, 4) assess the stability of the OCP as a function of time for alloy 22 exposed to gamma irradiation. Radiolysis measurements should be conducted using repository relevant waters in an autoclave system that allows continuous measurement of the OCP to be made up to 170 C. High temperature measurements are desirable because of the need to measure film stability and because this stability is temperature dependent. It would be desirable to measure the current-voltage response of the material in the gamma flux but this is of a lesser priority then measuring the stability of the OCP as a function of time. It would also be desirable to measure the film chemistry following long-term exposure to the ionizing gamma irradiation field but this is a lower priority because of the complexity of measuring film chemistry when samples are transported through air. Available gamma sources generally produce at least a factor of 100 times higher flux than that expected in the repository. Therefore, tasks no.'s 1 and 2 are needed to provide specific data on OCP shifts at repository relevant conditions. The current-voltage curves should be determined as a function of H_2O_2 concentration at repository relevant temperatures.

References

1. DOE Report-Dose Calculation for the Single CRM 21-PWR Waste Package with Drip Shield, BBAC00000-01717-0210-00017 REV00, p. 14.

2. DOE Report-Analysis/Model, "General Corrosion and Localized Corrosion of Waste Package Outer Barrier", ANL-EBS-Md-000003 REV 00, p. 55-56.

3. Fujita, N., M. Akiyama and T. Tamura, "Stress Corrosion Cracking of Sensitized Type 304SS in High Temperature Water Under Gamma Ray Irradiation", Corrosion, **Vol. 37** (1981) p. 335.

4. Glass, R.S., G.E. Overturf, R.A. Van Konynenburg and R.D. McCright, " Gamma Radiation Effects on Corrosion-I Electrochemical Mechanism for the Aqueous Corrosion Processes of Austenitic Stainless Steels Relevant to Nuclear Waste Disposal of Tuff", Corrosion Science, **Vol. 26** (1986) p. 577.

5. Herbert, D. G.O.H. Whillock and S.E. Worthington, "Zero-resistance Ammetry-its Application in Preventing the Corrosion of Stainless Steel in Cooling Waters", in Electrochemical Methods in Corrosion Research, Material Science Forum, **Vol. 192-194**, (1995), 469-476.

6. Jones, R.H., D.L. Styris, and E.R. Bradley, "Radiation Damage Effects in 16 MeV Proton and 14 MeV Neutron Irradiated Nickel and Niobium", ASTM STP 683, 1979, p. 346.

7. Mitchel, J.B.,"Exploratory Experiments Comparing Damage Effects of High-Energy Neutrons and Fission-Reactor Neutrons in Metals", UCRL-52388, Lawrence Livermore National Laboratory, California, January 12, 1978.

8. Reed, D.T., and R.A. Van Konynenburg, "Effect of Ionizing Radiation on the Waste Package Environment", TIC # 234975.

9. Saito, N., E. Kikuchi, H. Sakamoto, J. Kuniya and S. Suzuki, "Susceptibility of Sensitized Type 304 Stainless Steel to Intergranular Stress Corrosion Cracking in Simulated Boiling-Water Reactor Environments", Corrosion, **Vol. 53** (1997) p. 537.

10. Shikama, T., S.J. Zinkle, K. Shiiyama, L.L. Snead and E.H. Farnum, "Electrical Properties of Ceramics During Reactor Irradiation", J. of Nucl. Mater., **Vol. 258-263** (1998) p. 1867.

11. Shikama, T., and S.J. Zinkle, " Long Term Degradation of Electrical Insulation of Al_2O_3 Under High Flux Fission Reactor Irradiation", J. of Nucl. Mater., **Vol. 258-263** (1998) p. 1861.

12. Van Konynenburg, R., Lawrence Livermore National Laboratory, private communication, Dec. 2001.

13. Zinkle, S.J., P.J. Maziasz, and R.E. Stoller, "Dose Dependence of the Microstructural Evolution in Neutron-Irradiated Austenitic Stainless Steel", J. Nucl. Mater., **Vol. 206** (1993) p. 266.

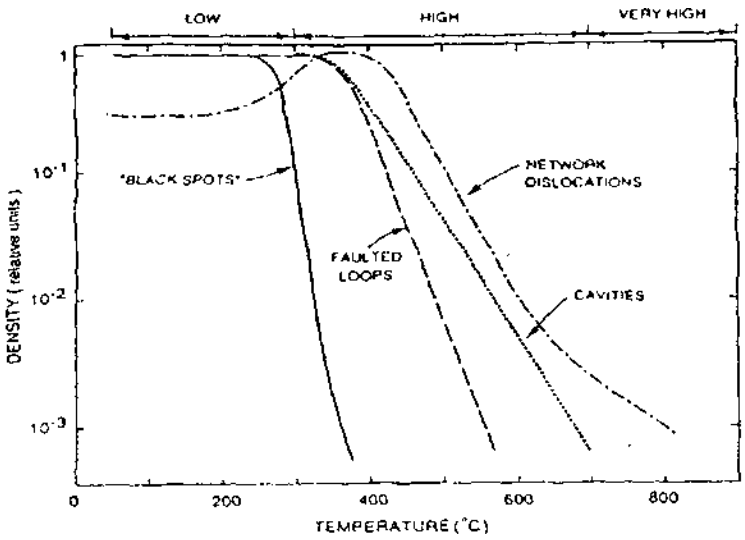

Figure 1 – Temperature dependence of the experimentally observed "saturation"densities of the various microstructural components in neutron-irradiated austenitic stainless steel. The microstructural data can be grouped into "low temperature", high temperature", and "very high temperature" regimes.

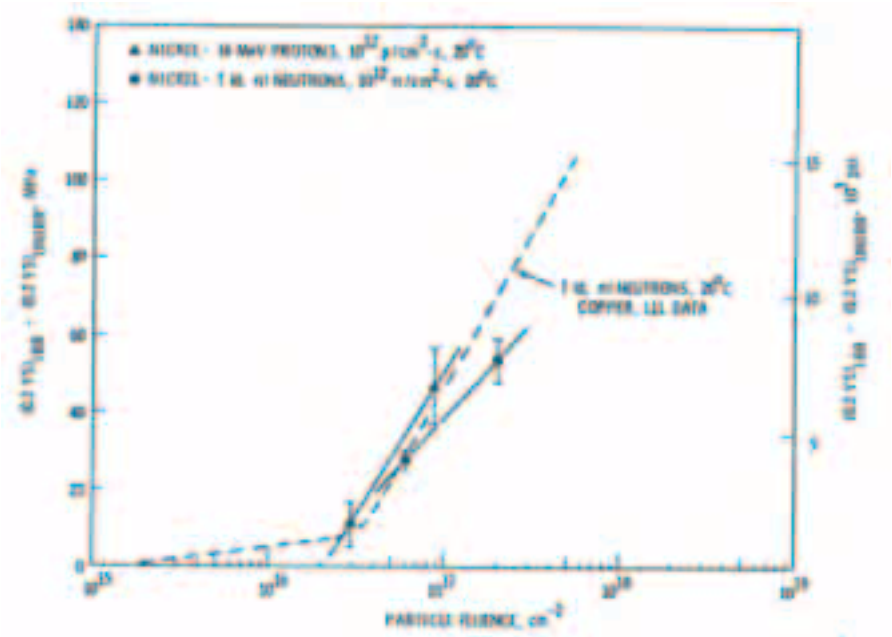

Figure 2 – Comparison of the yield stress increase in neutron- and proton-irradiated nickel and copper as a function of particle fluence.

19. Aspects of Waste Canister Corrosion Related to Oxidation and Scale Formation

Robert A. Rapp
The Ohio State University
Columbus, Ohio, USA

EDITORIAL NOTE

This volume, "A Compilation of Special Topic Reports," contains a series of reports that were prepared for the Waste Package Materials Performance Peer Review Panel to use as background and input to the peer review. Summaries drawn from the reports were also presented in Section 11 of the Panel's Final Report. The Panel used the reports as background and input for its review. Any views and comments expressed in the summaries and the full reports do not necessarily reflect the opinion and findings of the Panel. Further, opinions expressed in the reports are not necessarily those of the Panel or reflected in the Panel's reports and recommendations.

Abstract

Certain aspects of the corrosion expected for nuclear waste burial canisters involve mechanisms, measurements and interpretations that have been well studied and understood in terms of high-temperature corrosion studies. In particular, the subjects of hot corrosion, scale growth and adherence, the role of interfacial metal/scale structure in vacancy annihilation, and the segregation of impurity solutes to interfaces are discussed here. The initial formation of a very thin, adherent chromia-rich air-formed film seems important and advantageous to the long-term stability of the protective layer. Optimization of the initial surface preparation is recommended, and traditional electrochemical studies of passivation are suggested to offer little relevance to the problem.

Preface

Prior to a discussion of certain aspects of the corrosion situation expected upon the burial of radioactive waste for a very long time (10,000 years) in Yucca Mountain, NV, I wish to summarize my own expertise and experience in the corrosion field, so that the reader can put these comments in context and judge/evaluate them accordingly. Although I have a reasonable knowledge of the scientific and engineering aspects of aqueous corrosion, I have not studied in detail the structure, mechanism and growth kinetics of passive films in aqueous corrosion. On the other hand, for about 35 years, I have conducted research and reviewed and published studies involving the mechanisms of scale growth on metals and alloys in dry gaseous environments at

Special Topic Report prepared for the Waste Package Materials Performance Peer Review. The Final Report of the Peer Review was submitted to U.S. Department of Energy and Bechtel SAIC Company, LLC on February 28, 2002.

elevated temperatures. Over the past 15 years, Bernard Pieraggi, John Hirth and I have proposed detailed mechanisms for the annihilation of point defects, whose diffusion is involved in scale growth, by the climb of dislocations at the metal-scale interface. Likewise, over the past 20 years, I have published many studies which form the basis for an understanding of the mechanism of "hot corrosion", a high-temperature analog to "atmospheric corrosion" by a thin aqueous surface film. In a 1997 report[1] prepared for the Nuclear Regulatory Commission, Sylvain Larose and I reviewed the low-temperature (dry) oxidation of carbon steels and low-alloy steels for use as nuclear waste package materials. Despite my professional emphasis on corrosion phenomena at high temperatures, I feel that certain of the mechanisms and protective measures in high-temperature corrosion relate directly to the corrosion aspects for Alloy 22 in the burial of radioactive waste, as I shall attempt to demonstrate.

Introduction

Based on certain YMP reports describing the proposed waste burial system at Yucca Mountain, discussions held at the July 2001 NWTRB Workshop on Long-Term Extrapolation of Passive Behavior, and especially the report of Gustavo Cragnolino to that Workshop, certain aspects of the corrosion of the waste containment vessels are worthy of critical consideration. First, the Alloy 22 containment vessels will begin their service in an essentially dry air atmosphere at a temperature as high as 250C. Depending on many factors, such as the manipulation of ventilation cooling, the intrusion/seepage of ground water, the effectiveness of the Ti drip shields, etc., the Alloy 22 canisters could remain dry, e.g. only experience the slow growth of a protective chromia-rich film for a relatively long period (one hundred years or more). Ultimately, after sufficient cooling resulting from the decomposition of the nuclear waste, the relative humidity in the vault (depending on the local weather conditions) could exceed that necessary for condensation of a water film on this surface. Otherwise, some water could be deposited on the surface directly via seepage, etc., if the Ti drip shields should fail. In any case, an extended period of protective chromia-rich scale growth would precede the presence of any surface water film. Some extended period of cyclic wet and dry conditions could follow; of course, such wetting/drying cycles are particularly troublesome as they lead to the concentration of salts on the surface. Thereafter, the corrosion problem would become a rather unusual case of "atmospheric corrosion" of a *prefilmed* surface. This circumstance does not correspond to either of the two simpler corrosion mechanisms generally studied in the laboratory, and also dominating the attention of the laboratory studies for this application: "passivity" protection for the bare alloy, or atmospheric attack of the bare alloy. Some discussion of the atmospheric corrosion of a prefilmed surface will be presented.

In the estimation of life prediction for such an application, a principal unknown factor can be the occurrence of any "breakaway kinetics" resulting from the rupture, detachment or penetration of the protective film, whether it be a solid oxide or a hydrated passive film. One of the factors causing concern for the evaluation of the waste burial system is whether one can expect that vacancies active in supporting the diffusion of cations (or anions) through the protective film would experience a harmful coalescence (leading to local separation) at the metal/film interface, or whether vacancy annihilation at that interface would retain the attached

film. The specific preparation of the surface prior to exposure should play an important role in the action of the metal/film interface. These problems will be discussed in some detail.

Some concern has been expressed that minor impurities in the alloy, e.g. sulfur and phosphorus, would segregate and concentrate at the metal/film interface, thereby degrading the film adherence and affecting its interactive role with vacancies. The problem of interfacial segregation has been carefully studied at high temperatures and the resulting conclusions should also be valid at much lower temperatures. The effectiveness of certain reactive elements, e.g. Y or Ce for chromia films, in counteracting sulfur segregation and providing other favorable effects has been demonstrated, and will be discussed in this report.

Atmospheric Corrosion of Prefilmed Alloy 22 Surface

At the July 2001 NWTRB's Workshop on Passive Behavior, Gerry Gordon of the Yucca Mountain Project reported observations about the oxide film formed on Alloy 22. From AFM measurements, the thickness of the air-formed chromia-rich oxide formed on alloy 22 after oxidation at 200C for 45 days was about 32 angstroms, and little, if any, additional growth occurred after 120 days. Surprisingly, the passive chromia-rich film formed on Alloy 22 in an 85C, 1M NaCl aqueous solution of pH 1 exhibited about the same thickness. (This correlation would suggest significant physical and chemical similarities between the air-formed film and the passive water-formed film.) While an extrapolation of alloy recession to 10,000 years from measurements after 1.5 months is not justified, it seems clear that the oxidation rate in dry air in the range 200-300C (even following a parabolic rate law) can be considered absolutely negligible. Even iron and steels, the fastest oxidizing of all the practical alloy base metals, are estimated to suffer only about 15 microns of alloy recession with no breakaway kinetics after 1,000 years of oxidation in air at 250C[1]. Thus, it is clear that scaling of any alloy, but especially Alloy 22, resulting from air oxidation would represent no problem in alloy consumption/recession at the temperatures of the waste canister application. Likewise, the similar thickness and composition for the aqueous-formed passive film indicate no problem in metal recession resulting from uniform passive corrosion for 10,000 years or more. Cragnolino[2] reports a true steady-state passive current density (after 150 hours) in hot deaerated chloride-containing solutions of 1.0×10^{-8} amps/cm^2. This current density corresponds to an alloy recession rate of only about 0.1 σm/yr, extrapolating to a container life exceeding 100,000 years. (An important question about this argument, however, concerns the experimental use of a "deep" deaerated aqueous solution, to infer the rate of corrosion attack for an "atmospheric", thin, aerated aqueous film. Such a correlation needs to be demonstrated.) The point to be made here is that neither the low-temperature air-oxidation of the bare Alloy 22, nor the steady-state uniform passive aqueous corrosion of the bare Alloy 22 can lead to penetration of the proposed canister wall in 10,000 years.

However, the service life-cycle for the canister calls for the condensation or deposition of the potentially aggressive aqueous film on top of the existing steady-state air-formed oxide after many decades or hundreds of years. In fact, the growth of either the air-formed film or the passive film from aqueous attack is driven by a gradient in the electrochemical potentials for the

mobile ionic and electronic species in the product film. More simply, the gradient in the oxidation potential between the environment and the metal/film interface is responsible for the film growth in either case. If one considers that the full drop in oxidation potential already exists across the air-formed film at the time of introduction of the aqueous film, indeed, there is no immediate driving force for aqueous attack by the growth of the passive film. Then the effect of the salt-laden aerated aqueous film could initially only be to dissolve some small fraction of the air-formed film. There seems to be no apparent reason, except for the unlikely prospect of localized dissolution penetrating the air-formed film to reach the metal, that the formation or growth of a passive aqueous film would become relevant. Failing such penetration of the air-formed film, the only role of the aqueous film would be to support an atmospheric corrosion of the existing oxide film, essentially in the absence of a driving force (negligible gradient in oxidation potential). To understand better the nature of atmospheric corrosion, some principles demonstrated in its high-temperature analog "hot corrosion" will be discussed.[3]

At elevated temperatures, e.g. 1000C, certain sections of engineering systems, e.g. gas turbines for many applications, experience the deposition of a thin fused film of an aggressive salt usually based on fused sodium sulfate. Frequently, an accelerated corrosive attack results. The author has published extensive studies involving measurements of the solubilities of many oxides in fused sodium sulfate, the electrochemistry, and the mechanism of "hot corrosion". Figure 1 presents a plot of the measured solubilities of important oxides in fused Na_2SO_4 at 1200K.[3]. The ordinate scale, -log a_{Na2O}, is a quantitative measure of the melt basicity (an inverse analog to the pH in aqueous solutions). Thus, Fig. 1 displays measured plots for oxide solubilities which exactly follow the Pourbaix formalism for thermodynamics of aqueous solutions (except that the sense for the acid-base ordinate scale is reversed, according to the convention followed by fused salt chemists). Exactly similar "predictions" are made for the solubilities of oxides in aqueous solutions, the difference being that local equilibrium is seldom achieved for aqueous solutions near room temperature. Of particular importance for Alloy 22, Cr_2O_3 is seen in Fig. 1 to be a very acid oxide (in fused Na_2SO_4), so that in oxidizing gases the chromate CrO_4^{2-} ion is the dominant solute, but in a reducing environment, the solute CrO_2^- is important, as detailed in Fig. 2.[4]

Figure 3 presents a schematic depiction of the "negative solubility gradient" mechanism for steady-state hot corrosion.[5] Because the thin fused salt film supports a gradient in either melt basicity or oxidizing potential, or probably both, the local solubility for the protective adherent oxide film can change within the salt film. In case the oxide solubility is greater at the oxide-salt interface and lower farther out in the film, a "negative solubility gradient" exists within the film. Then the local dissolution of the oxide at the oxide-salt interface, the outward diffusion of the soluble ions down a concentration gradient, and the precipitation of the oxide as a non-protective particle in the salt film serves to convert an adherent protective oxide into non-protective particles in the salt matrix. In addition, the salt film may also preferentially attack the grain boundaries of the adherent oxide where impurities and segregants are concentrated. If the fused salt should succeed to reach the bare metal by such localized attack, dire circumstances would result, e.g. a metal sulfide could form at the metal-oxide interface, and the local basicity of the salt could be shifted by several decades, drastically increasing the local oxide solubility. These details were demonstrated in the hot corrosion of preoxidized Ni by Otsuka and Rapp[6], using

potentiometric sensors measuring the local basicity and oxidation state for the fused salt film during hot corrosion. This discussion of "hot corrosion" is provided here, because, except for certain details, the mechanism for atmospheric corrosion by a thin aqueous film must also correspond to a "negative solubility gradient" criterion for continuing attack, i.e. by dissolution of the protective film and reprecipitation of non-protective oxide particles in the film. As an important point, the atmospheric corrosion must also be driven by gradients in basicity and oxidation potential, factors that are not obviously present if the aqueous film resides on a preexisting protective oxide film.

In the field of hot corrosion, chromium is known to be the most effective element as an alloy or coating component to improve hot corrosion resistance. The rationalization for this behavior is one apparently shared with aqueous solution researchers in explaining the effectiveness of the chromate inhibitors. In hot corrosion, chromate (hexavalent Cr) is the dominant solute formed upon Cr_2O_3 dissolution. Because of the associated valence change, the solubility of Cr_2O_3 as CrO_4^{2-} depends upon the oxygen activity: proportional to $P_{O2}^{3/2}$. Because any aerated aqueous film will be most oxidizing at its film/gas interface, the precipitation of non-protective chromia particles in the aqueous film does not occur, because the "negative solubility gradient" is not satisfied. On the contrary, if some localized dissolution of the protective film would threaten to reach the bare metal, the resulting occurrence of a locally reduced site would lead to the deposition of Cr_2O_3 there, where its solubility is lowest. Figure 4 depicts schematically this protective action of chromium.[7]

The distinction between passive corrosion of an alloy in a "deep" aqueous solution (especially a deaerated solution) and "atmospheric corrosion" caused by a thin aerated surface film is significant, and seems to be overlooked in the current corrosion studies of Alloy 22. From hot corrosion experimentation, we know that studies involving deep melts have no relevance, but generally lead to excessively severe corrosion, because the oxide-salt interface has been shielded from the acidic oxidant SO_3. Likewise, if the fused salt contacts a susceptible metal in argon (deaerated gas), no hot corrosion occurs because an oxidant is lacking. Therefore, the existing electrochemical studies of passivity and measured values for steady-state current densities (as an estimate for the uniform corrosion rate) should be regarded with skepticism. On the other hand, for two good reasons, properly designed experimentation studying the atmospheric corrosion of a preformed oxide film on Alloy 22 are likely to demonstrate very low attack rates: 1. The preexisting film should support all of the difference in oxidation state which otherwise drives atmospheric corrosion, 2. The expected inherent protective nature of chromate solute should prevent any contact of the base alloy with the aqueous film in any case. To avoid the problems arising from cyclic wetting and drying of the Alloy 22 surface, however, a manipulation of the ventilation system should be considered so that the Alloy 22 canisters initially experience dry air oxidation for as long as possible, prior to some imposed cooling to permit condensation, but no wet/dry cycling. In any case, the proper direction for experimentation seems to be the study of atmospheric corrosion of prefilmed alloy surfaces. Electrochemical passivity studies do not seem to be relevant.

Role of the Metal-Scale Interface in Vacancy Annihilation; Effect of Surface Preparation

One of the questions posed at the July 2001 NWTRB Workshop was the uncertainty concerning the fate of vacancies supporting the diffusion of cations (or anions) in the growth of any barrier film on the alloy. In the event of vacancy coalescence to form voids at the metal/barrier interface, film separation or fracture could permit the contact of an aggressive aqueous film with the metal, perhaps supporting localized corrosion. The mechanism of vacancy annihilation at the metal-scale interface in the growth of oxide scales on metals at elevated temperatures has received significant clarification recently.[8-10] In brief, regardless of the individual crystallographic structures of the alloy substrate and the oxide grown at the surface, at least initially, some epitaxial relation(s) providing perfect contact between the two lattices will be established at the metal-scale interface. As illustrated schematically in Fig. 5, such an epitaxial interface can be considered to comprise a regular grid of "misfit dislocations" (compensating for the difference in lattice parameters for the two structures) and "misorientation dislocations" (corresponding to a minor tilt in the actual relative orientations from the ideal epitaxial arrangement). The misfit dislocations must be quite close together, e.g. every seven lattice planes of Ni for a [110] parallel epitaxy in the Ni/NiO interface, to account for a 14% difference in lattice spacing. The misorientation dislocations can be created by the intersection of the interface with a glide plane in the metal or the oxide, so these are generally less numerous.

As is well understood in bulk metals, vacancy annihilation occurs and is required for the climb of edge dislocations. The same applies for the metal/scale interface. A vacancy supporting cation diffusion in the growth of an adherent oxide arrives at the metal-scale interface and is annihilated (adding a cation to the scale) by the climb of the interface dislocations, as illustrated in Fig. 6. A misfit dislocation would climb into the metal, annihilating vacancies, but upon the necessary dissociation into glissile partials, return to the interface, to relieve the tensile stress created by its departure. (This sequence might be considered a "dislocation mill".) A misorientation dislocation would annihilate cation vacancies by climb within the interface. Only after some significant tangling of the interfacial dislocations (e.g. as might be supported by prior surface abrasion or creep in service, etc.) would the climb of these dislocations be blocked, so that vacancy agglomeration would lead to a local scale separation. Although perhaps not relevant to the Waste Storage problem, and certainly little considered by the aqueous corrosion community, such epitaxial interface structures and vacancy annihilation mechanisms must also apply for the growth of passive films on bare metals, insofar as the aqueous passive film is considered to be crystalline. In that case, the key to avoiding vacancy coalescence leading to void formation at the metal-scale interface is to start an oxidation or corrosion process with a surface that is relative free of deformation and residual stress. Certainly, the initial surface preparation plays a key role in deciding the state of the initial surface and therefore how the interface supports vacancy annihilation. Some observations in the low-temperature oxidation of iron support these arguments.

As seen in Fig. 7, Caplan and Cohen[11] showed that for the low-temperature oxidation of pure Fe (down to 400C) the scaling rates of cold worked (abraded) surfaces were about an order of magnitude higher than for an undeformed (electropolished) surface. The authors offered an outdated (and incorrect) interpretation, supposing that the abraded specimens possessed a higher

dislocation density in the metal to annihilate vacancies. The current author would interpret the differing kinetics as follows: the electropolished surfaces were able to form a larger oxide grain size and retain the epitaxial contact longer, thereby maintaining the low rate of parabolic scale growth without void formation. At such low temperatures, and especially for a chromia scale (film) on Alloy 22, diffusional growth occurs by cation (and perhaps anion) diffusion over short-circuit paths (grain boundaries) in the scale. Prior surface abrasion leads to a finer oxide grain size and therefore faster growth kinetics, besides a premature capitulation of the interface dislocations in their role for vacancy annihilation. Later studies[12,13] by Hussey et al. at the NRC of Canada (the world's experts in such studies) found similar kinetics for low-temperature (down to 200C) iron oxidation, and better scale adherence for coupons with electropolished surfaces (and therefore larger oxide grains) than for surfaces with smaller oxide grain sizes. The scale thicknesses for these studies ranged from hundreds to a few thousand angstroms, certainly thicker that those expected for Alloy 22. As already mentioned, for the Waste Canister application, the uniform corrosion rate is not an issue, but the adherence of the barrier film could be important. From the available studies, and implications from the modern mechanistic models, an initial surface with minimal strain giving better scale adherence would be favored for an electropolished surface. I recommend the consideration and implementation of such surface preparation studies in the ongoing experimentation. For the extremely thin oxide films relevant to Alloy 22 oxidation and corrosion, with proper surface preparation, I do not foresee any problem with retention of an adherent protective oxide film for 10,000 years. I might also suggest that the electroplating solution contain some soluble cerium ions, as these have been shown to produce various advantageous effects in both reducing scaling kinetics and scale adherence for chromia films both at high temperatures[14], and for aqueous corrosion.

Role of Interfacial Impurity Segregation

At the July 2001 NWTRB Workshop, Phillipe Marcus presented a schematic drawing of a passive film contacting the bare alloy (perhaps not relevant to the prefilmed Alloy 22 application). According to the illustration, sulfur in the alloy would accumulate/segregate (preferentially) at the alloy/film interface, leading to breakdown of the passive film and localized corrosion. Although Marcus must have some sort of experimental evidence to support this illustration (presentations were very limited in time), such a behavior for sulfur does not occur at *adherent* high-temperature metal/scale interfaces. To the extent that the preformed oxide film would protect the Alloy 22, and to the extent that any passive film would be crystalline, I would suggest that such a problem would not be expected for the Waste Canisters, based on the following considerations.

Luthra and Briant[15] treated the thermodynamics of segregation in alloys, especially the behavior of sulfur, boron and phosphorous in Ni-Cr-Al-Y alloys. Certainly, segregation of these solutes to grain boundaries and especially to the free alloy/gas interface is favored, as was shown by their experimental Auger observations.[16]. The poor adherence of oxide scales on high-sulfur alloys, especially for cycling oxidation, and the inhibiting effect of an yttrium or cerium alloy addition are also well known in high-temperature scaling. However, the sulfur does not segregate to an adherent (epitaxial) metal/scale interface, but only to local sites where scale

detachment has occurred, e.g. as a result of vacancy coalescence to form voids, i.e. to an interior alloy/gas interface. In many publications[17,18], the Grabke group has used scanning Auger to traverse adherent and locally detached oxide scales on metals. An adherent metal-scale interface did not contain sulfur, which is indeed logical since both the ion size for sulfur does not fit, nor is the bond energy for Fe-S competitive with the Fe-O bond. However, whenever vacancy coalescence would create an interfacial void, sulfur would quickly adsorb to the internal interface. This apparent detail in mechanism is important because it adds emphasis to the need for maintaining the adherent epitaxial metal-scale interface, e.g. using electropolished surfaces.

Concluding Remarks

The author has attempted to introduce certain aspects of the body of knowledge of high-temperature corrosion to interpret the low-temperature corrosion problem for Alloy 22 nuclear waste canisters. Some of the suggestions made here may seem unusual to the aqueous community, e.g. the lack of relevance of traditional electrochemical corrosion methods, the importance of initial surface preparation, etc., and these points require some further discussion and resolution. The author will be happy to receive comments and criticism of the presentation made here, in the hope of reaching a better understanding for the long-term corrosion mechanisms, problems, and rates.

References

1. S. Larose and R. A. Rapp, "Review of Low-Temperature Oxidation of Carbon Steels and Low-Alloy Steels for Use as High-Level Radioactive Waste Package Materials", Report CNWRA 97-003, Nuclear Regulatory Commission, Feb., 1997.

2. G. Cragnolino, "Long-Term Passive Dissolution and Localized Corrosion of Alloy 22", Report to NWTRB Workshop on Long-Term Extrapolation of Passive Behavior, July 19-20, 2001, Washington, DC.

3. Y. S. Zhang and R. A. Rapp, "Fundamental Studies of Hot Corrosion of Materials", Journal of Metals, Dec. (1994), pp. 47-55.

4. Y. S. Zhang, "Solubilities of Cr_2O_3 in Fused Na_2SO_4 at 1200K", J. Electrochem. Soc., **133**, (1986), pp. 655- 57.

5. R. A. Rapp and K. S. Goto, "The Hot Corrosion of Metals by Molten Salts", Molten Salts II, R. Selman and J. Braunstein, Eds., Electrochem. Soc., (1979), 159.

6. N. Otsuka and R. A. Rapp, "Hot Corrosion of Preoxidized Ni by a Thin Fused Na_2SO_4 Salt Film at 900C", J. Electrochem. Soc., **137**, (1990), pp. 46-52.

7. N. Otsuka and R. A. Rapp, "Effects of Chromate and Vanadate Anions on the Hot Corrosion of Preoxidized Ni by a Thin Fused Na_2SO_4 Film at 900C", ibid pp. 53-60.

8. B. Pieraggi and R. A. Rapp, "Stress Generation and Vacancy Annihilation during Scale Growth Limited by Cation-Vacancy Diffusion", Acta Metall., **36**, (1988), pp. 1281-89.

9. J. P. Hirth, B. Pieraggi and R. A. Rapp, "The Role of Interface Dislocations and Ledges as Sources/Sinks for Point Defects in Scaling Reactions", Acta Metall. Mater., **43**, (1995), pp. 1065-73.

10. B. Pieraggi, R. A. Rapp and J. P. Hirth, "Role of Interface structure and Interfacial Defects in Oxide Scale Growth", Oxid. Metals, **44**, (1995), pp. 63-79.

11. D. Caplan and M. Cohen, " Effect of Cold Work on the Oxidation of Iron from 400-650C", Corr. Sci., **6**, (1966), p. 321.

12. M. J Graham and R. J. Hussey, "The Growth and Structure of Oxide Films on Fe. I. Oxidation of (011) and (122) Fe at 200-300C", Oxid. Metals, **15**, (1981), pp. 407-20.

13. R. J. Hussey, D. Caplan, and M. J. Graham, "The Growth and Structure of Oxide Films on Fe. II. Oxidation of Polycrystalline Fe at 240-320C", Oxid. Metals, ibid., pp. 421-35.

14. B. Pieraggi and R. A. Rapp, "Chromia Scale Growth in Alloy Oxidation and the Reactive Element Effect (REE)", J. Electrochem. Soc., **140**, (1993) pp. 2844-50.

15. K. L. Luthra and C. L. Briant "Thermodynamics of Segregation in Alloys", Metall. Trans., **19A**, (1988), pp. 2091-2098.

16. C. L. Briant and K. L. Luthra, "Surface Segregation in MCrAlY Alloys", ibid., pp. 2099-2108.

17. H. J. Schmutzler, H. Viefhaus, and H. J. Grabke, "The Influence of the Oxide/Metal Interface Composition on the Adherence of Oxide Layers on Metal Substrates", Surface and Interf. Analysis, **10**, (1992), pp. 581-4.

18. H. J. Schmutzler, H. Viefhaus, and H. J. Grabke, " Investigation of the Oxide-Metal Interface Composition on the Adherence of Oxide Layers on Metal Substrates", Surface Interf. Anal., **10**, (1992), pp. 581-584.

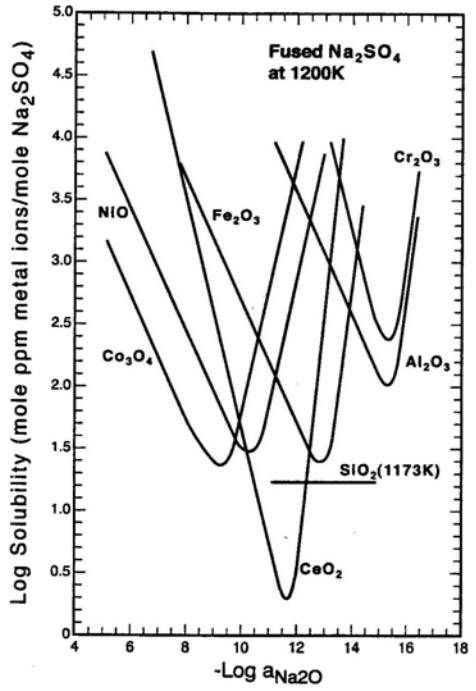

Fig. 1—Compilation of measured solubilities for several oxides in fused pure Na_2SO_4 at 1200 K.

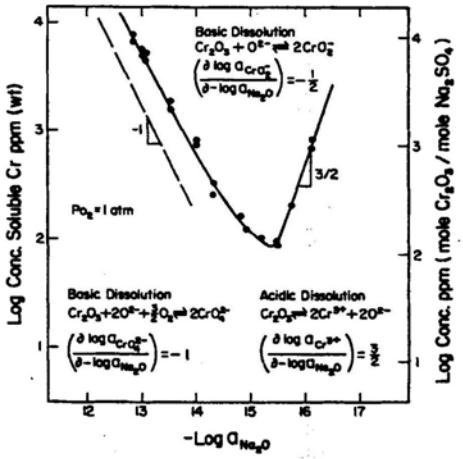

Fig. 2—Experimentally measured solubilities for chromium oxide in fused pure Na_2SO_4 at 1200 K and 1 atm oxygen.

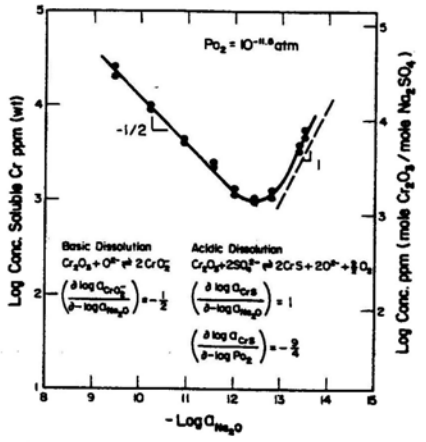

Fig. 3—Experimentally measured solubilities for chromium oxide in fused pure Na_2SO_4 at 1200 K and $10^{-11.5}$ atm.

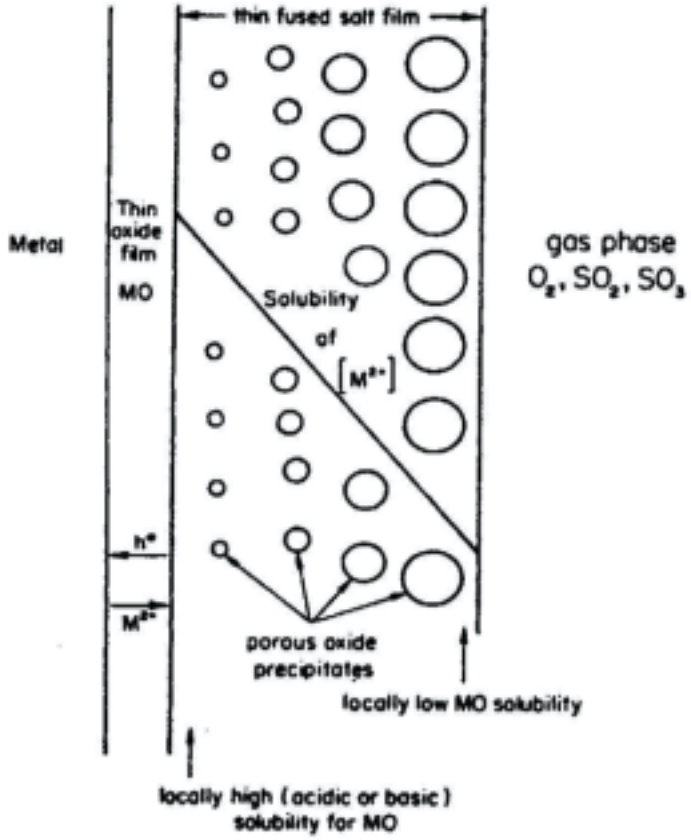

Fig. 3 —Reprecipitation of porous MO oxide supported by a negative solubility gradient in the fused salt film.

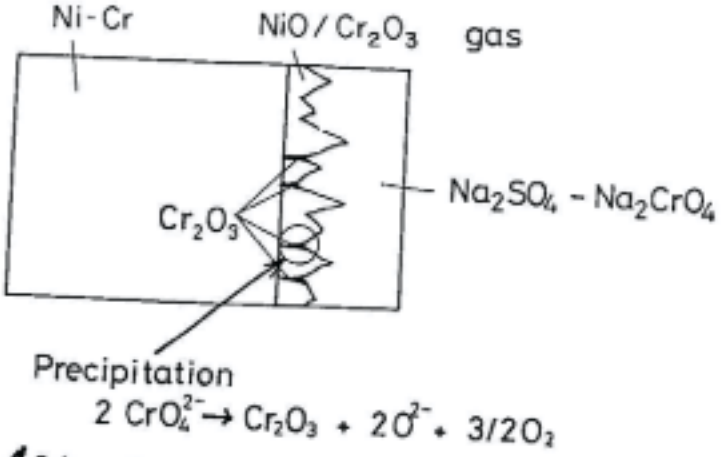

Fig. 4 Schematic representation of possible beneficial effect of chromium on hot corrosion of Ni-Cr alloy.

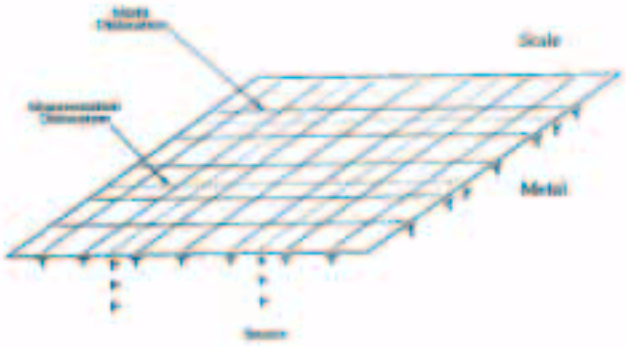

Fig. 5 — Schematic illustration of metal/oxide interface with parallel epitaxial orientation showing interfacial misfit and misorientation dislocations

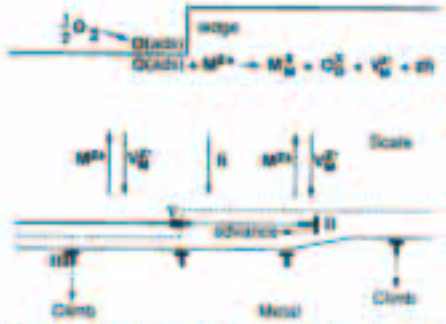

Fig. 6. Misfit and misorientation dislocations in the metal serve as interface sinks in the case of scale growth by cation/vacancy diffusion.

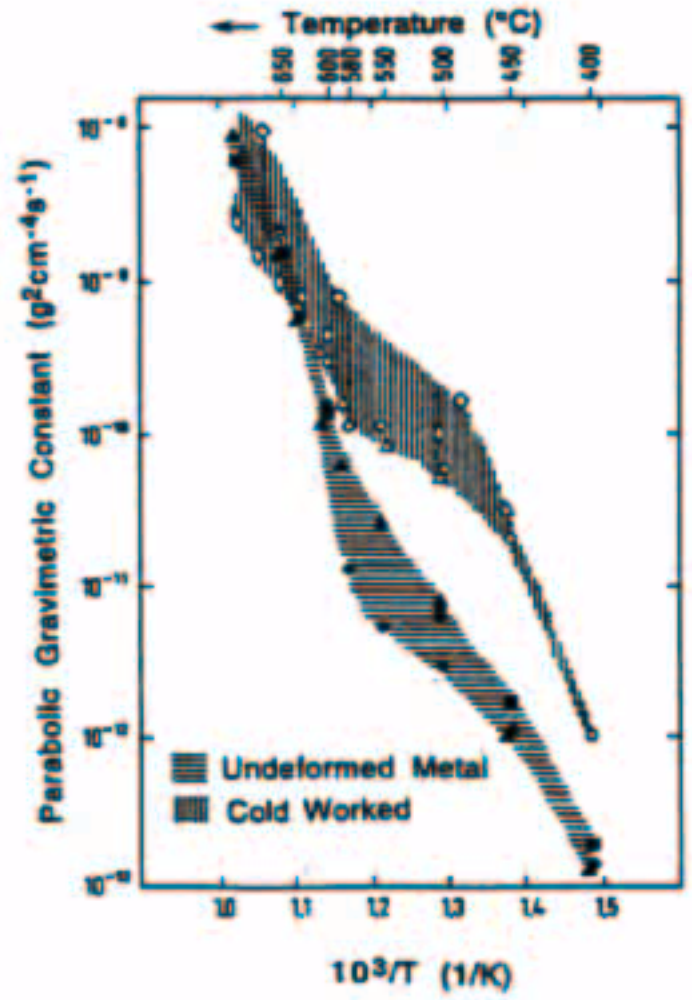

Figure 7 Influence of cold work on the oxidation rate of pure iron. The diagram clearly shows that the scaling kinetics of cold worked iron are faster than those of undeformed metal for temperatures below 650 °C. [Caplan and Cohen (1966)]

20. Interfacial Segregation in Nickel Base Alloys

Clyde L. Briant
Brown University
Providence, Rhode Island, USA

EDITORIAL NOTE

This volume, "A Compilation of Special Topic Reports," contains a series of reports that were prepared for the Waste Package Materials Performance Peer Review Panel to use as background and input to the peer review. Summaries drawn from the reports were also presented in Section 11 of the Panel's Final Report. The Panel used the reports as background and input for its review. Any views and comments expressed in the summaries and the full reports do not necessarily reflect the opinion and findings of the Panel. Further, opinions expressed in the reports are not necessarily those of the Panel or reflected in the Panel's reports and recommendations.

Introduction

The purpose of this report is to summarize the existing knowledge available on segregation to grain boundaries, oxide-metal interfaces, and surfaces in nickel-base alloys and to apply that knowledge to the particular problem under consideration. This problem concerns the storage of nuclear waste in the Yucca Mountain Repository. There is concern that over many years the material stored in this repository could be exposed to moisture, which in turn could lead to corrosion. It is also known that segregation to interfaces can enhance this corrosion. Thus one would like to know what segregants might be present on the interfaces that could lead to corrosive attack and whether or not segregation could increase during storage.

At the start of this report it is important to state certain restrictions that I have imposed. The first is that the report will only consider segregation. It will make no comment about how this segregation might affect corrosion. The second is that the temperature regime of interest, which is below 250^{o}C, is much lower than the range where laboratory experiments have been generally performed. Thus one must try to extrapolate information obtained at higher temperatures to this low temperature regime. In some places I will use a simple model to aid in this extrapolation. The third point is that, in general, much more work on segregation has been done on iron-base alloys than on nickel-base alloys. Thus I will also draw on the research on iron-base alloys where appropriate to discuss specific aspects of this problem. On this same point, there does not appear to be any segregation data available for the Hastelloy C-22, which is the alloy of interest for this project. However, there are a few studies on Hastelloy C-276 and these will be highlighted. Finally, I have not considered any effects that radiation damage could have on segregation.

Special Topic Report prepared for the Waste Package Materials Performance Peer Review. The Final Report of the Peer Review was submitted to U.S. Department of Energy and Bechtel SAIC Company, LLC on February 28, 2002.

In order to present these results, I will begin with grain boundaries, since intergranular corrosion would probably be of greatest concern. I will then consider surfaces, and finally the metal-oxide interface.

Grain Boundary Segregation

It is well known that impurity elements such as phosphorus, antimony, and tin segregate to grain boundaries in metals. The data which have demonstrated this segregation have almost all been obtained from experiments that employed Auger electron spectroscopy. The sample is fractured along the grain boundaries in the high vacuum spectrometer and then the exposed boundaries are analyzed. Many studies have now demonstrated the fundamental principles that control grain boundary segregation. (See Reference 1 for a review.) These are the following:

1. The amount of segregation increases with increasing bulk concentration of the segregant, provided the segregant remains in solid solution.
2. The amount of segregation increases with decreasing temperature, provided that the element remains soluble in the matrix.
3. As the temperature decreases, the time required to reach a given level of segregation increases.

However, there are two important ways in which the amount of segregation can be modified in complex materials. The first is that there can be site competition at the grain boundary between two elements. Experiments have shown that the element with the higher diffusion coefficient will reach the boundary first. This element may then keep another, more slowly diffusing element off the grain boundary [1]. The second point is that in segregation we are concerned with the concentration of an element that is in solid solution in the matrix. If the segregant is precipitated out as a second phase, it will not be free to segregate to the grain boundaries. For example, sulfur will readily segregate to grain boundaries in both iron and nickel and can make the boundaries very brittle. However, it is rarely observed on the grain boundaries of steel because it is usually precipitated as MnS. Similarly, Mulford [2] has shown that chromium and hafnium can both eliminate this segregation in nickel.

There have been a number of studies of grain boundary segregation of nickel-base alloys. Many of these are summarized in Table I. We list in this Table elements that were found to segregate to the grain boundaries and also impurity elements present in the bulk composition that were not found to segregate. It is clear from these examples that phosphorus is the primary segregant to the grain boundaries in these alloys. There are few elements that cause the formation of stable phosphides in either iron or nickel-base systems, so all of the phosphorus in the material would be free to segregate to the grain boundaries. The alloys listed in Table I all contain strong sulfide formers such as Cr and Mn, and these two elements would tend to lower the free sulfur concentration so much that this element would not segregate. The one time that sulfur was observed was in a weld where the high temperature of the welding process could dissolve any sulfides present and thus allow the sulfur to segregate. Two other elements that were observed to

segregate to grain boundaries in more than one study were boron and nitrogen. These elements would segregate very rapidly as interstitials. It is also important to note that silicon was not reported to segregate. It was detected in the Auger data reported in reference 3. However, it was found in equivalent amounts on both the grain boundaries and on transgranular fracture surfaces. This fact suggests it was either a precipitate or a contaminant. We note also that silicon is not frequently observed to segregate in steels. Finally, we point out that one study was performed on Hastelloy C276. Again, phosphorus was the only element that segregated. Although there does not appear to be any segregation data available for Hastelloy C-22, the current material of choice for use in Yucca Mountain, one would predict that phosphorus would be the primary segregant, since the chromium content of this material should eliminate sulfur segregation to grain boundaries.

A major concern for the particular problem under discussion here is very low temperature segregation. No experiments have been done in which samples were aged even at the peak temperatures that would be present in the Yucca Mountain Repository. In order to estimate the amount of segregation we have used the McLean isotherm [12] to predict the amount of grain boundary segregation. This is given by the following equation

$$C_{gbt} - C_{gbo} = (C_{gb\infty} - C_{gbo})(1 - \exp(4Dt/\alpha^2\delta^2)\mathrm{erfc}(2\sqrt{Dt}/\alpha\delta))$$

where C_{gbt} is the concentration on the grain boundary after time t, C_{gbo} is the initial concentration, $C_{gb\infty}$ is the concentration on the grain boundary at infinite time, D is the diffusion coefficient, α is the ratio of the equilibrium grain boundary concentration to the bulk concentration, and δ is the grain boundary thickness. Table II gives values used for the calculations. Since this equation is for an isothermal situation one could attempt to solve it in a step-wise fashion for a temperature profile. However, all indications from our calculations suggest this would significantly overestimate the amount of segregation. Therefore, we have chosen to determine the total amount of segregation at 250^{o}C, 180^{o}C, 85^{o}C, and 27^{o}C. Since at all of these temperatures, equilibrium is not reached even in 10000 years, this information should give an upper bound to the amount of segregation that would be expected for the different peak temperatures in the thermal profile.

Figure 1 shows the segregation profile for phosphorus for temperatures of 250^{o}C (Figure 1a), 180^{o}C (Figure 1b) and 85^{o}C (Figure 1c) and 27^{o}C (Figure 1d). We note several important points. First, the amount of segregation achieved decreased with decreasing temperature. This result shows that we the amount of segregation is kinetically limited since the driving force for segregation increases with decreasing temperature. Second, even in 10000 years the amount of segregation is significant only at 250 and 180^{o}C. However, these temperatures are reached only in the first two years, and at that time, the amount of segregation is 0.88 at.% and 0.03 at.%. These are extremely low levels of segregation. Thus we would expect that segregation would be minimal at these low temperatures.

Segregation to Free Surface

In this section we consider segregation of impurity elements to free surfaces. It is important to note that all of the results considered in this section will refer to segregation in high vacuum. The effect of an oxide coating on the surface will be considered in the next section.

There are a number of important differences between grain boundary segregation and surface segregation. These might be surprising, given that the basic mechanism of segregation, that is diffusion through the matrix to the interface, is the same in both cases. However, these differences do exist and it is important to list these before continuing this discussion.

(1.) The basic method of performing the experiments is different for the two types of segregation. As mentioned above, grain boundary segregation experiments are usually performed by annealing the sample at a given temperature for a specified time. The sample is fractured open, and if the sample has fractured along the grain boundaries, the boundaries may be inspected by Auger electron spectroscopy. In the surface heating experiments, the surface of the sample is usually cleaned by argon ion sputtering and then heated in the high vacuum spectrometer.

(2.) The total number of sites on the surface are many fewer than the total number of sites on grain boundaries throughout the material. Thus elements with much lower concentrations in the bulk could saturate the surface whereas they might have very low concentrations on the grain boundary. This fact should be especially noted for sulfur. In this author's experience, even for materials that have low sulfur concentrations and that also contain alloying elements that should precipitate sulfur, one can still observe strong sulfur segregation to the free surface.

(3.) The binding energy for an element to the surface may be different from that at a grain boundary. Thus one element may prefer the surface over the grain boundary or vice versa. In general, surface coverages are much greater than grain boundary coverages.

(4.) In surface heating experiments one generally finds that the initial kinetics of segregation are extremely rapid. After a few heating cycles, as described above, the rate of segregation decreases. It is assumed that this initial segregation to the surface occurs by rapid diffusion paths such as dislocation cores and grain boundaries. After repeated heating these rapid pathways are either depleted or are annealed out of the sample. There has been no evidence that these pathways have much effect on grain boundary segregation.

(5.) Site competition is observed more readily on the surface. This could be because the more surface active element simply covers the other element already on the surface rather than displacing it into the bulk.

(6.) Through repeated heating cycles followed by sputtering, one changes the amount of segregant in the bulk. For example, with enough heating and sputtering, one can completely deplete the free sulfur that is available to segregate and no longer observe it at the surface.

Let us now consider the experimental data. There have recently been a number of experimental studies in which surface segregation was studied in nickel-base alloys. The reason for the interest in this segregation was that it was thought that sulfur could lead to oxide spallation if the oxide formed over this sulfur. Although most of these tests were performed at elevated temperatures, we will begin with this information and use it to guide us in our discussion of segregation at lower temperatures. We will also draw on studies of iron base alloys.

Briant and Luthra [13] examined segregation in alloys with base compositions of Ni-23Co-20Cr-12.5Al. Some alloys had additions of yttrium to help prevent oxide spallation. Of particular interest for this report is the segregation of impurity elements. Sulfur was the primary element that segregated. Figure 2 shows the segregation as a function of time. The temperature of segregation was 1100^{o}C. Figure 3 shows the kinetics of sulfur segregation in well-annealed samples at different temperatures. Note that as the temperature decreases the time required to reach equilibrium increases significantly. In some alloys Briant and Luthra also found small amounts of phosphorus segregation.

Although very small amounts of sulfur in the bulk can lead to complete coverage, the amount of time required for depletion of sulfur through repeated heating and sputtering cycles is reflected by the amount available in the bulk. Figure 4 shows the number of heating cycles at 1000^{o}C required to deplete an R'N5 alloy of sulfur [14]. A cycle was defined as the time required to reach the equilibrium amount of segregation. The alloy represented by the plot in Figure 4a had been desulfurized prior to testing. The alloy represented by the plot in Figure 4b had not been desulfurized. One can see that only three cycles were required to completely eliminate segregation in the desulfurized alloys but that 6-10 cycles were required for the alloy that had not been desulfurized.

There has been one study in the literature [15] of surface segregation in Hastelloy C-276. Because of the importance of Hastelloy materials for the Yucca Mountain Project we summarize the results here is some detail. The way in which the experiments were performed was as follows. The sample, which was cold-worked, was sputter cleaned in the Auger spectrometer. It was then heated and held at temperature for one hour. In some cases at the end of this time the temperature was increased by 100^{o}C and then the sample held at the new temperature for another hour. In other cases, the sample was cooled to room temperature, cleaned, and then reheated to a new temperature. In some cases, repeat heatings were done and in other cases they were not. In Table III we have listed the elements present on the surface of the sample, along with comments regarding the segregation. The Table is divided by heating cycle. The temperatures that composed a given cycle are listed. Between heating cycles the sample was cooled to room temperature and sputter cleaned.

Several points should be noted about these results. The first is that in the cold worked samples segregation is detected at temperatures as low as 100 and 200^{o}C. The second is that the most common elements observed were C, O, N, P, and S. The third point is that with repeated cycles, the segregation patterns changed slightly.

After this series of heating cycles, the sample was fully recrystallized at 900°C for 500 minutes. It was sputter cleaned and then heated from 500 to 900°C and cooled back to 500°C. It appeared to take approximately four hours for this entire cycle. Figure 5 shows the surface concentrations. One notes that at the end of the cycle, P and S were the primary segregants on the surface.

The main conclusions to be drawn from these results, and most other studies on both iron and nickel base alloys, is that sulfur is the primary segregant in that it will displace other elements from the surface if there is sufficient concentration in the matrix. Other elements such as O, N, P, Si, and C can also segregate; however, in most cases they can be displaced by sulfur. There have also been reports of co-segregation of elements to the surface; that is, the presence of one element appears to stabilize that of another. These include Cr-N, Cr-S and Ni-Si [16-18].

One of the most useful results of the above study is that the authors examined segregation at very low temperatures. In the cold worked sample they observed segregation of C, O, S, and N at temperatures below 500°C in one hour. Similarly, Briant[18] has examined surface segregation in both 304L and 316NG stainless steel. His samples were annealed in the Auger spectrometer prior to collecting segregation data. In the 316NG stainless steel he did not observe impurity segregation at 300°C. At 400°C he observed small amounts of N and C and at 500°C he observed C, N, P, and S. In contrast in the 304L material he detected S at 300°C and saw significant segregation of sulfur at 400°C within 100 hours.

In order to consider the problem in a commercial application, it seems reasonable to make the following assumptions. First, the material will not be depleted of segregants the way material is after repeated heating and cooling cycles in the Auger spectrometer. Second, most of the rapid diffusion paths will be active; that is, what takes place in service should be equivalent to the first heating cycle in an Auger spectrometer. Therefore, if we apply the same kinetic model used for grain boundaries to the problem of surface segregation, we should obtain a very conservative answer, since it will employ diffusion coefficients for well-annealed bulk material. If we perform the calculation for sulfur, we find it will reach equilibrium in approximately 100 years if the peak temperature is 250°C. The only deterrent to segregation would be that site competition with other elements would slow down the sulfur segregation.

Thus it would seem likely that if segregation to a clean surface is the correct model, then the surfaces would rapidly become coated with impurities. However, as shown in the next section one must consider the fact that the surface is covered with an oxide. As will be shown there, it appears that the metal-oxide bond may inhibit most segregation and that the results reported in this section are actually relevant for the case of internal voids.

Segregation to the Oxide-Metal Interface

Segregation of impurities to the oxide-metal interface has been an area of great interest in recent years because of the problem of spallation of thermally grown oxides from the metal substrate upon cooling. It has been known for many years that additions of either yttrium or

hafnium to nickel-base alloys can be used to avoid this spallation problem and thus these elements have been added to the materials used in the turbine blades of aircraft engines to prevent this problem from occurring. What had not been worked out was why these elements had this beneficial effect. In the 1980s a new theory was proposed that has provoked much discussion [17,19]. The proposal posited that if sulfur was free in the metallic solid solution, it could segregate to the oxide-metal interface and cause embrittlement of that interface, just as it would do at grain boundaries. The role of the reactive elements, namely yttrium and hafnium, was to getter the sulfur as sulfides and eliminate the segregation.

The results of the investigations designed to test this theory have been very interesting. First there appears to be little doubt that extensive desulfurization causes an improvement in the adhesion of the oxide film [14, 19, 20]. However, what is missing is real proof that the importance of the reactive elements is to getter the sulfur. It is very difficult to perform Auger studies in which the oxide film will spall off the metal and expose the alloy underneath. The limited results suggest that although the rare earths may limit sulfur segregation to some extent, they probably have other beneficial effects as well [20].

The explanation that appears to be most consistent with the observations on oxide growth and spallation as well as with our knowledge of surface segregation and grain boundary segregation is that proposed by Grabke *et al* [16]. They examined an Fe-Cr alloy doped with sulfur. First, they noted that if they heated the alloy in high vacuum to 900^{o}C there was rapid sulfur segregation and that a monolayer was formed in a matter of minutes. They then performed the following experiment. They heated the sample to 500^{o}C in 10^{-5} mbar of oxygen to provide an oxide layer. They then heated the sample to 800^{o}C for 10 minutes. Practically no sulfur was observed and none was detected in sputter profiles through the thin oxide. They then oxidized the sample at 1000^{o}C in 10^{-2} mbar of oxygen. This produced a thick oxide that spalled off when the sample was cooled. Sulfur was found on the surface where the spallation had occurred. However, they also detected cavities on the spalled surface. They thus proposed that sulfur would segregate to the surface of the cavity once it had formed but not to the metal-oxide interface. The role of the reactive elements is to inhibit cavity formation. If sulfur does segregate to the surface of the cavity, it will lower the surface energy of the cavity and thus enhance its growth. This model is consistent with the proposal that sulfur segregates to creep voids [21] and that it also can segregate to a free surface and from that onto grain boundaries at a crack tip [22]. The important point to note is that in all of these cases, sulfur is not segregating to an oxide-metal interface but rather to a surface of an internal void that is equivalent to the free surface.

Therefore, for the problem under consideration in this report - low temperature segregation effects in a nickel base alloy - it would appear that unless voids form at the metal-oxide interface, it is actually unlikely that segregation will occur there. It has been pointed out that this interface between a metal and a ceramic is somewhat different from that of a grain boundary for two reasons [16]. First, because of the ionic nature of the atoms at the interface, it is unlikely that sulfur, an electronegative impurity, would segregate there. Second, if the oxide forms directly on top of the metal and bonds to it, it is not clear that there would be room for a segregated atom, or that the space available to it would be that different from that in the bulk. Thus, if we assume that an oxide forms immediately on the metal at room temperature, then it

seems unlikely that there would be significant segregation to the free surface or the metal oxide interface at the temperatures under consideration here.

Summary

In summary, one can show that some segregation is kinetically possible at the very long times considered in this project. However, almost all segregation will take place during the thermal transient at the beginning of storage. The peak temperature and the rate of cooling will be important parameters in determining how much segregation will result.

For grain boundary segregation, it would appear that the primary impurity that would segregate would be phosphorus. Sulfur will be gettered in the matrix and there is little evidence that silicon is a strong segregant.

Surface segregation could also occur if no metal oxide were present. In that case sulfur and phosphorus would be likely segregants. Since it is assumed that an oxide will be present at all temperatures, it seems unlikely based on all experimental evidence that segregation would occur. However, if internal voids were to form in some way, these elements could segregate to the surface of voids.

References

1. H.J. Grabke, in Impurities in Engineering Materials, ed. C.L. Briant, Marcel-Dekker, New York, 1999, p. 143.

2. R.A. Mulford, in Embrittlement of Engineering Alloys, ed. C.L. Briant and S.K. Banerji, Academic Press, New York, 1983, p. 1.

3. M. Guttmann, Ph. Dumoulin, N. Tan-Tai, and P. Fontaine, Corrosion, **37**, 416 (1981).

4. G.S. Was, H.H. Tischner, and R.M. Latanision, Metall. Trans. A, **12A**, 1397 (1981).

5. N. Pessall, G.P. Airey, and B.P. Lingenfelter, Corrosion, **35**, 100 (1979).

6. G.P. Airey, Corrosion, **35**, 129 (1979).

7. E.L. Hall and C.L. Briant, Metall. Trans. A, **16A**, 1225 (1985).

8. B.J. Berkowitz and R.D. Kane, Corrosion, **36**, 24 (1980).

9. C.L. Briant, Metall. Trans. A, **19A**, 137 (1988).

10. C.L. Briant and E.L. Hall, Corrosion, **43**, 539 (1987).

11. G. Was, Corrosion, 46, 319 (1990)

12. D. McLean, Grain Boundaries in Metals, Oxford Press, Clarendon, 1957, p.116

13. C.L. Briant and K.L.Luthra, Metall. Trans.A, **19A**, 2099 (1988).

14. C.L. Briant, W. Murphy, and J.C. Schaeffer, Scripta Metall., **32**, 1447 (1995).

15. J.J. Burton, B.J. Berkowitz, and R.D. Kane, Metall. Trans. A, **10A**, 677 (1979).

16. H.J. Grabke, D. Wiemer, and H. Viefhaus, Appl. Surf. Sci., **47**, 243 (1991).

17. C.L. Briant and R.A. Mulford, Metall. Trans.A, **13A**, 745 (1982).

18. C.L. Briant, Surf. and Int. Analysis, **13**, 209 (1988).

19. J.L. Smialek, Surf. and Interf. Analysis, **31**, 582 (2001).

20. P.Y. Hou, Oxidation in Metals, **52**, 337 (1999).

21. C.J. McMahon, Jr., Scripta Metall. **19**, 733 (1985).

22. D. Bika, J.A. Pfaendtner, M. Menyhard, and C.J. McMahon, Jr., Acta Metall. et Mater., **43**, 1895 (1995).

TABLE I
Grain Boundary Segregation in Nickel-Base Alloys

Alloy	Composition	Heat Treatment	Segregant	Elements Not Segregated	Ref.
Alloy 600	Ni-16Cr-6.59Fe-0.044C-0.40Si-0.25Mn-0.007S-0.007P-0.024Co	1150°C/1h	P	S,Si	3
		1150°C/1h + 600°C/100h	P	S,Si	3
		1150°C/1h + 500°C/1097h	P	S,Si	3
Alloy 600	Ni-15.2Cr-9.19 Fe-0.4Cu-0.21Si-0.032C-0.007P-0.004B	1100°C/0.5h + 700°C/100h	P, B, C	S	4
Alloy 600	Ni-15.36Cr-9.98Fe-0.04C-0.4Mn-0.17Si-0.38Cu-0.007S-0.01P-0.005B	Mill Anneal + 705°C/24 h	P, B	Si, S	5
		Mill Anneal + 649°C/100 h	P, B	Si,S	6
Alloy 600	Ni-16.32Cr-8.68Fe-0.24Mn-0.05C-0.007S-0.009P-0.0022B-0.015N	Mill Anneal + 650°C/100 h	P,N	S,Si,B	7
		Mill Anneal + 400°C/1000h	P,N	S, Si, B	7
Hastelloy C-276	Not Given	Commercial heat treatment + 482°C/100h	P		8
Alloy 182	Ni-14.3Cr-8.1Fe-0.63Si-7.19Mn-0.039C-0.42Ti-1.7Nb-0.045Ni-0.001S-0.015P	1200°C/3h + 600°C/1000h	P	S,Si	9
		As-Welded +620°C/24 h	P, N		9
Alloy 82	Ni-19.03Cr-0.81Fe-0.1Si-2.81Mn-0.011C-0.49Ti-2.55Nb-0.008N-0.001S-0.004P	As-Welded + 620°C/24h	P,S, B, N		10
Alloy X-750		Heat treatment not given; reference is a review paper	P		11

TABLE II
Values of Parameters Used in Segregation Calculations

Parameter	Value
C_{gbo}	0
$C_{gb\infty}$	40 at.%
α	1000
δ	1×10^{-9} m
Do	1.4×10^{-5} m^2/s
Q	45,380 cal/mole

TABLE III
Results on Surface Heating of Hastelloy C276
Data Taken from Reference 15

Cycle	Temperature	Elements Observed	Comments
First Heating Cycle	100	C, O	
	200	C, O, S	
	300	C, O, S, N	
Second Heating Cycle	100	C	Very slight segregation
	200	C, O	
	300	C, O, S	
Third Heating Cycle	400	P, C, O, S	
Fourth Heating Cycle	400	P, C, S	
	500	P,C, S, O, N	P, C, S significantly increased over 400^{o}C
Fifth Heating Cycle	500	P, C, S, N, O	
Sixth Heating Cycle	600	C, N, P, S, Si	Si segregated rapidly and then disappeared.
Seventh Heating Cycle	600	C, P, Si, N	S not observed; Si again was transient
Eight Heating Cycle	700	P, S, N	N quickly disappeared
Ninth Heating Cycle	700	P, S, N	
Tenth Heating Cycle	800	P, S	P disappeared
Eleventh Heating Cycle	900	P, S	P disappeared

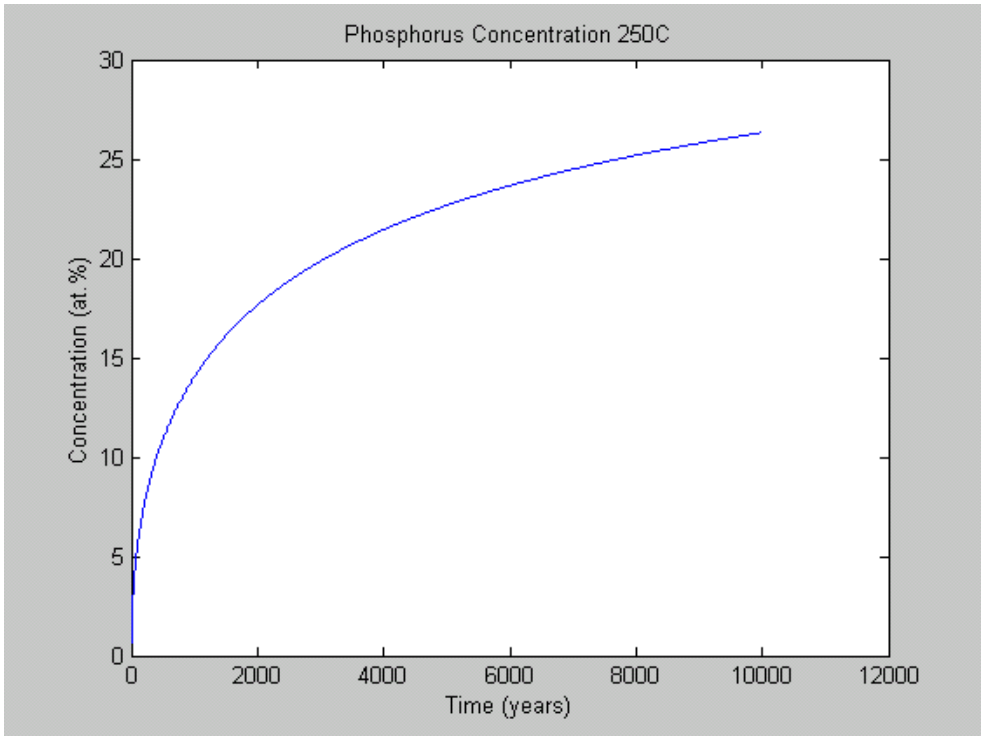

(a.)

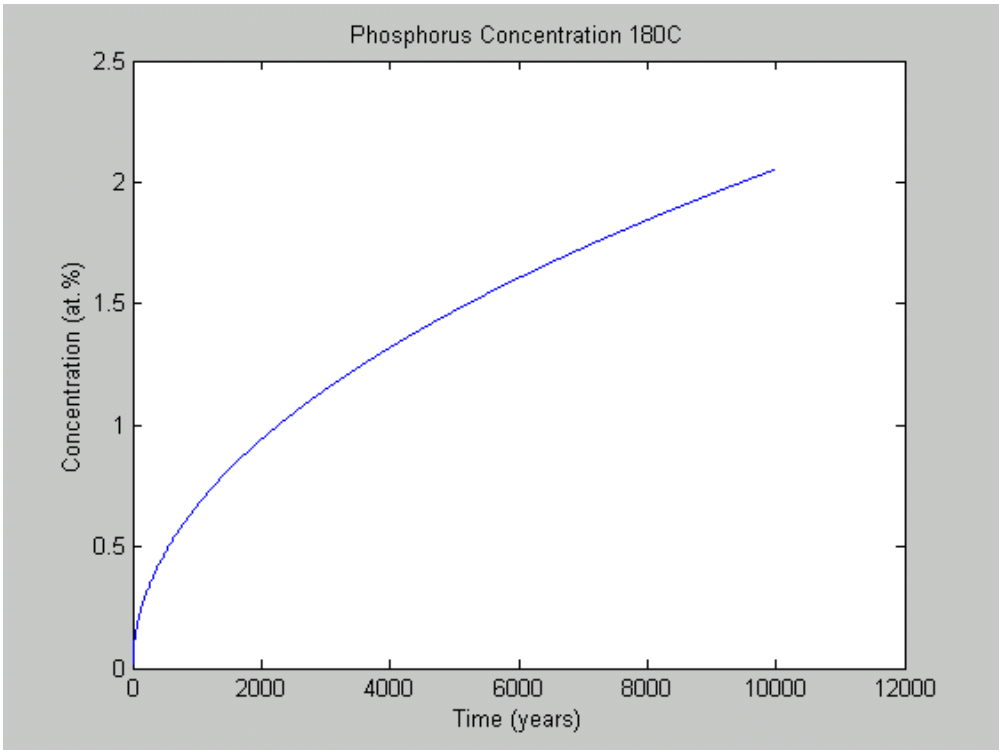

(b.)

Figure 1a - b – Calculated values of phosphorus segregation plotted as a function of time. (a.) Aging at 250°C for 10000 years. (b.) Aging at 180°C for 10000 years.

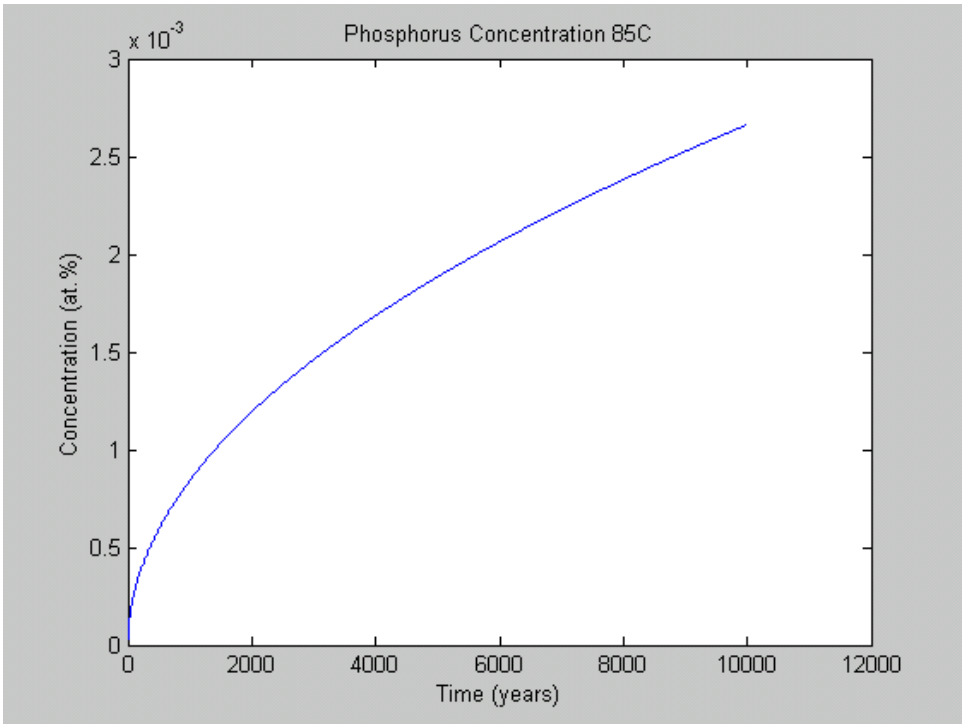

(c.)

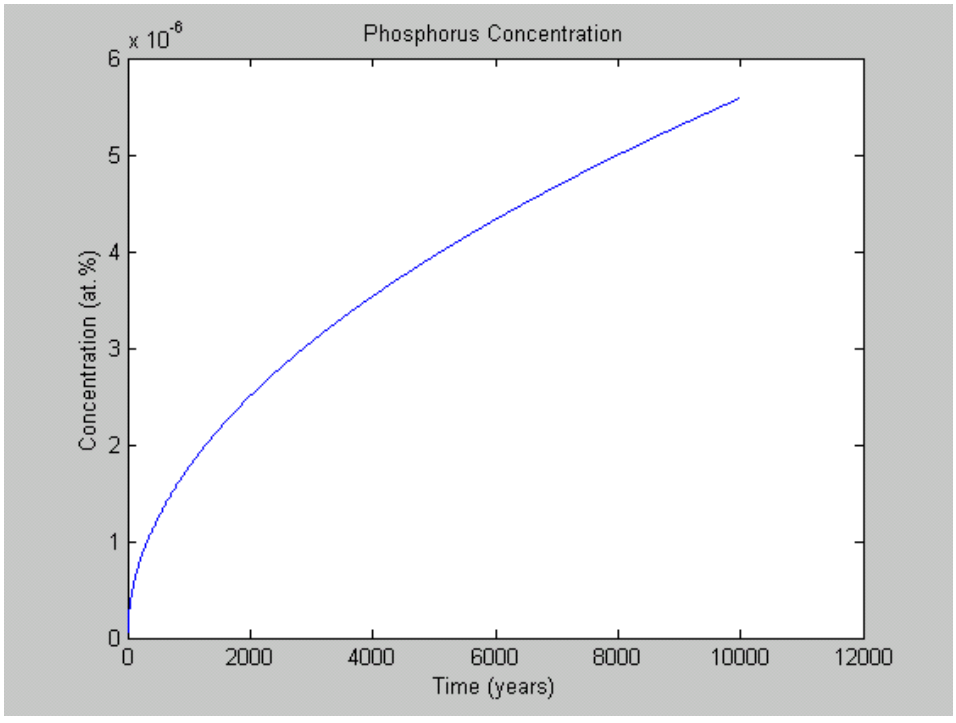

(d.)

Figure 1c - d – Calculated values of phosphorus segregation plotted as a function of time. (c.) Aging at 85°C for 10000 years. (d.) Aging at room temperature for 10000 years.

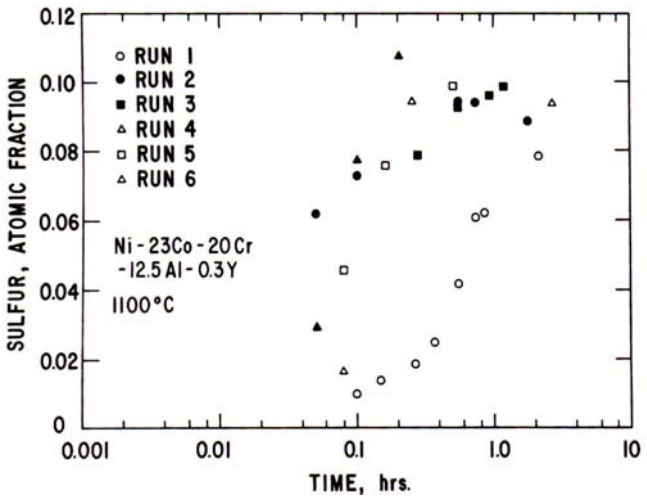

Figure 2 – Surface segregation of S at 1100°C in an Ni-Cr-Co-Al alloy. Data taken from reference 13

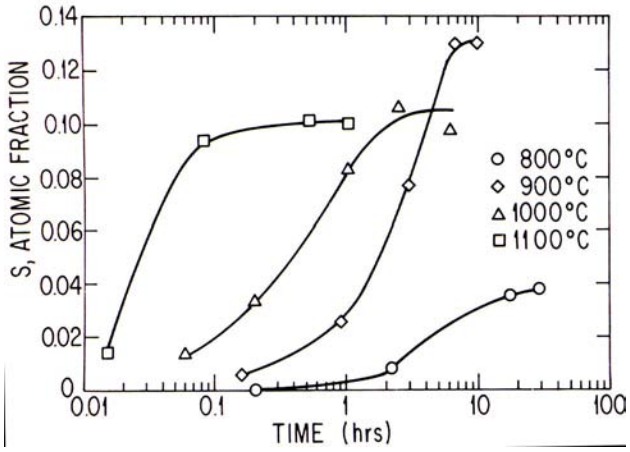

Figure 3 – Segregation of S plotted as a function of time. Data obtained at four different temperatures. Results taken from reference 13.

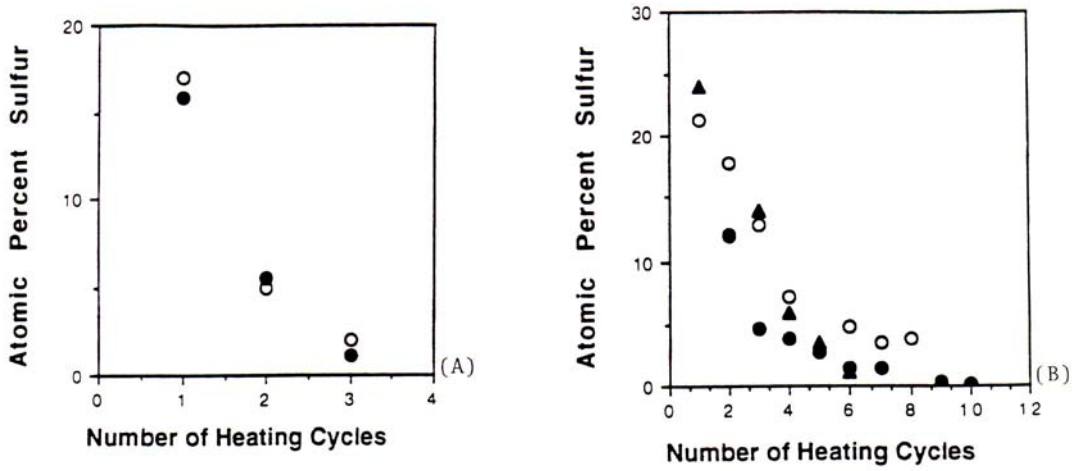

Figure 4 – Number of heating cycles to deplete material of sulfur. (a.) Material desulfurized prior to experiment. (b.) Material not desulfurized prior to experiment. Data taken from reference 14.

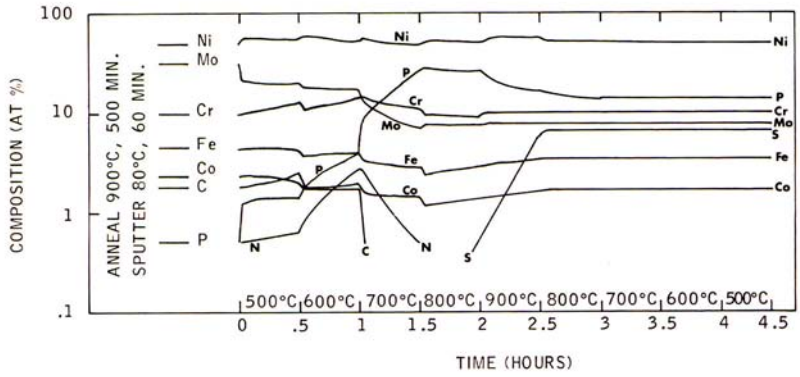

Figure 5 – Surface segregation in Hastelloy C-276. The sample was heated from 500 to 900°C and then recooled. Note the segregation of S and P. Data taken from reference 15.

21. Comments on Metallurgy and Fabrication of Alloy 22 Waste Packages

Stephen Floreen
Schenectady, New York, USA

EDITORIAL NOTE

This volume, "A Compilation of Special Topic Reports," contains a series of reports that were prepared for the Waste Package Materials Performance Peer Review Panel to use as background and input to the peer review. Summaries drawn from the reports were also presented in Section 11 of the Panel's Final Report. The Panel used the reports as background and input for its review. Any views and comments expressed in the summaries and the full reports do not necessarily reflect the opinion and findings of the Panel. Further, opinions expressed in the reports are not necessarily those of the Panel or reflected in the Panel's reports and recommendations.

The Cost of Staying Dry

The present strategy for minimizing corrosion damage by keeping the surface dry calls for temperatures on the order of 300∀C for long time periods. This may seem to be a good idea, but at least three detrimental phenomena can occur during prolonged exposures at such temperatures.

l. Creep

Creep will definitely occur in nickel base alloys at 300∀C. In fact, Gary Was and others have considered creep as the rate controlling process for the stress corrosion of Alloy 600 etc. in PWR environments. There is very little creep data available, and all of it appears to be confined to test times on the order of a few weeks. In view of the growing amount of nuclear waste, a program to measure creep rates over long times would be in order.

For present purposes, a ballpark estimate can be made using calculations for pure nickel. The attached Figure (upper left) shows the predictions made by Ashby et al for creep rates at different temperatures and stresses. At 300∀C and a very low stress of one MPa, the resultant creep strain after 100 years would be about 10 percent, and essentially complete stress relaxation is likely. Creep strains of this order will accelerate corrosion damage and may cause local tearing. Stress relaxation will wipe out the beneficial compressive stresses introduced by the post-weld laser treatment, and thus, make the weldments much more susceptible to stress corrosion.

Alloy 22 would have much greater creep strength, but the stresses would be much higher, especially if rock falls, earthquakes, etc. are considered. Thus, 10 percent creep is probably a

Special Topic Report prepared for the Waste Package Materials Performance Peer Review. The Final Report of the Peer Review was submitted to U.S. Department of Energy and Bechtel SAIC Company, LLC on February 28, 2002.

reasonable figure. In detail, the creep would not be uniform. An analysis of the nominal stress and temperature distribution in a container laying on its side would be needed to examine this question, and may be a good analysis to do.

It should also be noted that the materials within the container would creep. I will not attempt an analysis of this problem, except to say that the contents would sink to the bottom, and therefore, the heat sources would become concentrated at the bottom. Hence, local hot spots would develop that would accelerate creep.

Localized creep by itself could lead to ruptures. Even without fracture, the corrosion rates would increase as protective films were ruptured.

Creep could be minimized by design changes to lower the stress. At the least the supports the containers rest on need to be more carefully considered. Internal braces may be needed to lower the stress and to keep the package internals from sinking. However, the best thing to do is to lower the temperature.

2. Stress Relaxation

Stress relaxation refers to the decay in applied or residual stresses during elevated temperature exposure through a combination of small-scale creep and annealing processes. The classic case is a bolt holding two pieces together. With thermal exposures the bolt force will drop and eventually fully relax.

The relevance to the present problem is the post-weld laser treatment for creating residual compressive stresses in the welds. These stresses will be relieved by stress relaxation.

The attached figures (top right and bottom center) show examples of stress relaxation in iron base alloys. The test details are different so a direct comparison between the two is not instructive. The point to be made is that stress relaxation can occur at 300∀C. Tests of nickel base alloys by KAPL and Bettis show high-strength nickel alloys also relax at such temperatures. To my knowledge, this work has not been published. A literature search for relevant stress relaxation data is recommended along with an analysis of the effects of stress relaxation.

Even without more direct data, the creep rate data indicates that complete stress relaxation of the laser treated welds will have taken place after 100 years at 300∀C. Thus, the desire to stay dry destroys the method to protect the welds.

There does not appear to be any way to design around this problem. If you want to make use of residual stresses the temperature has to be lowered.

3. Precipitation Reactions

The Project staff has taken the approach that precipitation only becomes detrimental when 100 percent of the grain boundaries are covered. This is too optimistic. Detrimental effects from

secondary phases can result with very small amounts and with only a small fraction of the boundaries containing precipitates. If precipitates cause trouble, a little bit can go a long way. The author suggests that if precipitates are damaging, the effect may be observed an order of magnitude in time before 100 percent grain boundary coverage.

Detrimental effects of precipitation are likely to be most prevalent in the weld metal. Depending upon the welding details detrimental phases may be present from the start. Precipitation will occur faster than in base material, because of segregation in the cast structures of the weld. The laser treatment would help for a while but not for long enough. The rate of precipitation will increase with temperature of course, which is a penalty for higher temperature operation.

Summary

The desire to keep things dry produces a number of detrimental side effects. Thus, some consideration should be given to determine if there is some optimum temperature range that balances these competing factors. For the phenomena discussed above, a useful rule of thumb is that a 100 degree change in temperature produces a 10 fold change in rate. Is there some kind of rough yardstick of this kind that could be applied to the wetting problem? If there is, then some better focus could be directed to resolving this question.

22. Effects of Stress Relaxation on Stress Mitigation

Russell H. Jones
Battelle-Northwest
Richland, Washington, USA

EDITORIAL NOTE

This volume, "A Compilation of Special Topic Reports," contains a series of reports that were prepared for the Waste Package Materials Performance Peer Review Panel to use as background and input to the peer review. Summaries drawn from the reports were also presented in Section 11 of the Panel's Final Report. The Panel used the reports as background and input for its review. Any views and comments expressed in the summaries and the full reports do not necessarily reflect the opinion and findings of the Panel. Further, opinions expressed in the reports are not necessarily those of the Panel or reflected in the Panel's reports and recommendations.

The Project's primary plan to mitigate stress corrosion cracking involves the introduction of compressive stresses at closure welds where stress corrosion crack initiation and growth is most likely to occur. The outer closure weld will be induction heated and quenched while the inner closure weld will be laser peened. It has been demonstrated that compressive stresses are produced by both processes. Induction heating and quenching of a waste package mockup produced a change in the outer surface residual stress from a + 186 MPa to –497 MPa following quenching. The depth of the compressive layer was 7 mm. Laser peening produced a compressive stress of –90 MPa at the surface with the compressive layer extending to a depth of about 2 mm. Stress corrosion cracks will not propagate under compressive stresses; therefore, stress corrosion cracking is not an issue as long as residual compressive stresses exist. However, it is known that stress relaxation can occur in metals at relatively low temperatures by low temperature creep processes. The extent of relaxation is limited but the amount of strain needed to relax 500 MPa in alloy 22 is only 2.5×10^{-3} . Therefore, very little low temperature creep strain is needed to eliminate this mitigation method.

Relevant stress relaxation data on alloy 22 does not exist but some suggestion of the extent of relaxation that might occur is possible by looking at studies of other metals and alloys. For instance, using the Ashby map given by Floreen (1), high-purity nickel has a creep rate of 10^{-13} s^{-1} at 150 C and a stress/modulus ratio of 10^{-5}. This creep rate, assuming everything remains constant, will result in a creep strain of 2.5×10^{-3} in about 1,000 yrs. The starting stress/modulus ratio for the induction heated and quenched compressive layer is about 10^{-3} so the value of 10^{-5} is representative of the condition after considerable relaxation to a residual stress of 5 MPa. Other studies have shown low-temperature relaxation in alpha Fe (2), mild steel and copper (3) and cold drawn steel (4). Sanchez-Galvez and Elices (4) showed that a cold drawn steel with an ultimate tensile strength of 1500 MPa had a stress loss of 100 MPa (a strain of about 0.5×10^{-3})

Special Topic Report prepared for the Waste Package Materials Performance Peer Review. The Final Report of the Peer Review was submitted to U.S. Department of Energy and Bechtel SAIC Company, LLC on February 28, 2002.

in 10^5 hrs (about 4 yrs) at 20 C. Low-temperature creep/stress relaxation rates decrease with time so a linear extrapolation of these results is not correct but even with a decreasing relaxation rate it is very likely that a creep strain of 2.5×10^{-3} could occur in the lifetime of the repository in a cold drawn steel. A key question is whether it could occur in Alloy 22 during this time period.

The laser peening and induction heating and quenching process will produce residual stress gradients with the maximum near the surface decreasing to zero and then tensile stresses with increasing depth. Khadhraoui et al. (5) studied the stress relaxation of shot peened Inconel 718. This is a nickel base alloy as is alloy 22 and the shot peening produced a residual stress gradient similar to that obtained with induction heating and quenching and laser peening. Khadhraoui et al (5) found that a compressive residual stress of –800 MPa relaxed to –400 MPa in 100 hr at 600∀C . They also developed a model that could be useful in extrapolating their high temperature results to repository relevant conditions. This model closely matched their experimental results obtained at 600 and 650∀C and is expressed by equation 1:

$$dE_R\,(T,t)/dt = A\,(1 - \nu\,(T))(\,d\psi\,(T,t)/dt)\,\zeta_o \quad (1)$$

where E_R (T,t) is the macroscopic tensorial recovery strain, A is a proportional coefficient, T is temperature, t is time, (1 - ν (T)) is a measure of the remaining crystal defects at a given temperature T, ζ_o is a function of the strain associated with mobile dislocations in shot peened material, and $d\psi(T,t)/dt$ is given by equation 2 below:

$$d\psi\,(T,t)/dt = C \exp\,(-\div Q_o/kT)\,t^n \quad (2)$$

where $\div Q_o$ is the mean activation energy for migration of defects (i.e. dislocations), and C is a constant. While there are a number of parameters in this model, it should be possible to calibrate it for induction heated and quenched and laser peened material and therefore to predict the stress relaxation as a function of time.

As part of a study to measure the irradiation creep of Inconel 718 at 300∀C, Scholz and Matera (6) measured the thermal creep rate prior to irradiation. They found transient creep, that approached a creep rate of zero with time, produced a creep strain of 3×10^{-2} in 10^5 s (30 hrs) at a stress/modulus ratio of 10^{-3}. While 300∀C is about 100∀C higher than the expected repository temperature, the stress ratio is similar to that expected for the induction heated and quenched surface. A creep strain 10 times greater than needed to relax the –500 MPa from the induction heated and quenched surface was measured in only 30 hrs at 300∀C.

Clearly, the importance of the stress mitigation process to alleviating stress corrosion cracking and the fact that low temperature stress relaxation occurs in metals suggests that stress relaxation measurements be made of the compressive residual stresses in Alloy 22 following both induction heating and quenching and laser peening.

References

1. S. Floreen, "Composition Effects within the Chemical Specification for Alloy 22," Waste Package Materials Performance Peer Review, A Compilation of Special Reports, May 2002
2. P. Feltham, "Stress relaxation in Alpha-Iron at low temperatures", Phil. Mag, **Vol. 6**, (67), (1961) p. 847.
3. H.D. Chandler, "Transient creep in mild steel and copper at room temperature", Acta Metall. **Vol. 33**, No. 5 (1985) p. 835.
4. V. Sanches-Galvez and M. Elices, "The relationship between tensile strain, creep and stress relaxation in cold-drawn steels at low temperatures", Matl. Sci and Engr, **78** (1986) p. 1.
5. M. Khadhraoui, W. Cao, L. Castex and J.Y. Guedou, "Experimental investigations and modelling of relaxation behaviour of shot peening residual stresses at high temperature for nickel base superalloys", Materials Sci and Tech., **Vol 13**, (1997) p. 360.
6. R. Scholz and R. Matera, " Proton irradiation creep of Inconel 718 at 300∀C", J. of Nuclear Mater., **Vol 283-287** (2000) p. 414.

23. Corrosion of Nickel Base Alloys in Flue Gas Desulfurization Systems

John A. Beavers
CC Technologies Laboratories, Inc
Dublin, Ohio, USA

EDITORIAL NOTE

This volume, "A Compilation of Special Topic Reports," contains a series of reports that were prepared for the Waste Package Materials Performance Peer Review Panel to use as background and input to the peer review. Summaries drawn from the reports were also presented in Section 11 of the Panel's Final Report. The Panel used the reports as background and input for its review. Any views and comments expressed in the summaries and the full reports do not necessarily reflect the opinion and findings of the Panel. Further, opinions expressed in the reports are not necessarily those of the Panel or reflected in the Panel's reports and recommendations.

Emissions of sulfur dioxide SO_2 are a major shortcoming of the use of coal for electric power generation. These emissions are minimized by the use of low sulfur coal, the removal of sulfur prior to combustion, or scrubbing of the flue gas generated by the combustion of high-sulfur coal, referred to as flue gas desulfurization (FGD). Limestone and lime scrubbing are the most common methods for FGD. Counter current spraying with aqueous slurry of lime or limestone removes the SO_2 present in the flue gas. The slurry becomes very corrosive as a result of the absorption of the acid gases in the flue gas, including SO_2, HF, and HCl. The environment is a strongly acidic, oxidizing and comprised of a mixture of ionic species with chlorides.

Koch et al (1982) summarized the performance of construction materials for FGD systems. The most corrosive conditions were found in the pre-scrubbers, the ducts upstream of the re-heaters, and in the re-heaters. It was found that pitting and crevice corrosion of stainless steels and, to a lesser degree, nickel base alloys commonly occurred in these components. Stress corrosion cracking failures of stainless steels were found in the pre-scrubbers and in the re-heaters for these systems where higher temperatures and more acidic conditions were encountered. In most cases, the localized corrosion and SCC problems with metallic materials could be prevented by the application of higher alloyed materials.

Pre-scrubbers are defined as vessels through which the hot flue gas passes and is wetted without significant SO_2 removal. A very acidic environment is created in the pre-scrubber due to the presence of chlorides and SO_2 in the flue gas; pH values less than 2 have been measured. Moreover, a significant amount of chlorides can build up, ranging from a few thousand ppm in open loop systems to up to 100,000 ppm in closed loop systems. In addition to this corrosive

Special Topic Report prepared for the Waste Package Materials Performance Peer Review. The Final Report of the Peer Review was submitted to U.S. Department of Energy and Bechtel SAIC Company, LLC on February 28, 2002.

environment, abrasive conditions exist due to the high velocity gases and the presence of particulates. Extensive pitting has been observed on stainless steels, and even Inconel® Alloy 625 has suffered pitting attack. The most resistant alloys in pre-scrubber environments have been Hastelloy® C276 and Hastelloy® G, AL® 6X, and titanium. However even these corrosion resistant alloys have experienced localized attack in some severe applications. Hastelloy C276 experienced pitting rates of 25 um/y in one smelter gas scrubber (Tice 1974) and 10 um/y in a scrubber for a chemical waste incinerator (Kirchner 1975). In one application, high corrosion rates of titanium were observed, an effect that could be attributed to the low pH conditions in conjunction with the presence of fluorides and chlorides from the flue gas (Koch 1982).

Very corrosive conditions exist in the outlet ducts upstream of flue gas re-heaters due to the presence of high concentrations of chlorides and, to a lesser extent, fluorides and limited buffering from the lime or limestone slurry. The environment may have pHs less than 2. In the more aggressive environments, only titanium and nickel base alloys such as Hastelloy C-4, Hastelloy C-276, Inconel 625, and Hastelloy G have performed well. In one study of alloy performance in a corrosive outlet duct (Koch 1986), Hastelloy C276 and Hastelloy C22 performed the best of all of the nickel base alloys and stainless steels evaluated. Both exhibited low general rates of corrosion, were resistant to pitting, but exhibited some shallow crevice corrosion following 18 months of exposure. The location of corrosion was in a mixing zone of the duct where saturated flue gas from the scrubber at 55°C mixed with hot (150°C) flue gas from a bypass duct. The measured pH of the condensate at the location was 1.3 to 1.8 and the condensate contained 4800 ppm Cl, 2590 ppm F, and about 60,000 ppm SO_4.

Re-heaters are used to provide additional heat to the wet flue gas to raise the temperature above the dew point. This minimizes the formation of condensate in the downstream equipment, thereby allowing the use of less corrosion resistant materials down stream from the re-heater. The conditions inside the re-heater are typically more severe than in the outlet duct because of the increased temperature, for temperatures below the acid dew point of the gas. Localized corrosion and stress corrosion cracking of stainless steels has occurred in this application while nickel base alloys such as Hastelloy C-276, Hastelloy G and Inconel Alloy 625 have provided satisfactory performance. Never the less, some pitting attack of these alloys (about 25 um/y in the case of Hastelloy C-276) has been observed in reheater applications.

Thompson and Syrett (1992) used a statistical experimental design and electrochemical tests to investigate the localized corrosion behavior of several alloys in the complex environments comprised of a range of multiple ionic species and pH. The approach was highly successful and the single and mixed-ion contributions to corrosion were determined. The range of corrosion-resistant service for each of the alloys was determined. Hastelloy Alloy G-3 and Type 317L Stainless Steel were tested in simulated FGD solutions using a standard cyclic potentiodynamic polarization (CPP) procedure (ASTM G-61), a potentiostatic polarization procedure, and a modified version of the ASTM F-764 procedure. In the latter, specimens were potentiostated above the pitting potential for various times to produce pitting. The potentials of the specimens were then shifted to more negative values and the current versus time transients were measured for up to 16 hours. The process was repeated over a range of pitting times and final potentials until a potential was established above which pitting would continue and below

which complete passivation would occur for each pitting time. The data from the three types of tests were plotted on potential versus time curves. For the constant potential-time tests, each E_{pit} data point corresponded to the time to pit initiation at the test data potential and a data point with an arrow indicated that no pit initiation occurred in the time period measured. Time to pit initiation also was extracted from the CPP tests as the time to scan from the protection potential (established on the subsequent reverse scan), to the potential at which pits initiated. The protection potential values were also plotted on the same graphs and were obtained from either the CPP tests or from the modified ASTM F-746 tests. Each E_{prot} data point corresponded to the time pits were propagating, i.e, the time from pit initiation until pit repassivation.

Figure 1 shows data for Type 317L stainless steel in one of the simulated scrubber solutions. This figure shows that the E_{pit} and E_{prot} data are asymptotic to a potential defined as E_u, a unique pitting potential. The figure shows that the time to pit initiation decreased with increasing potential above this value while the potential required to passivate actively growing pits became more negative as the time the pit was allowed to propagate was increased. In a stochastic model for pit initiation, E_u is equivalent to the most active potential at which the pit nucleation frequency exceeds zero (Williams 1985).

In summary, field experience and laboratory testing of stainless steels and nickel base alloys for FGD applications demonstrate that Alloy 22 and other nickel base alloys of similar composition, such as Alloy C-276 and Alloy C-4, are highly resistant to localized corrosion in aggressive environments having pHs less than 2 and high chloride concentrations. While providing good overall performance, these alloys are not immune to corrosion attack and have experienced incipient pitting and crevice corrosion at rates of about 25 μm/y. This rate, if sustained, would be unacceptably high for the waste package, corresponding to 250 mm in 10,000 years. The results of a statistical designed experiment and electrochemical studies by Thompson (1992) demonstrate that protection potentials derived from CPP curves are conservative estimates of the actual potential for pit initiation.

References

1. R. W. Kirchner, "Corrosion of Pollution Control Equipment," Chemical Engineering Progress, **Vol. 71**, No. 3, 1975, p. 58.

2. G. H. Koch, J. A. Beavers, and N. G. Thompson, "Literature Review of FGD Construction Materials", Electric Power Research Institute, Palo Alto, CA, EPRI Report CS-2533, August 1982.

3. G. H. Koch and N. G. Thompson, "Localized Attack of Nickel-Containing Alloys in SO_2 Scrubber Environments," Journal of Materials for Energy Systems, American Society for Metals, **Vol. 8**, No. 2, September 1986, p197.

4. N. G. Thompson and B. C. Syrett, "Relationship Between Conventional Pitting and Protection Potentials and a New, Unique Pitting Potential," Corrosion, **Vol. 48**, No. 8, 1992, p. 649.

5. E. A. Tice, "Corrosion Tests in flue Gas Desulfurization Processes," Materials Performance, **Vol. 13**, No. 4, 1974, p. 26.

6. D. E. Williams, C. Westcott, and M. Fleischmann, J. Electrochem. Soc, **Vol. 132**, No. 8, 1985, p. 1804.

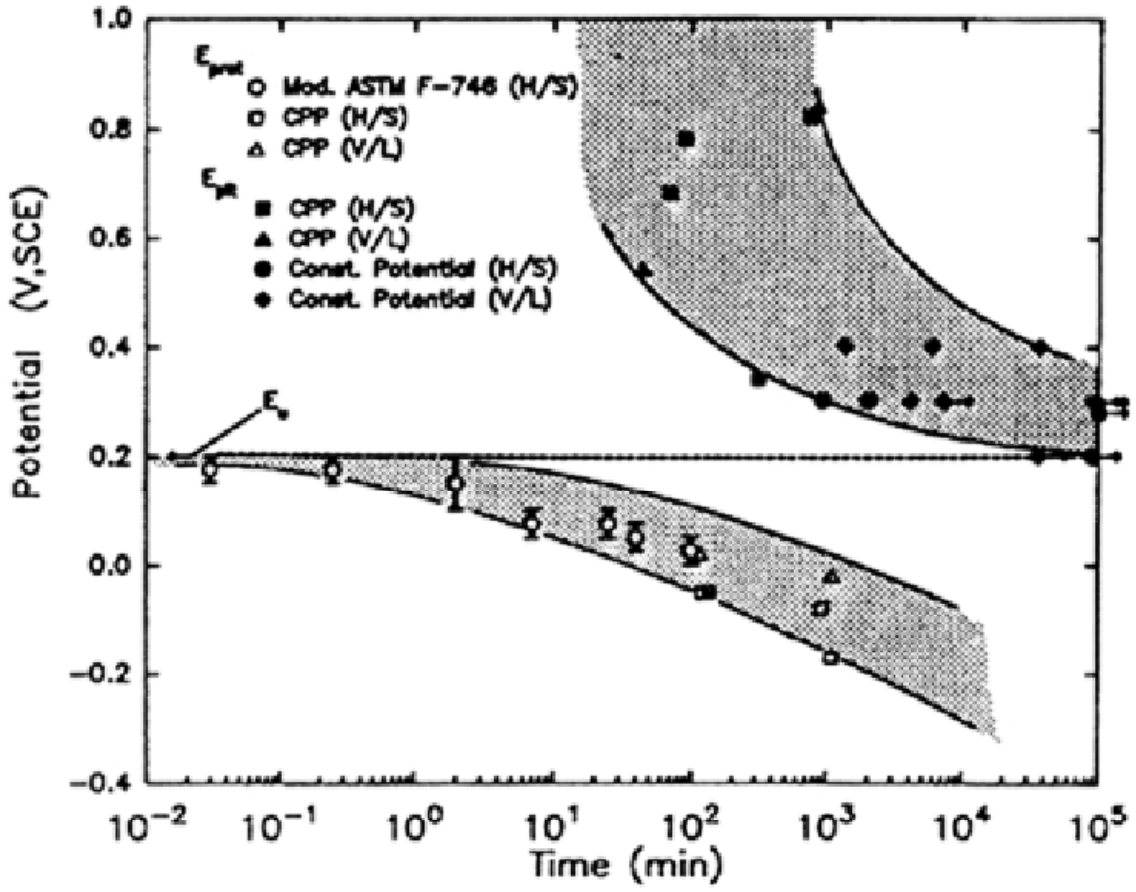

Figure 1 – Potential-Time relationship for E_{pit} and E_{prot} for Type 317L stainless steel in simulated scrubber solution.

24. Atmospheric Corrosion of Nickel Base Alloys

John A. Beavers
CC Technologies Laboratories, Inc
Dublin, Ohio, USA

EDITORIAL NOTE

This volume, "A Compilation of Special Topic Reports," contains a series of reports that were prepared for the Waste Package Materials Performance Peer Review Panel to use as background and input to the peer review. Summaries drawn from the reports were also presented in Section 11 of the Panel's Final Report. The Panel used the reports as background and input for its review. Any views and comments expressed in the summaries and the full reports do not necessarily reflect the opinion and findings of the Panel. Further, opinions expressed in the reports are not necessarily those of the Panel or reflected in the Panel's reports and recommendations.

Conventional ferritic and austenitic stainless steels are used extensively in atmospheric applications including marine atmospheres. Resistance to general corrosion increases with increasing chromium content of steel and general corrosion is negligible above a chromium content of about 12 percent (Johnson, 1980). Molybdenum free stainless steels, such as Type 410 or Type 304, experience staining and some pitting corrosion but addition of 2 to 3% molybdenum markedly increases resistance to attack (Larabee, 1945).

Nickel base alloys have excellent resistance to atmospheric corrosion even in marine environments. Boyd and Fink (1978) reported that Hastelloy Alloy C was bright and shiny, with no evidence of localized or general attack following 20 years marine exposure at the Kure Beach atmospheric corrosion test site. Mishka (1974) reported that Incoloy Alloy 825 corroded at a low rate of 0.06 mpy with superficial pitting (0.07 mils) following 7 years exposure at Kure Beach.

Stress corrosion cracking and hydrogen embrittlement are common problems for stainless steels in marine environments, primarily those alloys with high strength levels or a sensitized microstructure. Money and Kirk (1978) summarized the results of 5-year exposures of U-bends of a number of stainless steels and a few nickel base alloys at the Kure Beach test site. These included 304 and 316 stainless steels, Incoloy Alloys 800 and 825, Inconel Alloy 600, and Alloy 20-CB-3. None of the annealed, cold worked, or welded specimens failed by SCC but a high proportion of the stainless steel specimens that were sensitized underwent cracking. Incoloy Alloys 800 and 825, Inconel Alloy 600, and Alloy 20-CB-3 were resistant to cracking, even in the sensitized condition.

A few studies have been conducted in which the effect of sheltered versus exposed atmospheric conditions was evaluated. Feliu (1984) and Okorafor (1986) performed tests on

Special Topic Report prepared for the Waste Package Materials Performance Peer Review. The Final Report of the Peer Review was submitted to U.S. Department of Energy and Bechtel SAIC Company, LLC on February 28, 2002.

alloys other than stainless steels and nickel base alloys, probably because the latter are so resistant to corrosion that any effect would not be evident. The kinetics of corrosion of copper, zinc, steel, and aluminum were fitted to power laws for exposure periods of up to 8 years. For steel and aluminum, Feliu (1984) found that the corrosion rates Near Madrid Spain initially were higher for the fully exposed condition but the slopes for the power laws were higher for the sheltered exposure, such that the corrosion rates at the end of the eight-year period were higher for the sheltered exposure. The effect was most pronounced for aluminum. The slope for the sheltered exposure was larger than one (1.20), indicating an increasing corrosion rate with time; versus 0.85 for the fully exposed condition. The behavior was attributed to the accumulation of corrosive deposits and non-protective corrosion products on the sheltered metal surfaces. Okorafor (1986) observed similar behavior in exposure tests in Nigeria.

These results show that corrosion processes can occur in sheltered (no direct impingement of rain water) conditions. In addition, stress corrosion cracking of susceptible metals, e.g. sensitized stainless steels, occurs in marine open marine atmospheres. More corrosion resistant metals did not exhibit stress corrosion cracking.

Based on these results, any substitution of metals with less corrosion resistance than Alloy 22 for waste packages is not recommended. Clearly, 304/316 would fail under much more benign conditions. It is prudent to go with the best unless there is strong evidence that less resistant metals will work. There will be a strong economic incentive to use less expensive alloys. This should be evaluated carefully and materials substitutions allowed only with strong technical evidence to support long-term performance.

References

1. W. K. Boyd and F. W. Fink, "Corrosion of Metals in Marine Environments," Battelle Columbus Laboratories Report, MCIC-78-37, 103 pp, March 1978.
2. S. Feliu and M. Morcillo, "Corrosion Under Sheltered Exposure Sites in the Metropolitan Area of Madrid," British Corrosion Journal, p.64, June 1986.
3. M. J. Johnson and P. J. Pavlik, "Atmospheric Corrosion of Stainless Steels," Atmospheric Corrosion, NACE, Katy, TX, p. 461, 1980.
4. C. P. Larabee, "Corrosion of Steels in Marine Atmospheres and in Seawater," Transactions of the Electrochemical Society, **Vol. 87**, p. 171, 1945.
5. K. L. Money and W. W. Kirk, "Stress Corrosion Cracking Behavior of Wrought Fe-Cr-Ni Alloys in Marine Atmosphere," Materials Performance, **Vol. 17**, No. 7, p. 28, July 1978.
6. K. H. Miska, "Most Non-Ferrous Metals and Alloys Weather Well," Materials Engineering, **Vol. 79**, No. 4, p. 64, April 1974.
7. O. E. Okorafor, "Corrosion Under Sheltered and Unsheltered Sites in Awka, Nigeria," Corrosion Prevention and Control, **Vol. 19**, No. 3, p.143, 1984.

25. Corrosion of Stainless Alloys and Titanium in Peroxide Solutions

Roger Newman
UMIST, Corrosion and Protection Centre
Manchester, UK

EDITORIAL NOTE

This volume, "A Compilation of Special Topic Reports," contains a series of reports that were prepared for the Waste Package Materials Performance Peer Review Panel to use as background and input to the peer review. Summaries drawn from the reports were also presented in Section 11 of the Panel's Final Report. The Panel used the reports as background and input for its review. Any views and comments expressed in the summaries and the full reports do not necessarily reflect the opinion and findings of the Panel. Further, opinions expressed in the reports are not necessarily those of the Panel or reflected in the Panel's reports and recommendations.

Summary

Peroxide can cause uniform corrosion in a variety of pitting-resistant materials, but two completely different mechanisms are involved: transpassive dissolution, and HO_2^- complexation. These two topics are now reviewed, as they may be relevant to the condensed environment in Yucca Mountain where radiolytic formation of peroxide cannot be ruled out.

Transpassive corrosion of FeCr or NiCr based alloys can occur in highly oxidizing aqueous environments. In bleaching processes, such corrosion has been encountered with a variety of oxidants, especially chlorine dioxide, but also hydrogen peroxide. It may occur with hypochlorite, but only at concentrations higher than those usually used in pulp bleaching.

Transpassive corrosion in bleaching processes was discovered in nickel-base alloys, with stainless steels appearing immune. The reason for this is that iron (III) oxide or oxyhydroxide provides an adequately protective film in mildly alkaline environments, provided the conditions are not such as to promote pitting (i.e. the temperature is lower than the critical pitting temperature), and provided that there are no complexants of Fe(III) present. Nickel base alloys such as C-276 and C-22 have low iron contents and are prime candidates for transpassive corrosion. It is likely that an alloy could be engineered to provide optimum resistance to transpassive corrosion by including a critical content of iron and/or other elements that do not dissolve at the relevant potentials. It is not clear why NiO is so vulnerable to destruction of its passivating properties compared with Fe_2O_3 or FeOOH, but one can speculate that this involves

Special Topic Report prepared for the Waste Package Materials Performance Peer Review. The Final Report of the Peer Review was submitted to U.S. Department of Energy and Bechtel SAIC Company, LLC on February 28, 2002.

the very thin, crystalline, well-defined nature of the NiO film, compared with the more flexible nature of the range of products, including hydrated networks, that can form on iron.

Transpassive corrosion, or rather discoloration, has been observed in stainless steels when phosphonates are present, as these are complexants of Fe(III) and enable continuous dissolution of Cr(VI) to occur. This was essentially a cosmetic problem, but there are also some anecdotal cases of serious transpassive corrosion loss in stainless steels. Such problems may be due to extreme oxidant concentrations, presence of high levels of complexants such as EDTA, low water activity or perhaps particular values of pH where iron cannot provide a protective film.

At one time it was thought (e.g. by the author) that molybdenum dissolution was the main transpassive process occurring in this kind of corrosion, with Cr transpassivity being a subsidiary aspect. Now it appears that Cr transpassivity is both necessary and sufficient, although Mo definitely assists the process. There are various possibilities to inhibit this kind of corrosion, such as the use of silicates.

Titanium corrodes in alkaline peroxide solutions because the HO_2^- anion is a complexant for Ti(IV) as well as an oxidant. The corrosion has a fairly simple mechanism and appears to be well understood. The corrosion rate can be high, more than 10 mm/year in the worst cases. Low levels of calcium ions may act as effective inhibitors, as well as other species including magnesium, silicate and phosphate. Published corrosion-rate data may be unreliable because of very short test durations such as 1 hour. There are few data on the corrosion of titanium alloys in such media, but the rates and mechanism are probably similar to those of pure titanium. It is unlikely that low levels of elements such as Pd will block the corrosion significantly, but some experimentation may be worthwhile. It is possible that long-term corrosion rates will be higher with Pd or other electrocatalytic alloying elements, as these will catalyze the cathodic reaction.

General Background

Generation of aqueous peroxide by radiolysis can be expected at the surface of Yucca Mountain waste containers, and also on the drip shield, provided the conditions are such as to promote the retention of an aqueous phase. One can argue about the stability of peroxide under the repository conditions, but there are some factors, such as the presence of fluoride, that might lead to its stabilization. The purpose of this review is to consider the possible corrosion processes that might occur in the more extreme circumstances that could be envisaged. A full list of these would include crevice corrosion, transpassive corrosion and HO_2^- complexation. This review focuses only on the latter two possibilities, which are essentially uniform modes of corrosion. For historical reasons, the review of titanium corrosion is more elaborate than that of the stainless alloys; this should not be taken to mean that the author considers the risk to be higher for titanium components in the Yucca Mountain environment.

Note that each part (1 and 2) of this report has its own list of references.

PART 1 TRANSPASSIVITY OF STAINLESS ALLOYS

Transpassivity in alloys containing Cr or Mo is the oxidative dissolution of Cr or Mo from the passive film. The products are chromates or molybdates respectively (or chromic/molybdic acid at very low pH). This process is quite rare in the context of corrosion, because the potential required is very oxidising. However many surface treatment processes such as electropolishing or ac etching rely upon transpassive dissolution.

The relevant thermodynamic data according to Pourbaix [1] are:

$2CrO_4^{--} + 10H^+ + 6e = Cr_2O_3 + 5H_2O$
$E_0 = 1.311 - 0.0985\ pH + 0.0197 \log(CrO_4^{--})$

$MoO_4^{--} + 4H^+ + 2e = MoO_2 + 2H_2O$
$E_0 = 0.606 - 0.1182\ pH + 0.0295 \log(MoO_4^{--})$

From this we can see that transpassivity will be "easier" in alkaline than in acidic or neutral media (with oxygen as the oxidant), because the equilibria quoted are more steeply pH dependent than the oxygen electrode. For oxidants other than oxygen, this is not necessarily true (for example, the reduction of ClO_2 to ClO_2^- is pH-independent).

The first corrosion process involving transpassivity was probably that of stainless steel in concentrated nitric acid used for dissolution of spent nuclear fuel. Sometimes this corrosion is intergranular. The literature on this topic is quite confusing, and much work remains unpublished. However as far as one can gather, the potential reaches the required value not only from the oxidising action of nitric acid itself, but also from oxidising impurities. This case will not be considered further in this review. The case of nitric acid is exceptional in that it involves an acidic environment.

Mo transpassivity occurs at a significantly lower potential than that of Cr. However the atomic percentage of Mo in industrial Ni[Fe]-Cr-Mo alloys is never higher than ca. 11% (in the C-276 alloy). Mo dissolution alone is unlikely to destabilize the passive film to the extent that high corrosion rates on the order of 1 mm/year will occur. However the onset of Mo transpassivity may and does facilitate the onset of Cr transpassivity. For example, work carried out by Laing (PhD thesis, UMIST, to be published) showed that 316SS reacted faster than 304SS with alkaline permanganate solution. More controversially, it may be suggested that Mo alloying degrades the resistance of NiCr alloys to transpassive corrosion in bleaching media. There are a number of less well-defined possibilities: for example, the gradual accumulation of products from very mild transpassive dissolution (of Mo in the first instance) may generate a more catalytic surface for the cathodic reaction – a kind of autocatalytic transpassivity. These products may be oxides, but could also be porous metallic layers.

Work in progress has shown that the potential of Ni base alloys in the presence of strong oxidants tends to remain for some time around a hump in the anodic polarization scan (as

measured without oxidant present) which is due to Mo transpassivity. After this period Mo is apparently depleted and the potential may rise to the Cr transpassivity region.

According to thermodynamics, the loss of Mo and Cr should not completely destabilize the passive film on a nickel alloy, as NiO is quite stable under many of the conditions where transpassive dissolution has been observed. Some fundamental research is required on the reasons for the relative ease of destruction of Ni-induced passivity by dissolution of alloying elements. This may be connected with the ultra-thin, crystalline, well-defined nature of the nickel oxide passive film. In contrast, mildly basic transpassive conditions seem to allow the ready formation of a protective iron-rich film upon loss of Cr and Mo from a stainless steel. This may not be the well-defined passive film that is familiar from studies in media such as borate buffer. The resistance of stainless steels to transpassive corrosion may rely upon a thicker, more hydrated or polymeric, amorphous iron-rich product, and this would help to explain why nickel is not able to achieve a similar level of protection upon loss of Cr and Mo (since nickel cannot form such networks). Thus iron base alloys can be resistant to transpassive corrosion under conditions where nickel base alloys are corroded[8]. This explains why the use of Ni base alloys in ClO_2 bleaching, designed to resist localized corrosion better than available stainless steels, led to the first widely reported cases of transpassive corrosion. It was found that only a modest iron content was required to resist this kind of environment.

Peroxide is about as oxidising as ClO_2, and it is not surprising that transpassive corrosion can also occur in peroxide bleaching, and obeys similar rules. The relevant thermodynamic data for some important oxidants are:

$H_2O_2 + 2H^+ + 2e = 2H_2O$
$E_0 = 1.776 - 0.0591pH + 0.0295 \log(H_2O_2)$

$ClO_2 + e = ClO_2^-$
$E_0 = 1.160 + 0.0591 \log (p_{ClO2}/(ClO_2^-))$

$ClO_2 + 4H^+ + 5e = Cl^- + 2H_2O$
$E_0 = 1.511 - 0.0473\ pH + 0.0118 \log(p_{ClO2}/(Cl^-))$

$ClO^- + 2H^+ + 2e = Cl^- + H_2O$
$E_0 = 1.715 - 0.0591\ pH + 0.0295 \log((ClO^-/(Cl^-))$

Many of these species are possible buffers; we also have to remember that:

H_2O_2/HO_2^- pK = 11.63

and

[8] Incidentally, the fact that surfaces with no remnant of the original passive film, only an iron-rich oxide, still resist localized corrosion in the presence of chloride is one of many pieces of evidence that the composition of the passive film has nothing to do with localized corrosion resistance.

$HClO/ClO^-$ pK = 7.49

Uniform Corrosion of Ni Base Alloys in ClO_2 Bleaching

Since the literature of peroxide corrosion of Ni base alloys is quite sparse, but is entirely analogous to similar transpassive corrosion in ClO_2 bleaching, the latter is now reviewed.

The first relatively scientific studies of transpassive corrosion in Ni base alloys were made by Canadian workers [2-4] and by Arlt and others [5,6]. Alloys such as C-276 were already in satisfactory use for chlorine bleaching, including certain blends of chlorine and chlorine dioxide, but when the chlorine dioxide concentration was increased there was an alarming incidence and rate (several mm per year) of general corrosion[9]. Newman and Garner played some part in the diagnosis of transpassive corrosion via discussions with Wensley et al. [2,3]; however at that time the role of Mo in enhancing corrosion was overestimated. This was not settled until recently, when Ernst [7] during her PhD work showed that simple NiCr alloys were, if anything, more susceptible to transpassive corrosion than complex NiCrMo alloys (but the role of low levels of iron alloying in the long term corrosion rate has not been examined in detail).

Arlt et al. [5,6] introduced a very important concept, namely that iron was protective against transpassive corrosion, and they hinted that there was a neat symmetry between the amount of iron required to protect against this form of uniform corrosion and the amount of chromium required to produce passivity in acids. There can be little doubt that whatever controls the formation of a protective Cr_2O_3 film on stainless steels is also controlling the protection by iron against transpassive corrosion. According to the percolation model of alloy passivity [8], this reflects a geometrical requirement for 3D connectivity of a gel-like layer of the protective oxide, in the form of an oxyhydroxide network.

An important finding was that the key factor in producing transpassive corrosion was the substitution of chlorine by ClO_2. The reason for this appears to be the rise in corrosion potential especially at near-neutral pH values, as discussed by Outi [9] among others. Peroxide can produce similar potentials to ClO_2, but the exact relationship between the two oxidants has not been established as a function of pH.

High-alloy stainless steels were bound to find a market in bleach plant after the discovery of their relative immunity to transpassive corrosion, and a number of papers of varying degrees of objectivity have been published in the corrosion press on this topic [10-16]. Many of these emanate from steel producers. The important factor, obviously, is the ability to provide immunity to localized corrosion (by alloying sufficiently to remain below the CPT and CCT of the alloy) while providing enough elements, including iron, that are not dissolved transpassively.

[9] This led to the substitution of Ni base alloys by titanium in some plants, which worked perfectly until ClO_2 was substituted by alkaline peroxide, which corroded titanium by a complexation reaction of HO_2^- .

The exact pH dependence of transpassivity in high-alloy stainless steels has not been established. There may be a narrow window where the iron based passive film is not protective and rapid transpassive corrosion can occur. This would probably be close to neutral or slightly acid pH, and would probably depend on the co-presence of chloride.

Alloy C-22 has not been much investigated in terms of transpassive corrosion. Since it does not contain enough iron to form a protective film, it must be considered susceptible to this form of corrosion, but not to the extent of alloy C-276 which has a very high Mo content. The transpassivity of Mo undoubtedly assists the transpassive dissolution process on this alloy.

Transpassive corrosion of stainless steel can occur in particular circumstances. In the case investigated by Laycock et al. [17], the presence of a complexant of Fe(III) (a phosphonate) aggravated alkaline peroxide corrosion that would normally have been stifled by formation of an iron-based protective film. However the result was cosmetic damage. If some other product were to have a high level of EDTA or a similar chelating agent, it may attack stainless steel in a more substantial manner; one should note however that such cases the environment would be vastly higher in both oxidant and complexant than anything that could exist in Yucca Mountain. The author has come across cases of persistent transpassive corrosion (leading to product contamination and significant though not dramatic metal loss) in industrial non-aqueous environments where passivity of iron was diminished owing to lack of water. For any material affected by this kind of corrosion, one also needs to consider the presence of other dissolved species that have the potential to form insoluble compounds, such as silicates.

It is possible that fluoride, present in the Yucca Mountain groundwater, could act as both a complexant of Fe III and (by the same token) a stabilizer of peroxide. This raises some interesting possibilities for experimental work.

References: Transpassive Corrosion of Stainless Alloys

1. M. Pourbaix, Atlas of Electrochemical Equilibria, NACE/CEBELCOR, Houston (1976).

2. D A Wensley and D C Reid, Corrosion/93, Paper No. 433, NACE, Houston (1993).

3. D A Wensley, D C Reid and H. Dykstra, Corrosion/90, Paper No. 537, NACE, Houston (1990).

4. A. Nadezhin, J. Richard, J. Coster, G. Volpe and C. Thompson, Corrosion/92, paper #320, NACE, Houston (1992).

5. N. Arlt, W. Heimann and T. Ladwein, Corrosion/91, Paper #198, NACE, Houston (1991).

6. N. Arlt, C. Gillesen, T. Ladwein and E. Michel, Corrosion/93, Paper #434, NACE, Houston (1993).

7. P. Ernst, PhD thesis, UMIST (1999).

8. Q. Song, R.C. Newman, R.A. Cottis and K. Sieradzki, J. Electrochem. Soc., **137**, 435 (1990).

9. V. Outi, Technical Research Centre of Finland Research Notes, pp. 3-46, 1994.

10. J. Olsson, B. Jonsson and R. Davison, Corrosion/2001, Paper #425, NACE, Houston (2001).

11. I. Aho-Mantila, P. Pohjanne, O. Hyokyvirta and K. Saarinen, in Stainless Steel '99, 3rd European Congress Proceedings, Vol. 1: Marketing and Application (Italy), pp. 271-279 (1999).

12. D.E. Bardsley, in Proc. 8th International Symposium on Corrosion in the Pulp and Paper Industry (Stockholm, 1995), pp. 75-82, Swedish Corrosion Institute, 1995.

13. P Andreasson and L Troselius, Swedish Corrosion Institute Report #1995:8.

14. D.L. Reichert, Corrosion/96, Paper #467, NACE, Houson (1996).

15. B. Wallen, M. Liljas and P. Stenvall, Corrosion/92, Paper #322, NACE, Houston (1992).

16. A.H. Tuthill and D.E. Bardsley, Corrosion/92, Paper #323, NACE, Houston (1992).

17. N.J. Laycock, R.C. Newman and J. Stewart, Corros. Sci., **37**, 1637-1642 (1995).

PART 2 PEROXIDE COMPLEXATION CORROSION OF TITANIUM

Unexpected corrosion problems affecting titanium in peroxide bleach plant were discovered in the 1970s. The news did not travel rapidly, and belated awareness of the problem, even in countries with advanced pulp and paper industries, was very costly. The corrosion rates in extreme cases, with high pH and temperatures above 70^{o}C, could be as high as 50 mm/year.

The essential mechanism of peroxide corrosion of titanium is not in doubt. The hydrogen peroxide anion, HO_2^-, forms some kind of soluble complex with Ti(IV). This immediately explains why the problem is found in alkaline environments, since the pK_a value for

$$H_2O_2 = HO_2^- + H^+$$

is about 11.6 at ambient temperature.

For the present review we have not searched the chemistry literature in detail, but there must be better knowledge of the Ti(IV)-peroxide complex than is displayed in the corrosion literature. There seems to have been no significant advance since Russian work in the mid-1970s [1].

Nature of the Corrosion Product

Although the complexation of Ti(IV) by peroxide seems the obvious explanation of the high corrosion rates in the Ti-peroxide system, authors have generally proposed rather complicated reaction schemes and have not often tried to relate them to electrochemical reaction kinetics. One reason for this may be that oxide products are often observed, even in cases of rapid corrosion, and a formal reaction scheme to account for their presence is sought. Authors tend to propose multi-stage reactions such as

$$Ti + OH^- + HO_2^- = Ti(OH)_2O_2\ (aq)$$

[following the Russian work, e.g. ref 1], followed by

$$Ti(OH)O_2 + 2OH^- + H_2O = Ti(OH)_4 + HO_2^-$$

In other words, the peroxide is considered as a kind of catalyst. Little or no solution analysis has been done to see how much of the soluble complex escapes; experience from other corrosion systems suggests this is probably at least 50% and probably 90%, so the oxide or hydroxide product may be a red herring kinetically, although it can possibly be important in other respects:

- Interaction with inhibitors such as Ca^{++} [10]

- Improvement of adhesive bonding in aerospace applications [2]

- Improvement of bone growth and adhesion in surgical implants [4,11,13]

No-one seems to have suggested that the soluble complex may be ionic, but it would not be surprising if the chemistry literature shows this to be the case.

The most recent corrosion study [15] concludes that the final products are $HTiO_3^-$ and oxygen, a proposal that denies any role to the equilibrium complexation tendency of peroxide for Ti(IV). Yet a yellow product is known to exist in the titanium-peroxide system [4], and other metals such as tantalum form well-characterised and brightly coloured soluble peroxide complexes. It is probably safe to conclude that the authors of the corrosion studies have only a limited knowledge of the real nature of the soluble Ti(IV)-peroxide complex.

Corrosion studies have focused on alkaline solutions, but physiological studies related to bone growth on titanium implants have used neutral pH values. The postulated source of peroxide in the body [4,12] is the inflammatory response which involves activity of

macrophages. At neutral pH the peroxide is almost all in the form of H_2O_2, and there is correspondingly little corrosion; however there is a mild complexation and dissolution-reprecipitation cycle that gradually builds up a bluish outer layer on top of the barrier TiO_2 film over a period of a few weeks [4,11] – Figure 1. This layer may be important in bone adhesion. The implied corrosion rate of about 1 σm/year can be explained by the solubilization of the oxide by the low concentration of HO_2^- that exists at this pH. Only at pH values less than about 5 would this action become completely negligible. Interesting studies on bone adhesion have shown strong effects of metal ions, included in a peroxide pretreatment solution, on the subsequent apatite nucleation process at the titanium surface [13].

Electrochemical Characteristics of Titanium in Alkaline Peroxide Media

Most studies have shown an anodic limiting current density (current independent of potential), which is typical of metal dissolution controlled by the solubility of a stable metal-ion complex – Figure 2. In this case, as pointed out by Rasten et al. [14], the anodic Tafel coefficient b_a is infinity. Other authors claim that the value is around 250 mV [15]. In any event, it is much larger than the cathodic Tafel coefficient, associated with activation-controlled peroxide reduction, which seems to be about 120 mV [15]. It is relatively easy to obtain good agreement between weight loss and the polarization resistance measured electrochemically, using these or similar *b* values for the conversion. In near-neutral solution the difference in the passive current due to peroxide addition is undetectable in short-term experiments – Figure 3.

One would expect the open-circuit (corrosion) potential to drop when the corrosion rate increases, and such behaviour has indeed been reported by Saarinen et al. [6] who showed typical potentials of +100 mV (SHE) at low corrosion rates and –300 mV (SHE) at high corrosion rates – Figure 4. The same phenomenon was noted in plant monitoring by Hyokyvirta et al. [16]. Similar though smaller effects were noted by Andreasson [10], but Wyllie et al. [9] stated that the potential generally increased with peroxide addition. There will certainly be competing effects in this respect: increasing the peroxide concentration will increase the rate of the cathodic reaction (thus tending to raise the potential) but also increases the rate of the anodic reaction, which will have the opposite effect.

Corrosion Rate as a Function of pH, Temperature and Peroxide Concentration

The problems in bleach plants triggered a number of studies [3,5-10,14-15]. Some of these will not be considered in detail, as the authors allowed peroxide to decompose in a "realistic" way during the tests, which makes the results impossible to interpret (e.g. ref 6). Others (e.g. ref 9) are vague about how they handled this issue, as well as that of pH control under conditions where additions of peroxide were made during a test (if a test is being conducted at pH 12 or 13, hydrogen peroxide acts as an acid and lowers the pH). Others used very short immersion times to avoid peroxide decomposition, but generally were not confident in quoting peroxide levels to better than $\pm$ 30%.

Workers at RMI Titanium [7,8] published the results of a widely-quoted but in our view rather impatient study. To consider the results, one must first believe (or suspend one's disbelief) that a 0.5 to 1 hour test duration is sufficient to give valid corrosion-rate data. In the RMI work, the peroxide concentrations of interest ranged from 0.2 to 0.4 g/l, the temperature from 65 to 80°C, and the pH from 10 to 12.5 – Table 1. Data related to inhibitors and chelating agents will be considered later on. The corrosion rates at 70°C and 0.2-0.3 g/l peroxide (without other additions) rose from ca. 0.1 to ca. 10 mm/year as the room-temperature pH was increased from 10 to 12, suggesting that the corrosion rate is closely related to the HO_2^- concentration, but not via a simple proportionality – Table 2. A very steep increase in corrosion rate, for this temperature, occurred when the pH was increased from 11 to 12. Surprisingly, the corrosion rate at 65°C and pH 12.0 was very low, less than 0.1 mm/year. This result is not explained by the authors and may be an artifact of their short test duration. It certainly does not fit in with any simple theoretical model of the corrosion process. Saarinen et al. [6] carried out similar studies at 85°C and found similar corrosion rates at high pH, up to 12 mm/year. Their solutions were more complicated, and the concentrations of species were varying during the tests. It is difficult to make any detailed analysis of these results. These authors also examined grade 5 titanium (Ti-6Al-4V alloy), and found it had a higher corrosion rate than grade 2.

According to Andreasson [10], there are "critical" conditions for corrosion of titanium in alkaline peroxide media, an observation that supports (at least in part) the 65°C "threshold" of Schutz and Xiao [7,8]. For tests conducted under a variety of hot conditions in a pilot plant, she concluded that pH 11 (measured at room temperature) was a critical point (see data in Tables 3 to 5). This could be due to the appearance of significant HO_2^- in the solution, although the rise in corrosion rate around this pH is certainly steeper than the rise in HO_2^- level. Since all her solutions contained calcium, magnesium and chloride, some of the abrupt transitions in corrosion rate could be due to thresholds in the behaviour of some inhibitor (see next section). However, Rasten et al. [14] also displayed a "critical" concentration of peroxide (0.3 to 0.4 g/l) in solutions of very high pH such as 12.0, with no inhibitors present. Crucially, comparison of their electrochemical and weight-loss data shows that there was a time-dependent film breakdown phenomenon, suggesting that it is important to allow an adequate testing time, at least on the order of many hours. Such effects may invalidate the apparent thresholds in peroxide concentration, temperature or pH reported by several authors.

Varjonen and Hakkarainen [5] carried out a standard type of corrosion investigation at 80°C, using grade 5 titanium, and found that significant damage due to peroxide occurred at pH 10.5 but not at pH 9.5. The general principle was stated that one can achieve an acceptable corrosion rate by ensuring that the HO_2^- concentration does not exceed a critical level. This is easier said than done, and inhibition may be a better route in practice.

According to Wyllie et al. [9], black films can form when excess peroxide (5 to 10 g/l) is added to high-pH solutions, giving relatively low corrosion rates even when there is a very high HO_2^- concentration. However they stated that these films were easily wiped off the metal and could not be relied upon in practice. This was a study in which one could question the control of pH and peroxide.

The study of Been and Tromans [15] is useful in that it contains some data for low temperatures. For example, the corrosion rate at 10°C and 0.15M peroxide was 0.35 mm/year. They showed that the corrosion rate was relatively constant with time (over 3 hours) for the more aggressive conditions, but tended to decay to low values in less aggressive solutions such as pH 10, 0.05M peroxide. The validity of electrochemical impedance for the estimation of corrosion rate was demonstrated. The impedance diagrams were very simple in nature, because the anodic charge transfer resistance is essentially infinity, so the measured resistive components relate essentially to the cathodic reduction of peroxide, which like oxygen reduction on passive metals always gives a clean, ideal impedance response (the authors gave a more complicated explanation and gave a lot of attention to the capacitive component(s) in the impedance response).

Been and Tromans [15] did not carry out a systematic study as a function of pH and peroxide concentration, but it appears that they consider the corrosion process to be diffusion-controlled by escape of a titanium complex from the surface. This is, of course, the obvious first hypothesis as to the mechanism in such a system, and it is frustrating that published data are so poorly suited to testing it.

We are not aware of any long-term studies showing the effects of noble alloying elements such as Ni and Pd. One can anticipate that these will accumulate and may for example catalyze peroxide reduction (a detrimental effect) or block anodic dissolution (a beneficial effect). Some experimentation in this are, using the alloy proposed for Yucca Mountain, would be useful.

Inhibitors

It is feasible to inhibit alkaline peroxide corrosion of titanium using low levels of calcium ions. This was part of a patent granted in 1983 [3], which also referred to strontium and barium ions. The test durations were quite short, usually 1 hour. Other inhibitors such as silicates, magnesium ions and phosphates are less effective (or at least require much higher concentrations). The presence of complexants such as EDTA or phosphonates (used to stabilize the peroxide against decomposition) is also relevant to the effect of calcium since it can be complexed by these same additives. This issue seems to be quite complicated and not fully addressed in the literature.

According to Rasten et al. [14], magnesium stops working as an inhibitor above e.g. 80°C and/or pH 13. It is not known how calcium behaves under extreme conditions.

Schutz and Xiao [7,8] showed apparently convincing results related to the effects of calcium ions. Expanded application guidelines were suggested for temperatures over 65°C, based on very encouraging corrosion rates such as 0.05 mm/year at pH 12, 0.2 to 0.3% peroxide and 10 ppm calcium ions. However the exposure times were very short (0.5 to 1 hour), and we would not advise reliance on such data without longer-term testing. The authors stated that even at fairly high levels of chelant (e.g. EDTA, DTPA), the calcium continued to work effectively. It is hard to see how calcium could operate by simple adsorption, and indeed Andreasson [10] states

that Ca and Mg are found in the passivating oxide layer. Apparently the oxide film can extract calcium from the solution even when it is in the form of a stable complex.

Conclusions: Peroxide Corrosion of Titanium

1. Peroxide-induced corrosion of titanium occurs only in alkaline media because the complexant is HO_2^- not H_2O_2.
2. There are few data for near-ambient temperatures because the main interest in the literature is related to the pulp and paper industry, which uses temperatures in the region of 70-80^oC for peroxide bleaching.
3. The corrosion rate is very roughly proportional to the HO_2^- concentration in some studies, but many data also show passivation-like or threshold behaviour as a function of relevant variables. There is evidence that there may be short-term passivity that breaks down with time near reported "thresholds", which should therefore be treated with caution.
4. In view of the last comment, test times should not be too short. One hour is not long enough. However for longer testing a more elaborate system is required to maintain peroxide concentration and pH.
5. Remarkably low levels of calcium ions in the region of 10 ppm can inhibit corrosion dramatically, although one suspects that some data are unreliable because of very short test times. Magnesium ions, silicates and phosphates are other possible inhibitors. Inhibition by calcium is reported not to be degraded by the presence of normal amounts of complexants or peroxide stabilizers such as EDTA.

References: Peroxide Complexation Corrosion of Titanium

1. T.M. Sigalovskaya, et al., Zasch. Met., **12**, 363 (1976).
2. A.K. Rogers, K.E. Weber and S.D. Hoffer, "The alkaline peroxide prebond surface treatment for titanium: the development of a production process", SAMPE Quarterly, July 1982, pp 13-18.
3. US Patent #4,372,813, Feb 8 1983 (Clerbois et al.): "Process for inhibiting the corrosion of equipment made of titanium".
4. J. Pan, D. Thierry and C. Leygraf, "Electrochemical and XPS studies of titanium for biomaterial applications with respect to the effect of hydrogen peroxide", J. Biomedical Mtls. Res., **28**, 113-122 (1994).
5. O.A. Varjonen and T.J. Hakkarainen, "Corrosion behaviour of titanium (grade 5) in alkaline hydrogen peroxide bleaching solution – laboratory experiments", Corrosion/94, Paper #425, NACE, Houston (1994).

6. K. Saarinen, J. Ramo and T. Korvela, "Corrosion performance of titanium in alkaline hydrogen peroxide environments", in Titanium '95: Science and Technology, pp 1886-1894, Institute of Materials, London (1995).

7. R.W. Schutz and M. Xiao, "Practical windows and inhibitors for titanium use in alkaline peroxide bleach solutions", Corrosion/95, Paper #427, NACE, Houston (1995).

8. R.W. Schutz and M. Xiao, "Expanded windows for titanium use in the pulp/paper peroxide bleach plant", in J. Testing and Evaluation, **24** (2), 119-122 (1996).

9. W.E. Wyllie II, B.E. Brown and D.J. Duquette, "The corrosion of titanium in alkaline peroxide bleach liquors", Corrosion/95, Paper #421, NACE, Houston (1995).

10. P. Andreasson, "The corrosion of titanium in hydrogen peroxide bleaching solutions", in Proceedings of International Symposium on Corrosion in the Pulp and Paper Industry (May 1995), pp 119-126, Swedish Corrosion Institute (1996).

11. J. Pan, D. Thierry and C. Leygraf, "Hydrogen peroxide toward enhanced oxide growth on titanium in PBS solution: Blue coloration and clinical relevance", J. Biomedical Mtls. Res., **30**, 393-402 (1996).

12. A. Montague, K. Merritt, S. Brown and J. Payer, "Effects of Ca and H_2O_2 added to RPMI on the fretting corrosion of Ti6Al4V", J. Biomedical Mtls. Res., **32**, 519-526 (1996).

13. C. Ohtsuki, H. Iida, S. Hayakawa and A. Osaka, "Bioactivity of titanium treated with hydrogen peroxide solutions containing metal chlorides", J. Biomedical Mtls. Res., **35**, 39-47 (1997).

14. E. Rasten, R.E. Antonsen, A. Bjorgum, J. Krysa and R. Tunold, "The stability of the passive film on titanium in alkaline solutions with peroxide ions", in Proceedings of Eurocorr '97 (Trondheim, 1997), pp 683-688.

15. J. Been and D. Tromans, "Titanium corrosion in alkaline hydrogen peroxide", Corrosion, 56, 809-818 (2000).

16. O. Hyokyvirta, P. Pohjanne, A. Heinavaara, J. Hirvonen and A. Lewenstam, "The corrosion of titanium and some other construction materials during hydrogen peroxide bleaching according to the field measurements", in Environmental Degradation of Materials and Corrosion Control in Metals, eds M. Elboudjani and E. Ghali, pp 205-222, CANMET, Ottawa (1999).

TABLE 1
Conditions Used in the RMI Titanium Study [7,8]

MATRIX OF TEST CONDITIONS FOR CORROSION EVALUATION OF GR.2 TITANIUM SAMPLES IN HOT ALKALINE PEROXIDE SOLUTIONS

H_2O_2 Concentration (wt.%)	Temp. (°C)	pH	Inhibitor Addition	Chelating Agent Addition (Molar Ratio $X:Ca^{+2}$)
0.2 - 0.3	65	12.0	none	none
	70	10.0 - 12.5	none	none
	75	12.0	none	none
	80	9.5 - 12.0	none	none
	65	12.5	1 ppm Ca^{+2}	none
	70	11.0 - 12.0	1 - 100 ppm Ca^{+2}	none
	80	10.0 - 12.0	1 - 200 ppm Ca^{+2}	none
	70	12.0	50 - 200 ppm Mg^{+2}	none
	70	12.0	100 ppm Ca^{+2} + 100 ppm Mg^{+2}	none
	70	12.0	100 - 10,000 ppm SiO_3^{-2}	none
	70	12.0	100 ppm Ca^{+2}	EDTA (2.5:1, 1:1, 1:2)
	70	12.0	100 ppm Ca^{+2}	DTPA (2.5:1, 1:1, 1:2)
0.3 - 0.4	70	12.5	none	none
	80	12.5	none	none
	70	12.5	200 ppm Ca^{+2}	none
	70	12.5	100 ppm Ca^{+2}	EDTA (1:1, 1:2)
	80	12.5	200 ppm Ca^{+2}	none
	80	12.5	100 ppm Ca^{+2}	EDTA (1:1, 1:2)

TABLE 2
Corrosion Rate Data from the RMI Titanium Study, without Inhibitors [7,8]

CORROSION RATE OF GR.2 TITANIUM AS A FUNCTION OF pH IN 0.2-0.3% H_2O_2 SOLUTIONS AT 70° AND 80°C

Temperature (°C)	pH	Corrosion Rate	
		mm/y	mpy
70	10.0	0.07	2.7
	10.3	0.28	11
	10.6	0.91	36
	10.9	2.44	96
	11.2	0.48	19
	11.3	1.55	61
	11.5	2.06	81
	12.0	8.89	350
	12.1	8.43	332
	12.2	10.90	429
	12.4	10.62	418
80	9.5	0.12	4.7
	10.0	1.73	68
	11.2	5.56	219
	12.0	13.78	542

TABLE 3
Conditions for Tests Carried Out in Pilot Bleaching Plant, by Andreasson [10]

Test-packet	C_{NaClO_2}, g/l	pH	Temp. °C	Exp. time, h
1	3,2	11,4	78	72
2	3,0	11,0	79	485
3	2,3	10,6	76	286
4	2,8	10,9	71	648
5	2,5	10,6	80	168
6	2,5	11,0	79	168
7	2,4	10,9	79	168

TABLE 4
Calcium, Magnesium and Chloride Concentrations for the Tests of Andreasson [10]

Test-packet	Ca^{2+}, mg/l	Mg^{2+}, mg/l	Cl, mg/l
1	42	7,3	30
2	42	7,3	30
3	42	7,3	30
4	23	9,1	52
5	25	2,8	15,9
6	25	2,8	15,9
7	25	2,8	15,9

TABLE 5
Corrosion Rates Measured by Andreasson in a Pilot Bleaching Plant
(See Tables 3 and 4 for Conditions)

Test packet	gr.2 mm/år	gr.5 mm/år	gr.7 mm/år	gr.9 mm/år	gr.12 mm/år
1	8,7 9,1	25,9 23,3	8,9 9,3	17,1 17,6	3,1
2	4,64 4,65	14,1 13,6	3,24 2,99	9,20 9,17	1,72
3	0,0011 0,0010	0,832 0,740	0,0011 0,0009	0,036 0,067	0,0017 0,0016
4	0,0004 0,0006	1,08 1,29	0,0002 0,0004 *	0,007 0,138*	0,0002 0,0001
5	0,0082 * 0,0003 *	2,324* 2,376*	0,0006 0,0006	0,0788 0,310	0,0007 0,0006
6	0,361* 0,383*	5,526* 5,133*	0,0015 0,020	1,1256 1,204	0,071 0,096
7	0,004* 0,001*	4,707* 4,792*	0,0010 0,0003	0,331 0,390	0,001 0,001

*indicates welded coupons

TABLE 6
Corrosion Rate Data from the RMI Titanium Study, with Calcium Inhibitor Added [7,8]

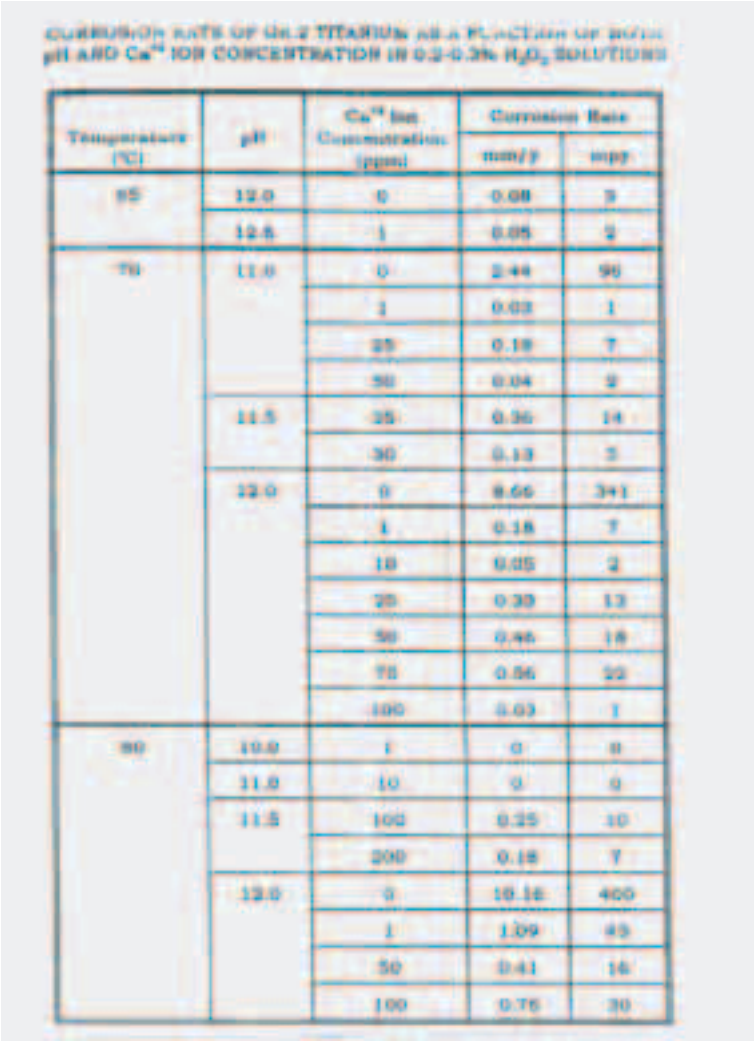

CORROSION RATE OF GR.2 TITANIUM AS A FUNCTION OF BOTH pH AND Ca^{++} ION CONCENTRATION IN 0.2-0.3% H_2O_2 SOLUTIONS

Temperature (°C)	pH	Ca^{++} Ion Concentration (ppm)	Corrosion Rate mm/y	Corrosion Rate mpy
95	12.0	0	0.08	3
	12.8	1	0.05	2
70	11.0	0	2.44	96
		1	0.03	1
		25	0.18	7
		50	0.04	2
	11.5	25	0.36	14
		30	0.13	5
	12.0	0	8.66	341
		1	0.18	7
		18	0.05	2
		25	0.30	13
		50	0.46	18
		75	0.56	22
		100	0.03	1
80	10.0	1	0	0
	11.0	10	0	0
	11.5	100	0.25	10
		200	0.18	7
	12.0	0	10.16	400
		1	1.09	43
		50	0.41	16
		100	0.76	30

TABLE 7
Corrosion Rate Data from the 1983 Clerbois Patent, Showing the Effects of Several Inhibitors (Ca, Sr, Ba)

Example No	NaOH g/l	Sequestering Agent g/l *	Brand name and grade	Inhibitor g/l	Type	H_2O_2 g/l Beginning	H_2O_2 g/l End	time hours	pH	weight loss by measurement of polarisation resistance mean mm/year	weight loss by measurement of polarisation resistance inhibition %	weight loss by direct measurement sample 1 mm/year	weight loss by direct measurement sample 2 mm/year	weight loss by direct measurement inhibition %
1	1	1	Clarene S	-	—	4.1	4.1	1	10.4	19.1	0	11.4	32	0
2	1	1	Clarene S	1	$(NaPO_3)_6$	4.0	4.0	1	10.4	11.6	39.3	11.0	10.8	65.6

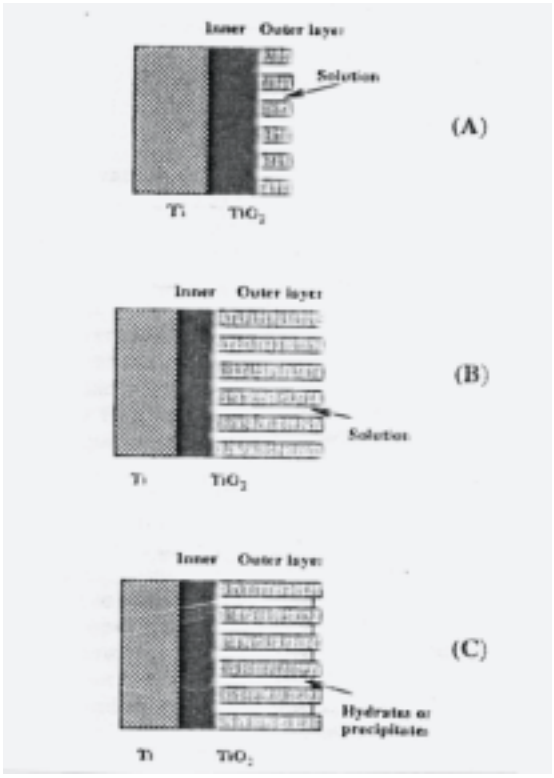

Figure 1 – Mechanism of coloured layer formation on titanium In near-neutral peroxide solution [11]. (A) Without H_2O_2; (B) with H_2O_2, earlier stage; (C) with H_2O_2, later stage, when blue color appears.

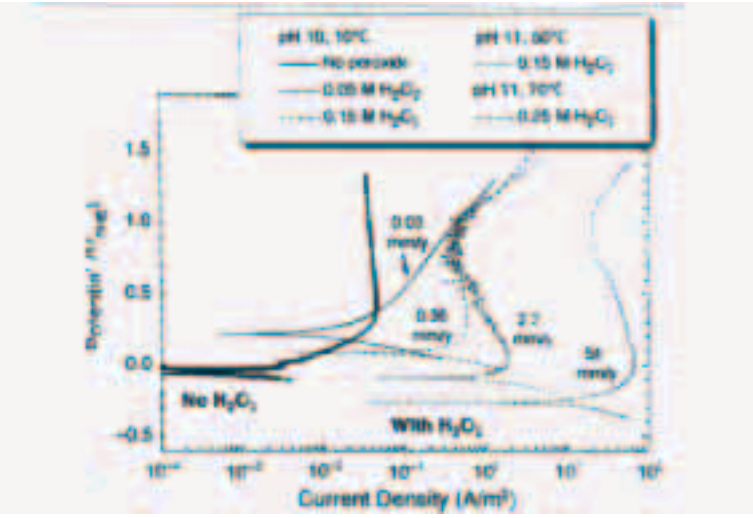

Figure 2 – Anodic behaviour of titanium in various alkaline peroxide solutions, showing anodic limiting current density due to complexation of the passive film.

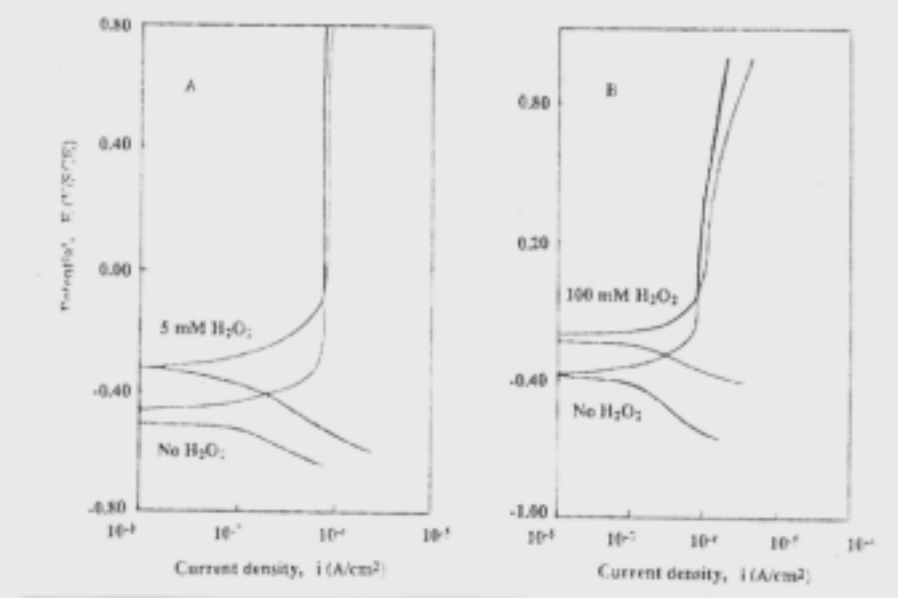

Figure 3 – Anodic behaviour of titanium in near-neutral physiological medium containing peroxide, showing little or no enhancement of the passive current [4]. Polarisation rate: 10 mV/min; A: no N_2 deaeration; B: deaeration by N_2.

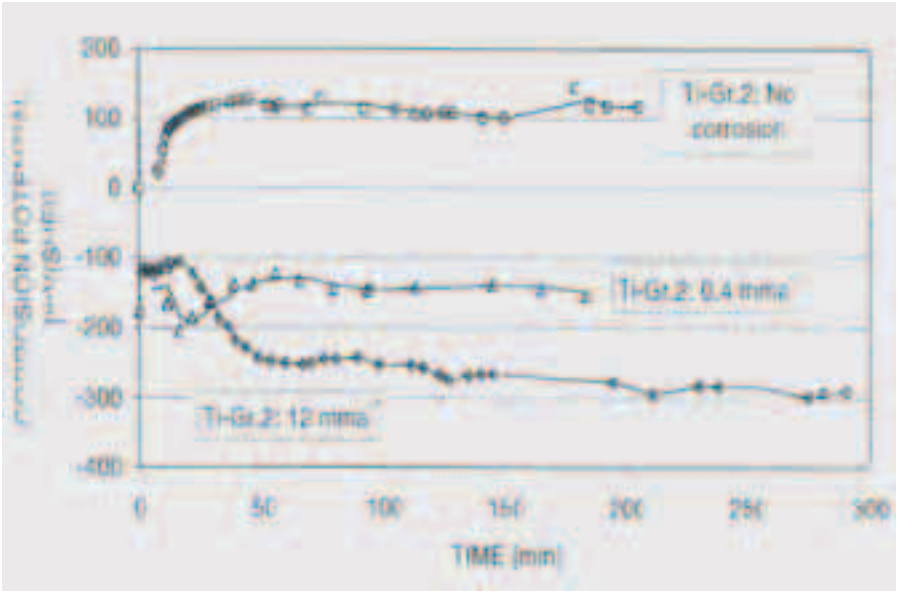

Figure 4 – Typical corrosion potentials observed during corrosion of titanium in alkaline peroxide solution, showing drop in potential at high corrosion rates [6].

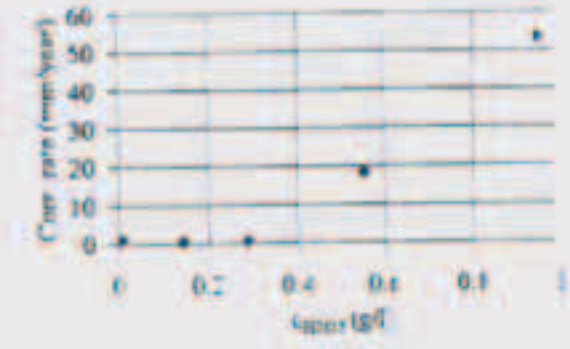

Corrosion rate vs. CH_2O_2 at pH=12 and temp.= 90°C by AC-Impedance

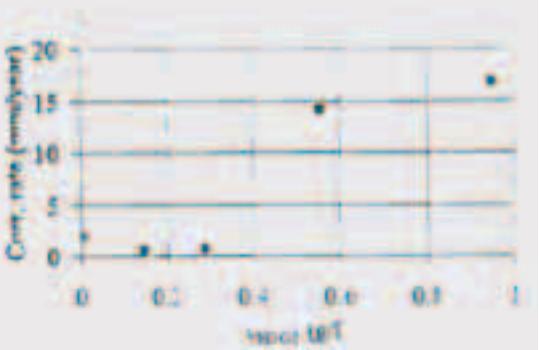

Corrosion rate vs. CH_2O_2 at H=12 and temp.= 90°C by polarisation curves

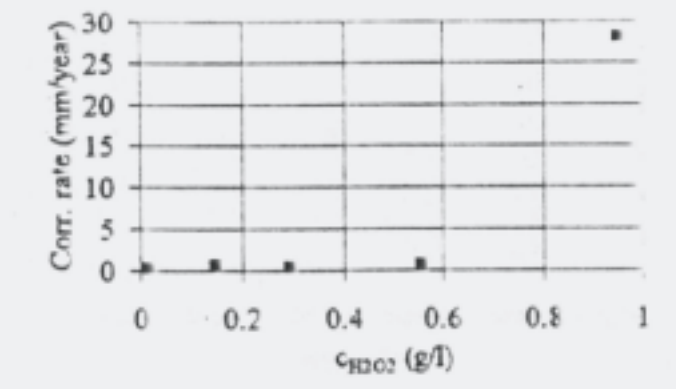

Corrosion rate vs. CH_2O_2 at pH=12 and temp.= 90°C by weight loss

Figure 5 – Data from Rasten et al. [14] showing higher corrosion rates measured electrochemically than by weight loss at e.g 0.55 g/l peroxide because there was a time-dependent breakdown of passivity.

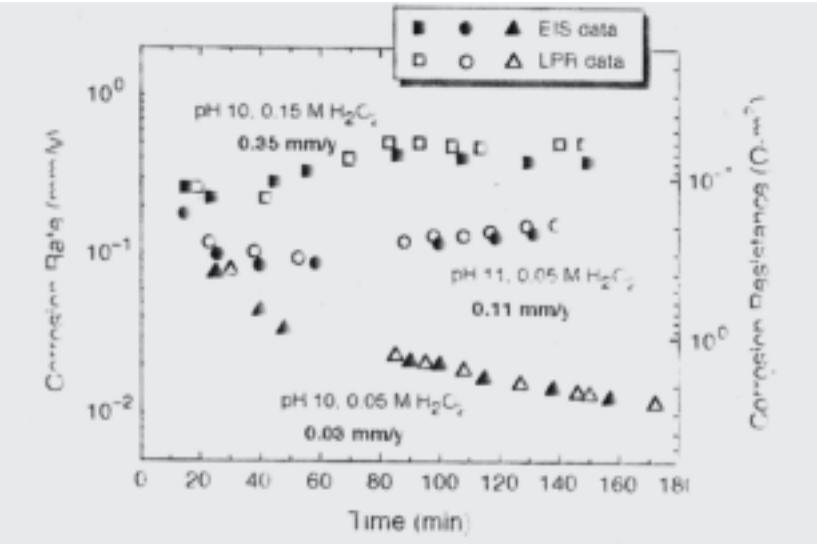

Figure 6 – Different trends of corrosion rate with time depending on pH and peroxide level, from ref. 15. Comparison of LPR data with weight loss tests (indicated in bold font in mm/yr) and EIS data.

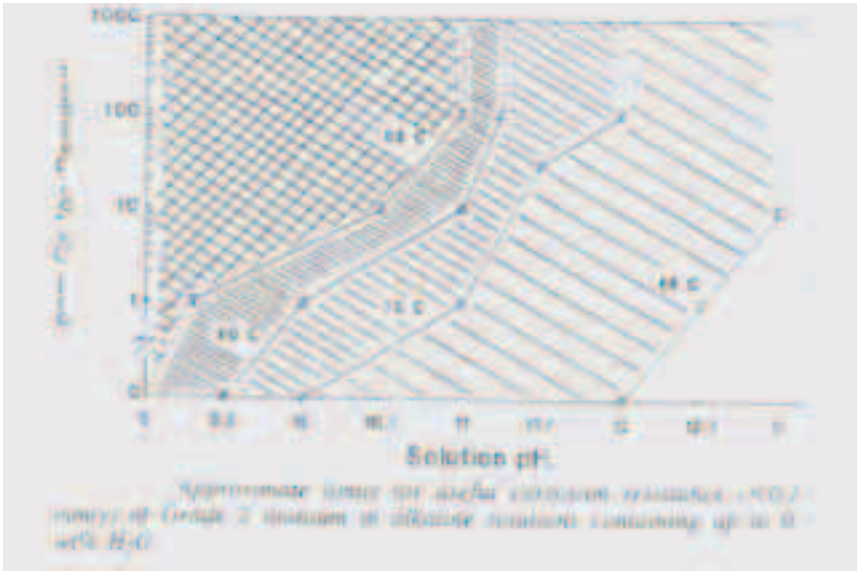

Figure 7 – Suggested application limits of titanium in inhibited bleach solutions, from the RMI Titanium study [7,8].

26. Assessment of Potential Stress Corrosion Cracking (SCC) Failure of Alloy 22 Waste Container

Carl E. Jaske
CC Technologies Laboratories, Inc
Dublin, Ohio, USA

EDITORIAL NOTE

This volume, "A Compilation of Special Topic Reports," contains a series of reports that were prepared for the Waste Package Materials Performance Peer Review Panel to use as background and input to the peer review. Summaries drawn from the reports were also presented in Section 11 of the Panel's Final Report. The Panel used the reports as background and input for its review. Any views and comments expressed in the summaries and the full reports do not necessarily reflect the opinion and findings of the Panel. Further, opinions expressed in the reports are not necessarily those of the Panel or reflected in the Panel's reports and recommendations.

The mechanical integrity assessment of Alloy 22 waste containers must consider the possibility that crack-like flaws may initiate and grow by stress-corrosion cracking (SCC). SCC may occur at fabrication flaws and areas of stress concentration. The major stress of concern is residual stress from the fabrication process. The most likely area for fabrication flaws, stress concentrators, and high residual stress are the weld joints.

Fracture mechanics is used to evaluate the potential for crack-like flaws to grow or to result in component failure. Fracture mechanics can be applied deterministically or probabilistically. In the former case, conservative values of fracture toughness, SCC rates, flaw sizes, and residual stress are used, while in the latter case statistical distributions of these values are used.

The critical crack size is that at which failure is predicted to occur. The minimum critical crack size is computed when deterministic fracture mechanics (DFM) is employed, whereas a likely distribution of critical crack sizes is computed when probabilistic fracture mechanics (PFM) is employed. The maximum SCC rate is used for DFM analyses, while the distribution of probable SCC rates is used for PFM analyses.

An important issue that must be address in applying either DFM or PFM to waste canisters is the effect of long-term aging on material properties. Long-term exposures at elevated temperature can reduce fracture toughness. Thus, a flaw that is initially below the critical size can become critical without any growth if aging significantly degrades the fracture toughness of the material. Material aging also may increase SCC rates. For these reasons, the effects of material aging must be quantified and included in the DFM or PFM model.

Special Topic Report prepared for the Waste Package Materials Performance Peer Review. The Final Report of the Peer Review was submitted to U.S. Department of Energy and Bechtel SAIC Company, LLC on February 28, 2002.

Figure 1 illustrates the application of DFM to remaining life prediction.[1] The input data are crack sizes measured by inspection, crack growth rate, fracture toughness, and degradation of fracture toughness with time. K_I is the applied stress intensity factor, K_{ISCC} is the threshold stress intensity for SCC, and K_{Ic} is the fracture toughness. Crack growth must be evaluated when $K_I \varnothing K_{ISCC}$, and fracture is predicted to occur when $K_I \varnothing K_{Ic}$. The crack can grow with time until either a leak or a fracture is predicted.

For PFM, the distributions of crack size, growth rate, fracture toughness, and change in fracture toughness are evaluated to predict probabilities of growth, leaking, and fracture. The Monte Carlo method is often used to apply PFM.

Both the increase in crack size (a) and decrease in critical crack size must be considered for fracture prediction. Increasing crack size in a waste container requires a mechanism for active crack growth, such as SCC. Decreasing critical crack size in a waste container requires an aging mechanism that reduces fracture toughness. Thus, both SCC growth and material aging must be quantified and evaluated for waste containers.

For a closed cylinder, two types of fracture are possible. First, a surface crack can grow until it reaches a critical depth where it suddenly penetrates the wall and results in a leak. Second, a surface crack or through-wall flaw can grow to a critical length where sudden rupture of the cylinder occurs. The first type of fracture may possibly occur in a waste container, but the second type is highly unlikely. The reasons are that Alloy 22 is expected to have reasonably high fracture toughness even if it undergoes long-term aging and the main stress is a residual stress. Residual stress is relieved by crack growth. Experience with engineering alloys, even those with much lower toughness than Alloy 22, shows that a primary sustaining stress, such as internal pressure, must be present to result in sudden fracture. Therefore, only the through-wall penetration or leak scenario needs to be evaluated for waste canisters.

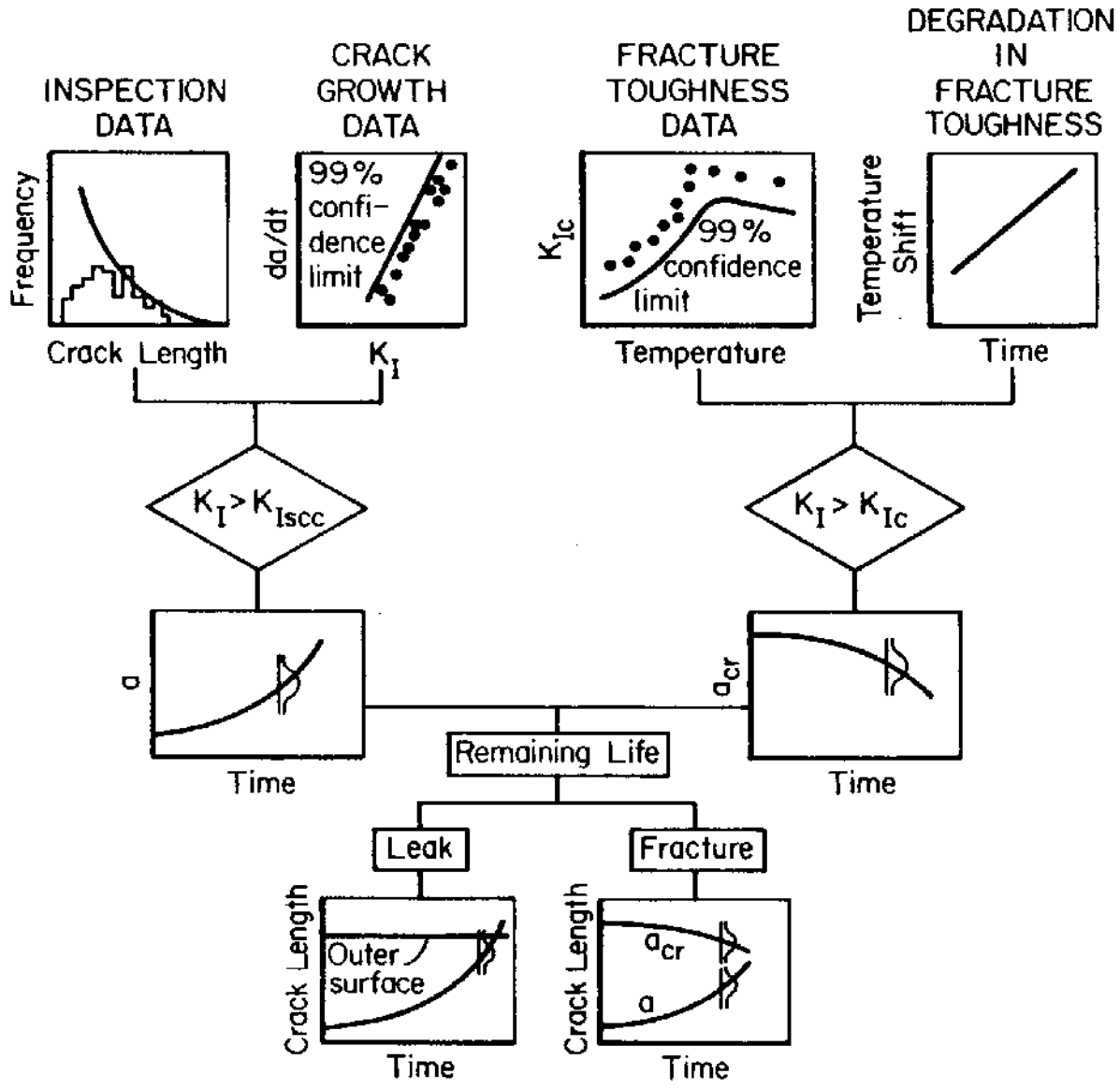

Figure 1. Typical procedure for remaining life assessment using fracture mechanics.[1]

REFERENCE

1. C. E. Jaske, "Techniques for Examination and Metallurgical Damage Assessment of Pressure Vessels," Performance and Evaluation of Light Water Reactor Pressure Vessels, PVP – Vol. 119, ASME International, New York, pp. 103-114.